

**STABILITY OF THE SHORELINE AT FORT ANNE**

**NATIONAL HISTORIC SITE**

**Final Report to**

**Parks Canada  
Department of Canadian Heritage**

**Contract No. NHS/SWNS 94-05**

**by**

**Graham R. Daborn  
Carl L. Amos  
Harold A. Christian  
and  
Michael Brylinsky**

**May 1995**

**ACER Publication No. 37**

## 1.0 EXECUTIVE SUMMARY

In order to assess the prospects for and appropriate design of remedial works to protect the embankments at Fort Anne National Historic Site from continuing erosion, a research programme to examine hydrodynamic and sedimentological processes in neighbouring portions of the Annapolis Basin and Estuary was conducted from 12 to 18 June 1994. The project was a cooperative exercise involving three research groups : the Acadia Centre for Estuarine Research, the Atlantic Geoscience Centre (Bedford Institute of Oceanography), and the Institute for Marine Dynamics (National Research Council of Canada, Ottawa). The combined intellectual and material resources of these three groups was essential to the success of the project. Each group also provided 'in-kind' resources in order to enable the project to be completed.

Recording current meters were deployed at three locations in the central axis of the estuary, and at three other locations on the Fort Anne foreshore, to provide data for construction and calibration of a hydrodynamic model. These data were forwarded to the Institute for Marine Dynamics for modelling purposes.

Geotechnical investigations were conducted by the Atlantic Geoscience Centre. Four soil cores were obtained using a portable gravity percussion sampler. Observations during coring indicated that the embankment of the southwest ravelin consists of marine clays with interbedded saltmarsh roots. A small landslide occurred on the seaward face of this slope in March 1994. The laminations exposed by the slip indicate that the embankment is a natural deposit, representing a local topographic high. Vertical standpipes have been installed at the four coring sites along the slope to assist with detection of further movements, and with identification of any internal slip surface. These piezometer pipes are suitable for the monitoring of groundwater levels in the embankment.

Granulometric tests of cores indicate that the 'red mud' that overlies the glacial till is a silty clay (56% silt, 44% clay) of post-glacial origin. Shear tests confirm previous observations that it is overconsolidated, and has a plasticity index of 29% (liquid limit 55%; plastic limit 26%). Undrained shear strength of undisturbed core subsamples ranged from 180 to 690 kPa.

As a result of observations made during the early field study, plans to reinstate the rockfill berm at the toe of the slope were advanced, and the work was completed by Parks personnel during the summer. Calculations of slope stability indicate that without the rock fill that had eroded away, the slope was unstable; emplacement of approximately 1000 tonnes of rock has reestablished stability for the near future, however, further remediation is required. It is also recommended that water levels in the standpipes be monitored regularly for assessment of the groundwater table.

A series of seven deployments of 'Sea Carousel', a field-deployable annular flume, was made along the axis of the Annapolis Estuary to examine the *in situ* shear strength and erodibility of the bottom sediments. The field study was a cooperative effort of the Acadia Centre for Estuarine Research and the Atlantic Geoscience Centre. Field measurements were made of water column salinity, temperature and suspended solid concentrations at each 'Sea Carousel' site. Grab samples were taken for analysis of sediment and biological characteristics.

Difficulties were experienced in maintaining position during the two-hour long deployments at stations nearest Digby because of strong winds. Nonetheless, complete deployments were successfully made in the Estuary (the region between the Annapolis Causeway and Goat Island),

the area of greatest significance for modelling purposes. Results of 'Sea Carousel' deployments showed that the sediment surface in the inner Annapolis Basin in the vicinity of Fort Anne is highly erodible, exhibiting erosion at critical shear stresses of 0.3 to 0.6 Pa. The results are conformable with those of remolded sediments examined in laboratory flumes at the Acadia Centre for Estuarine Research and the Canada Centre for Inland Waters.

Analyses of grab and core samples at each of the anchor stations indicates that the abundance and diversity of benthic organisms is greater at stations in the Basin than in the Estuary. Although polychaete worms are numerically dominant throughout, a greater variety of polychaetes and crustaceans is present in the coarser sediments characteristic of the Basin. In the Estuary, the finer sediments are actively disturbed (bioturbated) by burrowing invertebrates. Chlorophyll and carbohydrate concentrations in sediments of the Estuary suggest that biological production is lower in the Estuary than the Basin, although in some respects the station nearest to Fort Anne appears anomalously high. The intertidal fauna at Fort Anne is poorly developed, reflecting the instability of the surface. The burrowing amphipod *Corophium volutator*, is numerically dominant, and its activities may increase susceptibility of the surface sediment to resuspension. Remedial action to transform the intertidal mudflat at Fort Anne into a rocky shore might increase benthic production as well as minimise further erosion.

Recommendations arising from the study include :

1. That discussions regarding engineering solutions for protection of the embankment and saltmarsh against erosion be initiated immediately.
2. That a multidisciplinary team be established to develop and select appropriate engineering solutions.
3. That solutions considered should address two problems : erosion of the Fort embankment and residual marsh at the high water level; erosion of exposed intertidal silty-clay by tidal resuspension. Possible solutions to be considered should include : rebuilding of Queen's Wharf; reconstruction of the groyne (i.e., the "Scottish"? wharf) at the junction of Allain River and the Annapolis Estuary; rockfill protection of remnant saltmarshes; covering of exposed intertidal sediments by a more erosion-resistant material.
4. That water table levels in the embankment be monitored regularly.
5. That the position of rocks laid down as part of recent remedial work should be monitored in order to detect continued movement.
6. That a mid-summer survey of benthic intertidal fauna be conducted.
7. That experiments be designed and conducted to examine the feasibility of sealing the exposed intertidal sediment to prevent its further loss.

## TABLE OF CONTENTS

1.0	Executive Summary	ii
2.0	Introduction	1
2.1	Acknowledgements	4
3.0	Objectives	5
4.0	Field Operations	7
4.1	Introduction	7
4.2	Current Meter Deployments	7
4.3	Anchor Stations	12
4.4	Intertidal Studies	12
5.0	Physical Oceanography of the Annapolis Basin and Estuary	13
5.1	Long Term Records	13
5.2	Anchor Station Data	14
5.3	Summary	14
6.0	Geotechnical Investigations of Fort Anne Foreshore	21
6.1	Introduction	21
6.2	Methodology	21
6.3	Core Sampling	21
6.4	Historical Information on Measures to Combat Slope Instability	22
6.5	Conclusions	23
7.0	Slope Stability of the Southwest Ravelin	25
7.1	Introduction	25
7.2	Geotechnical Site Investigations - 1993-94	25
7.3	Inferred Regional Topographic Changes Since Deposition	27
7.4	Laboratory Shear Strength Testing	27
7.5	Slope Geometry from Geographic Survey	28
7.6	Analysis of Slope Stability	28
7.7	Discussion of Results	31
7.8	Recommendations for Further Remediation	32
8.0	Sedimentological Studies of the Annapolis Estuary	34
8.1	Introduction	34
8.2	Field Survey	34
8.3	Results	35
8.4	Interpretation	72
8.5	Laboratory Study	72
8.6	Results	74
8.7	Interpretations	88



9.0	Biological Constituents of the Annapolis Basin and Estuary	89
9.1	Introduction	89
9.2	Subtidal Benthic Fauna	89
9.3	Biological Properties of Subtidal Sediments	94
9.4	Intertidal Fauna	95
10.0	Summary	101
11.0	Conclusion and Recommendations	104
12.0	References Cited	106
13.0	Appendices	
A.	Graphic Summaries for 1994 Geotechnical Borings on Southwest Ravelin	109
B.	Boundary Conditions for the Analysis of Slope Stability	114
C.	Photographs of Gravity Cores, Stations S2 to S8, Annapolis Basin and Estuary	132
D.	Grain Size Analyses of Gravity Cores	139
E.	Benthic Fauna at Subtidal Stations of the Annapolis Basin and Estuary, June 1994	170

## LIST OF FIGURES

Figure 2.1	Landslip at Fort Anne, March 1994.	2
Figure 2.2	Landslip at Fort Anne, March, 1994. High water.	2
Figure 4.1	Annapolis Basin and Estuary, showing location of anchor stations (S1-8), and Aanderaa current meter locations (C1-3).	8
Figure 4.2	Annapolis Estuary in the Vicinity of Fort Anne, showing S4 current meter deployment locations (#1 - 3) and intertidal transect (T).	9
Figure 4.3	S4 Current Meter Station 2, near "Scottish?" Wharf.	10
Figure 4.4	View toward "Scottish?" Wharf and S4 Station 2.	10
Figure 4.5	Intertidal Transect No. 2.	11
Figure 4.6	Red Clay exposed near S4 Station 2.	11
Figure 5.1	Long term records of current velocity and direction, salinity, temperature and water depth at station C1, near Fort Anne, Annapolis Estuary, June 1994.	16
Figure 5.2	Long term records of current velocity and direction, salinity, temperature and water depth at station C2, near Goat Island, Annapolis Estuary, June 1994.	17
Figure 5.3	Long term records of current velocity and direction, salinity and temperature at station C3, in the Annapolis Basin, June 1994.	18
Figure 5.4	Salinity-temperature profiles at anchor stations S2 to S5 in the Annapolis Estuary, June 1994.	19
Figure 5.5	Salinity-temperature profiles at anchor stations S6 to S8 in the Annapolis Basin, June 1994.	20
Figure 7.1	Tilt angle data recorded by Parks Canada, from aluminum plates installed on rotated timbers projecting from the base of the embankment referred to as the southwest ravelin. Plates numbered 5 and 6 appeared to continue their rotation, perhaps along with No. 2, whereas others were now settling, due to undermining by sea action. A major erosion event appears to have occurred about 100 days after the commencement of record-keeping, in June 1993.	26

Figure 7.2	Plasticity chart modified from Jacques, Whitford & Associates Ltd. (1985), combining index property data from Allain Creek area with that of the intertidal red clay exposed seaward of the southwest ravelin. Note that the mudflat clay plots as an intermediate material. It was tested and was found to be 56% silt and 44% clay. Its position above the A-line indicates that it is of glacial origin.	29
Figure 7.3	Profile IB 900 to 913, from the crest of the southwest ravelin to the intertidal zone. Position of the groundwater table is inferred from direct observation and standpipe testing. The approximate depth of rock fill is indicated, along with the most likely position of the slip surface within the slope. This profile shows the slope before major erosion. Note the stepped backscarp and rotated timbers, indicating that slippage had previously occurred.	30
Figure 8.1	Correlation between 'Sea Carousel' current velocity measurements measured by electromagnetic current meter and estimated by analysis of videotape imagery.	37
Figure 8.2	Time series of 'Sea Carousel' deployment at anchor station S2.	38
Figure 8.3	Time series of 'Sea Carousel' deployment at anchor station S3.	39
Figure 8.4	Time series of 'Sea Carousel' deployment at anchor station S4.	40
Figure 8.5	Time series of 'Sea Carousel' deployment at anchor station S5.	41
Figure 8.6	Time series of 'Sea Carousel' deployment at anchor station S6.	42
Figure 8.7	Time series of 'Sea Carousel' deployment at anchor station S7.	43
Figure 8.8	Time series of 'Sea Carousel' deployment at anchor station S8.	45
Figure 8.9	Correlations between suspended sediment concentration and optical backscatter sensor reading, during 'Sea Carousel' deployment at anchor station S2.	46
Figure 8.10	Correlations between suspended sediment concentration optical backscatter sensor reading, during 'Sea Carousel' deployment at anchor station S3.	47
Figure 8.11	Correlations between suspended sediment concentration optical backscatter sensor reading, during 'Sea Carousel' deployment at anchor station S4.	48
Figure 8.12	Correlations between suspended sediment concentration and optical backscatter sensor reading, during 'Sea Carousel' deployment at anchor station S5.	49
Figure 8.13	Correlations between suspended sediment concentration optical backscatter sensor reading, during 'Sea Carousel' deployment at anchor station S6.	50

Figure 8.14	Correlations between suspended sediment concentration optical backscatter sensor reading, during 'Sea Carousel' deployment at anchor station S7.	51
Figure 8.15	Correlations between suspended sediment concentration and optical backscatter sensor reading, during 'Sea Carousel' deployment at anchor station S8.	52
Figure 8.16	Relationship of shear stress and depth in 'Sea Carousel' deployment at anchor station S2.	55
Figure 8.17	Relationship of shear stress and depth in 'Sea Carousel' deployment at anchor station S3.	56
Figure 8.18	Relationship of shear stress and depth in 'Sea Carousel' deployment at anchor station S4.	57
Figure 8.19	Relationship of shear stress and depth in 'Sea Carousel' deployment at anchor station S5.	58
Figure 8.20	Relationship of shear stress and depth in 'Sea Carousel' deployment at anchor station S6.	59
Figure 8.21	Relationship of shear stress and depth in 'Sea Carousel' deployment at anchor station S7.	60
Figure 8.22	Relationship of shear stress and depth in 'Sea Carousel' deployment at anchor station S8.	61
Figure 8.23	Relationship between erosion rate and bed shear stress at anchor stations S2 to S5 in the Annapolis Estuary.	62
Figure 8.24	Settling rate experiments at anchor stations S2 to S5 in the Annapolis Estuary.	63
Figure 8.25	Change in shear strength with depth in gravity core from anchor station S2.	65
Figure 8.26	Change in shear strength with depth in gravity core from anchor station S3.	66
Figure 8.27	Change in shear strength with depth in gravity core from anchor station S4.	67
Figure 8.28	Change in shear strength with depth in gravity core from anchor station S5.	68
Figure 8.29	Change in shear strength with depth in gravity core from anchor station S6.	69
Figure 8.30	Change in shear strength with depth in gravity core from anchor station S7.	70
Figure 8.31	Change in shear strength with depth in gravity core from anchor station S8.	71

Figure 8.32	Calibration of optical backscatter sensors in ACER Laboratory Carousel experiments, Run 1.	75
Figure 8.33	Calibration of optical backscatter sensors in ACER Laboratory Carousel experiments, Run 2.	76
Figure 8.34	Relationship between lid rotation of ACER Laboratory Carousel and measured current velocity.	77
Figure 8.35	Correlation between Electromagnetic Current Meter reading and velocity estimated from video record.	78
Figure 8.36	Time series of ACER Laboratory Carousel experiment using sediment from anchor station S3, Run 1.	79
Figure 8.37	Time series of ACER Laboratory Carousel experiment using sediment from anchor station S3, Run 2.	80
Figure 8.38	Time series of ACER Laboratory Carousel experiment using sediment from anchor station S3, Run 3.	81
Figure 8.39	Relationship between shear stress and depth in sediment, ACER Laboratory Carousel, Run 1.	83
Figure 8.40	Relationship between shear stress and depth in sediment, ACER Laboratory Carousel, Run 2.	84
Figure 8.41	Relationship between shear stress and depth in sediment, ACER Laboratory Carousel, Run 3.	85
Figure 8.42	Comparison of Laboratory and Sea Carousel determinations of relationship between shear stress and erosion rate.	86
Figure 9.1	Abundance of benthic organisms at stations S2 to S8 in the Annapolis Basin and Estuary, 1994.	90
Figure 9.2	Abundance of dominant benthic species in the Annapolis Basin and Estuary, 1994.	92
Figure 9.3	Relative abundance of dominant benthic species at stations S2 to S8 in the Annapolis Basin and Estuary, 1994.	93
Figure 9.4	Water content and % organic carbon of sediments from stations S2 to S8 in the Annapolis Basin and Estuary, 1994.	96
Figure 9.5	Carbohydrate concentrations of sediments at stations S2 to S8 in the Annapolis Basin and Estuary, 1994.	97

Figure 9.6	Chlorophyll concentrations of sediments at stations S2 to S8 in the Annapolis Basin and Estuary, 1994.	98
Figure 9.7	Intertidal Transect on Fort Anne Shore.	99
Figure 9.8	Relative abundance of benthic intertidal fauna along Fort Anne transect.	100

## LIST OF TABLES

Table 4.1.	Locations of S4 Current Meter deployments, Fort Anne foreshore, June 1994.	7
Table 5.1.	Deployments of Aanderaa Current Meters in the Annapolis Basin.	13
Table 7.1.	Summary of engineering properties for soils encountered. The saturated unit weight ( $\gamma_s$ ), effective cohesion intercept ( $c'$ ), effective angle of internal friction ( $\Phi'_i$ ), undrained shear strength ( $C_u$ ), and the ratio of peak to remoulded undrained shear strength, or sensitivity ( $S_i$ ), are listed for each soil shown in the section diagrams.	32
Table 7.2	Summary of slope stability calculations, including loading conditions (drained versus undrained), state of tide, existence of rockfill at toe of embankment and resultant factor of safety derived from the Bishop-Simplified, Janbu and Morgenstern-Price methods. Factor of safety is defined as the ratio of the sum of the resisting forces (soil shearing resistance) to the driving forces (gravitational loads). A factor of safety less than 1 indicates that an unstable condition exists.	33
Table 8.1.	A summary of station locations of the Sea Carousel and general conditions.	36
Table 8.2.	A summary of the erosion characteristics of the Sea Carousel stations occupied in Annapolis Basin. (Bed state is herein subdivided into five major groups on the basis of erosion threshold and friction angle ( $\Phi$ ). These are (1) stable beds where $\Phi > 10^\circ$ ; (2) unstable beds where $\Phi < -10^\circ$ ; (3) neutral beds where $-10^\circ > \Phi > 10^\circ$ ; (4) fluidized beds where $-10^\circ > \Phi > 10^\circ$ and where $\tau_o \Rightarrow 0$ ; and (5) surface bed strengthening attributed to biostabilization.)	36
Table 8.3.	A summary of the correlation between measured suspended sediment concentration (SSC) and voltage output from the Optical Backscatter Sensors (OBS) of Sea Carousel.	45
Table 8.4.	A summary of the peak erosion rates (EP) for Type I erosion detected by Sea Carousel at stations FA2 to FA5 (inner stations). The remaining stations have not been included as the seabed at these outer stations is largely composed of sand.	54
Table 8.5.	A summary of the mean mass settling rates determined during the still water settling period carried out at the latter stages of each Sea Carousel deployment of the inner stations in Annapolis Basin.	54
Table 8.6	A summary of the bulk physical properties of gravity cores collected at each of the Sea Carousel stations.	64
Table 8.7.	A summary of the surface sediment character at stations FA2 to FA7. No sample was collected at FA8 due to ship drift.	72



Table 8.8.	A summary of results on the erosion of sediments from FA3 using Lab Carousel.	74
Table 8.9.	The peak erosion rates (EP) and prevailing bed shear stresses during the erosion of station FA3 grey mud in the Laboratory Carousel.	87

## 2.0 INTRODUCTION

Graham R. Daborn  
Acadia Centre for Estuarine Research  
Acadia University

Erosion of the shoreline adjacent to Fort Anne National Historic Site has continued during the last few years until very little remains of the extensive saltmarsh that formed the seaward boundary of the Fort prior to and during the early 1950s. It is apparent that the fringing saltmarsh provided part of the necessary protection of the Fort embankments. With its disappearance, wave action has been directed at the foot of the embankment on the Annapolis Estuary (i.e., west) side, resulting in continuing and increasing instability of the 18<sup>th</sup> century cribwork and the embankment that it supports (Daborn *et al.* 1993a). In March 1994 a 4 m section of the southwest ravelin slipped down below the high water level, leaving an exposed surface that is susceptible to erosion by waves at high water, and to precipitation at all times (Figures 2.1 and 2.2). During May 1994, a skeleton became exposed as a result of continued surficial erosion in the same area; this burial has been tentatively associated with events of the early part of the 18<sup>th</sup> century (Dunn 1992, Cybulski 1994, Wallace 1994), prior to the establishment of the cribwork that is now exposed as a consequence of erosion.

In addition to wave action on the embankment itself, previous studies have shown that the sediments forming the beach in front of the embankments are eroding during every flood tide. This erosion results from resuspension of a fine red clay that has become exposed as a consequence of the removal of an overburden of grey marine muds that elsewhere underlie saltmarshes in the Allain River area (Daborn *et al.* 1992). Observations in 1994 suggested that erosion of this red clay will probably continue as long as it is exposed to water, resulting in a steady increase in the slope of the beach, and increased vulnerability of the embankments of the Fort (Daborn *et al.* 1993a).

In order to develop an appropriate strategy to protect Fort Anne in both short and long terms, it is necessary to understand the basic processes involved in the erosion, and to have sufficient knowledge of the environmental properties that prevail in the immediate area. Present knowledge suggests that the cribwork laid down in the 18<sup>th</sup> century had not been exposed until the latter half of the present century; it is critical to determine the changes in dynamic processes in the Annapolis Estuary that were responsible for initiating the present erosion process. Previous studies (Daborn *et al.* 1992, 1993a) had concluded that the present phase of erosion began in the late 1950s or early 1960s. This time period was coincident with the construction of the Annapolis Causeway (1960), the deterioration of Queen's Wharf, and several changes associated with bridges in the Annapolis Estuary and Allain River.

Chief among the physical properties requiring study are the nature of the sediments being eroded, particularly their grain size and susceptibility to erosion. A rock mass was originally placed on the cribwork when it was constructed, but much of this mass has migrated away from the site, or fallen down between the cribs as a result of movements associated with tidal rise and fall, and the action of waves and ice. At high tide wave action continues to remove fine sediments that lie beneath the cribs, so that some of the timbers exhibit movement in an upward or downward direction, particularly during spring tides. The stability of the embankment has been reduced as a result. An assessment of slope stability, which necessitates information on slope characteristics, sediment

Figure 2.1.  
Landslip at  
Fort Anne,  
March 1994



Figure 2.2  
Landslip at Fort Anne,  
March 1994.  
High Water.

properties, and mass concentrations, is an essential requirement for development of appropriate remedial measures.

The Acadia Centre for Estuarine Research (ACER) was requested by Canadian Heritage to design and coordinate a research project aimed at obtaining information necessary for the planning of remedial measures. Because of the interdisciplinary nature of the processes involved, and the necessity for unique instrumentation for examination of sediment properties *in situ*, the Centre established a cooperative study team with personnel from the Atlantic Geoscience Centre (Geological Survey of Canada, Bedford Institute of Oceanography). This team has previously worked on integrated, cooperative studies of sediments in the Minas Basin and the Miramichi Bay (Brylinsky *et al.* 1992, Daborn *et al.* 1993b).

ACER acted as coordinating agent, subcontracting with AGC for certain aspects of the field work. Operating funds were provided under contract NHS/SWNS 94-05.

In addition, the Institute for Marine Dynamics of the National Research Council of Canada (Ottawa) was recruited to develop linked hydrodynamic and sedimentological models that could be used for assessment of the most efficacious protective measures for the Fort. Data on current velocities, sediment erodibility, sediment properties, suspended sediment concentrations, and salinity/temperature conditions in the Annapolis Basin and Estuary were collected on behalf of the Institute to provide input for the calibration of the models.

In order to develop an assessment of present conditions on the shoreline and in the Annapolis Basin, and to provide data for calibration of hydrodynamic and sedimentological models, the project was organised into six major activities :

1. monitoring of water movements on the Fort Anne shore;
2. examination of physical processes acting in the Annapolis Basin as a whole, with particular reference to the region between the Annapolis Causeway and Goat Island (i.e., the Estuary);
3. examination of the properties of sediments on the foreshore at Fort Anne, and assessment of the stability of the embankments that have been subject to erosion;
4. determination of sediment properties and erodibility of submersed sediments in the Annapolis Estuary and Basin;
5. laboratory investigation of sediment properties to compare with *in situ* measurements made in the field;
6. examination of deposited sediments on the Fort Anne shore for evidence of bioturbation or other biological influence on sediment erodibility.

## 2.1 Acknowledgements

The Department of Fisheries and Oceans provided use of the M/V *Vigilance* for deployment and retrieval of the Aanderaa current meters. We are particularly appreciative of the efforts and professionalism of the Captain and crew of the *Vigilance*, and to Terry Matheson for making the vessel available.

The ACER field crew included Dr. Michael Brylinsky, Jamie Gibson, Stephen Mockford and Ken Meade, all of whom worked long hours with both enthusiasm and reliability. Jamie Gibson contributed a great deal of additional time and effort assisting Ms. Nathalie Sigouin and David MacDonald to collect water and sediment samples from the vicinity of Fort Anne for use in the laboratory flumes.

We are very grateful for the assistance provided by Fort Anne personnel, especially the Superintendent, Ms. Lillian Stewart, Roland Clayton and Sid Burrell.

We also acknowledge the continuing support of Project Manager Warren Peck, and Parks Canada staff members Brenda Dunn and Birgitte Wallace-Ferguson, who have added greatly to our appreciation of the historical context of the site and its physical evaluation.

### 3.0 OBJECTIVES

#### A. Monitoring Dynamic Processes in the Annapolis Basin and Estuary

1. To obtain long-term (14 day) records of current velocity and direction at three locations along the axis of the Annapolis Basin and Estuary for calibration of the hydrodynamic model;
2. To obtain short-term (several tidal cycles) measurements of current velocity and direction at sites on the Fort Anne foreshore for calibration of the hydrodynamic model;
3. To obtain salinity and temperature profiles at stations in the Annapolis Basin and Estuary for calibration and validation of the hydrodynamic model.

#### B. Geotechnical Investigations of the Fort Anne Embankments

1. To obtain representative soil samples from within the zone of slope instability, in order to determine the presence of any internal shear planes or surfaces;
2. To provide soil material for geological description, in order to determine the nature and degree of interbedding, as well as to classify the soil engineering behaviour;
3. To install groundwater monitoring wells within the previously-drilled sample holes to provide a means of measuring the elevation of the groundwater table within the embankment. Monitoring is to be carried out on an intermittent basis during periods of heavy rain in the spring.

#### C. Slope Stability

1. To determine the existing stability of the embankment of the southwest ravelin at Fort Anne;
2. To assess the benefit of placing a rock berm at the base of the embankment to replace rock fill that has migrated from the site as a result of erosion.

#### D. Sedimentology of the Annapolis Estuary and Basin

1. To obtain direct *in situ* measurements of threshold stresses for erosion of surficial sediments deposited subtidally along the axis of the Annapolis Estuary and Basin;
2. To determine stillwater settling rates of eroded sediments under ambient conditions of salinity and temperature for comparison with laboratory flume studies;
3. To obtain gravity cores from each station location for determination of bulk density, vane shear strength, grain size, and evidence of bioturbation;
4. To examine the relationships between erosion threshold of sediments deposited and allowed various times to consolidate in a laboratory flume, for comparison with *in situ* measurements.

### E. Biological Influences on Sediment Stability

1. To obtain samples of deposited sediments along the axis of the Annapolis Basin and Estuary to characterise the benthic fauna from the perspective of its influence on sediment stability;
2. To obtain samples of deposited sediment on the Fort Anne shore to record and describe the infaunal community.



## 4.0 FIELD OPERATIONS

Graham R. Daborn  
Acadia Centre for Estuarine Research  
Acadia University

### 4.1 Introduction

Field work was carried out between 12 June and 2 July 1994. The team was divided into three groups, one of which was responsible for ship-board operations (primarily anchor stations for deployment of 'Sea Carousel' and associated activities), and the other two for land-based work at the Fort. Anchor station operations (q.v. below) were coordinated by Dr. Michael Brylinsky, and shore-based operations by Harold Christian and Dr. Graham R. Daborn.

### 4.2 Current Meter Deployments

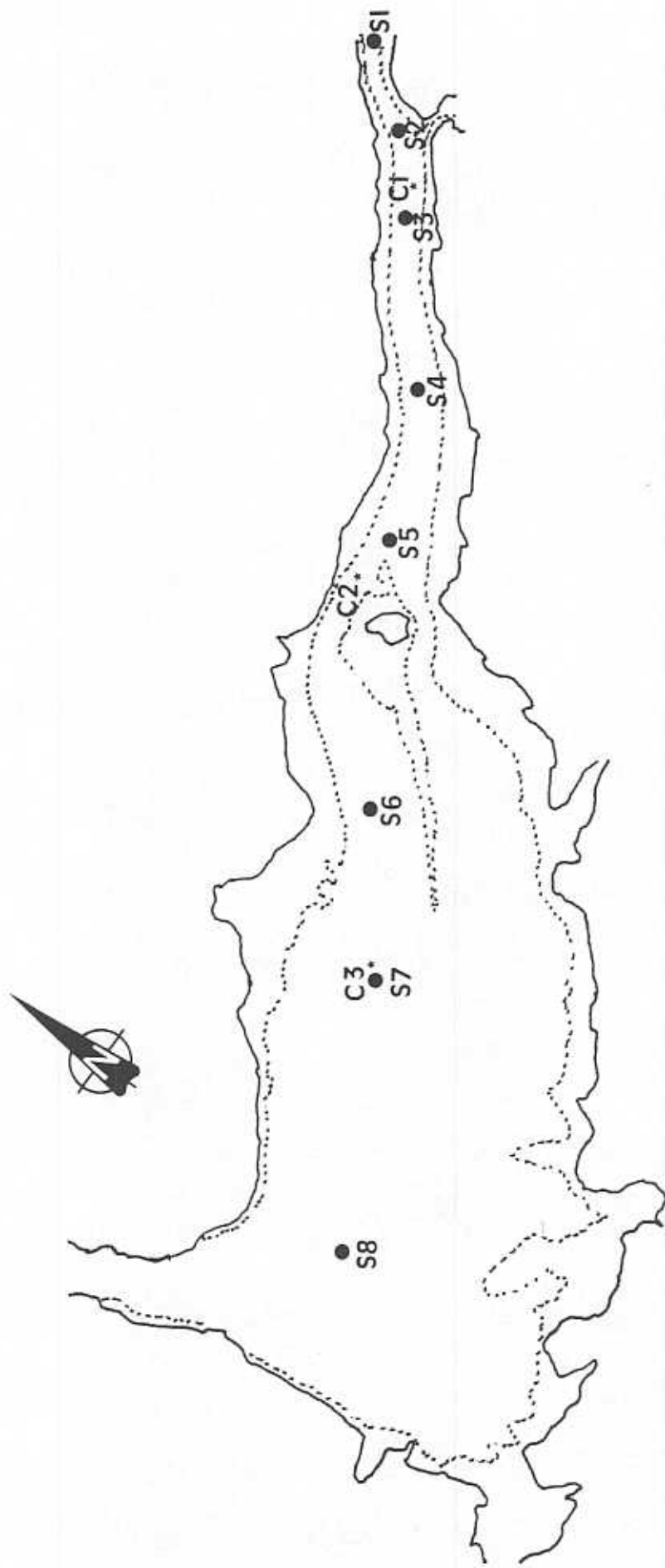
Three Aanderaa RCM4™ recording current meters were leased from ASL Environmental Sciences Limited (British Columbia), and deployed for a 14-day period at three locations along the principal axis of the Annapolis Basin and Estuary. Locations of the stations (C1-C3) are indicated in Figure 4.1. Each instrument was suspended at a height of 5 m above the bottom, and recorded current velocity and direction, water temperature and conductivity. The two instruments deployed east of Goat Island also recorded pressure, primarily reflecting changes in water depth over the tidal cycle. The instruments were set to record at 10-second intervals, and these data were internally averaged over 10-minute periods.

An Interocean™ S4 recording current meter was loaned to ACER by Dr. Carl Amos. This instrument (Figures 4.3 and 4.4) was deployed at three locations on the Fort Anne shoreline to obtain information regarding current velocities and direction over the intertidal zone. Locations of the deployments are shown in Figure 4.2, and details given in Table 4.1 :

Deployment #	Location	Times*	# Tides
1	44° 44.92' N 65° 31.78' W	In : 21:05 12 June Out : 09:09 14 June	3
2	44° 44.79' N 65° 31.66' W	In : 11:47 14 June Out : 11:00 17 June	6
3	44° 44.92' N 65° 31.66' W	In : 12:40 17 June Out : N/A 24 June	14

\* AST

Table 4.1. Locations of S4 Current Meter deployments, Fort Anne foreshore, June 1994.



- S1 - S8
- ▲ C1 - C3

Figure 4.1 Annapolis Basin and Estuary, showing location of anchor stations (S1-8), and Aanderaa current meter locations (C1-3).

Figure 4.2 Annapolis Estuary in the Vicinity of Fort Anne, showing S4 current meter deployment locations (#1 - 3) and intertidal transect (T).

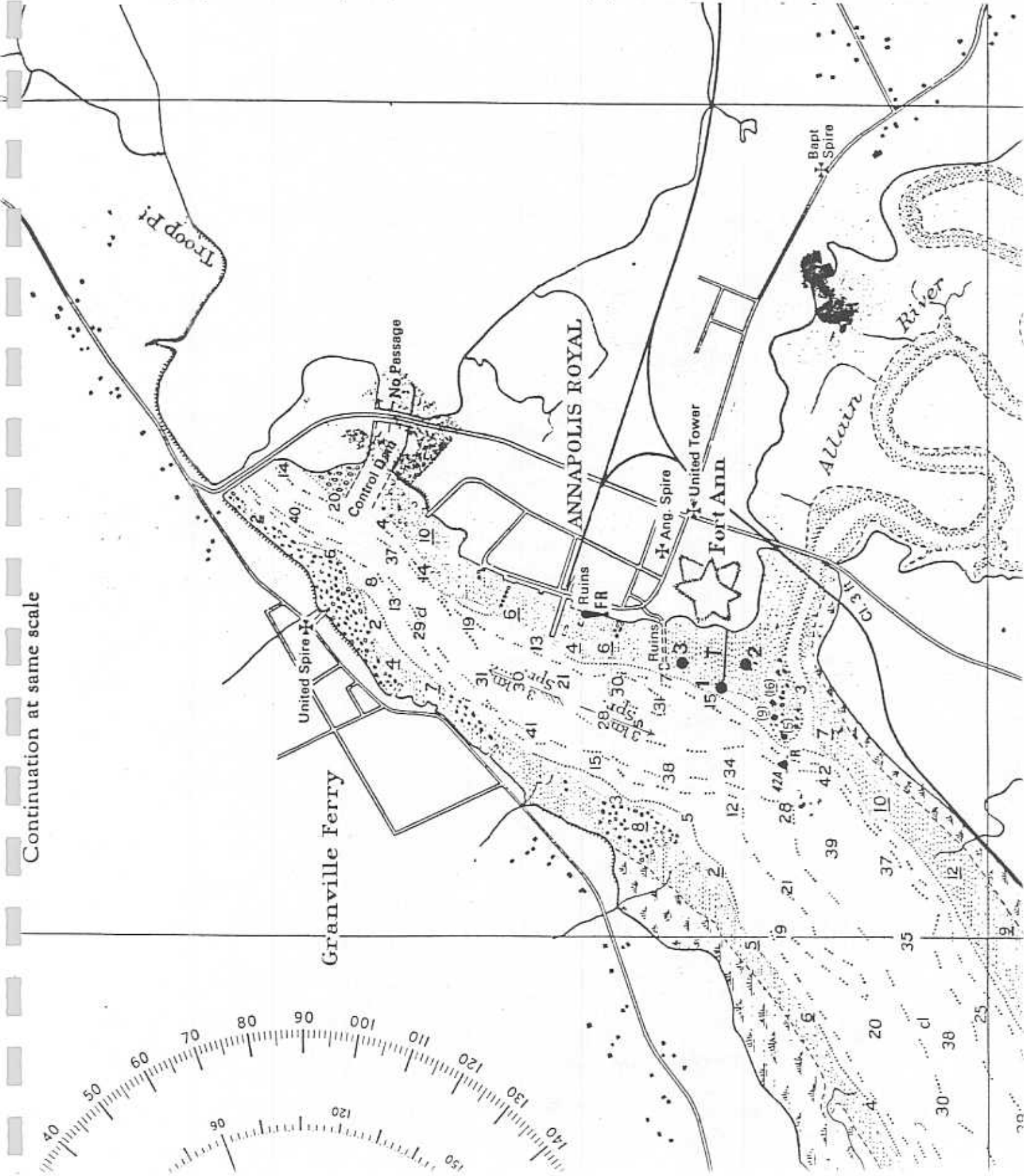


Figure 4.3.  
S4 Current Meter  
Station 2, near  
"Scottish"? Wharf

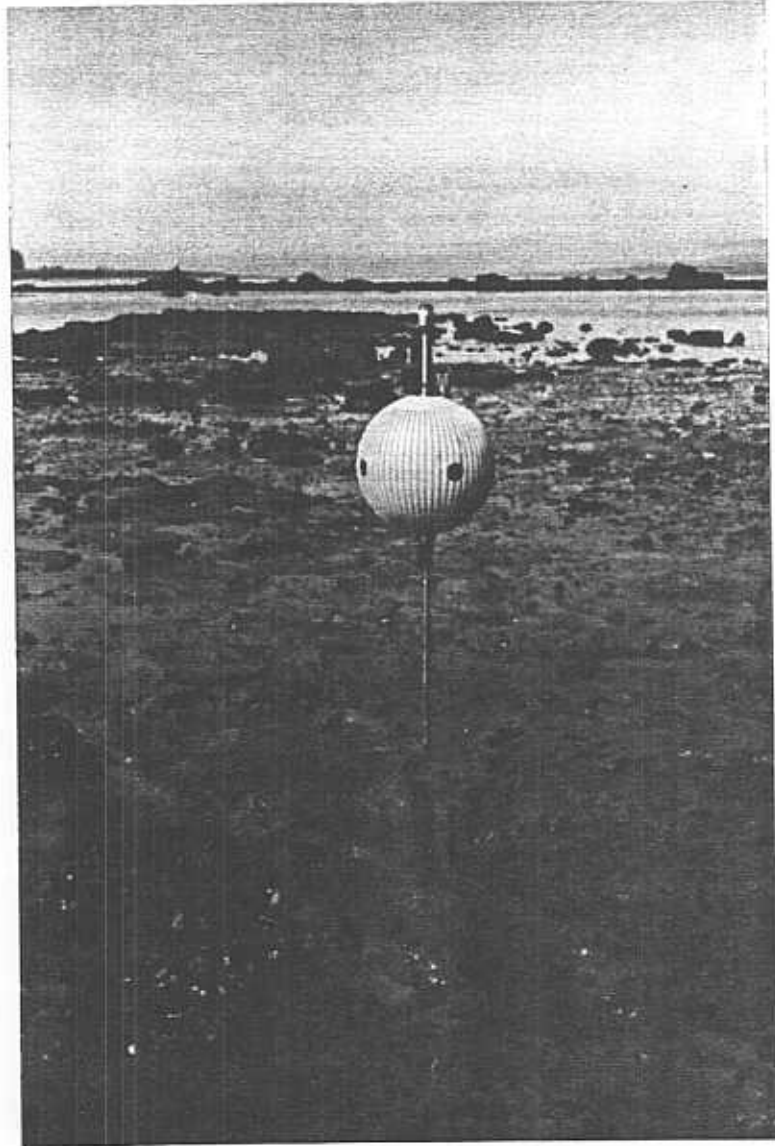


Figure 4.4  
View toward  
"Scottish"? Wharf  
and S4 Station 2.



Figure 4.5 Intertidal Transect No. 2  
(Arrow indicates S4 Station #1)

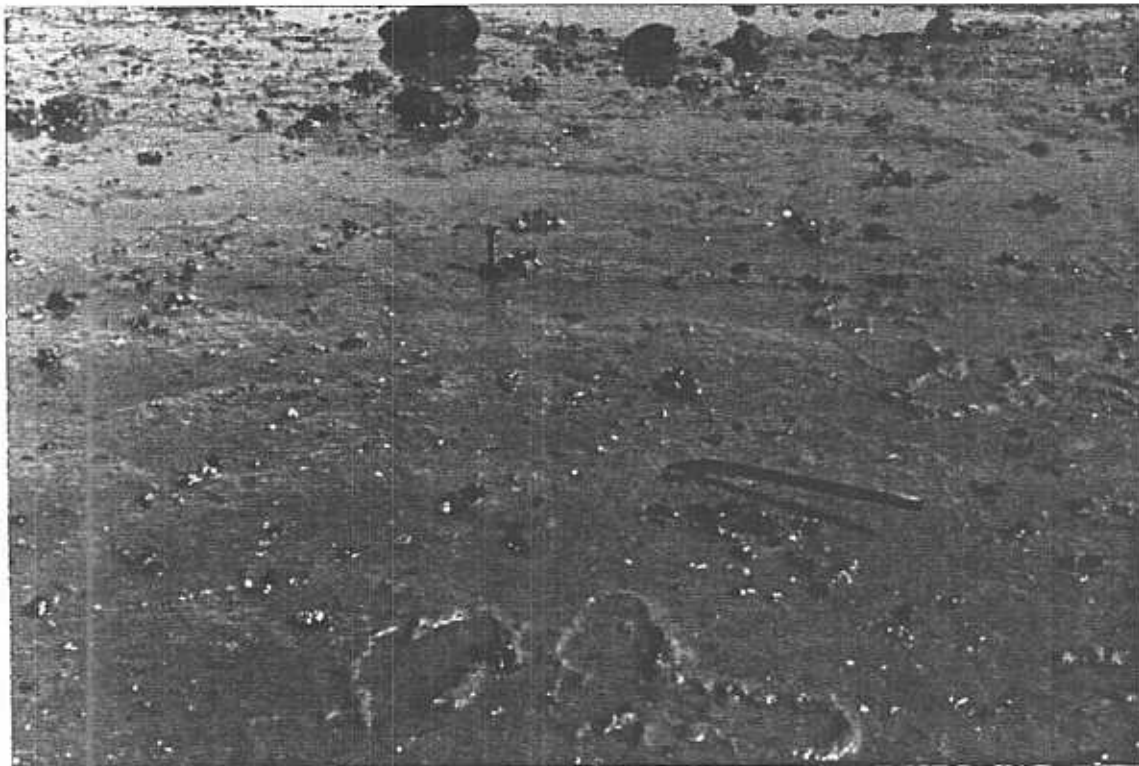


Figure 4.6 Red clay exposed near S4 Station # 2.  
(Metal posts represent a 1993 bed-level monitoring station.  
Both posts were originally c. 60 cm above the substrate.  
Ice has bent one post over and driven the other into the substrate).



### 4.3 Anchor Stations

A local scallop-dragger, the "*Gail and Troy*" was leased to provide a platform for 'Sea Carousel' operations. The vessel was anchored at eight pre-determined locations along the axis of the Annapolis Estuary and Basin, from the vicinity of the Annapolis Causeway to the centre of the Basin east of Digby (Figure 4.1). Locations of stations finally occupied were recorded using a Magellan 1500 GPS. At each anchor station, three anchors were set (one bow and two at the stern) to keep the vessel from moving too much under the influence of wind and current. Because the dragger lies high in the water, it was very susceptible to wind, particularly in the Basin west of Goat Island, and the planned anchor station S8 had to be abandoned before the 'Sea Carousel' deployment was complete. At several other stations, also, deployment of 'Sea Carousel' had to be shortened because of wind drift of the vessel. Anchor station S1 proved to have a rocky substrate, and was not occupied.

At each anchor station, a profile of the water column was taken using an EMP 2000 recording conductivity/temperature/depth meter. The bottom was then sampled using a wide-barrel AGC gravity corer, and a Van Veen grab. Core samples were sealed in plastic core liners, labelled, and stored for subsequent examination. Grab samples were opened on deck, and syringe subsamples taken for analysis of sediment bulk properties (cf. Section 8.2), organic matter, chlorophylls and carbohydrates (cf. Section 9.2).

A set of five or six grab samples was taken with a 15 cm Ekman Grab at each station. The samples were then sieved through 0.5 mm mesh sieves, and the residue stored in 4% formalin for subsequent analysis of the fauna.

Following benthic sampling, 'Sea Carousel' was deployed on site (cf. Section 8.0).

### 4.4 Intertidal Studies

In order to obtain estimates of the concentrations of red clay resuspended on each tide, six 1 L water samples were taken by hand from the surface water as the tide ebbed from the Fort Anne foreshore. Samples were filtered through pre-weighed 0.45  $\mu\text{m}$  Nuclepore™ filters, dried and reweighed.

A transect of stations was established on 16 June from the base of the southwest ravelin across the foreshore to the low tide mark. The transect ended near the location of the first deployment of the S4 current meter (cf. Figures 4.2 and 4.5). At 20 m intervals, three core samples were taken using a 5.7 cm diam. hand-held sampler for analysis of benthic invertebrates. Sample locations were selected using a randomised sample procedure. Samples were bagged separately, sieved through 0.5 mm sieves, and fixed in formalin for identification and enumeration.

## 5.0 PHYSICAL OCEANOGRAPHY OF THE ANNAPOLIS BASIN AND ESTUARY

Graham R. Daborn  
Acadia Centre for Estuarine Research  
Acadia University

In order to obtain direct field measurements in support of the modelling exercise being conducted by the National Research Council of Canada, current meters were deployed at three locations along the axis of the Annapolis Basin and Estuary, and at three locations on the foreshore of Fort Anne.

### 5.1 Long Term Records

Locations of the current meters are shown in Figure 4.1 and listed in Table 5.1 :

Station No.	Instrument No.	Location	Deployment Statistics
C1	8207	44°44.07'N 65°32.13'W	5 m above bottom Time on: 13.46 AST 13 June Time raised : 13.00 AST 29 June
C2	8208	44°42.56'N 65°36.28'W	5 m above bottom Time on: 14.25 AST 13 June Time raised: 13.30 AST 29 June
C3	6353	44°39.98'N 65°40.61'W	5 m above bottom Time on: 15.05 AST 13 June Time raised: 14.00 AST 29 June

**Table 5.1. Deployments of Aanderaa Current Meters in the Annapolis Basin.**

Selection of these locations was made in order to provide a reasonably complete coverage of the main Basin up to the Annapolis Causeway.

Results from the current meters are shown in Figures 5.1 to 5.3.

Tidal range in the Estuary varied from 5 to 8 m during the deployment. At high and low water, abrupt changes in water depth often occurred (cf. Figures 5.1 and 5.2) that are attributable to interactions between the tidal water of the Estuary, and regulated flows through the Annapolis Causeway and out of Allain River.

Maximum and mean current velocities were greater at the outer station (up to 70 cm.sec<sup>-1</sup> and averaging c. 25 cm.sec<sup>-1</sup>) than at either of the two stations inside Goat Island (50-65 cm.sec<sup>-1</sup> and averages about 20 cm.sec<sup>-1</sup>). Flood-ebb inequality is also more pronounced in the Basin (Figure



5.3) than in the estuary (Figures 5.1 and 5.2). Tidal currents are strongly reversing at all three stations, but there is a clearer tendency towards a rotary current at the Basin station (Figure 5.3).

During the 14 days of deployment, temperature and salinity (as conductivity) both increased, in association with warmer weather and decreased freshwater output from the River. The temperature and conductivity signals at the central station just above Goat Island are much more irregular than at the other two stations (Figure 5.2). This may be attributed to the confounding effects of flow around the island.

## 5.2 Anchor Station Data

At each anchor station occupied for 'Sea Carousel' and grab sampling, temperature and salinity profiles of the water column were recorded using an EMP 2000 recording CTD. Results are shown in Figures 5.4 and 5.5. Maximum water depth during these profiles depended upon the stage of the tide; hence the depth of the bottom measurement in a profile represents the near-bottom water at that station at the time of sampling.

Stations between the Annapolis Causeway and Goat Island exhibit a significant degree of stratification, with a layer of less saline, somewhat warmer water overlying a deeper layer of more saline water with which it is partially mixed. Because of the partial mixing, the salinities of bottom water are 28 to 30‰, which represent the salinity regime to which deposited sediments are exposed. Stratification is more strongly developed at the inner stations, and these profiles suggest that three layers may exist: a surface layer of 1 to 2 m, an intermediate layer from 2 to 4 m depth in which salinity increases in a step-wise manner (especially at stations 2-4), and the lowermost layer of relatively high salinity. Station 5 was over the main (northerly) channel of the estuary, where turbulent mixing is greater as a result of the high velocities occurring in that channel (cf. Figure 5.2); consequently the temperature-salinity profile exhibits more consistent patterns of change with depth. Previous studies have indicated that the structure of the water column in the inner portion of the estuary is influenced by sluicing and generation activities of the Annapolis Tidal Generating Station (Daborn *et al.* 1992, 1993a).

Stratification of the water column was still evident at two stations to the seaward of Goat Island, in the Annapolis Basin, but the most westerly station (S8 - Figure 5.5) exhibited a completely mixed condition. Because of the relatively greater volume of seawater at these stations, bottom salinities are higher, around 32‰.

## 5.3 Summary

The Annapolis Basin and Estuary form a complex system because of the shape of the basin, its geographic orientation, its restricted connection with the Bay of Fundy, and the relatively discrete sources of freshwater input. Goat Island lies at the junction between the Basin and the Estuary. On the seaward side of Goat Island, current and wave action are both high, resulting in a well-mixed water column. Deposited sediments are coarse-grained, dominated by sand, as a result of tidal sorting (cf. Daborn *et al.* 1991 and Table 8.7 herein).

Between Goat Island and the Annapolis Causeway, wind fetch is restricted, and although tidal currents are still quite high, freshwater issuing through the Causeway is inclined to remain at the surface, and to track more closely along the northern shore, resulting in a longitudinal stratification

(Daborn *et al.* 1993a). Bottom sediments in this stretch are increasingly dominated by silts and clays (Table 8.7 and Daborn *et al.* 1991).

The different current and sediment regimes on either side of Goat Island are reflected in the biological inhabitants of the bottom (cf. Section 9.0).

## Inner Station (CM #8207)

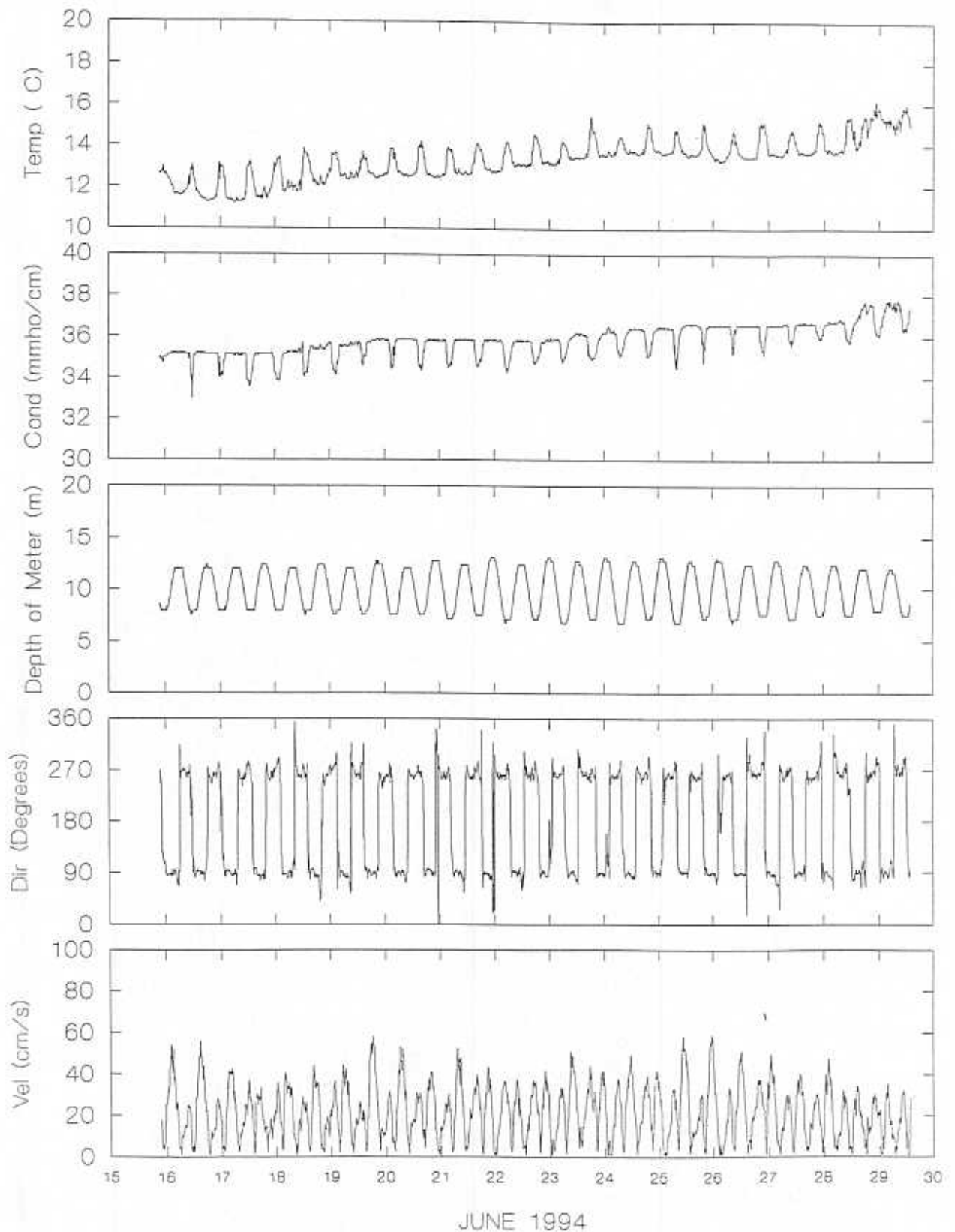


Figure 5.1 Long term records of current velocity and direction, salinity, temperature and water depth at station C1, near Fort Anne, Annapolis Estuary, June 1994.

## Centre Station (CM #8208)

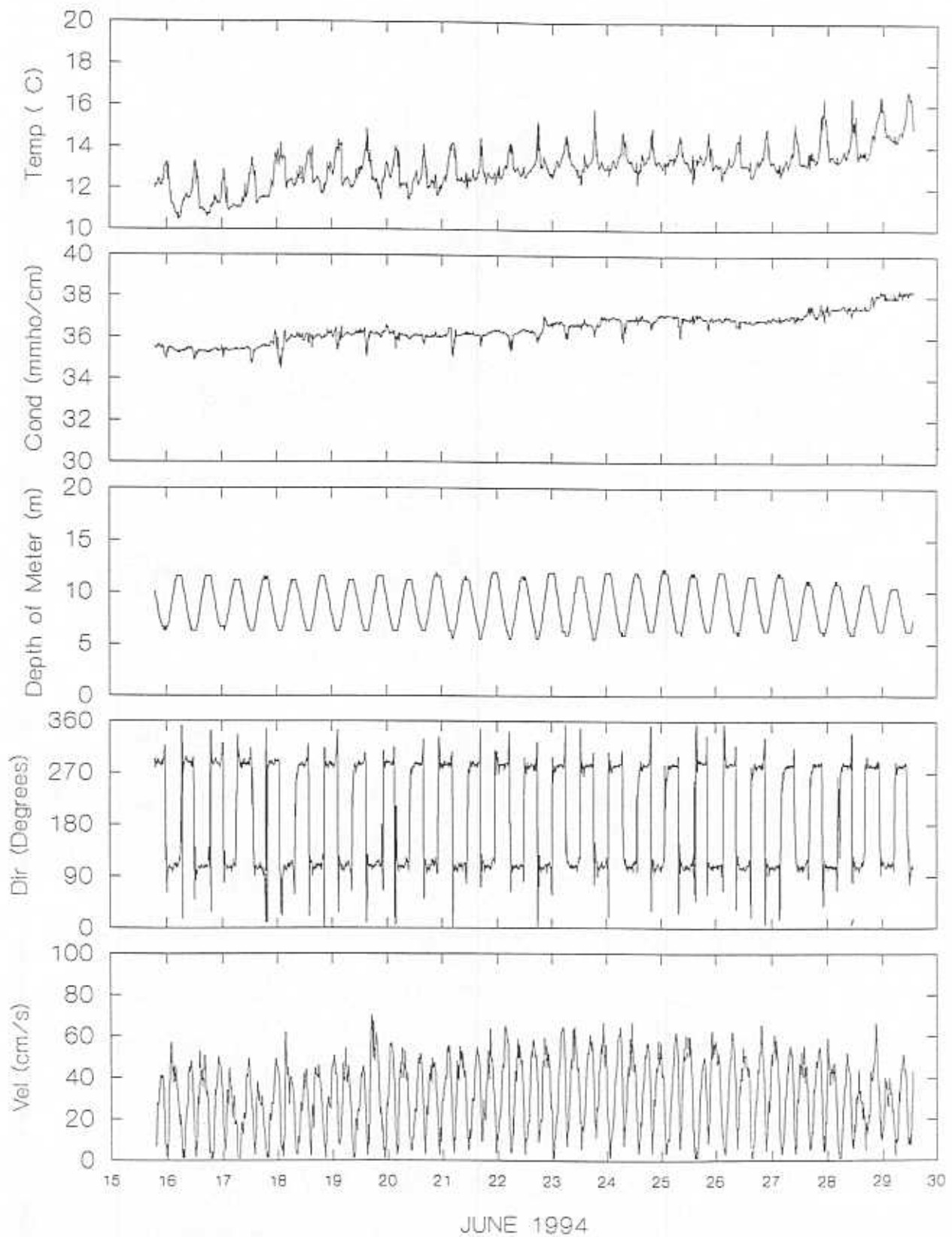


Figure 5.2 Long term records of current velocity and direction, salinity, temperature and water depth at station C2, near Goat Island, Annapolis Estuary, June 1994.

## Outer Station (CM #6353)

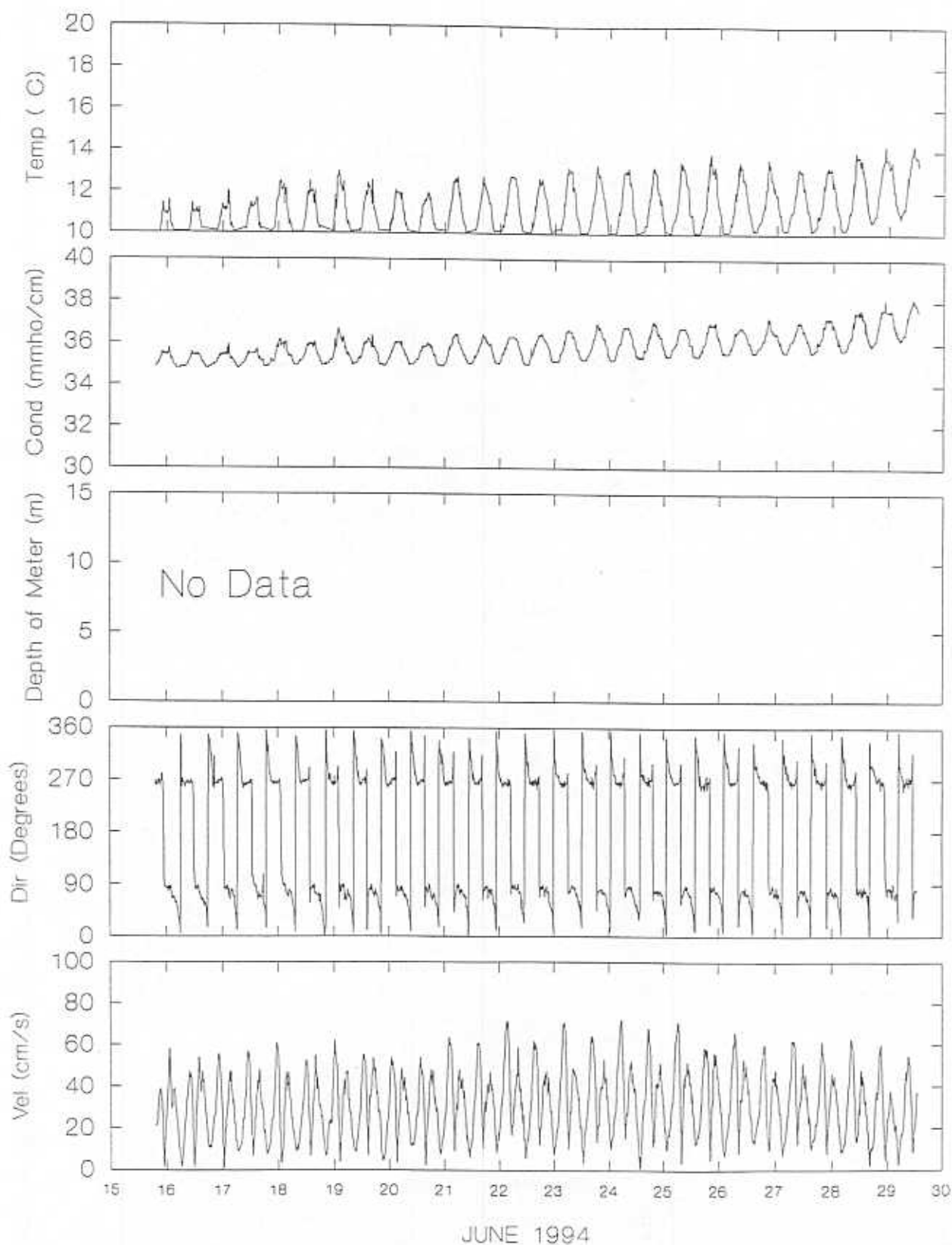


Figure 5.3 Long term records of current velocity and direction, salinity and temperature at station C3, in the Annapolis Basin, June 1994.

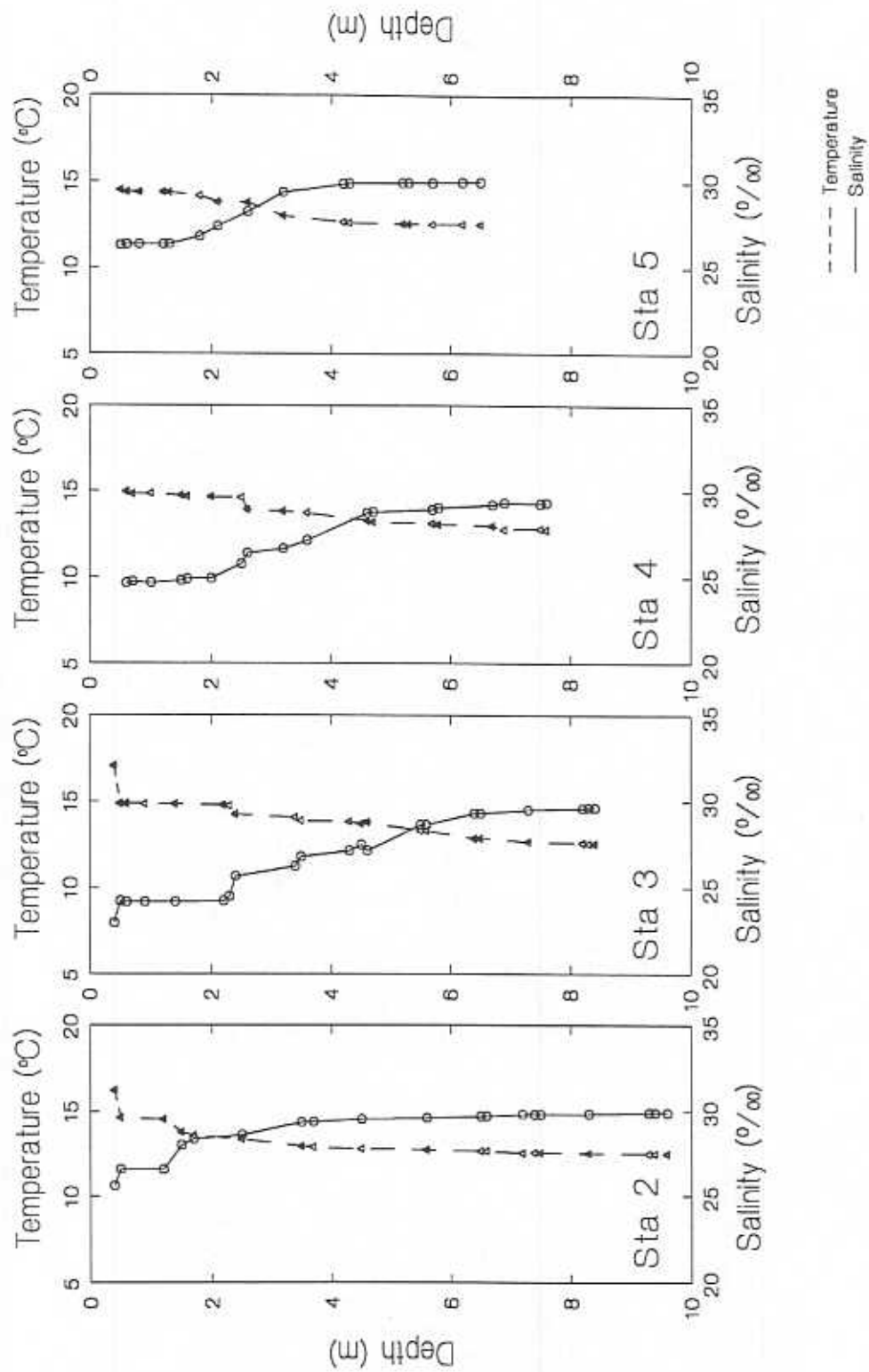


Figure 5.4 Salinity-temperature profiles at anchor stations S2 to S5 in the Annapolis Estuary, June 1994.

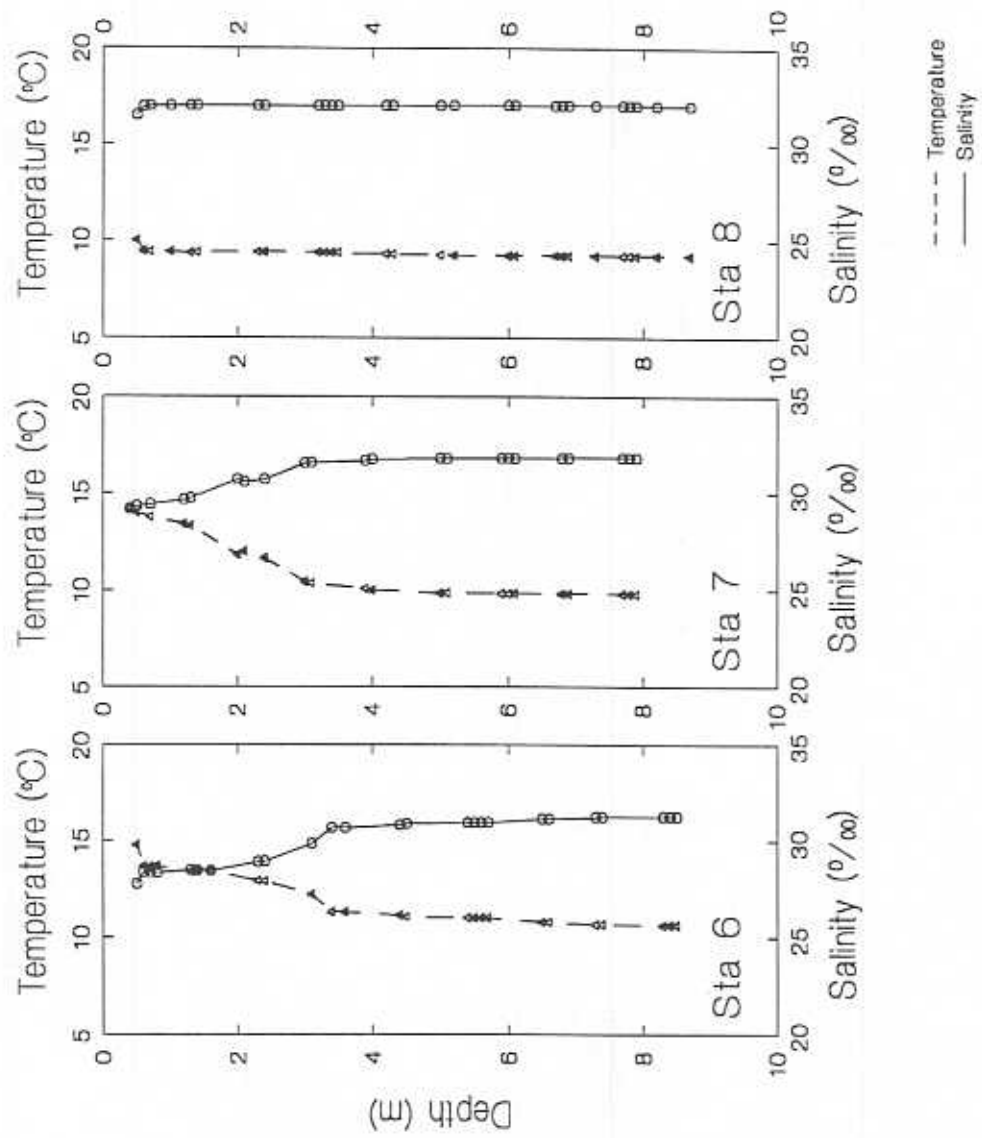


Figure 5.5 Salinity-temperature profiles at anchor stations S6 to S8 in the Annapolis Basin, June 1994.



## **6.0 GEOTECHNICAL INVESTIGATIONS OF FORT ANNE FORESHORE**

H.A. Christian  
Atlantic Geoscience Centre  
Geological Survey of Canada

### **6.1 Introduction**

This field site investigation was initiated at the request of Parks Canada and the Acadia Centre for Estuarine Research to address a need for enhanced geotechnical and geological data in the vicinity of the southwest ravelin of Fort Anne. Objectives of the study are given above in section 3.0. This chapter constitutes AGC project report FA94077.

### **6.2 Methodology**

Field work was carried out on this phase of the project from 30 June to 2 July 1994.

To ensure that soil samples taken were of high quality, AGC provided all sampling and well-installation equipment. Soil sampling was conducted using a gravity percussion system, utilizing a 20 kg weight suspended on a cable run through a block at the top of a 10 m high tripod. The weight was raised and lowered by hand so that each drop travelled a distance of at least 1 m. The weight was dropped onto a bearing pad mounted on a conductor rod screwed into the top of a thin-walled aluminum sampling tube, 76 mm in diameter and 3 m in length. An internal piston assisted in sample recovery and was connected to the tripod on a cable of fixed length. At the desired location, the sample was driven into the ground until the point at which 20 blows failed to advance the tube more than 2 cm. After sampling, the tubes were pulled with a chain hoist mounted in the apex of the tripod. The tubes were then cut to size, capped, labelled and waxed and packed for shipment to AGC. Upon arrival at AGC, soil samples were placed into refrigerated storage for later analysis.

The open sample holes were then used as convenient holes for installation of groundwater wells. A 74 mm diameter clear PVC pipe was inserted into each hole, and backfilled with 20 cm of fine blasting sand to prevent water-borne entry of fines from the soil surrounding the borehole. Each standpipe was flushed with seawater to remove any cuttings, and labelled. The wells were then pumped dry and covered with vented caps.

### **6.3 Core Sampling**

Field work commenced on 30 June with mobilization of all equipment to the southwest ravelin, using the cart path on top of the embankment as an access route. The tripod was set up over the desired point on the slope. Sites were chosen to represent the entire slope, over a difference in elevation of approximately 12 m. The vegetative cover was removed by hand to expose the soil surface before sampling began. The following summary details work at each site.

1. SAMPLE 94BH1    30/06/94    Recovery 0 - 1.73 m (tube)

Location : 5.5 m horizontal distance from crest of slope, near wooden survey stake.

2. SAMPLE 94BH2    30/06/94    Recovery 0 - 1.21 m (tube)

Location : Taken at base of slope, within recently eroded slump scar (cf. Figures 2.1 and 2.2). The ground underfoot was partly remoulded slumped soil from higher on the slope (to a depth of 20 cm). It was at this elevation that soil liquefaction was observed during a previous visit to the site in March 1994. We encountered soft clay 1 m below the ground surface, which caused the sampler to plug with soil; the remainder of hole was drilled to 2.4 m, but the sample would not enter the tube. The problem of sample bypass is commonly encountered when attempting to sample profiles where clays become progressively softer with depth.

3. SAMPLE 94BH3    01/07/94    Recovery 0 - 1.39 m (tube)

Location : Taken beside 94BH2. We observed thin zones of squeezing clay closing the hole after removal of the sample tube, at a depth below ground surface of about 1 m. The bottom part of the open hole appeared to be unstable and prevented full penetration of the groundwater well pipe. We also observed that there existed a bench of very soft remoulded clay below the cribwork, in front of the slump scar, at the same elevation as the squeezing clay seams in this sample hole. These squeezing clay strata appear to be at roughly the same elevation at which human remains were recently found.

4. SAMPLE 94BH4    01/07/94    Recovery 0 - 0.25 m (bagged)

Location : Taken upslope of 94BH1, half way to uppermost survey stake. A short sample was taken which fell out of the tube and was bagged. The sampler plugged with organic debris and unfortunately we could not recover the sample from 0.25 to 3 m.

### 6.3.1 Drilling Notes

The most interesting finding arising from this field work was the detection of soft, squeezing clays within the soil profile, which appear to be natural intact strata and appear to outcrop within the slump scar at the elevation of the base of the cribbing. The actual subsurface conditions beneath the cribbing are presently unknown, as sampling was not conducted there owing to the probability of encountering wood at depth. The soft clay zone within the embankment represents a weak substrate which may have been recognised as such by the early engineers. It would be of considerable interest from a historical point of view to determine whether the cribbing was installed to provide a more stable base upon which soil earthworks could be raised.

### 6.4 Historical Information on Measures to Combat Slope Instability

From the rotated positions of the wooden cribbing, as indicated by the timbers projecting at right angles to the embankment, it is evident that slope instability has developed within the underlying deposit, after the embankment was re-engineered. The trigger for slope failure may therefore have been present beforehand, in the form of weak subsurface materials which had a predisposition to failure under load, which would likely have been initiated by local slope oversteepening, possibly brought about through past shoreline erosion. Dunn (1992) referred to historical records that describe the condition of this part of the Fort prior to any major intervention by man, as being basically the same as at present, with the sea washing the base of the slope. Apparently, no tidal marsh existed at that time.

Dunn (1992) also referred to continued complaints from French engineers about 'the disastrous [sic] effects resulting from a combination of spring neap tides and the Fort's subsoil'. This is very useful information, as it indicates that tidal drawdown was recognized as an important factor in inducing slope instability on these oversteep slopes. Tidally-induced residual porewater pressures have been found to constitute a controlling factor in the stability of many coastal soil deposits and indeed has led to some very large movements in Scandinavian clays (Bjerrum 1971, Terzaghi 1956).

Thus, the rise of the tide increases porewater pressure within the adjacent soil embankment. These pressures remain for a period of time after the tide falls, so that on the ebb tide the gravitational load of the embankment is increased by the amount of water held within the soil. Combined with the cutting action of the waves breaking upon the unprotected toe of the embankment at high water, the drawdown effect can lead to ongoing instability which can only be corrected by replacing eroded mass and by protecting the toe from wave action.

The evidence of the importance of upwelling groundwater was apparent in March 1994, when a site visit encountered fully liquefied clay soil at the base of the embankment, in the area where the later June observation noted outcropping of softened remoulded clay. As soil is eroded by sea action, the unavoidable consequence is an increase in hydraulic gradients and a localized reduction in effective stress -- and therefore in overall stability of the embankment.

Also noteworthy is the observed tendency for compacted clays found on the intertidal zone to lose their cohesion when newly exposed to seawater, after which they become unstable and are much more readily eroded. The same softening process may occur within the embankments of the Fort, under the influence of percolating groundwater.

Where slumping has exposed the soil profile on the embankment, the soil stratigraphy was observed to consist of a continuous sequence of thinly interbedded sands and silty clays, with beds being roughly horizontal. Thus, any water infiltrating during periods of heavy rain into the backslope would ultimately emerge on the exposed face of the embankment. If the embankment face were to become impervious, as it must do during the winter when it is frozen, porewater pressure is likely to rise, further reducing stability. The most critical time to monitor porewater pressure therefore is during periods of heavy rain, during a spring thaw.

## **6.5 Conclusions**

From an engineering point of view, the problem of localized slumping of the embankment may simply be a reactivation of an earlier movement. Evidently, rotational movement has occurred at some point in the past, as shown by the backward tilting of cribbing at right angles to the slope. This is in itself evidence of deep-seated instability. The instability may be due to several factors, including oversteepening of the embankment by construction of the Fort itself, or upward hydraulic gradients during heavy rains, which lead to a progressive softening and reduction in shearing resistance within the zone of overstress. Alternatively, the instability may have resulted from a reduction in resisting forces through loss of the mass of soil, rocks and cribbing work at the base of the slope. From a historical point of view, the early engineers may have considered the placement of rockfilled cribbing as the best means of providing a stable foundation from which they could steepen the Fort's embankments. It is apparent that the soft clays within the embankment are a natural feature and may have prompted them to take this approach in their design. According to

Dunn (1992) it seems that the sea action was attacking the base of the embankments as it does at present.

To correct these problems, the first and most obvious solution has already been implemented, namely replacing the eroded mass at the base of the slope. This will ensure a more stable slope, at least in the short term, and hold groundwater pressures in check. Provided that groundwater seepage pressures are not too high, long term stability may simply require occasional maintenance of the rockfill berm. The next obvious task was to carry out detailed slope stability analyses, drawing on the geometry of the failure as indicated, together with soil engineering parameters derived from laboratory testing. Results of these tests are outlined in Section 7.

In lieu of groundwater table elevation data from the site, some basic assumptions had to be made for the analysis of slope stability, which can be checked once empirical data are available. If instability proceeds unabated, then a more stringent engineering examination will be warranted to determine whether a reduction in the elevation of the groundwater table would have a sufficient beneficial effect to assist the stabilisation. Under those circumstances, remediation would require drainage (or other removal) of any surface water ponded in the moat or otherwise infiltrating the slope, and perhaps covering the seaward side of the embankment with an impermeable blanket.

## **7.0 SLOPE STABILITY OF THE SOUTHWEST RAVELIN**

H.A. Christian  
Atlantic Geoscience Centre  
Geological Survey of Canada

### **7.1 Introduction**

The accurate analysis of the stability of a natural or manmade soil embankment depends to a large degree on a detailed knowledge of site conditions, including the variation in soil type with depth, the material behaviour under both rapid (undrained) and long-term (drained) loading conditions, the location of the groundwater table within the slope and its variability over time. The existence of weak layers or previously-sheared layers is of considerable importance, as existing landslides are reactivated at lower stress levels than initially, especially if the soils involved have a predisposition to strain-soften, or suffer significant strength loss during initial failure.

### **7.2 Geotechnical Site Investigations - 1993-94**

Two site investigation programs were directed at providing data on specific questions given above. A 1993 investigation sampled eroding strata over the intertidal zone, directly in front of the southwest ravelin. These samples were removed to the Atlantic Geoscience Centre and were tested in a geotechnical laboratory as part of this component of the study (Jacques, Whitford & Associates Ltd. 1994), to provide soil strength parameters for a static stability analysis of the embankment itself. Also, shallow cone penetration tests were carried out in the red clays exposed across the intertidal zone, to establish the *in situ* shear strength profile (Daborn *et al.* 1993). The samples were also tested for engineering index properties, including plasticity and grain size distribution.

A 1994 investigation program was aimed at characterizing the actual soil profile at the location of the receding embankment, at the end of the wooden cribworks. There was ample evidence of active instability, ranging from revegetated depression areas on the slope indicating previous slippage and subsidence, as well as fresh toe failures, developed by wave undercutting. Upwelling groundwater was observed at the base of the slope in late March, revealing that the recent loss of toe material had resulted in an aggravation of the problem, as seepage pressures were no longer in balance with overburden pressures. Groundwater exit points on the slope were found to be fully liquefied and seepage was noted from horizontal sand seams exposed in the back of the undercut slope, to a height of several metres above high tide level. This excessive groundwater flow was not evident later in 1994, at the time soil borings were conducted, presumably due to drier conditions.

The wooden timbers forming part of the cribbing were observed to be undergoing some continued motion, as indicated by Figure 7.1. Note that two timbers were undergoing upward rotation, whereas others were subsiding from their present position of between 20 and 35° with respect to the horizontal. Subsidence is taken to be indicative of undermining through soil erosion by wave action, whereas upward rotation is believed to indicate rotational slippage of the seaward side of the embankment. This allowed a rough estimation of the position of the point of rotation and the depth of movement was established.



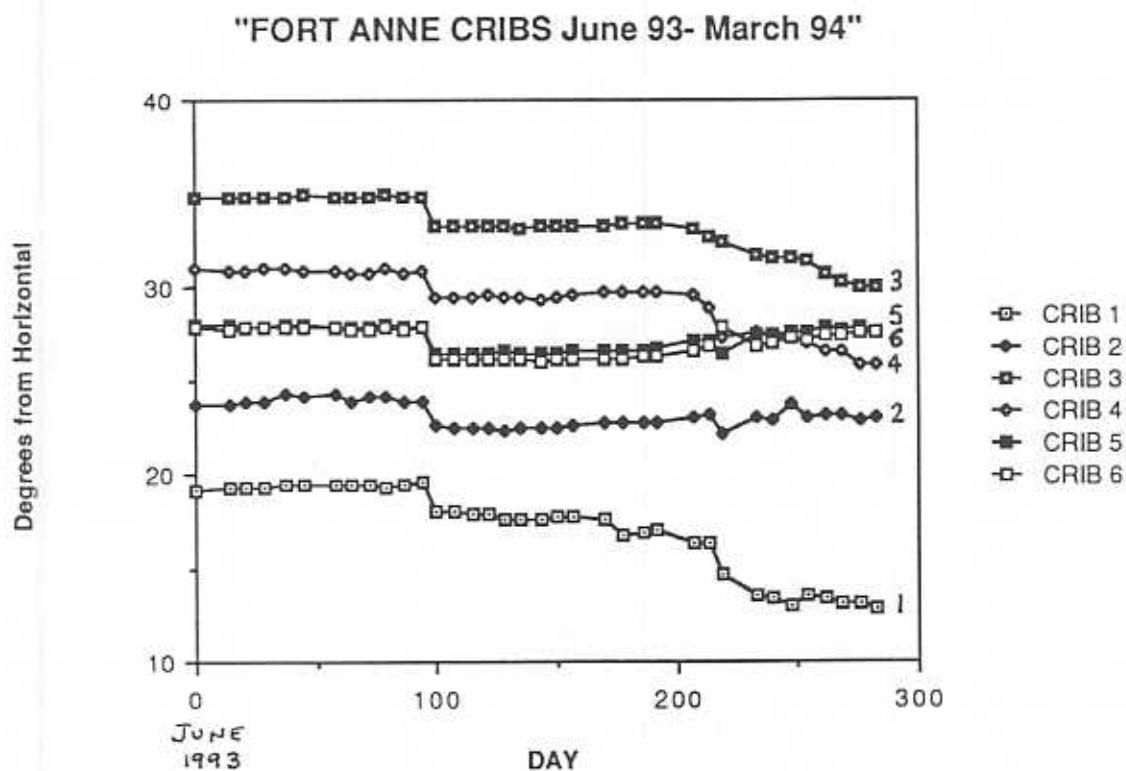


Figure 7.1 Tilt angle data recorded by Parks Canada, from aluminum plates installed on rotated timbers projecting from the base of the embankment referred to as the southwest ravelin. Plates numbered 5 and 6 appeared to continue their rotation, perhaps along with No. 2, whereas others were now settling, due to undermining by sea action. A major erosion event appears to have occurred about 100 days after the commencement of record-keeping, in June 1993.

Soil investigations in 1994 established that the soil profile was layered, consisting of a thin cover of topsoil or fill at the crest of the slope, underlain by a thick sequence of horizontally stratified sand and silt. This in turn was underlain by stiff red clay, which appeared to contain thin soft clay layers, at an elevation equivalent to the bottom layer of exposed wood timbers. Human remains were found immediately below this level (Wallace 1994, Cybulski 1994). Soil borings terminated in this unit and did not reach the elevation of the intertidal mudflat, due to unstable borehole conditions. The appearance and consistency of this red clay appeared identical to soil samples obtained in 1993 over the mudflat (Appendix A). Consequently, it was concluded that the red clay did indeed extend beneath the Fort and was part of a regional deposit.

A geotechnical foundation investigation was carried out in an area about 40 m north on the Queens Wharf. In their report, Golder Associates (1982) reported encountering a similar stratum of stiff reddish clayey silt, overlying till. Another geotechnical investigation, at the location of the northern bridge abutment on Allain Creek was carried out and described in Jacques, Whitford & Associates Ltd. (1985). Therein, a deep soil unit was encountered underlying a grey marine silt and was referred to as a "reddish brown silty clay". It was tested to define its creep behaviour, as there was a concern regarding the stability of the bridge abutment. Soil borings encountered glacial till at a depth of 32 m below ground surface, which would suggest that the overlying soil deposits are post-glacial and probably were laid down as shallow-water deposits reworked from glacial outwash sediments, roughly 2000 years ago.

### 7.3 Inferred Regional Topographic Changes Since Deposition

The stiff consistency of the red clay noted over the intertidal area (Daborn *et al.* 1993) provided an opportunity to determine that the present topography is quite modified from the post-depositional condition, with there being as much as 25 m eroded locally from the Fort Anne mudflat. As the Fort itself was constructed on a natural topographic high (Dunn 1992), there are strong indications that the surficial red clays and layered sands were deposited over a short period of time, but were thereafter extensively excised and eroded by stronger fluvial activity than presently exists, as the ice sheet ablated. R. Stea (personal communication, 1993) commented that this fine-grained, reddish silty clay unit could be seen as far up the Annapolis River as Middleton.

### 7.4 Laboratory Shear Strength Testing

Jacques, Whitford & Associates Ltd. (1994) reported on the results of triaxial and direct shear testing program performed on red clay samples provided by the Atlantic Geoscience Centre, which were taken from the intertidal mudflat in front of the southwest ravelin in 1993.

Undisturbed soil specimens were first removed from the sample tubes and were tested under consolidated undrained triaxial compressional shear conditions. The effective stress shear strength parameters thus obtained were as follows:

$\Phi'_r$	Angle of internal friction	24°
$c'$	effective cohesion intercept	0

Soil specimens were also prepared and tested in direct shear, to determine the remoulded shear strength parameters, which were as follows:



$\Phi_f$	Angle of internal friction	12°
$c'$	effective cohesion intercept	0

The liquid limit averaged 55 percent and the plastic limit was found to be 26 percent. The plasticity index was therefore 29 percent. Natural moisture contents averaged 31 to 32 percent by weight, slightly above the plastic limit, indicating that the soil deposit had undergone a significant amount of consolidation since deposition, under higher overburden stress than presently exists. High undrained shear strengths inferred from *in situ* cone penetration tests confirmed that the red clay deposit over the intertidal zone was lightly overconsolidated, which Daborn *et al.* (1993) attributed to erosion of overburden. The soils tested were found to contain 56 percent silt and 44 percent clay by weight and were classified as a high plasticity clayey silt. Figure 7.2 illustrates the plasticity data in graphical form, after Jacques, Whitford & Associates Ltd. (1985). The soil encountered on the intertidal mudflat plots as a material that is intermediate between the surficial silt and reddish clay soils, encountered at the Allain Creek bridge abutment.

### 7.5 Slope Geometry from Geographic Surveys

The Nova Scotia College of Geographic Sciences provided survey data, collected on three separate occasions over a two-year period, on three slope-normal profiles on the seaward side of Fort Anne. The section denoted as IB 900 to 913 corresponded to the southern end of remaining (intact) wooden cribbing, on the seaward face of the southwest ravelin. This geometry was taken as being typical of the adjacent portion of the slope, before major loss of rock fill and wave undercutting had occurred (Figure 7.3). The depth of rock fill was assumed to be as indicated in Figure 7.3, based on soundings made with a steel rod between wood timbers.

The various soil strata are indicated therein, based on the 1994 soil borings. The position of the groundwater table is also indicated. During heavy rains, groundwater was observed to be exiting the slope immediately above the rock berm. There is little doubt that the cribbing in the vicinity of the southwest ravelin was by then generally in a poor condition, having rotated along a wide front by as much as 35° from its original horizontal position, over an unknown period of time, possibly due to wave undermining and slope destabilization.

### 7.6 Analysis of Slope Stability

The calculation of slope stability was performed to arrive at a measure of the factor of safety against static failure, which can be defined as the ratio of driving to resisting forces. By definition, a factor of safety equal to unity exists along an active failure surface within a soil mass. Temporal changes in pore water pressure may act along this surface, as a result of movements of the groundwater table. Seasonal fluctuations in the position of the groundwater table or phreatic surface can alter the effective stress regime within the soil mass and may lead to the onset of failure through a reduction in the shear strength. Likewise, a removal of soil material from the toe of the slope can cause instability to develop, through a reduction in the resisting forces. Removal of toe protection has two, very negative consequences:

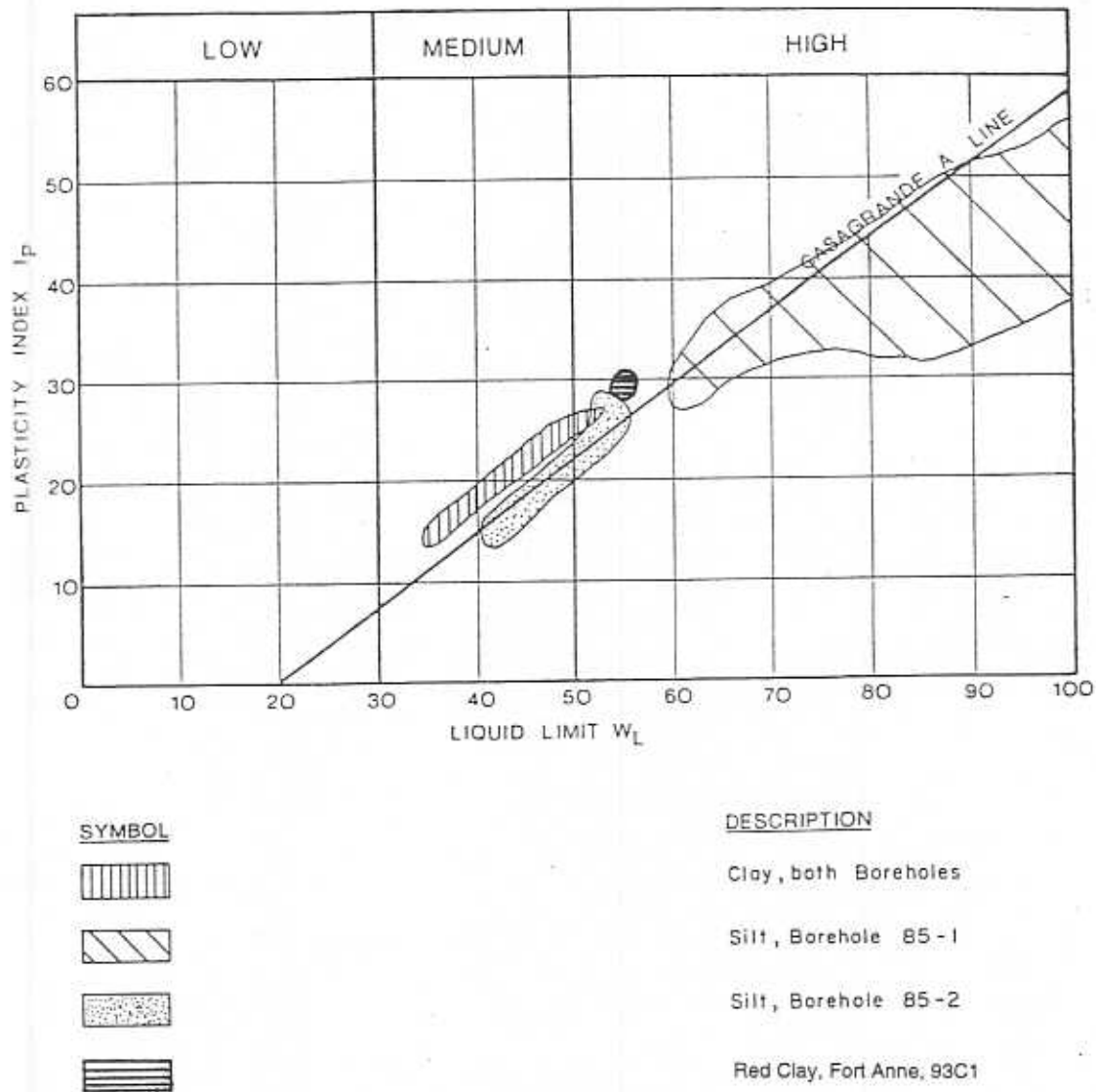


Figure 7.2 Plasticity chart modified from Jacques, Whitford & Associates Ltd. (1985), combining index property data from Allain Creek area with that of the intertidal red clay exposed seaward of the southwest ravelin. Note that the mudflat clay plots as an intermediate material. It was tested and was found to be 56% silt and 44% clay. Its position above the A-line indicates that it is of glacial origin.

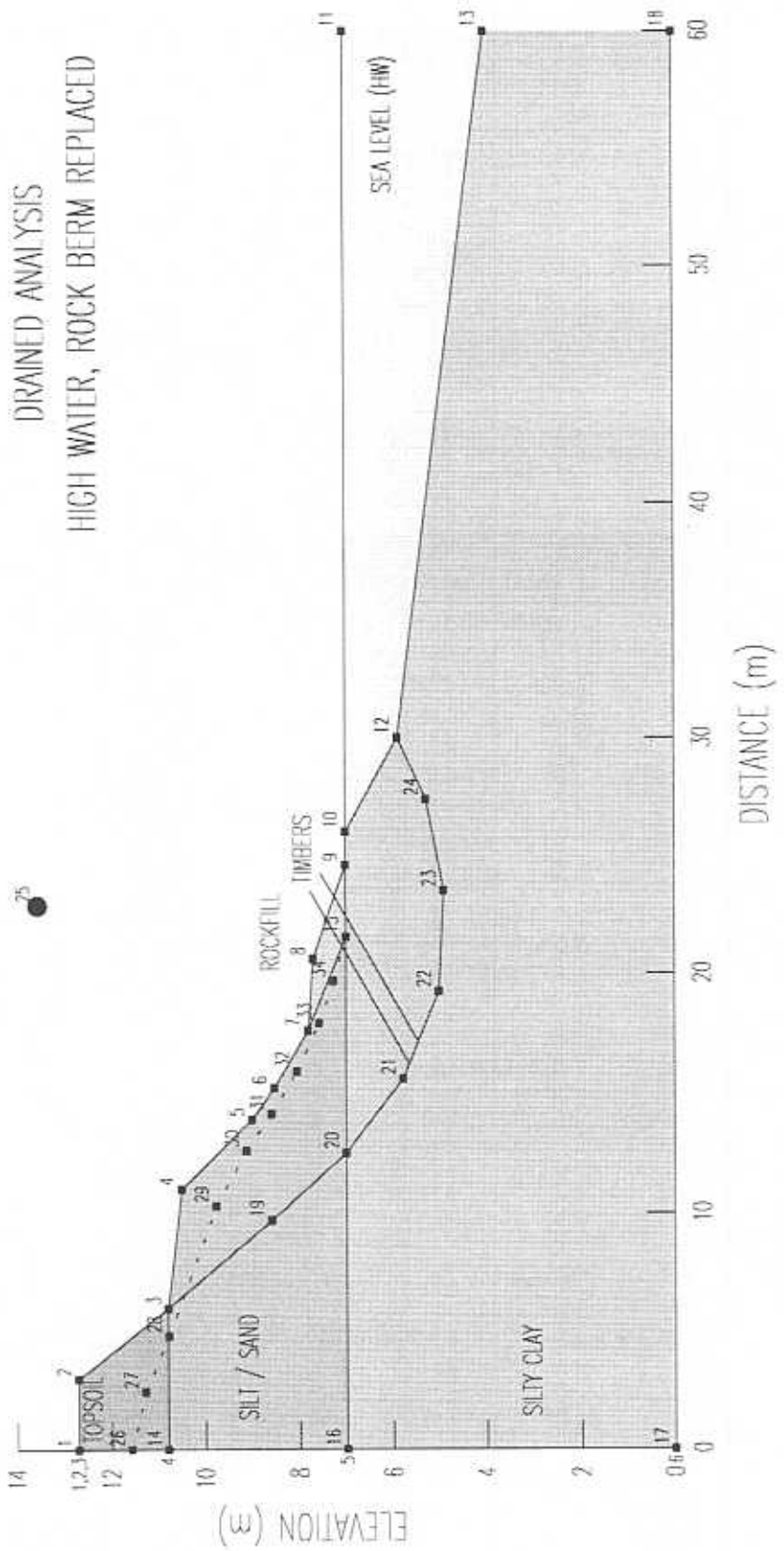


Figure 7.3 Profile IB 900 to 913, from the crest of the southwest ravelin to the intertidal zone. Position of the groundwater table is inferred from direct observation and standpipe testing. The approximate depth of rock fill is indicated, along with the most likely position of the slip surface within the slope. This profile shows the slope before major erosion. Note the stepped backscarp and rotated timbers, indicating that slippage had previously occurred.

1. The counterbalancing forces holding groundwater pressures and downslope translation in check are removed, causing local heave or seepage liquefaction failure at the most critical point, where resisting forces are mobilized during shear. Upwelling seepage, over a period of time, can erode finer-grained particles from the soil matrix (piping), resulting in an increase in soil permeability, a loss of shear strength and in future, excessive flows of groundwater from the slope. (Rock fill was possibly recognized by the early engineers at the Fort as a beneficial means of surcharging the weak slope, improving static stability).
2. Where parent soils provide a means of developing a natural shoreline-armouring deposit which resists wave action, the protection of the weaker parent material within the slope is more assured. Disintegration and loss of the cribworked rock berm after depletion of the salt marsh probably led to the local incursion of the sea into the southwest ravelin, through wave erosion during extreme high tides. 1994 was reportedly a year of some of the highest tides in the last decade (G.R. Daborn, personal communication, 1993).

The methods of analysis adopted covered the range of expected loading conditions, with the two principal conditions being short-term (undrained) loading, at times wherein erosion of toe material proceeded at a rapid rate; versus long-term loading, wherein drained shear strength behaviour governed stability. These established procedures are described in detail by Morgenstern and Sangrey (1978) and are beyond the scope of this report. The three analytical methods employed were:

1. Bishop Simplified Method
2. Janbu Method
3. Morgenstern-Price Method

Of these methods, the Morgenstern-Price formulation is the only approach that satisfies both moment and force equilibrium and is therefore rigorous in the satisfaction of interslice forces. Slope stability software SLOPE/W was used in the analysis of the factor of safety. Input conditions and soil parameters are given in Table 7.1, wherein strength parameters were obtained from the triaxial testing carried out on the red clay samples tested and reported in Jacques, Whitford & Associates Ltd. (1994). Detailed sections and loading conditions are given in Appendix B (Section 13).

### **7.7 Discussion of Results**

Of particular importance was the observation that there existed a number of shallow soft layers of red clay beneath the Fort in the vicinity of the southwest ravelin. From a sensitivity analysis, it was found that reducing the soil shear strength to the fully remoulded condition along a failure plane within the red clay resulted in factors of safety that fell below unity. Therefore, this assumption was deemed to be acceptable, both from the observational and analytical points of view, as this was evidently a pre-existing landslide that had been recently remobilized. Direct shear testing, in accompaniment with triaxial testing, established that the remoulded strength was half the peak (intact) shear strength.

Soil Type	$\gamma_s$ (kN/m <sup>3</sup> )	$c'$ (kPa)	$\phi'$ (°)	$C_u$ (kPa)	$S_t$
Rockfill (Basalt)	27	0	-	-	-
Topsoil (Sandy loam)	17	0	35	10	-
Stratified Soil (Sand & Silt)	18	0	35	15	-
Red Clay (Remoulded)	19	0	12	10	1
Red Clay (Intact, lightly overconsolidated.)	19	0	24	60 if $Z < 22\text{m}$ 0.3 $P_o'$ if $Z > 22\text{m}$	5

**Table 7.1. Summary of engineering properties for soils encountered. The saturated unit weight ( $\gamma_s$ ), effective cohesion intercept ( $c'$ ), effective angle of internal friction ( $\phi'$ ), undrained shear strength ( $C_u$ ), and the ratio of peak to remoulded undrained shear strength, or sensitivity ( $S_t$ ), are listed for each soil shown in the section diagrams.**

The results of the slope stability computations are detailed in Table 7.2. Note that the presence of the rockfill berm at the toe of the slope profoundly influences stability; thus a loss of this important resisting mass was a major factor in reactivating the failure. Also, note that the lowest factors of safety exist at low tide, wherein groundwater held within the slope has a larger destabilizing effect. Short-term stability through undrained loading was not found to be a concern, as factors of safety ranged from 1.68 to 1.71, depending to a small degree on the presence of the rock berm.

### **7.8 Recommendations for Further Remediation**

It was evident that replacement of the rock berm, to at least the elevation indicated in the levelling surveys conducted by the Nova Scotia College of Geographic Sciences, would increase the factor of safety to just above 1.0, which is barely sufficient to prevent further movement. It should be borne in mind that this finding is based on a number of assumptions regarding the soil variability at the site and is founded on only a rudimentary knowledge of the soil shear strength behaviour, arrived at through a minimum of laboratory testing.

In view of the beneficial but marginal improvement stability gained by replacement of the rock berm, further remedial measures may be required to ensure continued stability. These might involve increasing the amount of rock fill, or lowering the groundwater table within the slope by installing drains. It is essential to ensure that the toe area is not further undermined by wave action.

It is recommended that groundwater table levels be monitored in the standpipes established in 1994, during the March to May period and reported to the Atlantic Geoscience Centre, to check that the assumption made in the analysis was valid. A lower groundwater table position within the slope would significantly improve the overall static stability of the site.

Run No.	Loading Condition	Tidal Condition	Rock Berm in Place	Bishop Simplified	Janbu	Morgenstern Price
1	Undrained	Low Water	No	1.82	1.66	1.71
2	Drained	High Water	No	0.94	0.86	0.89
3	Drained	Low Water	No	0.86	0.80	0.81
4	Undrained	Low Water	Yes	1.79	1.64	1.68
5	Drained	High Water	Yes	1.22	1.07	1.10
6	Drained	Low Water	Yes	1.12	1.00	1.02

**Table 7.2 Summary of slope stability calculations, including loading conditions (drained versus undrained), state of tide, existence of rockfill at toe of embankment and resultant factor of safety derived from the Bishop-Simplified, Janbu and Morgenstern-Price methods. Factor of safety is defined as the ratio of the sum of the resisting forces (soil shearing resistance) to the driving forces (gravitational loads). A factor of safety less than 1 indicates that an unstable condition exists.**



## 8.0 SEDIMENTOLOGICAL STUDIES OF THE ANNAPOLIS ESTUARY

Carl L. Amos  
Atlantic Geoscience Centre  
Bedford Institute of Oceanography

### 8.1 Introduction

Development of a comprehensive hydrodynamic and sedimentological model suitable for assessment of possible engineering solutions to the problem of shoreline erosion at Fort Anne requires detailed information on the behaviour of deposited sediments. Traditionally, such information has been derived from analyses of sediments removed from the field to a laboratory. These procedures are of limited value because of changes in behaviour of the sediment associated with its removal, transportation and remoulding (Amos and Mosher 1985). The extent of these changes is generally unknown. In addition, it has become apparent that biological processes associated with the disturbing effects of burrowing organisms (bioturbation) and the stabilizing effects of burrow construction or plant exudates (biostabilization), may be of great significance in determining sediment behaviour (Nowell *et al.* 1981, Meadows and Tufail 1986, Paterson and Daborn 1991, Daborn *et al.* 1993).

For these reasons it was considered desirable to obtain as much information as possible about sediment properties *in situ*. This portion of the study constituted a cooperative project between the Atlantic Geoscience Centre, the Institute for Marine Dynamics (N.R.C.) and the Acadia Centre for Estuarine Research. It was based upon direct, *in situ*, measurements of sediment erodibility using a remotely-deployable flume, together with sampling and subsequent laboratory analyses of sediments. Results of the N.R.C. flume studies have been reported in Sigouin and MacDonald (1994).

### 8.2 Field Survey

#### 8.2.1 Equipment and Methods

##### a) Sea Carousel

Sea Carousel is a benthic annular flume capable of submarine measurement of seabed erodibility (Amos *et al.* 1992). The annulus is 2 m in diameter, 0.3 m high and 0.15 m wide. It is equipped with three optical backscatter sensors to monitor water turbidity, a Marsh-McBirney® current meter to monitor azimuthal and vertical flow, a lid rotation sensor and an underwater camera that views the eroding bed through a window in the side of the annulus. The system is operated from the surface through an RS-232 communication link to a submerged data logger/controller. The digital driver motor is controlled by a similar link to a second computer. Real time video is monitored on a video display and logged on VHS tape.

Flow is induced by rotation of the lid to which are attached eight paddles. Azimuthal flow is transformed to bed stress based on velocity gradients derived in a series of laboratory tests. Bed stress is increased in the flume in a series of steps. Erosion rate is defined as the increase in suspended mass through time. Eroded depth is derived assuming spatially-constant erosion under the flume, and by measures of bulk density made at the site (*circa* 1400 kg/m<sup>3</sup>). The profile of shear strength with depth is derived by assuming that the applied fluid shear stress ( $\tau$ ) is equivalent



to the shear strength ( $\tau_b$ ) of the sediment when erosion ceases, and that this strength is the critical value ( $\tau_c$ ) at which sediment at that depth will begin to be eroded  $\tau = \tau_b = \tau_c$ . The critical shear stress for incipient erosion of the sediment surface (the erosion threshold) is evaluated as the surface ( $z = 0$ ) intercept of the best-fit line of shear strength versus depth. See Amos *et al.* (1992) for a detailed description of the methods and results.

#### b) Seabed Sampling

A medium Van Veen grab was used to collect bulk samples of the seabed at each station. Two small syringe cores were collected from the surface of each grab for purposes of examining microfabric and macrostructure. The syringe cores were held vertically to prevent disturbance, and frozen onboard using dry ice. Small unit volumes of sediment were also collected from the sediment surface for CHN ratios, polysaccharides, and chlorophyll *a* content. These were collected from three depths in each grab sample: 1, 8 and 15 cm. Thereafter, the bulk sample was retained for future analysis of benthic fauna. Grab samples from stations FA2<sup>1</sup> and three were also used for studies of resuspension, settling, and biostabilization within the Laboratory Carousel at Acadia University.

A wide-barrel AGC gravity corer was deployed at each site. The corer was equipped with 50 lb of lead and a 1 m long barrel. The barrel was equipped with a one-way valve at the top (to prevent draw-out on removal of the corer from the seabed) and a leaf core catcher at the base. The corer was allowed to free fall from 1 to 2 m above the seabed. The purpose was to obtain undisturbed samples of the sediment surface and about 0.6 to 0.8 m of the underlying material. Cores were stored vertically, packed to prevent motion, and sealed with wax to prevent loss of moisture. The cores were collected for analysis of the major physical properties. These properties are: water content; grain size; bulk density; acoustic velocity; vane shear strength; and sediment texture, lithology, and structure.

### 8.3 Results

#### 8.3.1 Summary

Eight sites, FA1 to FA8 (= S1-8 in Figure 4.1), were chosen for Sea Carousel deployments. These sites extend from the vicinity of the tidal power plant to the outer region of Annapolis Basin along a transect that followed the main tidal channel (Figure 4.1). Site FA1 (the innermost) was abandoned as the seabed was composed of gravel and cobbles. Other sites yielded good data, although the outer two stations were aborted early because of ship drift. Station FA2 (S2) was located immediately off Fort Anne and had a surface very similar to the red clay found cropping out on the tidal flats. Stations FA3, FA4, and FA5 (= S3-5) were located landward of Goat Island and were situated on what appeared to be marine grey clay. Stations FA6, FA7, and FA8 were situated on non-cohesive silt and sand. A summary of the Sea Carousel deployments is given in Table 8.1.

---

<sup>1</sup> In this section, anchor stations are referred to by labels commencing with "FA"; these correspond to the anchor stations referred to elsewhere and labelled S1-8 in Figure 4.1. (i.e., FA5 here = S5 elsewhere).

STATION	LAT	LONG	DEPTH (m)	TEMP (C)	SALINITY (ppt)
FA2	44 44.549	65 31.348	9.2	12.5	29.9
FA3	44 43.966	65 32.125	8.4	12.5	29.6
FA4	44 43.654	65 32.994	7.5	12.7	29.3
FA5	44 42.461	65 35.513	6.4	12.5	30.0
FA6	44 41.070	65 38.784	8.6	10.6	31.3
FA7	44 39.616	65 40.418	8.5	9.8	31.8
FA8	44 38.245	65 43.703	8.2	9.2	32.0

Table 8.1. A summary of station locations of the Sea Carousel and general conditions.

The time-series of the *in situ* erosion tests undertaken at stations FA2 to FA8 are presented in Figures 8.2 to 8.8, respectively. The figures show that full deployments were obtained at stations FA2, FA3, FA4, and FA6. The remaining stations were disrupted because of ship drift during deployments. The quality of data is thus better at the inner stations than at the outer ones. Nevertheless, it was possible to detect bed erosion rates, erosion types, friction angles and mass settling rates in almost all cases. These results are summarised in Table 8.2.

STATION	EROSION THRESHOLD ( $\tau_c$ ; Pa)	FRICTION ANGLE ( $\Phi$ )	EROSION TYPE	BED STATE
FA2	0.3	0	I	NEUTRAL
FA3	0.6	19	I/II	STABLE
FA4	0.2	17	I	STABLE
FA5	0.2	8	I	NEUTRAL
FA6	0.5	0	--	NEUTRAL
FA7	0.9	--	I	--
FA8	0.5	6	I	NEUTRAL

Table 8.2. A summary of the erosion characteristics of the Sea Carousel stations occupied in Annapolis Basin. (Bed state is herein subdivided into five major groups on the basis of erosion threshold and friction angle ( $\Phi$ ). These are (1) stable beds where  $\Phi > 10^\circ$ ; (2) unstable beds where  $\Phi < -10^\circ$ ; (3) neutral beds where  $-10^\circ > \Phi > 10^\circ$ ; (4) fluidized beds where  $-10^\circ > \Phi > 10^\circ$  and where  $\tau_c \Rightarrow 0$ ; and (5) surface bed strengthening attributed to biostabilization.)

The inner stations were of very low erosion resistance and high erosion rates by comparison to similar studies in the Bay of Fundy (Amos *et al.* 1994). Erosion was largely Type I (benign) which means that a limited amount of material would be removed by each erosion event. However, it would appear that each tidal inundation induces erosion thereby promoting net scour. Station FA2 showed anomalously high erosion rates even within Annapolis Estuary itself. The overall bed state was one of low consolidation (neutral), and therefore exhibited a high susceptibility to erosion.

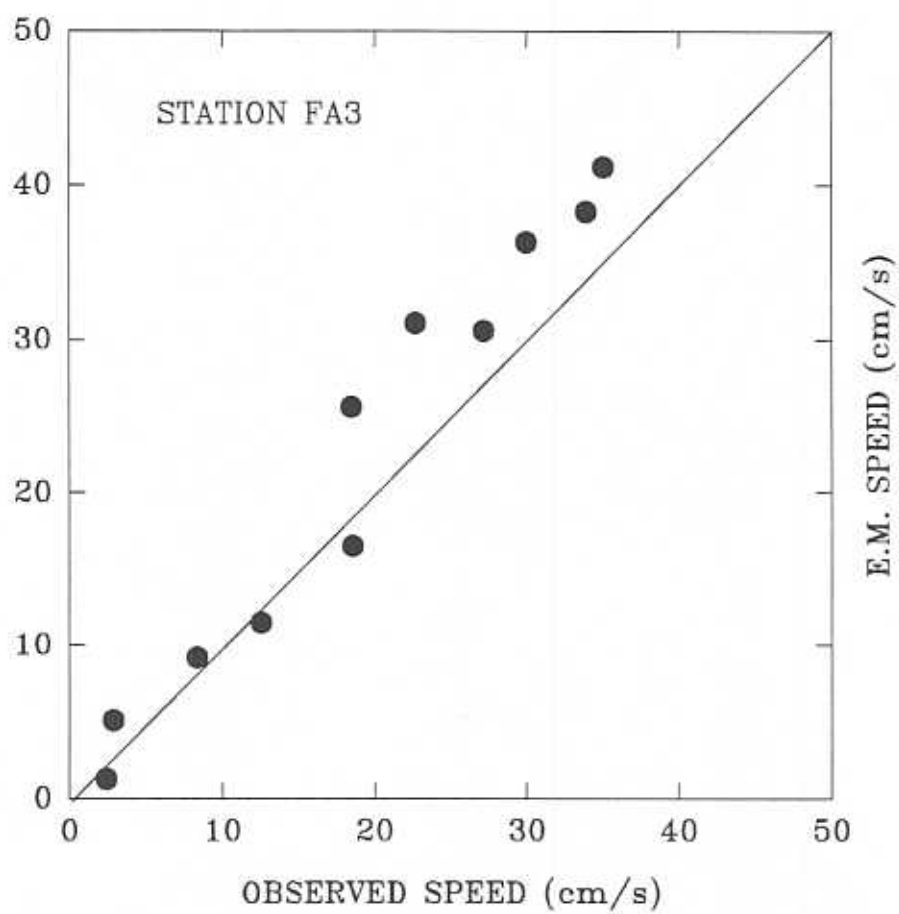


Figure 8.1 Correlation between 'Sea Carousel' current velocity measurements measured by electromagnetic current meter and estimated by analysis of videotape imagery.

## SEA CAROUSEL - ANNAPOLIS BASIN

STATION FA2 - 15 JUNE, 1994

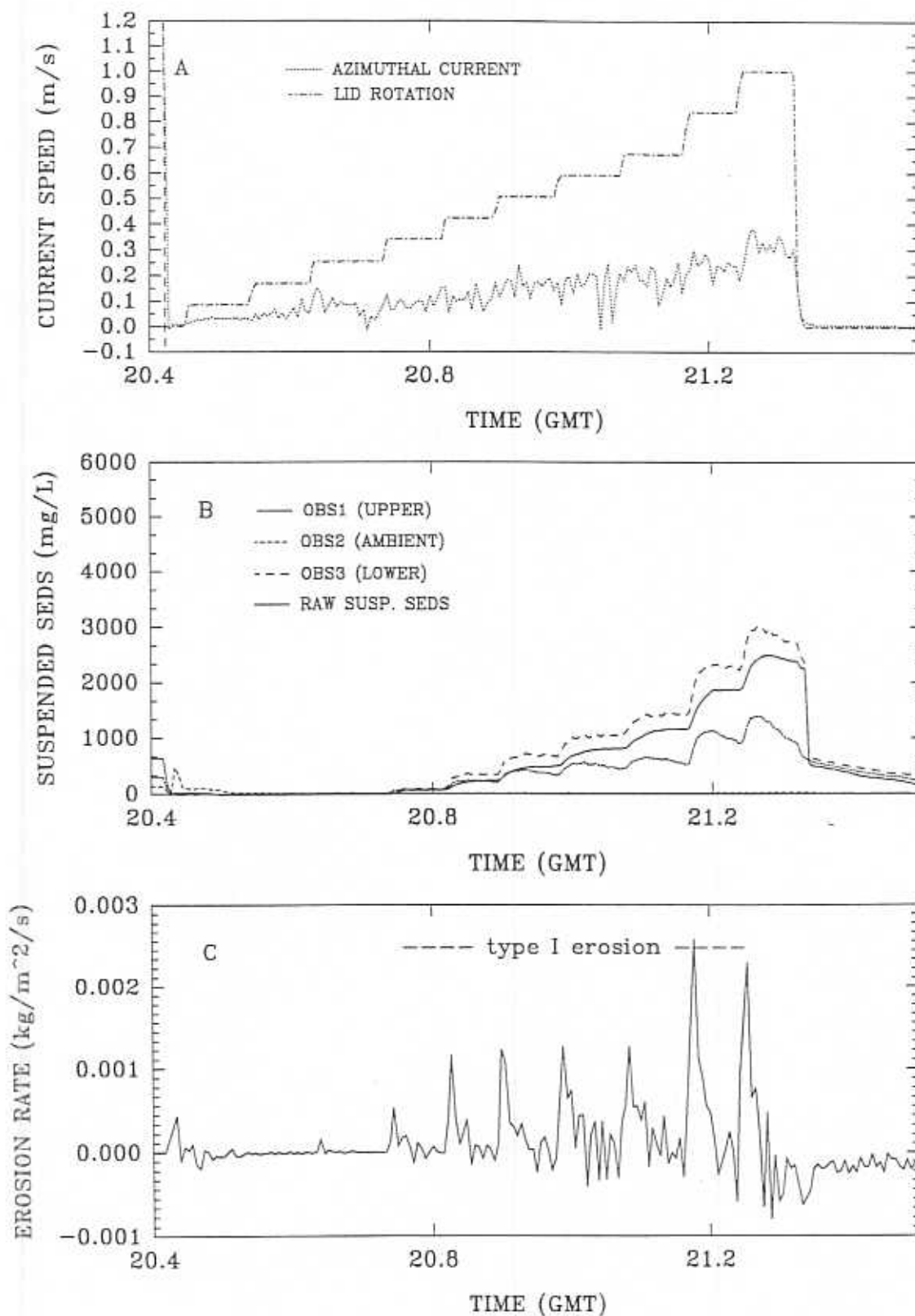


Figure 8.2 Time series of 'Sea Carousel' deployment at anchor station S2.

## SEA CAROUSEL - ANNAPOLIS BASIN

STATION FA3 - 16 JUNE, 1994

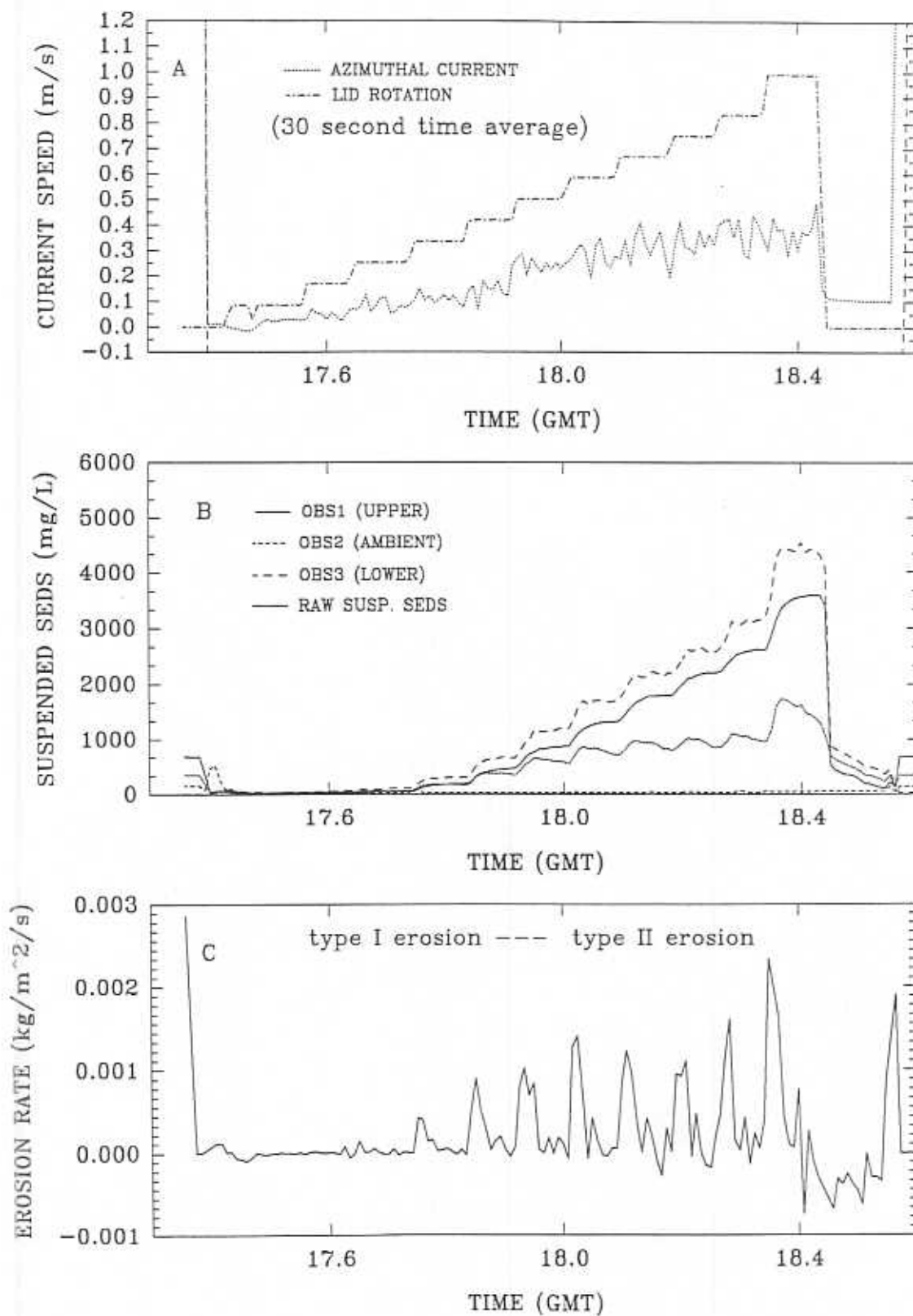


Figure 8.3 Time series of 'Sea Carousel' deployment at anchor station S3.

## SEA CAROUSEL — ANNAPOLIS BASIN

STATION FA4 — 16 JUNE, 1994

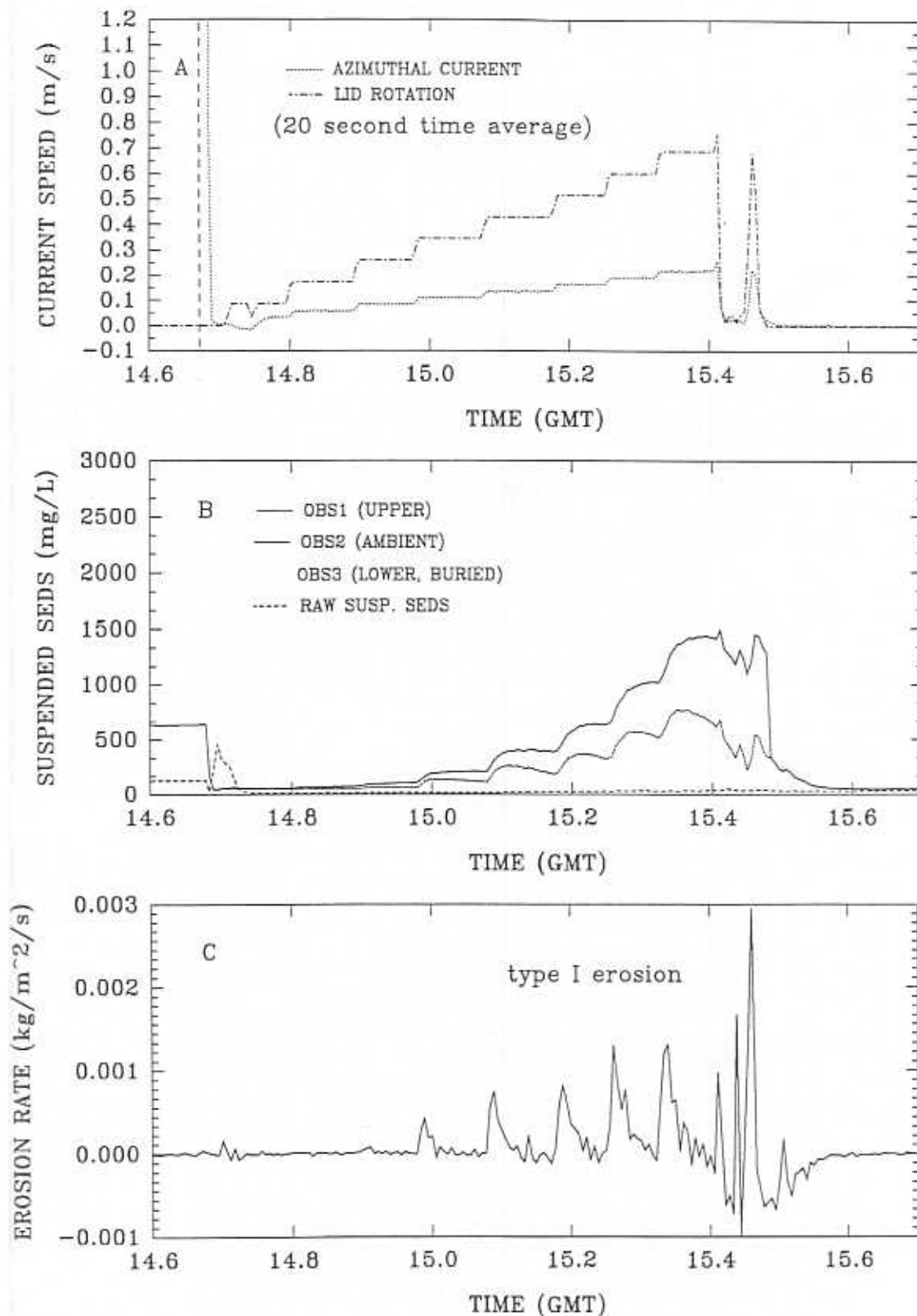


Figure 8.4 Time series of 'Sea Carousel' deployment at anchor station S4.

## SEA CAROUSEL - ANNAPOLIS BASIN

STATION FA5 - 15 JUNE, 1994

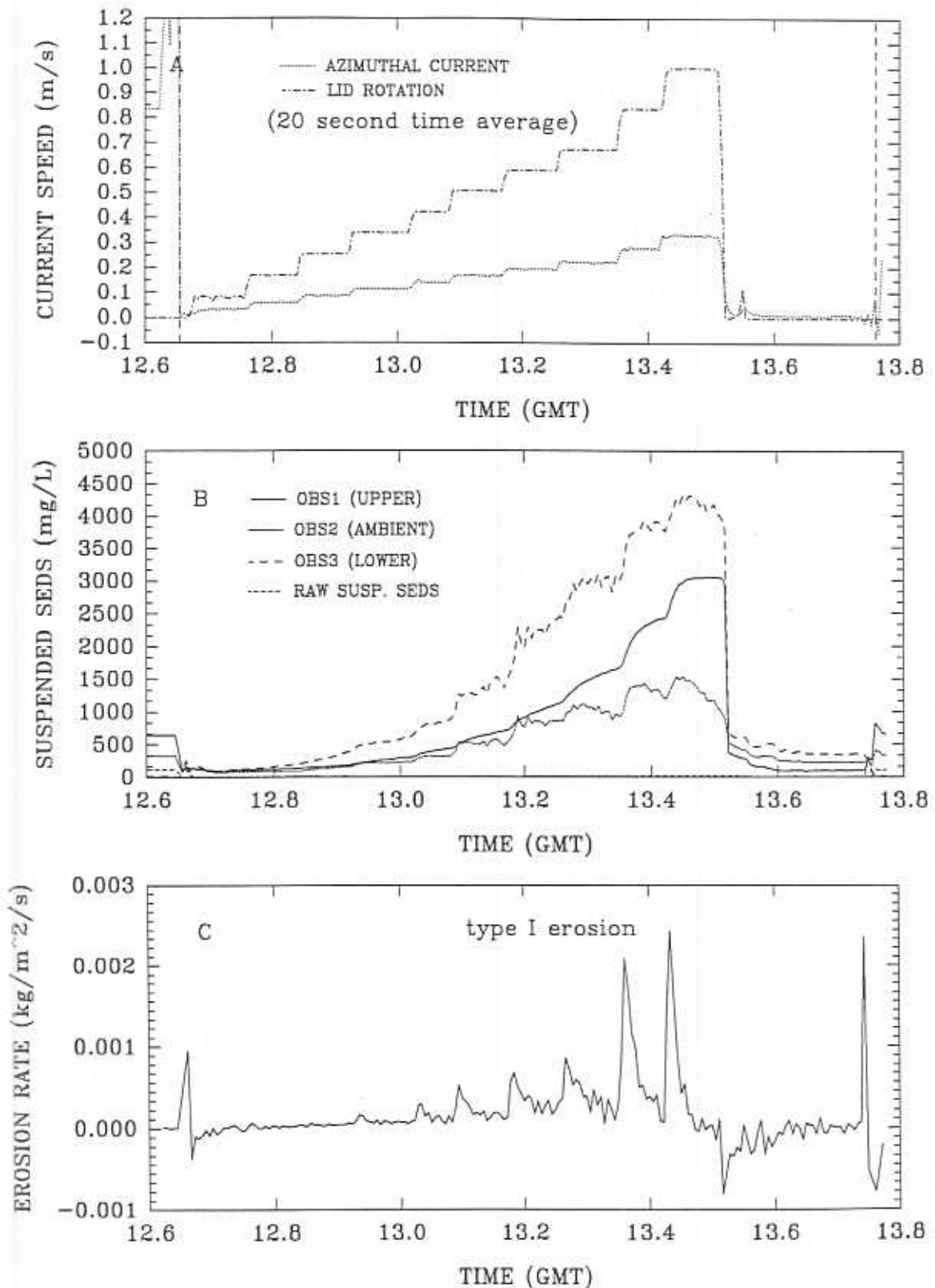


Figure 8.5 Time series of 'Sea Carousel' deployment at anchor station S5.



## SEA CAROUSEL - ANNAPOLIS BASIN

STATION FA6 - 16 JUNE, 1994

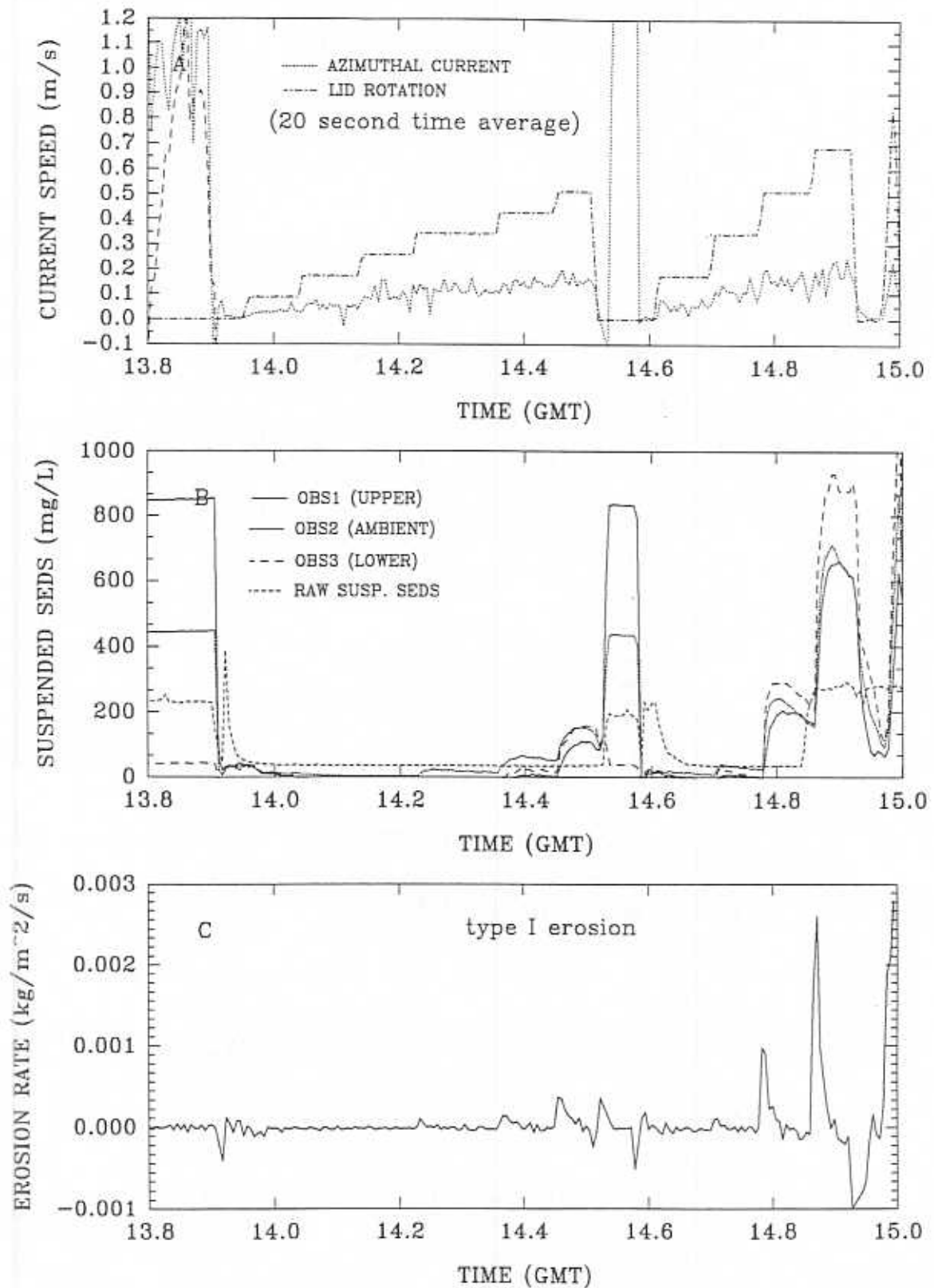


Figure 8.6 Time series of 'Sea Carousel' deployment at anchor station S6.

## SEA CAROUSEL - ANNAPOLIS BASIN

STATION FA7 - 16 JUNE, 1994

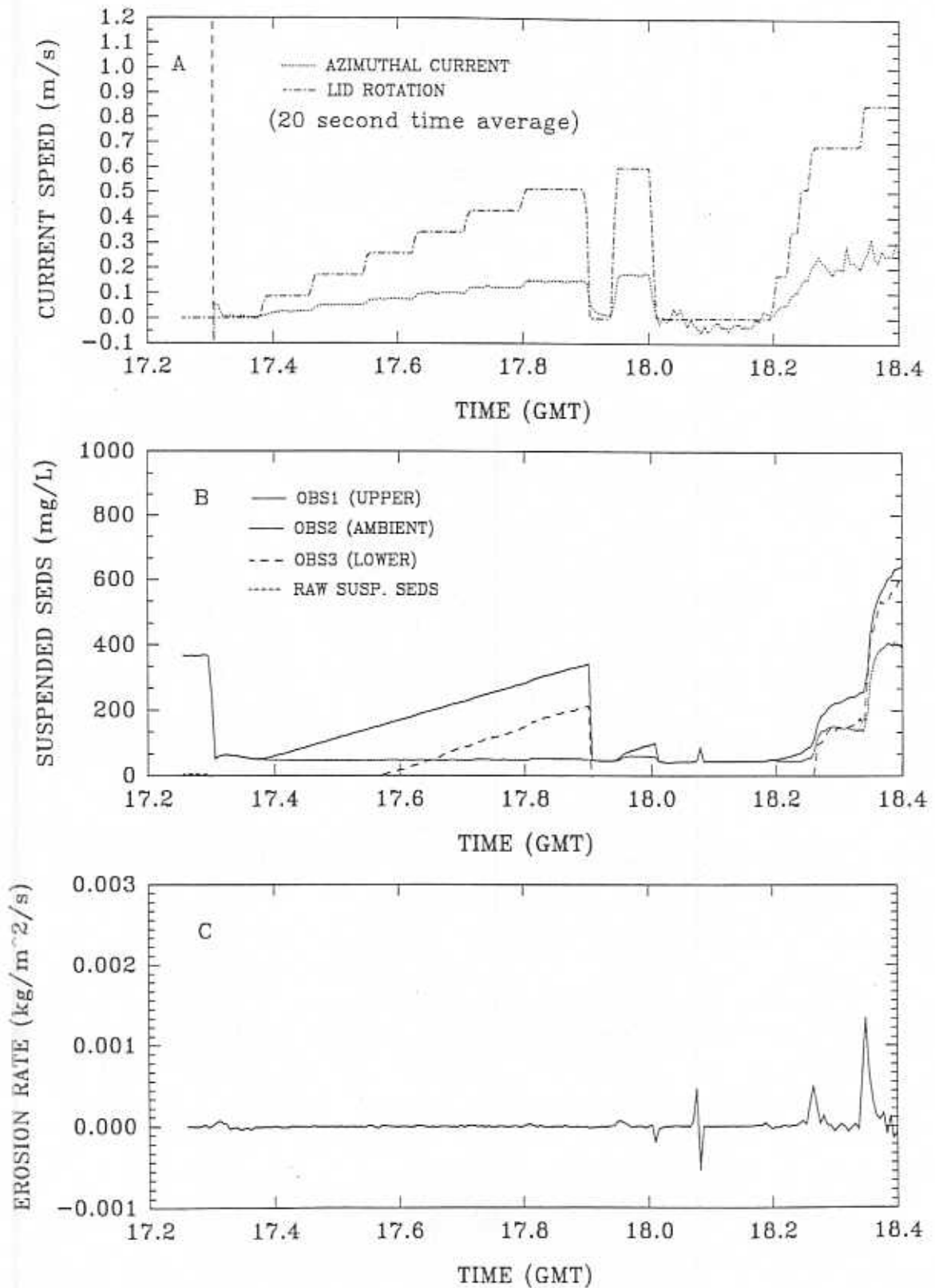


Figure 8.7 Time series of 'Sea Carousel' deployment at anchor station S7.

## SEA CAROUSEL - ANNAPOLIS BASIN

STATION FA8 - 16 JUNE, 1994

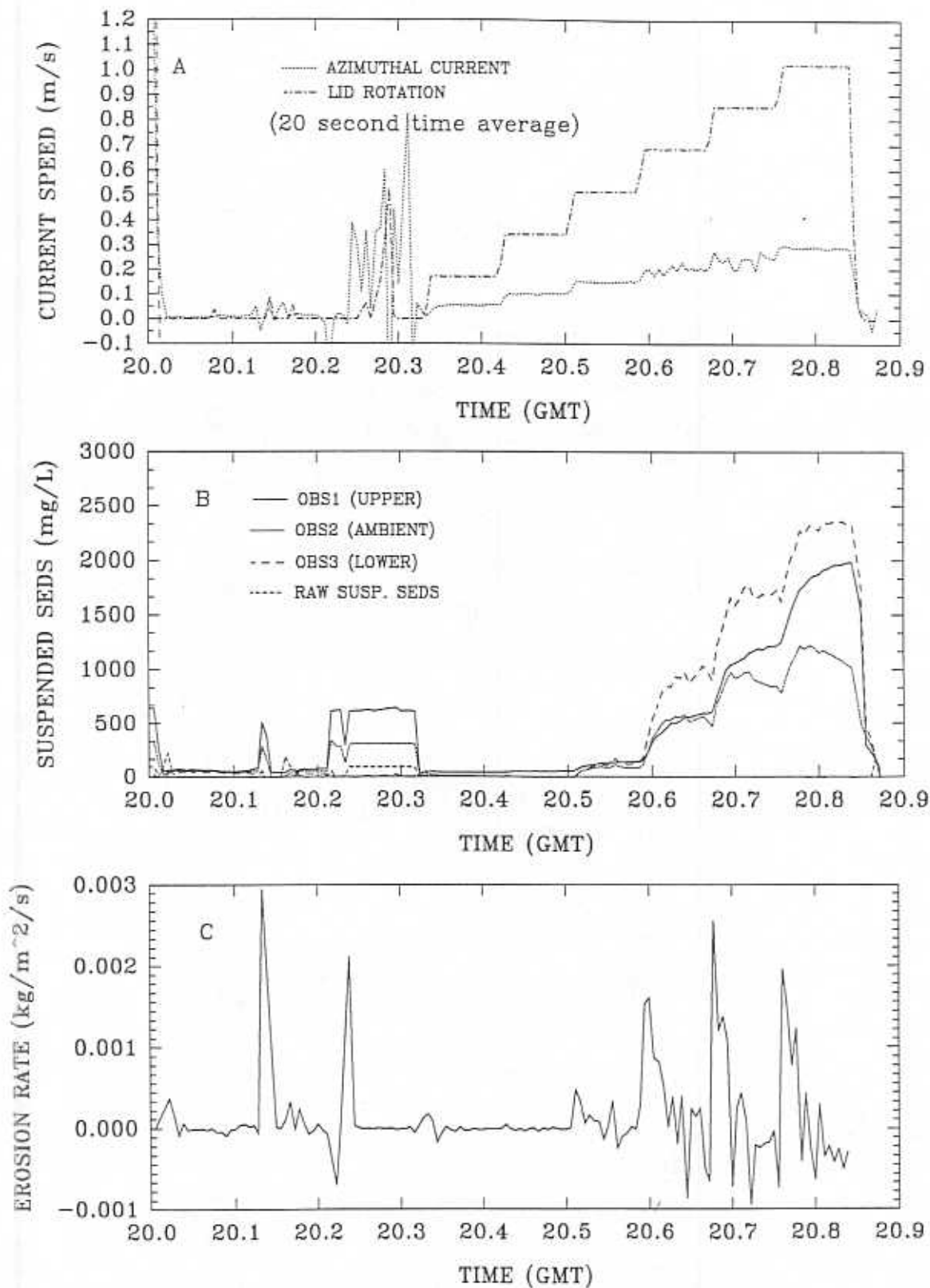


Figure 8.8 Time series of 'Sea Carousel' deployment at anchor station S8.

### 8.3.2 Sensor Calibration

The current meter output was transformed to current speed using the following algorithm:

$$U_y = 0.00306(EM_{\text{voltage}}) \text{ m/s}$$

$$U_w = 0.00306(EM_{\text{voltage}}) - 0.03 \text{ m/s}$$

where  $U_y$  and  $U_w$  are the azimuthal and vertical current speeds respectively. Observed current speed was determined from high-resolution video records of the erosion experiment. The relationship between the observed and predicted azimuthal currents is shown in Figure 8.1. Notice that the relationship is good up to 0.2 m/s. Above this value the observed current is lower than the measured. This we attribute to the fact that the video observes the bed and the water column to about 0.10 m above it. The current meter, on the other hand is about 0.2 m above the bed and is subject to higher flows.

The detection of suspended sediment concentration within the Carousel is dependent on the relationship between filtered mass derived from pumped samples from the flume, and the output voltage from the OBS sensors. The calibration plots for each station are shown in Figures 8.9 to 8.15. In all cases, very high correlations were derived:

STATION	EQUATION	$r^2$
FA2	SSC = -127 + 2.51(OBS)	1.0
FA3	SSC = -121 + 2.79(OBS)	0.98
FA4	SSC = -74 + 2.51(OBS)	0.98
FA5	SSC = -58 + 2.42(OBS)	0.98
FA6	SSC = -165 + 3.46(OBS)	0.98
FA7	SSC = -20 + 1.36(OBS)	0.92
FA8	SSC = -82 + 2.34(OBS)	0.98

**Table 8.3.** A summary of the correlation between measured suspended sediment concentration (SSC) and voltage output from the Optical Backscatter Sensors (OBS) of Sea Carousel.

The calibrations are valid for the upper OBS only (OBS1) as the pump sample was derived from this height. The lower OBS (OBS3) was not correlated with pumped material because of the dangers of concentration gradients near the bed. Thus OBS3 was assigned the same slope as the upper OBS, but the offset was defined on the basis of the still water value.

### 8.3.3 Threshold Stresses for Bed Erosion

The erosion thresholds of the inner stations were consistently low, varying between 0.2 and 0.3 Pa. By comparison, the thresholds of the outer stations vary between 0.4 and 0.7 Pa. The inner stations are amongst the weakest to have been monitored by Sea Carousel in the Bay of Fundy. For example, typical erosion thresholds on the Minas Basin tidal flats were between 1.0 and 1.5 Pa (Amos *et al.* 1992); that is, they were up to seven times stronger than off Fort Anne.

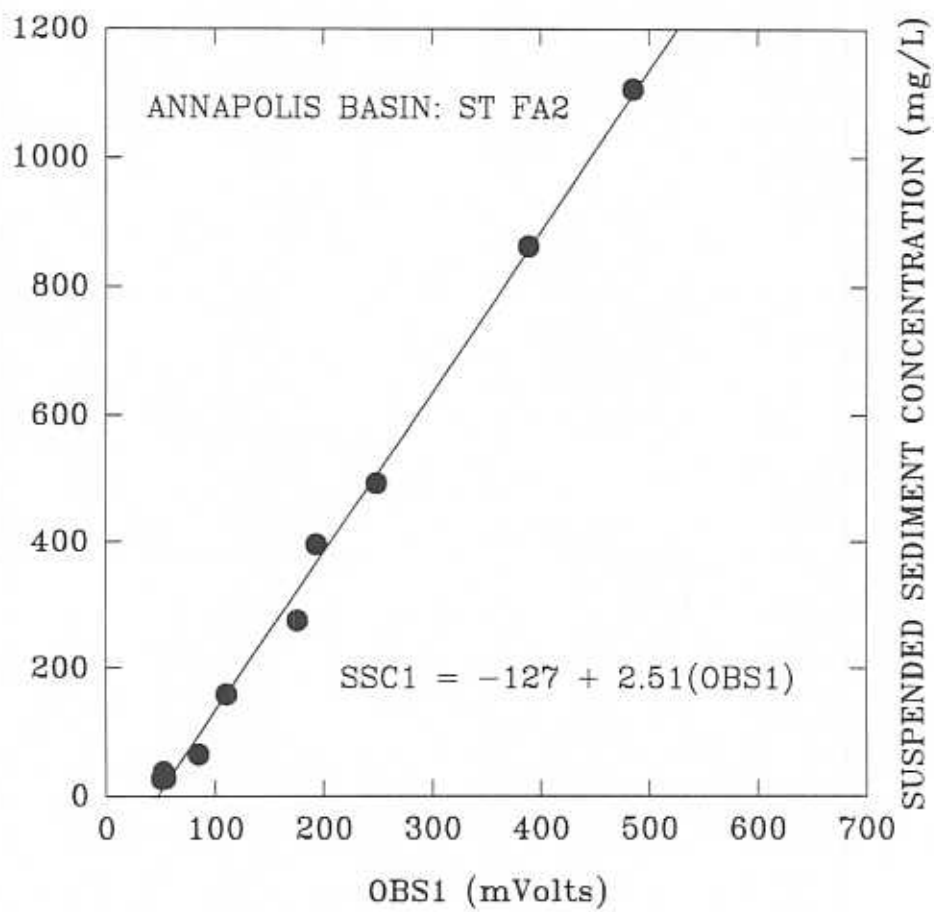


Figure 8.9 Correlations between suspended sediment concentration and optical backscatter sensor reading, during 'Sea Carousel' deployment at anchor station S2.

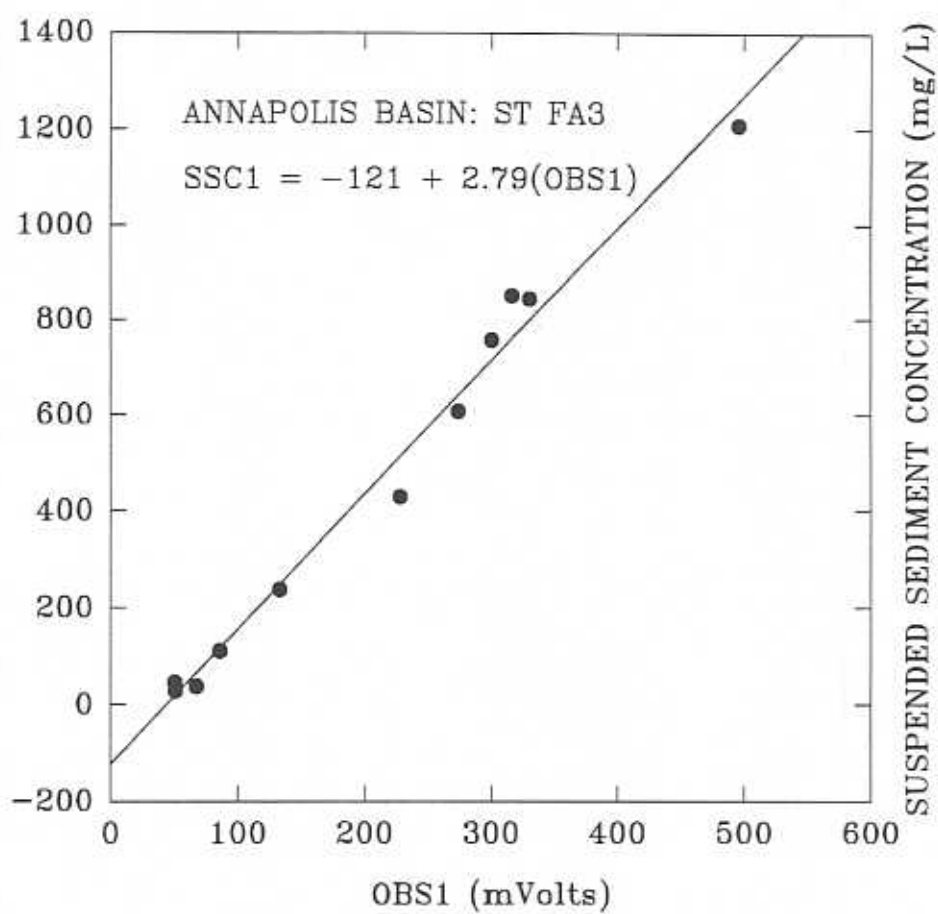


Figure 8.10 Correlations between suspended sediment concentration optical backscatter sensor reading, during 'Sea Carousel' deployment at anchor station S3.

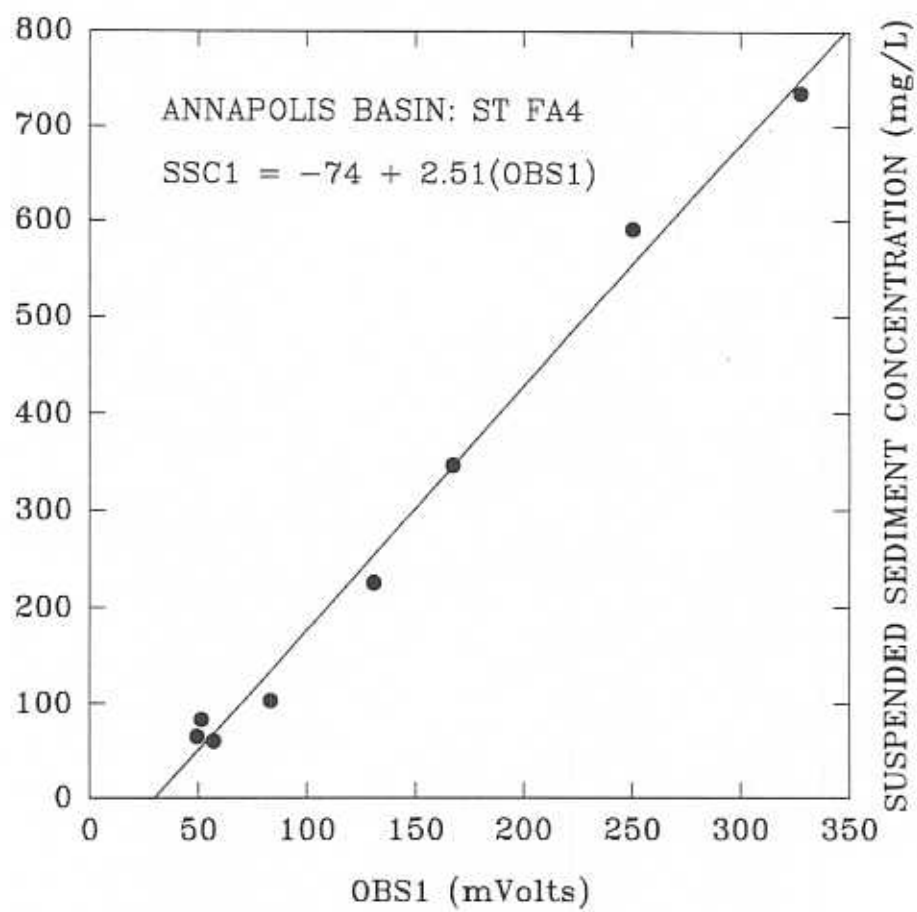


Figure 8.11 Correlations between suspended sediment concentration optical backscatter sensor reading, during 'Sea Carousel' deployment at anchor station S4.



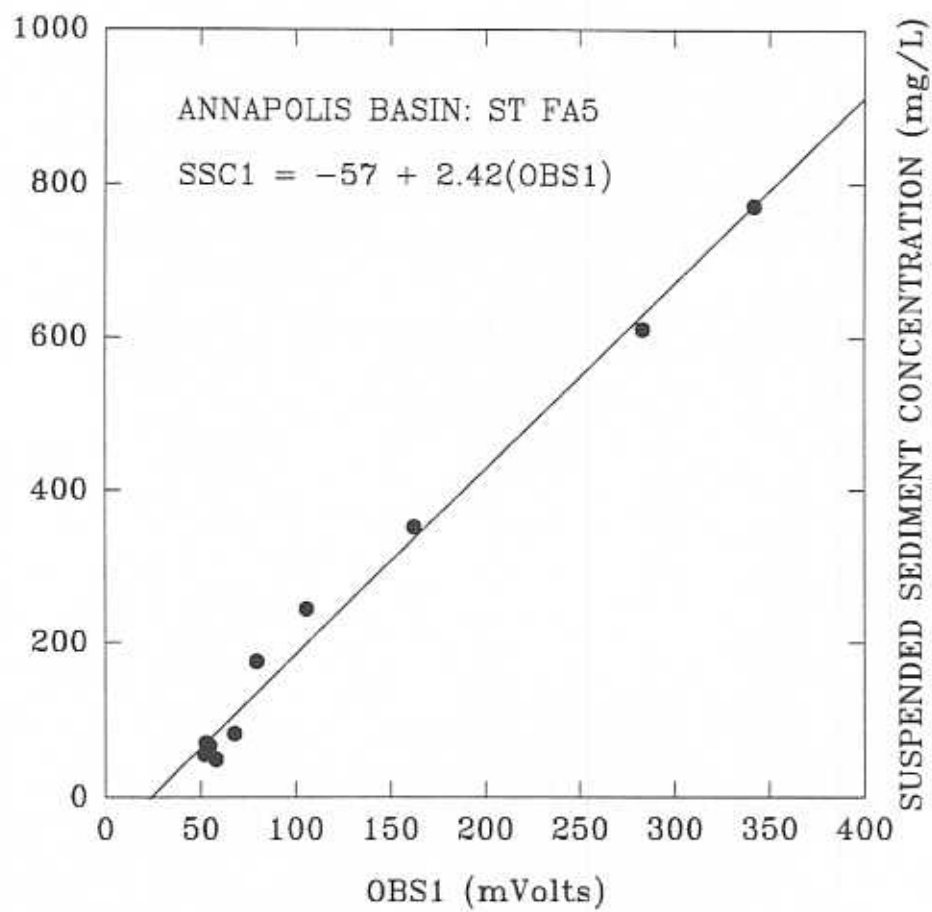


Figure 8.12 Correlations between suspended sediment concentration and optical backscatter sensor reading, during 'Sea Carousel' deployment at anchor station S5.

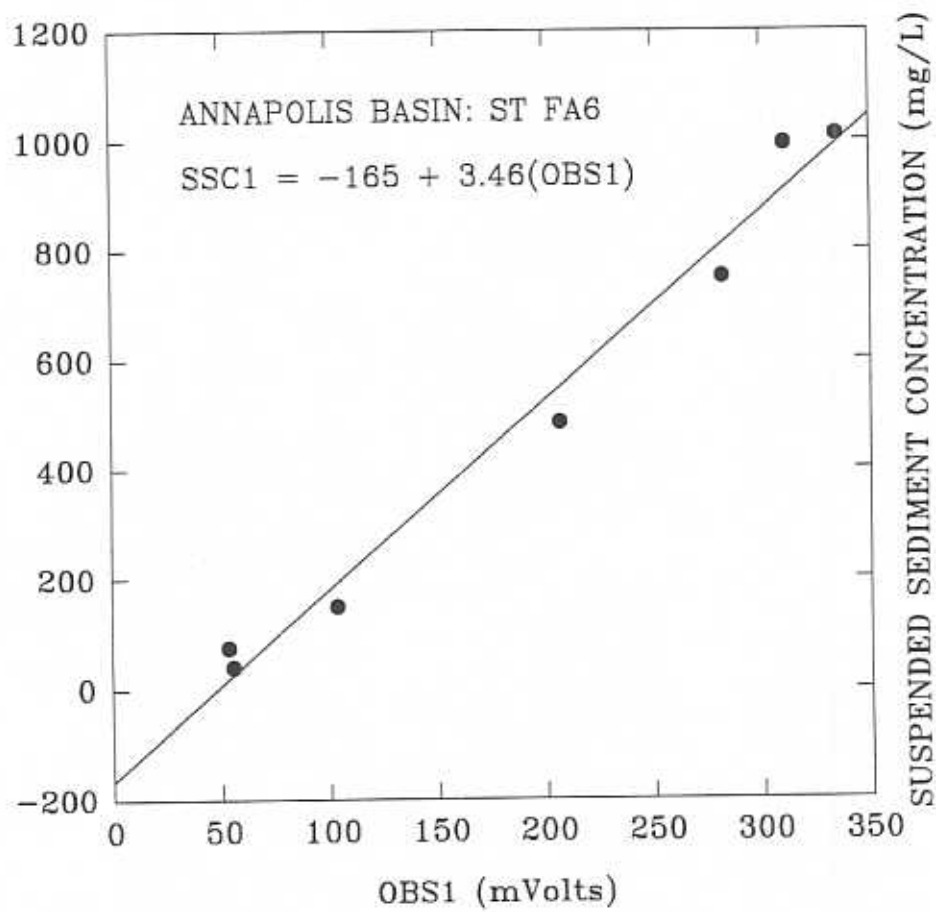


Figure 8.13 Correlations between suspended sediment concentration optical backscatter sensor reading, during 'Sea Carousel' deployment at anchor station S6.

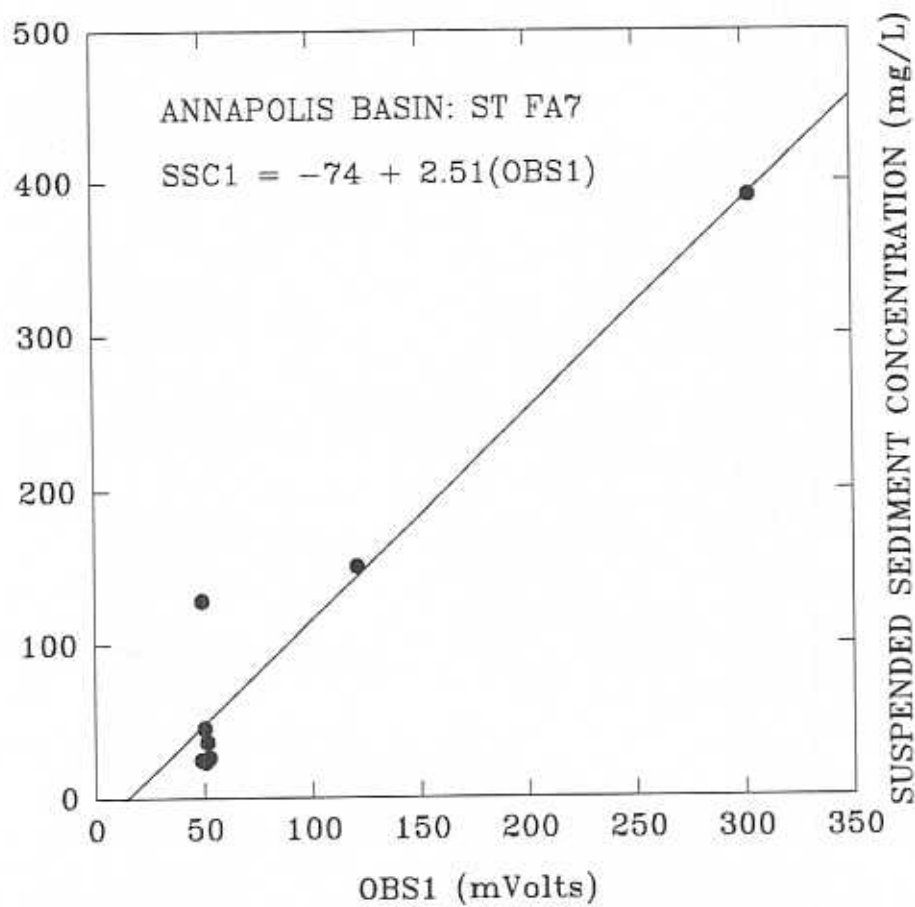


Figure 8.14 Correlations between suspended sediment concentration optical backscatter sensor reading, during 'Sea Carousel' deployment at anchor station S7.

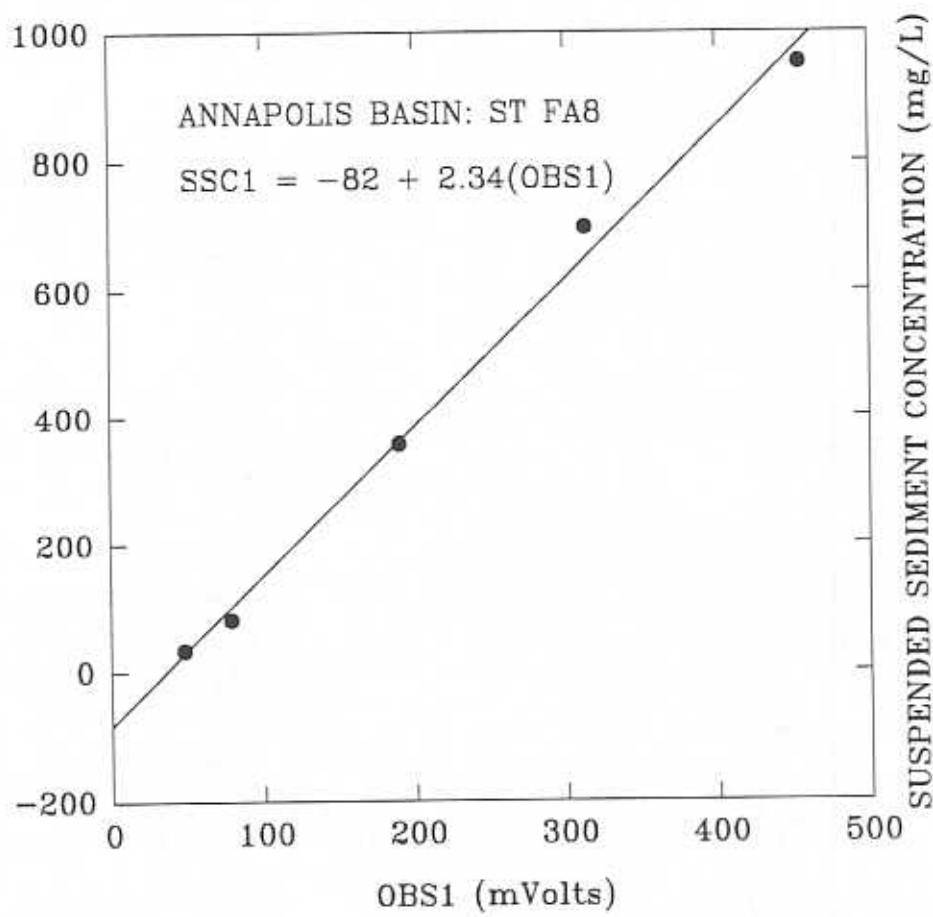


Figure 8.15 Correlations between suspended sediment concentration and optical backscatter sensor reading, during 'Sea Carousel' deployment at anchor station S8.

The resistance to erosion did not increase significantly with depth below the mudline. This becomes evident in Figures 8.16 to 8.22, which illustrate synthetic cores of stations FA2 to FA8, respectively. Notice that at station FA2 there is no strength gain with depth, suggesting that once the erosion process had begun, it would continue provided the applied stress was maintained. This, at first sight, conflicts with the observation of Type I erosion within Sea Carousel at station FA2. However, it reflects the fact that the surface sediments at this location may be unconsolidated, resulting from the relatively recent deposition of red clay resuspended from the nearby shoreline. It may also reflect a stress reduction due to increases in suspended sediment concentration during the erosion process.

### 8.3.4 Erosion Rates

The erosion rates are illustrated in the time-series plots of Figures 8.2 to 8.8. Notice that, in each case, there is a distinct peak in erosion rate at the beginning of each speed increment (EP) and that erosion decreases sharply after the initial peak. This peak has been plotted against the applied bed shear stress in Figure 8.23. There appears to be a positive linear correlation between EP and bed shear stress ( $\tau_o$ ) of the form:

$$EP = 0.0035(\tau_o - \tau_c) \text{ kg/m}^2/\text{s}; r^2 = 0.48$$

where  $\tau_c$  is the erosion threshold determined from the figure when  $EP = 0$ . In this case  $\tau_c = 0.06$  Pa. This is an extremely low value for an erosion threshold, but it corresponds quite well with the threshold determined by Sigouin and MacDonald (1994) for their grey mud ( $\tau_c = 0.09$  Pa). Also, the form of the relationship between EP and excess bed shear stress, is the same as that used by Sigouin and MacDonald (1994) to derive their erosion threshold.

Much of the scatter in the results comes from the relatively high erosion rates exhibited at station FA2 (off Fort Anne). The red clays of the tidal flats appear to overlie the more typical grey marine clays at this site (see later section). The rapid erosion of these red clays, observed over the tidal flats, would agree with the subtidal results reported herein.

STATION	EROSION RATE (kg/m <sup>2</sup> /s)	BED SHEAR STRESS (Pa)
FA2	$5 \times 10^{-4}$	0.07
FA2	$1.2 \times 10^{-3}$	0.22
FA2	$1.2 \times 10^{-3}$	0.30
FA2	$1.3 \times 10^{-3}$	0.45
FA2	$1.3 \times 10^{-3}$	0.52
FA2	$3.9 \times 10^{-3}$	0.60
FA2	$3.8 \times 10^{-3}$	0.67
FA3	$5.0 \times 10^{-4}$	0.15
FA3	$1.0 \times 10^{-3}$	0.34
FA3	$1.6 \times 10^{-3}$	0.76
FA3	$2.2 \times 10^{-3}$	0.72
FA3	$1.3 \times 10^{-3}$	0.71
FA4	$4.0 \times 10^{-4}$	0.20
FA4	$8.0 \times 10^{-4}$	0.29

FA4	$9.0 \times 10^{-4}$	0.39
FA4	$1.3 \times 10^{-3}$	0.48
FA4	$1.3 \times 10^{-3}$	0.48
FA5	$3.0 \times 10^{-4}$	0.29
FA5	$5.0 \times 10^{-4}$	0.34
FA5	$7.0 \times 10^{-4}$	0.40
FA5	$9.0 \times 10^{-4}$	0.43
FA5	$2.1 \times 10^{-3}$	0.53
FA5	$2.4 \times 10^{-3}$	0.63

Table 8.4. A summary of the peak erosion rates (EP) for Type I erosion detected by Sea Carousel at stations FA2 to FA5 (inner stations). The remaining stations have not been included as the seabed at these outer stations is largely composed of sand.

### 8.3.5 Deposition Rates

The still water settling rates for material eroded from the seabed at stations FA2 to FA5 (the inner stations) were determined based on the rate of change in suspended sediment concentration during the latter stages of each deployment. The time-series of these settling periods are shown in Figure 8.24. The estimation of the mean mass settling rate follows the method given in Amos and Mosher (1985). These mass settling rates are summarised in Table 8.5.

STATION	SETTLING RATE (m/s)
FA2	$3.9 \times 10^{-4}$
FA3	$9.0 \times 10^{-4}$
FA4	$9.1 \times 10^{-4}$
FA5	$6.5 \times 10^{-4}$

Table 8.5. A summary of the mean mass settling rates determined during the still water settling period carried out at the latter stages of each Sea Carousel deployment of the inner stations in Annapolis Basin.

The settling rate at station FA2 is remarkably close to the 50<sup>th</sup> percentile of the fall velocity observed by Sigouin and MacDonald (1994) for the grey and red muds, and which were  $4 \times 10^{-4}$  and  $3 \times 10^{-4}$  m/s respectively. These values are very low indeed, and are amongst the lowest detected in the Bay of Fundy system. Again, it suggests that the material at station FA2 is unique by comparison with the rest of the Basin, and that there is a link in behaviour between the intertidal red muds and the material comprising the seabed at station FA2.

### 8.3.6 Physical Properties

The gravity cores collected at each of the Sea Carousel stations were split and logged for sedimentological and bulk physical properties. Photographs were taken of the cores during logging; these are recorded in Appendix C (Figures 13.1 to 13.11).

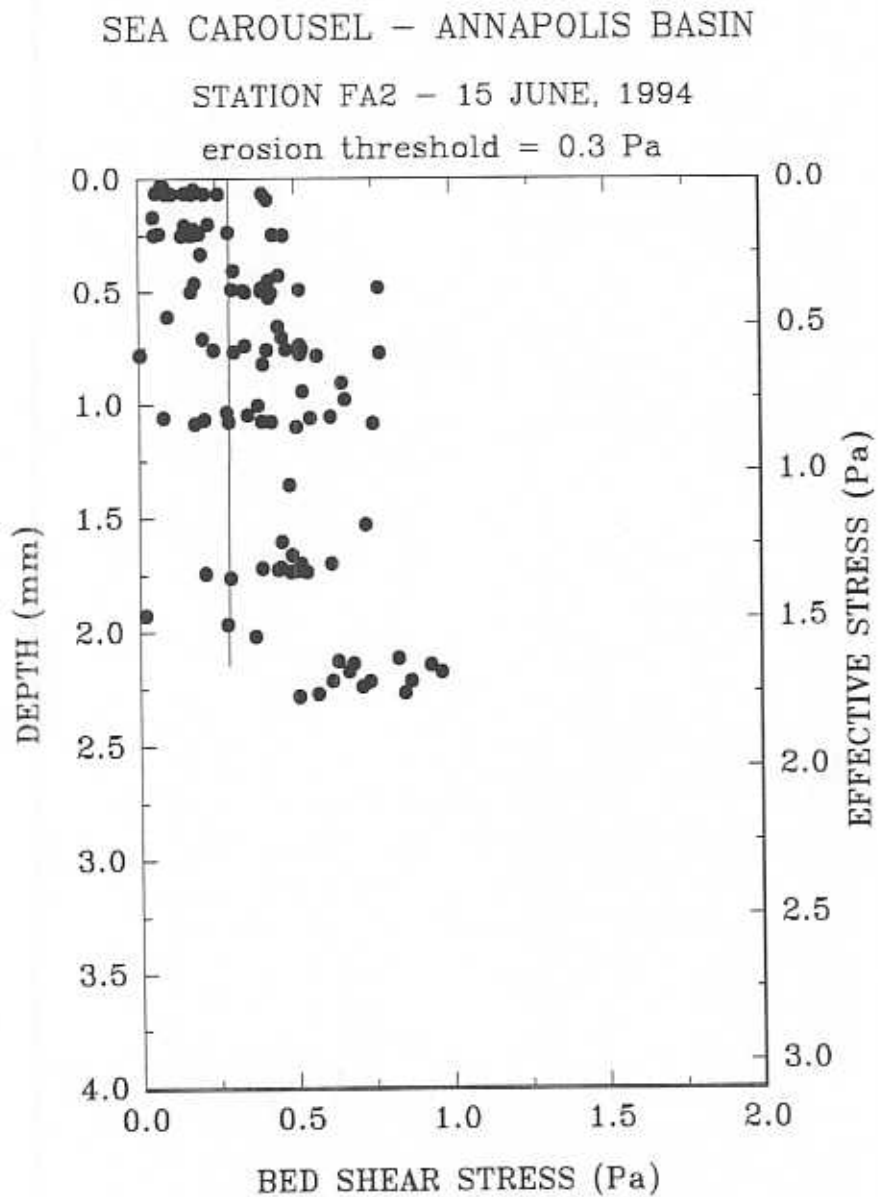


Figure 8.16 Relationship of shear stress and depth in 'Sea Carousel' deployment at anchor station S2.



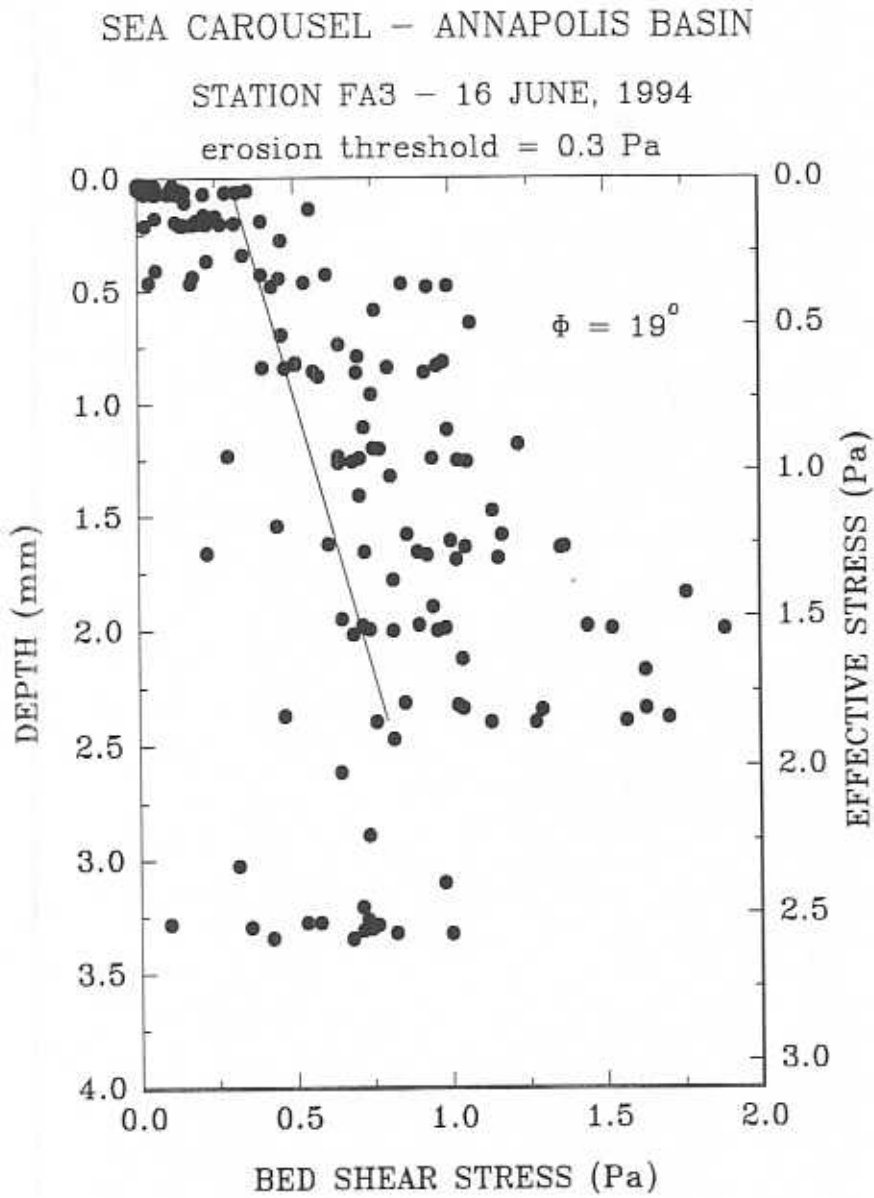


Figure 8.17 Relationship of shear stress and depth in 'Sea Carousel' deployment at anchor station S3.

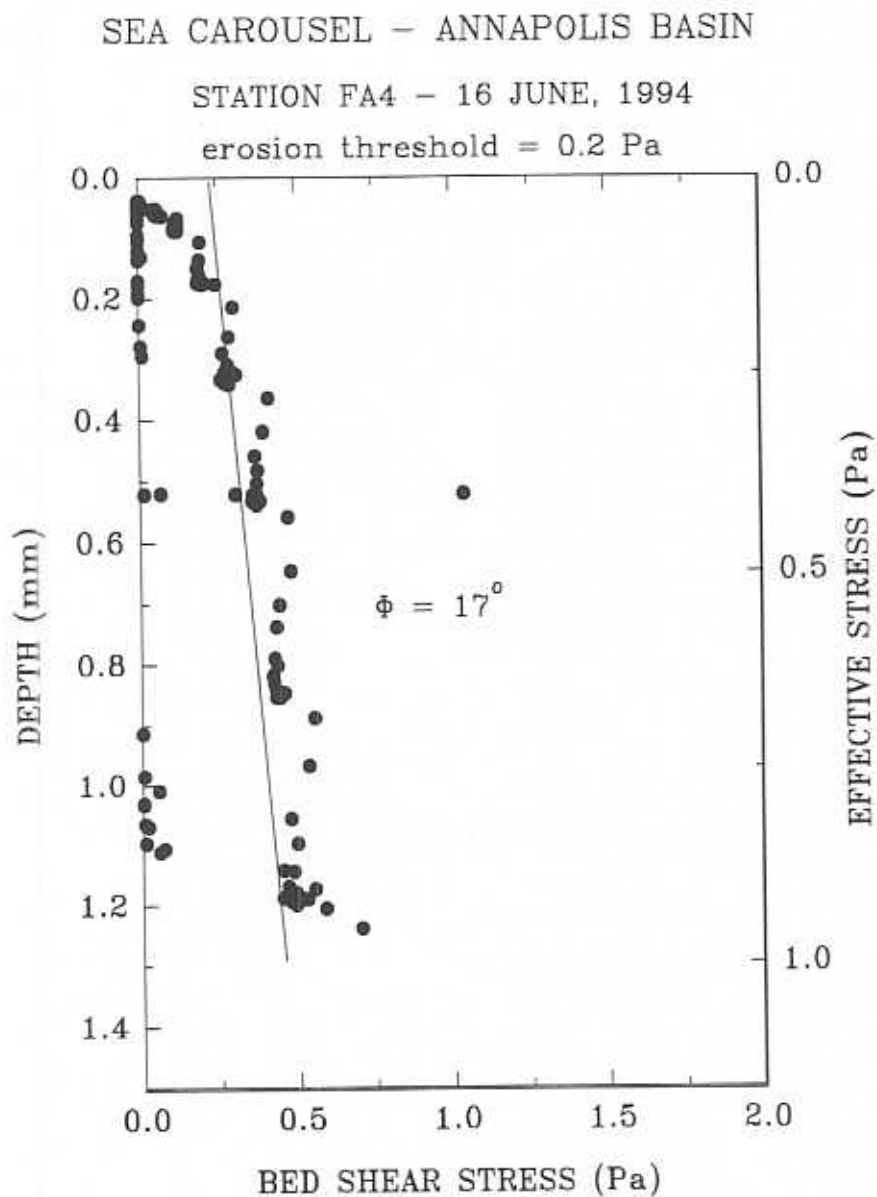


Figure 8.18 Relationship of shear stress and depth in 'Sea Carousel' deployment at anchor station S4.

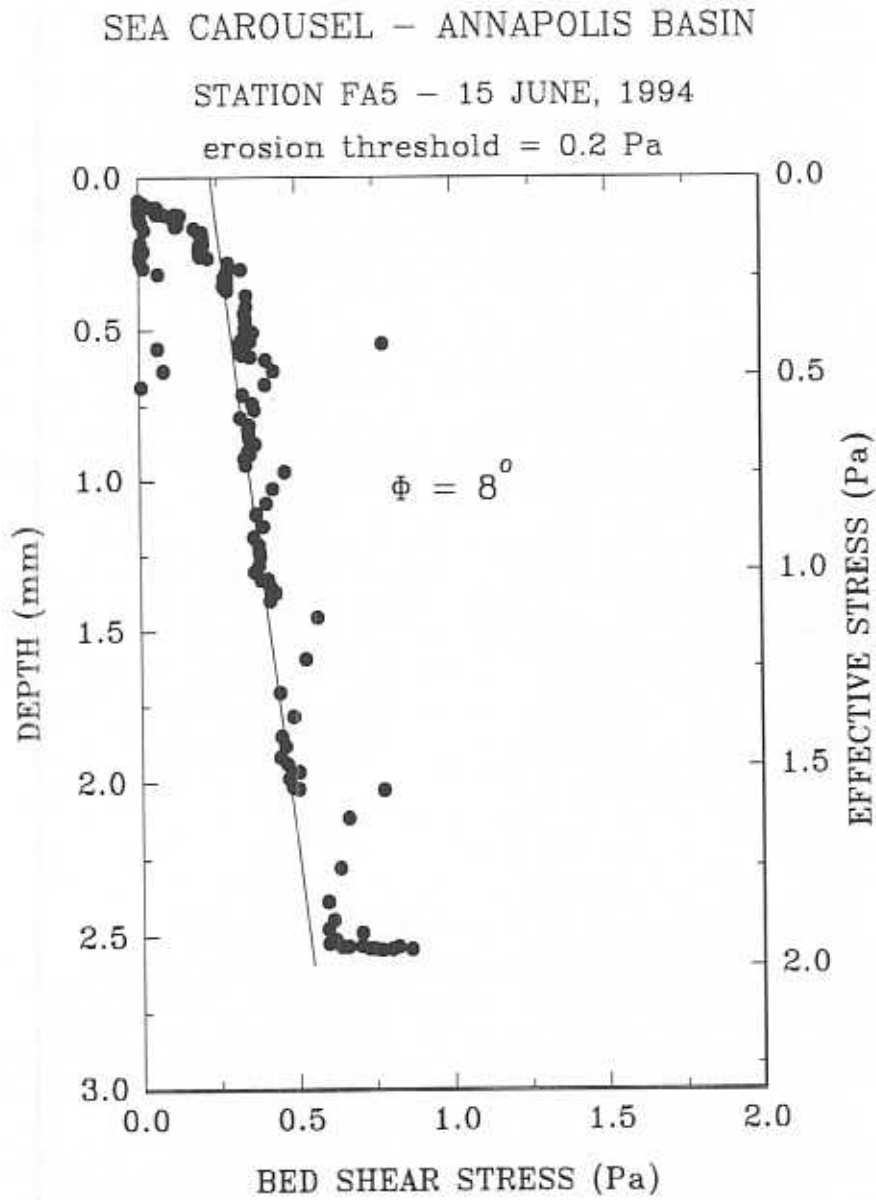


Figure 8.19 Relationship of shear stress and depth in 'Sea Carousel' deployment at anchor station S5.

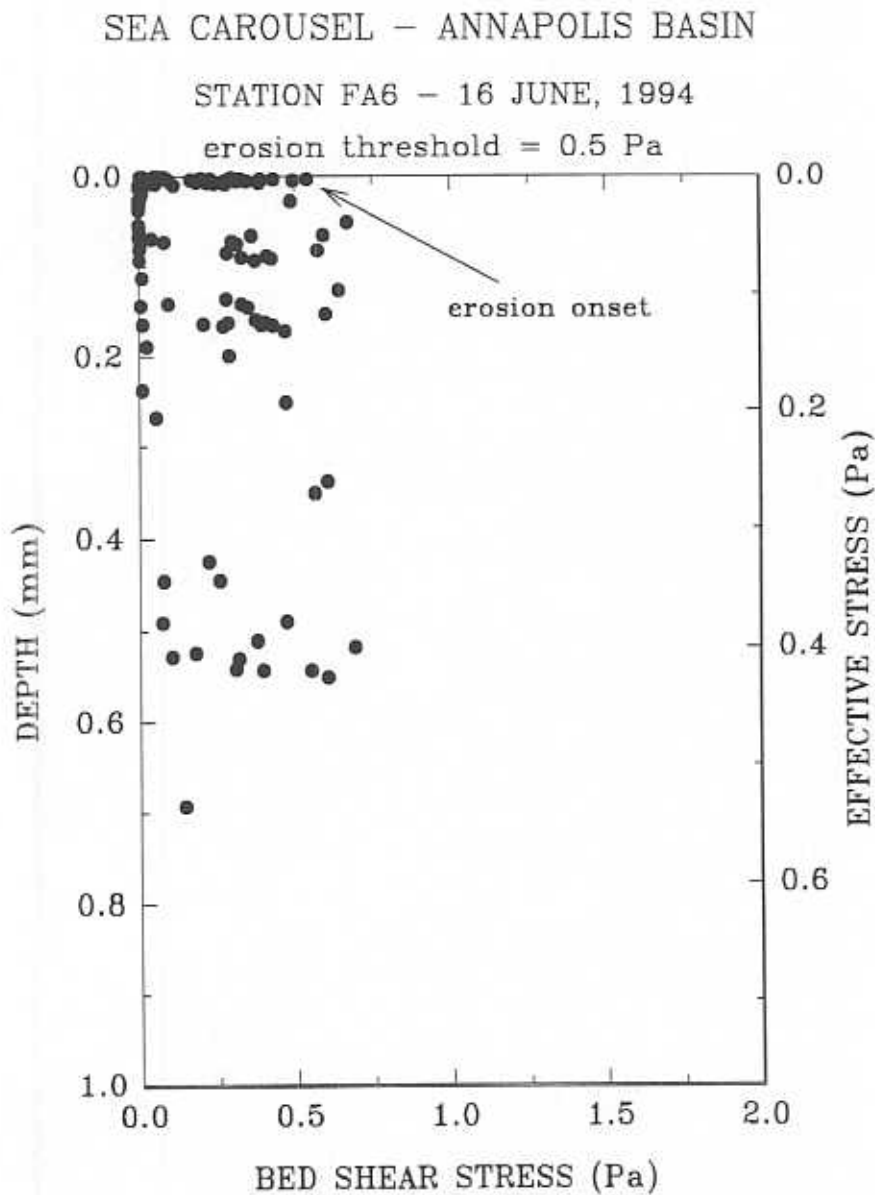


Figure 8.20 Relationship of shear stress and depth in 'Sea Carousel' deployment at anchor station S6.

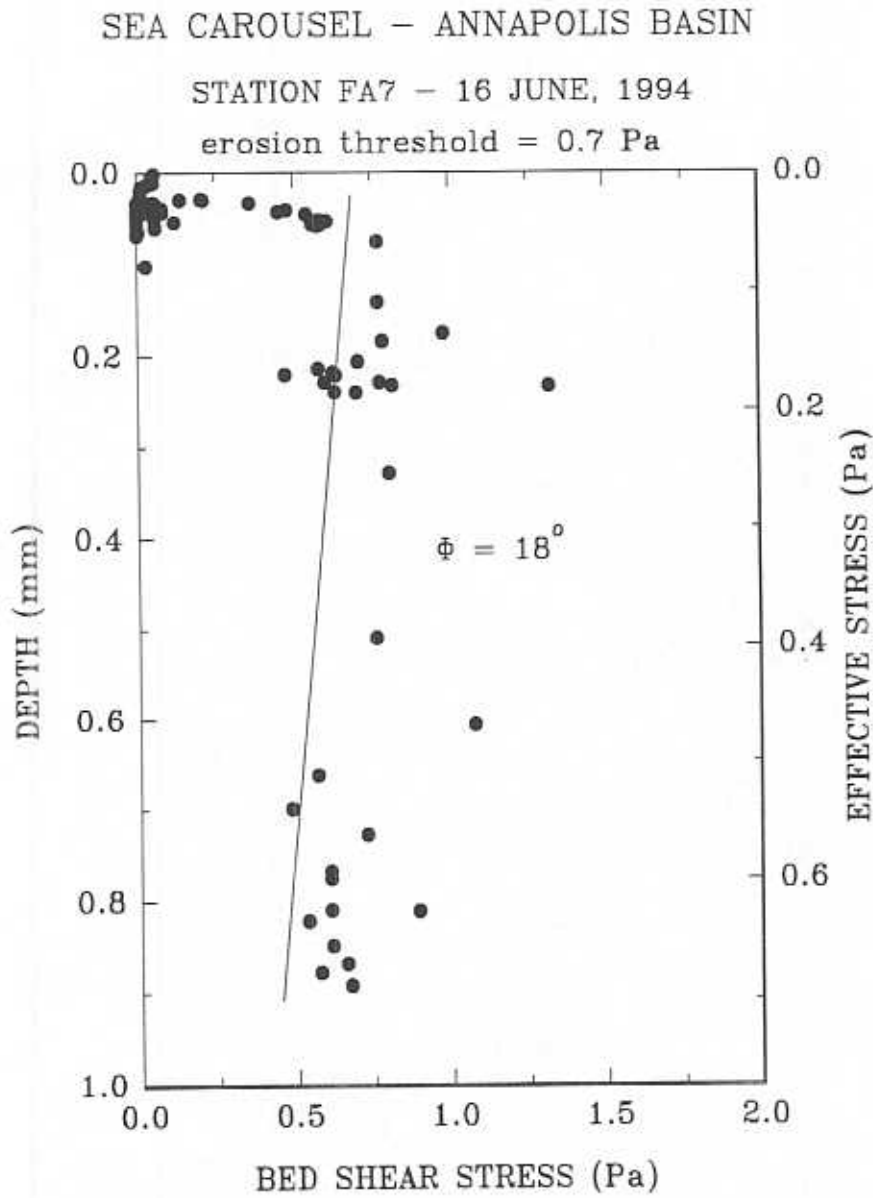


Figure 8.21 Relationship of shear stress and depth in 'Sea Carousel' deployment at anchor station S7.

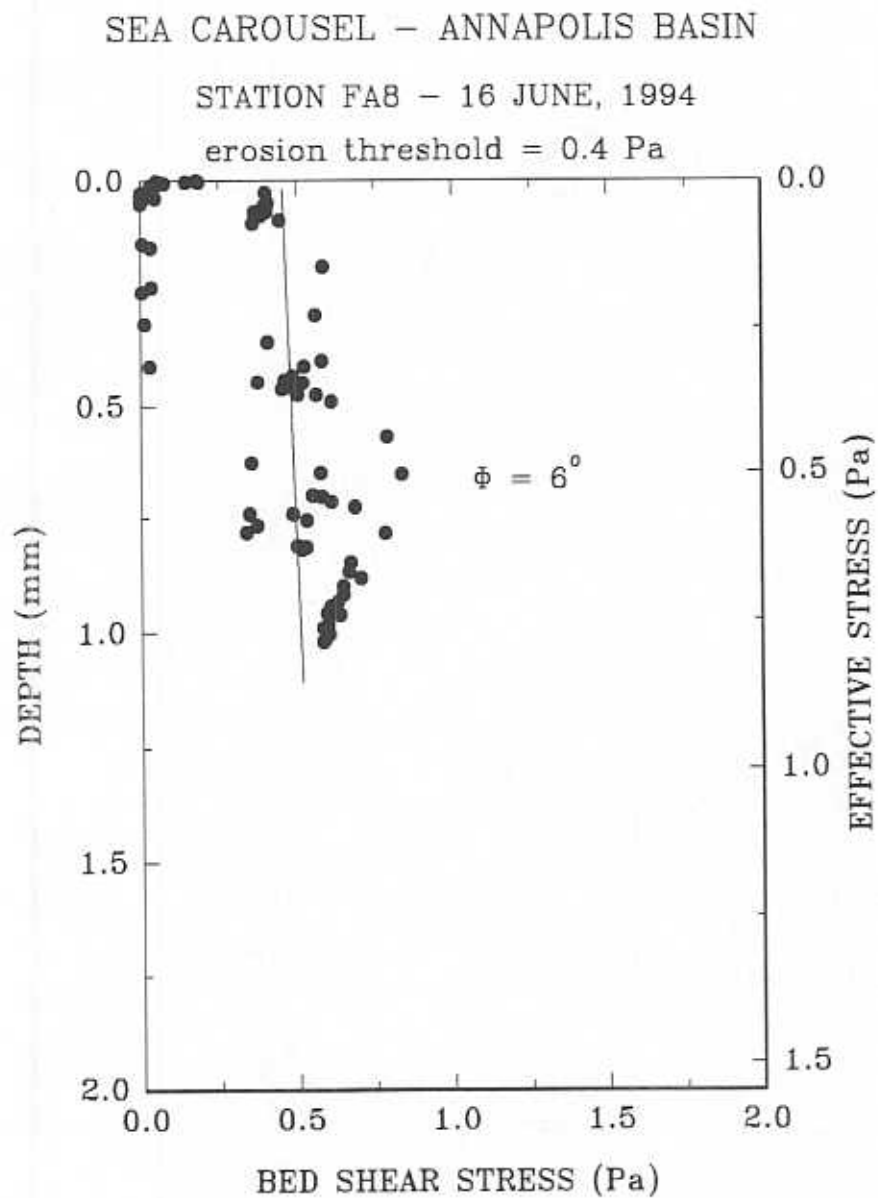


Figure 8.22 Relationship of shear stress and depth in 'Sea Carousel' deployment at anchor station S8.

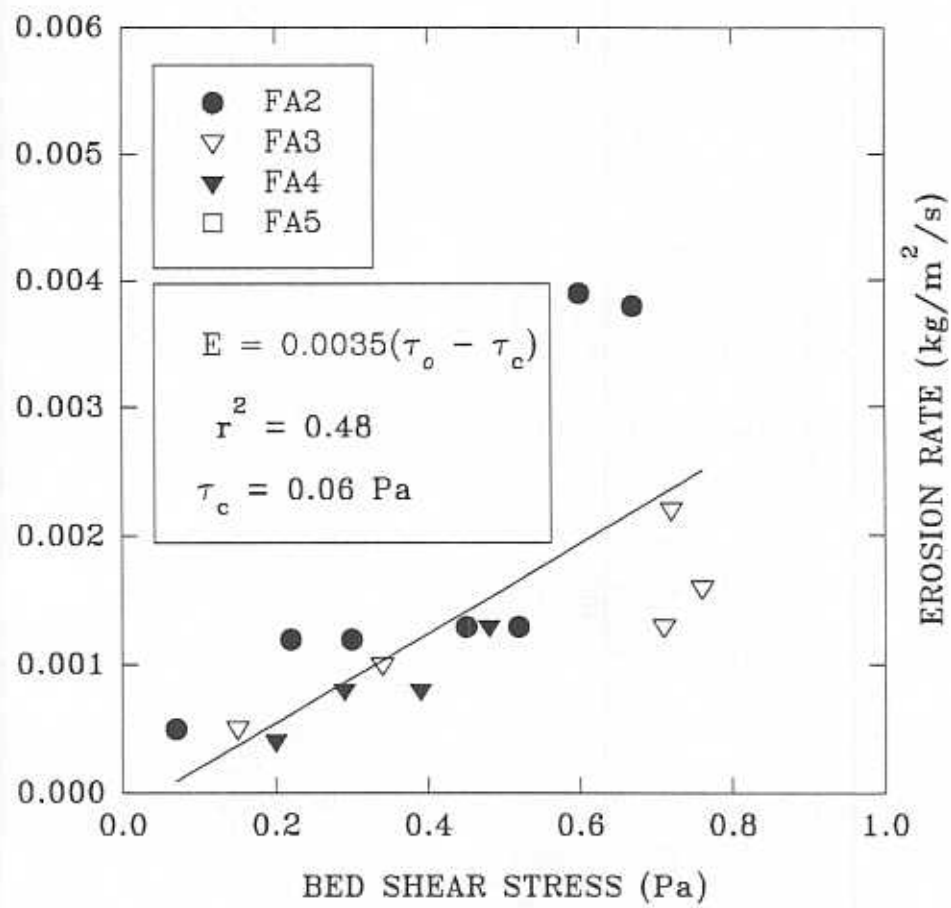


Figure 8.23 Relationship between erosion rate and bed shear stress at anchor stations S2 to S5 in the Annapolis Estuary.



settling experiment – Annapolis Basin, 1994

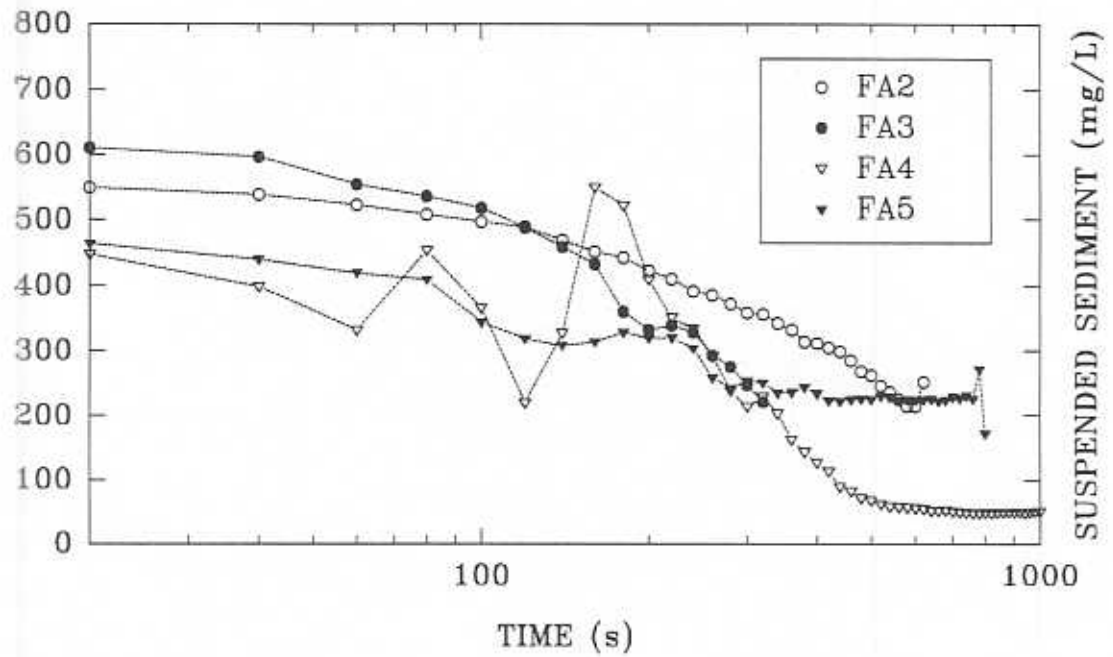


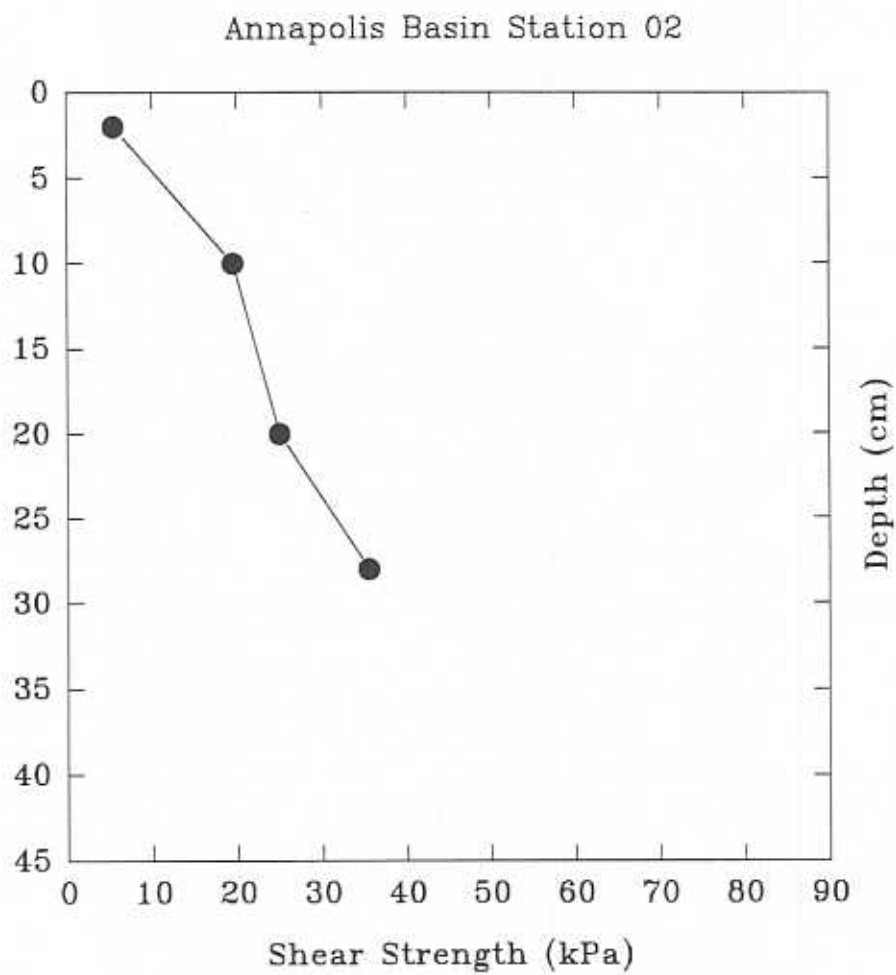
Figure 8.24 Settling rate experiments at anchor stations S2 to S5 in the Annapolis Estuary.

The inner stations (FA2 to FA5) were characterised by highly bioturbated, reduced muds, whereas the outer stations (FA6 and FA7) were of mixed lithology and composition. Station FA2 was distinguished by an oxidized surface layer, 3 cm thick, that was reddish in colour much like the colour of material found on the adjacent tidal flats (cf. Figure 13.1). Any evidence of lamination had been destroyed by the presence of worm tubes which have produced a relatively-low bulk density (Table 8.6). The vane shear strength is plotted against depth in Figures 8.25 to 8.31. The bulk physical properties for station FA2 (Figure 8.25) showed a friction angle of 24°, which corresponds to that derived by H. Christian (see Section 7.4) from core samples taken on the red muds immediately below the Fort. It would thus appear likely that the material underlying station FA2 is the same material that is being eroded from the tidal flats off Fort Anne. The interstitial water salinity at a depth of 25 cm in the core from station FA2 was 28 ppt. This suggests that either the material was deposited under saline conditions, or the unit has been ventilated through bioturbation. This latter option is unlikely given the steady increase in vane shear strength to 40 kPa at a depth of 30 cm.

Stations FA3 and FA4 are also highly bioturbated and strongly reduced, forming a surface layer of grey mud (Figures 13.2 to 13.6). They exhibit the highest water contents of the station transect and also the lowest friction angles. The correspondingly low erosion thresholds (0.2 Pa) measured by Sea Carousel may, therefore, be explained in terms of the strong effects of bioturbation. This is supported by the measures of shear strength (Figures 8.20 and 8.21) which show only slight increases with depth to a maximum value of 10 kPa.

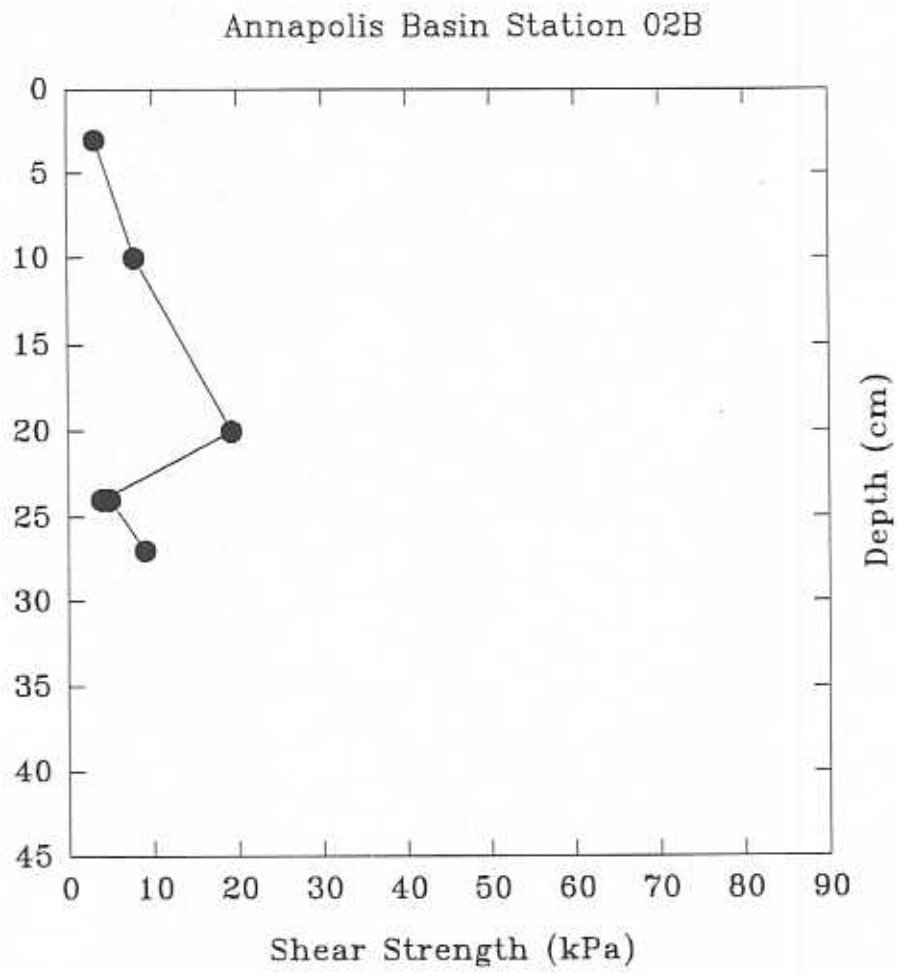
STATION	DEPTH (cm)	BULK DENSITY (kg/m <sup>3</sup> )	WATER CONTENT (% dry)	FRICITION ANGLE (degrees)
FA2	6	1482	97	--
FA2	16	1502	95	--
FA2	25	1533	83	24
FA3	8	1423	111	--
FA3	20	1421	129	--
FA3	31	1349	149	--
FA3	41	1417	128	5
FA4	35	1515	100	11
FA5	2	1504	88	--
FA5	10	1599	77	--
FA5	20	1550	80	--
FA5	30	1704	54	--
FA5	40	1601	65	14
FA6	2	1648	59	--
FA6	10	1737	52	--
FA6	20	1680	54	--
FA6	30	1751	53	6
FA7	6	1837	33	35

Table 8.6 A summary of the bulk physical properties of gravity cores collected at each of the Sea Carousel stations.



Note: Shear strength measured with the 25mm Controls Penetrometer.

Figure 8.25 Change in shear strength with depth in gravity core from anchor station S2.



Note: Shear strength measured with the sensitive vane (3, 10, 20, 27 cm depths) and regular vane (24 cm depth) of the Soiltest CL 600 Torvane.

Figure 8.26 Change in shear strength with depth in gravity core from anchor station S3.

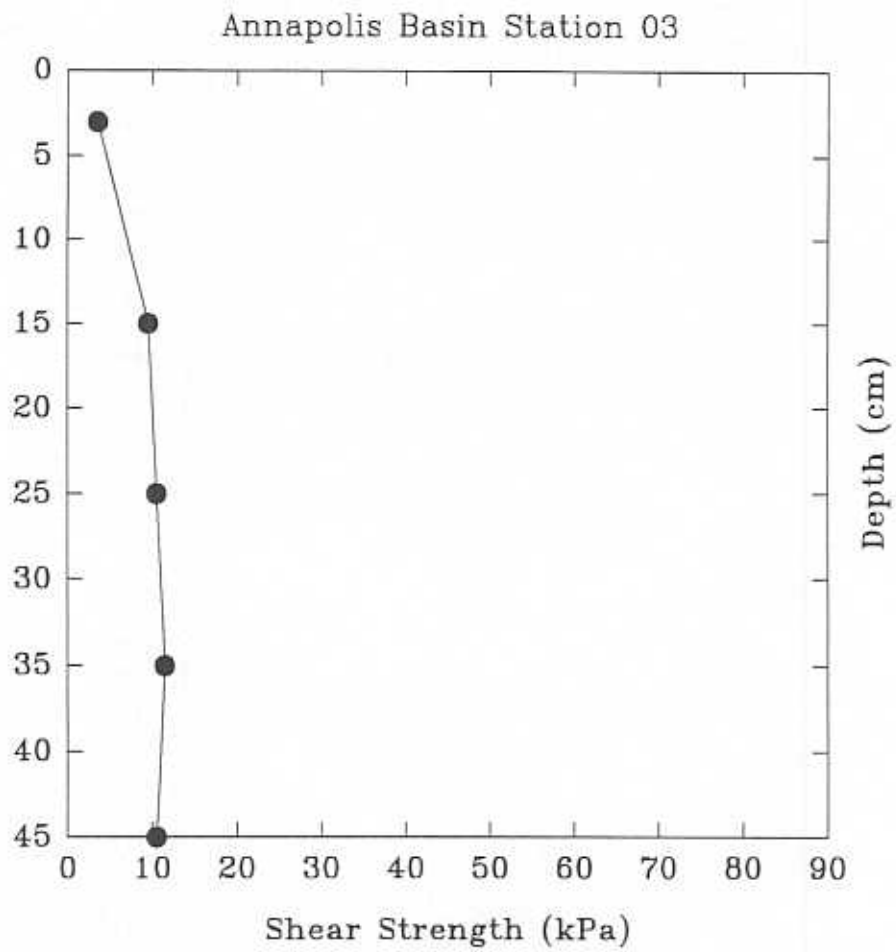


Figure 8.27 Change in shear strength with depth in gravity core from anchor station S4.

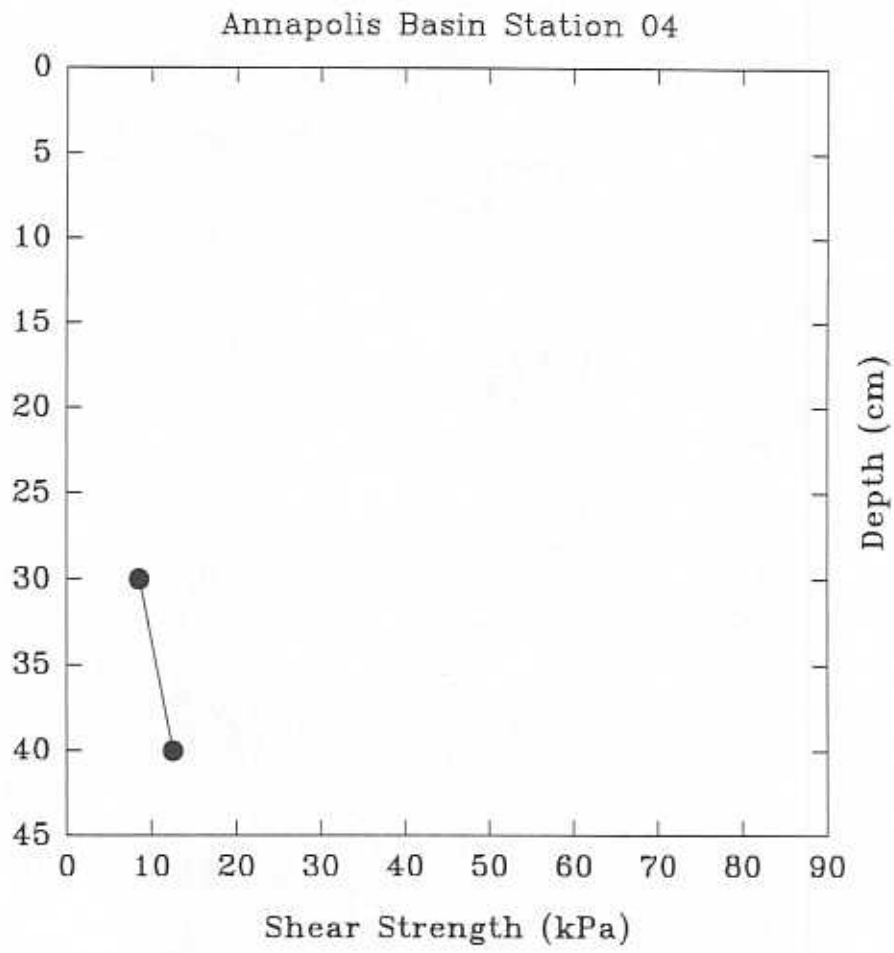


Figure 8.28 Change in shear strength with depth in gravity core from anchor station S5.

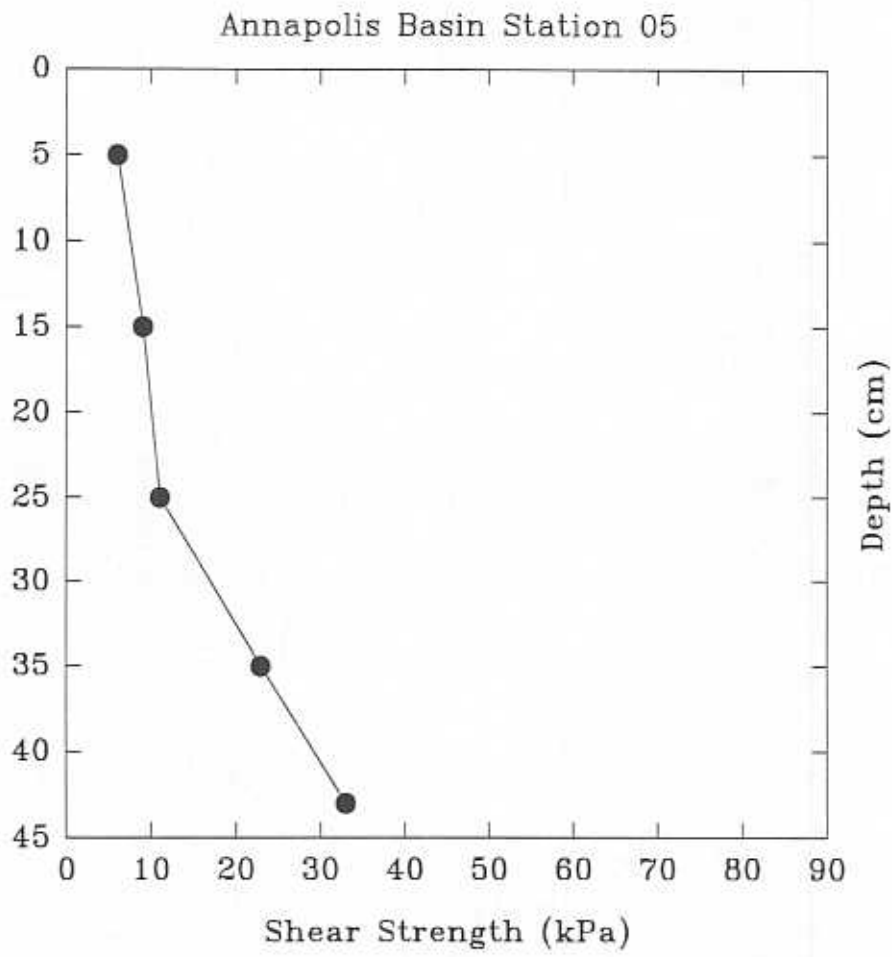


Figure 8.29 Change in shear strength with depth in gravity core from anchor station S6.



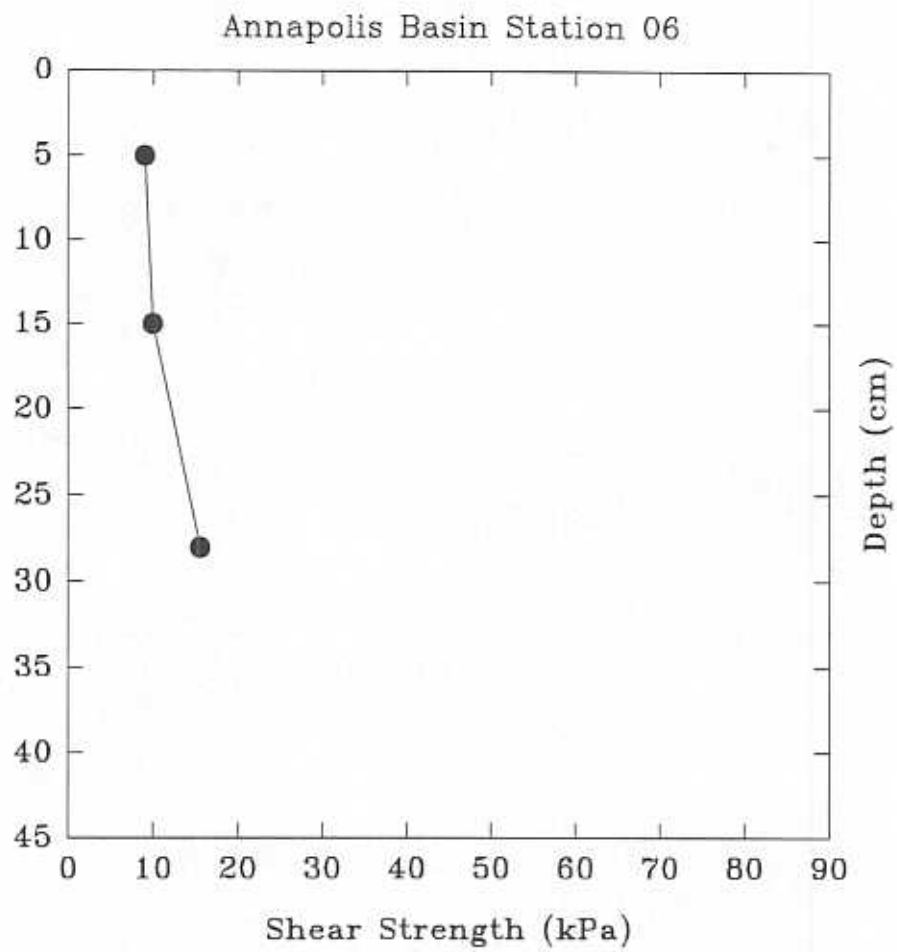


Figure 8.30 Change in shear strength with depth in gravity core from anchor station S7.

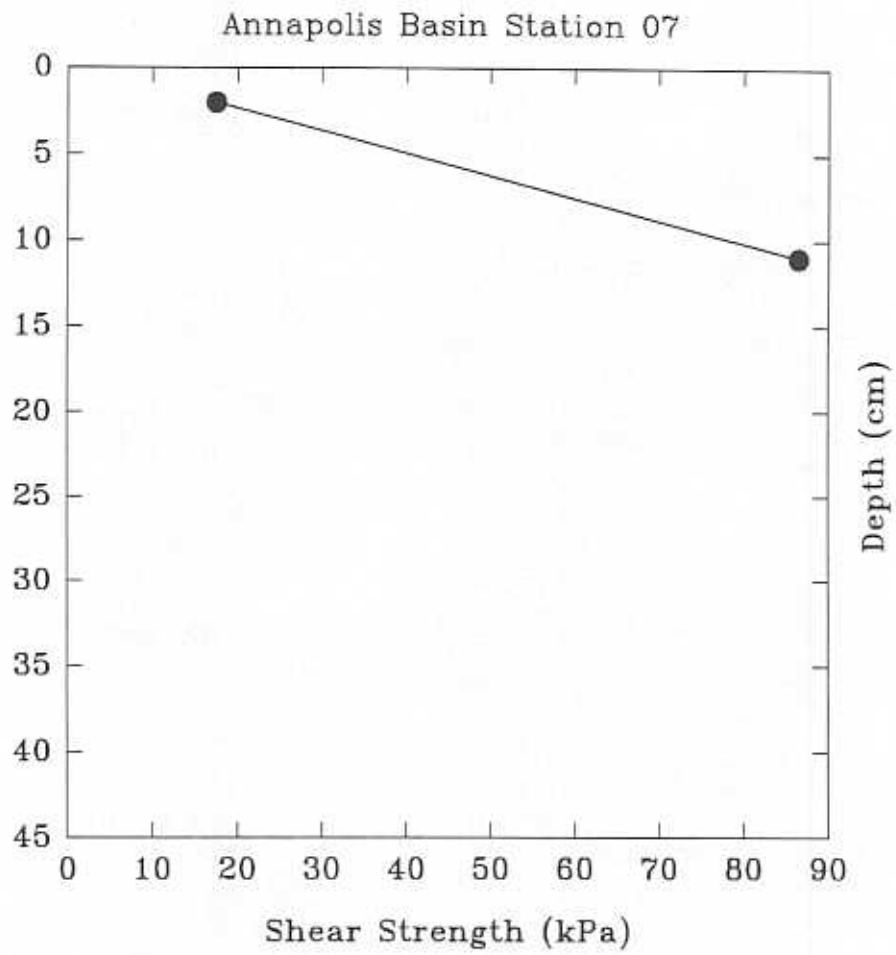


Figure 8.31 Change in shear strength with depth in gravity core from anchor station S8.

STATION	ORGANIC CARBON CONTENT(%)	SAND CONTENT(%)	SILT CONTENT(%)	CLAY CONTENT(%)
FA2	1.68	3	53	44
FA3	1.59	6	55	39
FA4	1.80	4	57	39
FA5	0.91	19	55	26
FA6	0.74	39	42	19
FA7	0.28	80	12	8

Table 8.7. A summary of the surface sediment character at stations FA2 to FA7. No sample was collected at FA8 due to ship drift.

Plots of the grain size histograms are given in the appendix. The trend in sediment texture shows a consistent increase in sand content and decrease in mud content with distance down the Estuary and Basin. A distinct difference takes place between the inner stations, which are predominantly clayey silts, and the outer stations which are predominantly silty sands. Station FA2 has the highest clay content and the lowest sand content, though there is no significant difference in texture between it and stations FA3 and FA4. The organic carbon content also shows a trend of decreasing amount seawards. This would in part govern the trends in the water content discussed above.

#### 8.4 Interpretation

The results from the Sea Carousel show that the seabed in the inner part of Annapolis Basin (inside Goat Island) is of low stability and readily eroded. The lowest stability was found immediately off Fort Anne. Furthermore, the rate of erosion (for a given bed shear stress) is also greatest off the Fort, and the rate of settling is lowest. The bed surface at this site is composed of the red mud found cropping out across the tidal flats in front of the Fort. The inference is that this material has probably resettled in the channel following its erosion from the intertidal zone nearby. These observations support the predictions of the hydrodynamic and sediment model constructed by the National Research Council (Willis *et al.* 1995).

#### 8.5 Laboratory Study

##### 8.5.1 Equipment and Methods

Laboratory Carousel is an annular flume situated at Acadia Centre for Estuarine Research. It is used to undertake calibration and manipulative experiments on natural sediments examined *in situ* using Sea Carousel. Consequently, it is of the same dimensions as Sea Carousel. That is, it is 2 m in diameter with an annulus width of 0.15 m. It may be filled with seawater to a maximum depth of 0.50 m, but is nominally maintained at 0.30 m to mimic the flume depth in Sea Carousel. It is fitted with a rotating lid that sits at the water surface with eight paddles beneath that are spaced equidistantly around the lid. The speed of lid rotation is controlled by an Empire 0.75 Hp DC motor and Focus controller and power supply. The speed of flow is detected by a model 523 (0.5" head size) Marsh-McBirney electromagnetic current meter. The meter is situated 0.20 m above the base of the flume, where it records azimuthal (tangential) and vertical components of the flow field. Three Optical Backscatter Sensors (OBS's) are housed in the wall of the flume at heights of 0.02

(OBS2), 0.09 (OBS1), and 0.20 m (OBS3) above the base of the flume. The OBS's are calibrated to suspended sediment mass by pump sampling from three ports in the side of Lab Carousel at the heights of the OBS's. Samples were collected approximately two minutes after each increase in lid rotation. Approximately 200 ml were filtered through Millipore, glass fibre filters. The tared dry weight was plotted against OBS voltage output and a least-squares, best fit regression line derived.

Data on the two components of current speed and the three OBS channels are logged at 1 Hz using a Campbell Scientific CR10 data logger. All data are stored on a PC which is interfaced to the data logger via an RS232 link. A Hi8 Sony video camera records bed erosion and flow in the lower 30 mm of the water column. The video is used to examine the depth of bed erosion, the size and mechanics of bed erosion, the presence and nature of bedload transport (surface creep or saltation), as well as the presence or absence of a viscous sub-layer, and the velocity gradient in the lowermost parts of the benthic boundary layer. Each experiment was carried out in a manner similar to that adopted with Sea Carousel. That is, the current speed was increased incrementally in a series of steps, each step lasting 15 to 20 minutes. The experiment terminated when saturation of the OBS sensors took place; at which point the flow was stopped and a period of mass settling was monitored.

A series of experiments was undertaken using natural seawater collected at Hall's Harbour, Bay of Fundy, Nova Scotia. A bulk sample from station FA3 was used in the laboratory study. A description of the method of emplacement and the procedures is found in Sigouin and MacDonald (1994). In summary, bed was moulded onto the base of the flume with a spatula. This was done because of time delays in settling experienced earlier. The bed was smoothed and subsequently inundated slowly with seawater. No attempt was made to suppress the growth of microorganisms.

### 8.5.2 Sensor Calibration

Only two OBS sensors were operating during this series of experiments (OBS1 - the middle sensor; and OBS2 - the lower sensor). The calibration of these sensors to suspended sediment concentration (SSC) showed considerable scatter (Figures 8.32 and 8.33). Nevertheless, the following relationships were derived for a concentration range of  $0 < \text{SSC} < 3500 \text{ mg/L}$ :

$$\begin{aligned} \text{SSC1} &= -0.399 + 0.0014(\text{OBS1}) \text{ g/L}; r^2 = 0.84 \\ \text{SSC2} &= -0.637 + 0.0017(\text{OBS2}) \text{ g/L}; r^2 = 0.89 \end{aligned}$$

where the OBS outputs are in millivolts.

Sigouin and MacDonald (1994) used lid rotation as their index of flow. We have correlated this with observed current speed ( $U_y$ ). The observations were made from high-resolution video tapes taken of the lowermost 5 cm of the after column. Particle trajectories were determined and the distanced travelled over each frame was used to compute the current speed. The resulting correlation with lid rotation (ROT) is shown in Figure 8.34. The relationship follows the linear function:

$$U_y = 1.46 + 300(\text{ROT}) \text{ cm/s}; r^2 = 0.98$$

where ROT is measured in hertz. In a similar fashion, the EM flow meter installed in the Laboratory Carousel has been calibrated against the video observations. Again, a highly significant linear relationship was found between the two variables of the form:

$$U_y = 3.03 - 0.222(EM) \text{ cm/s; } r^2 = 0.98$$

where EM is the output of the EM current meter in millivolts. This relationship is shown in Figure 8.35.

## 8.6 Results

### 8.6.1 Summary

Three (3) laboratory experiments were carried out on an emplaced sample from station FA3. The first experiment (LE1) was undertaken on remoulded material. Two subsequent laboratory experiments were carried out (LE2 and LE3). In these cases, the bed was redeposited from suspension, thus mimicking the natural process of sedimentation. A summary of these experiments, the consolidation times, and the erosive characteristics is given in Table 8.8.

EXPERIMENT NUMBER	SETTLING TIME (days)	WATER TEMP(C)	EROSION THRESHOLD (Pa)	FRICTION ANGLE (degrees)
LE1	--	22	1.1	-54
LE2	4	22	0.8	-43
LE3	7	24	1.5	-37

**Table 8.8.** A summary of results on the erosion of sediments from FA3 using Lab Carousel.

Time-series of the three experiments are given in Figures 8.36 to 8.38. The material used in the test and the method of bed emplacement have been described by Sigouin and MacDonald (1994). The material used in this study was collected from the region of grey mud at station FA3, approximately 1 km downstream of Fort Anne. The time-series show that all experiments were influenced by an unsteady current speed and by sensor saturation during the mid portions of the experiments. The results from this study should be viewed, therefore, only as a guide.

Each experiment lasted about two hours. Current speed was increased in a series of steps up to a peak of 0.4 m/s. The duration of each step in speed was about 15 minutes. Erosion was terminated once the OBS sensors became saturated, at which point a phase of settling commenced. In experiment LE1, settling took place in still water. In experiments LE2 and LE3, settling took place under a series of decreasing current speeds.

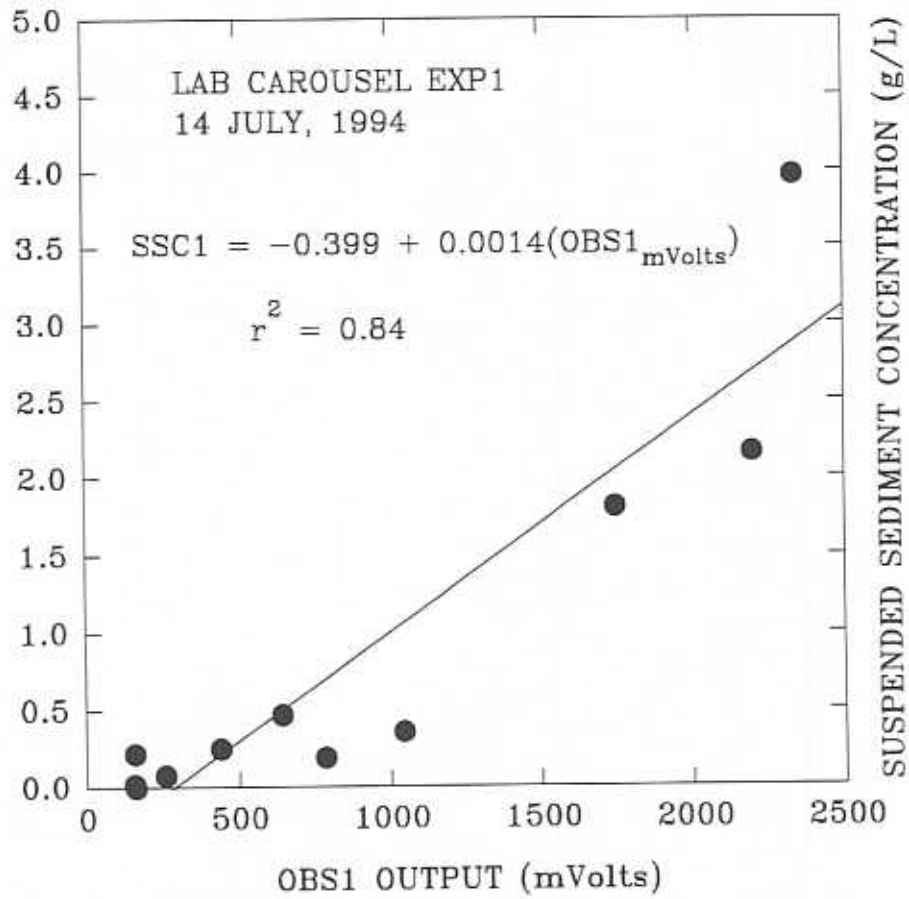


Figure 8.32 Calibration of optical backscatter sensors in ACER Laboratory Carousel experiments, Run 1.

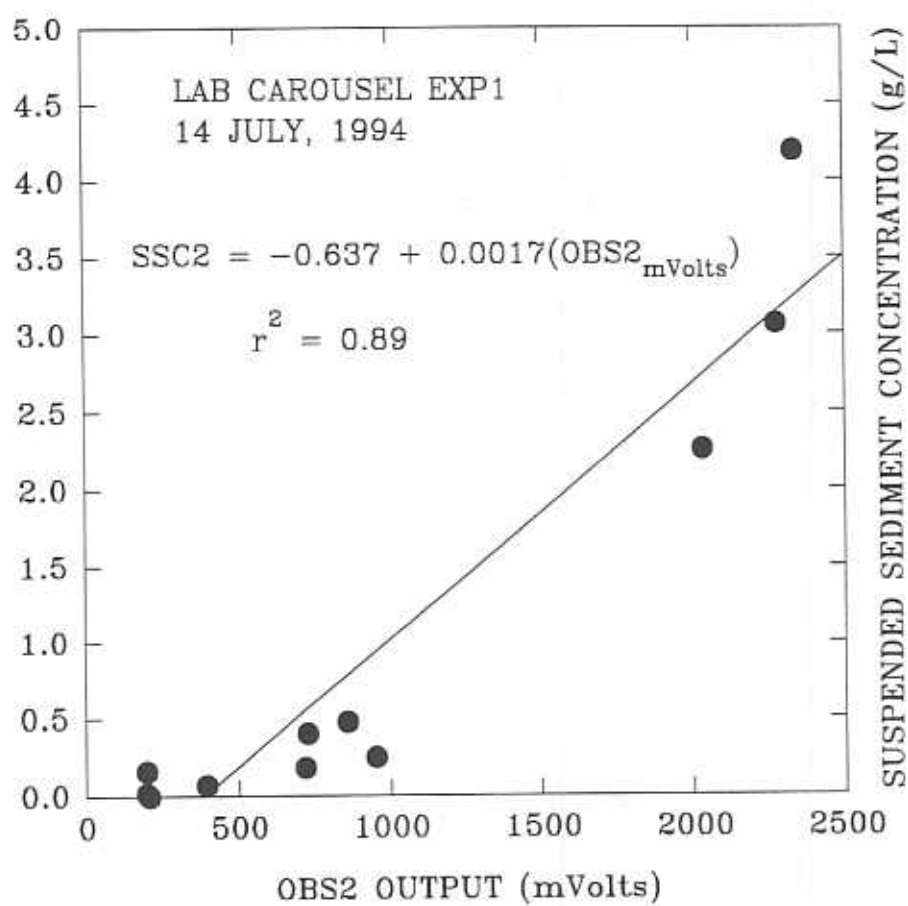


Figure 8.33 Calibration of optical backscatter sensors in ACER Laboratory Carousel experiments, Run 2.



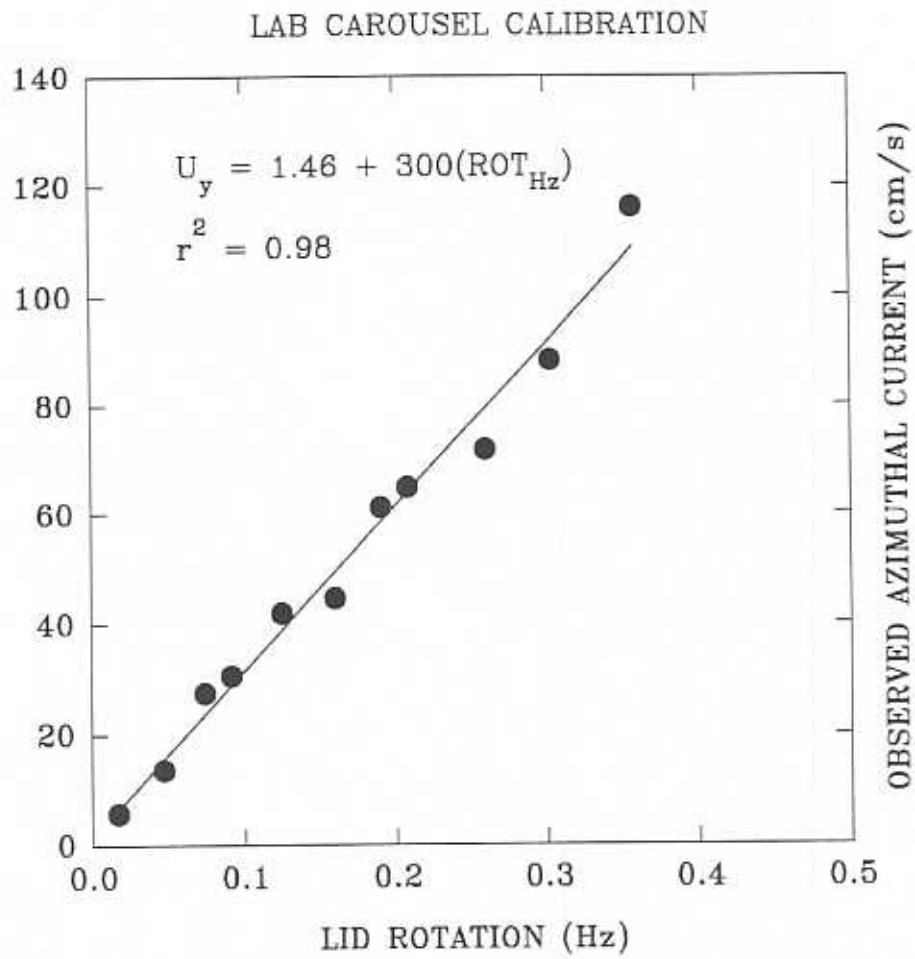


Figure 8.34 Relationship between lid rotation of ACER Laboratory Carousel and measured current velocity.

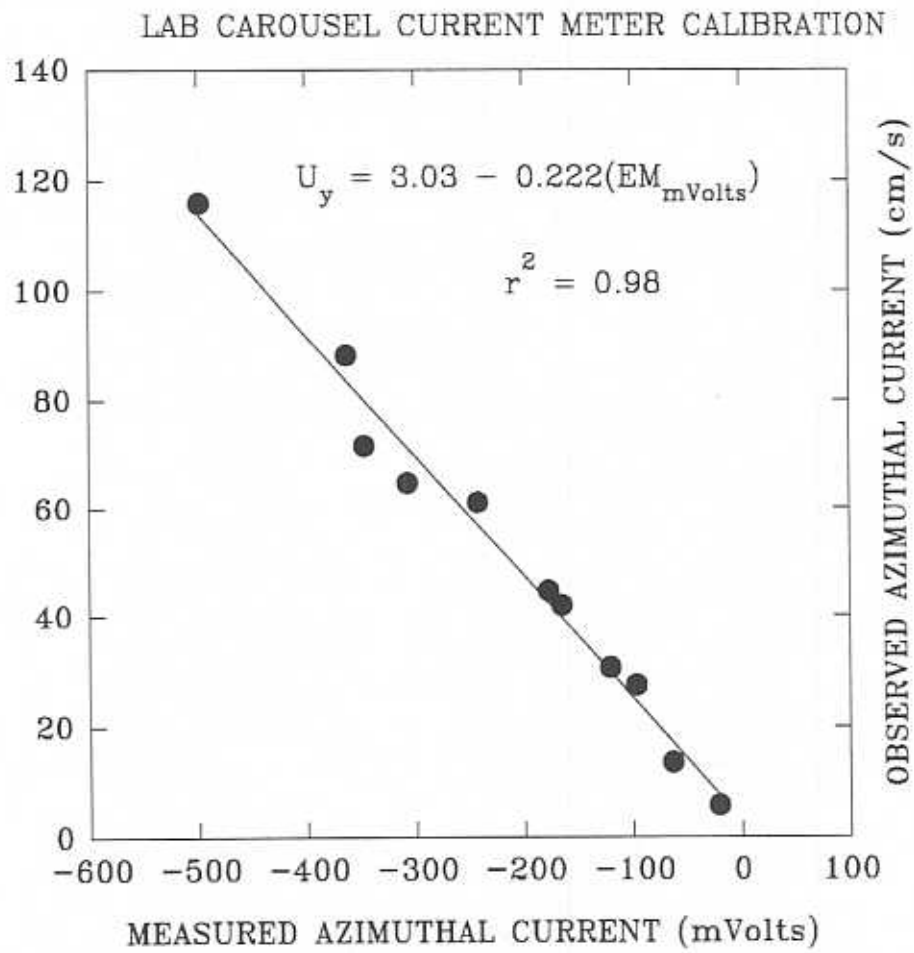


Figure 8.35 Correlation between Electromagnetic Current Meter reading and velocity estimated from video record.

## LAB CAROUSEL - EXP1

FORT ANNE (FA3) - 14 JULY, 1994

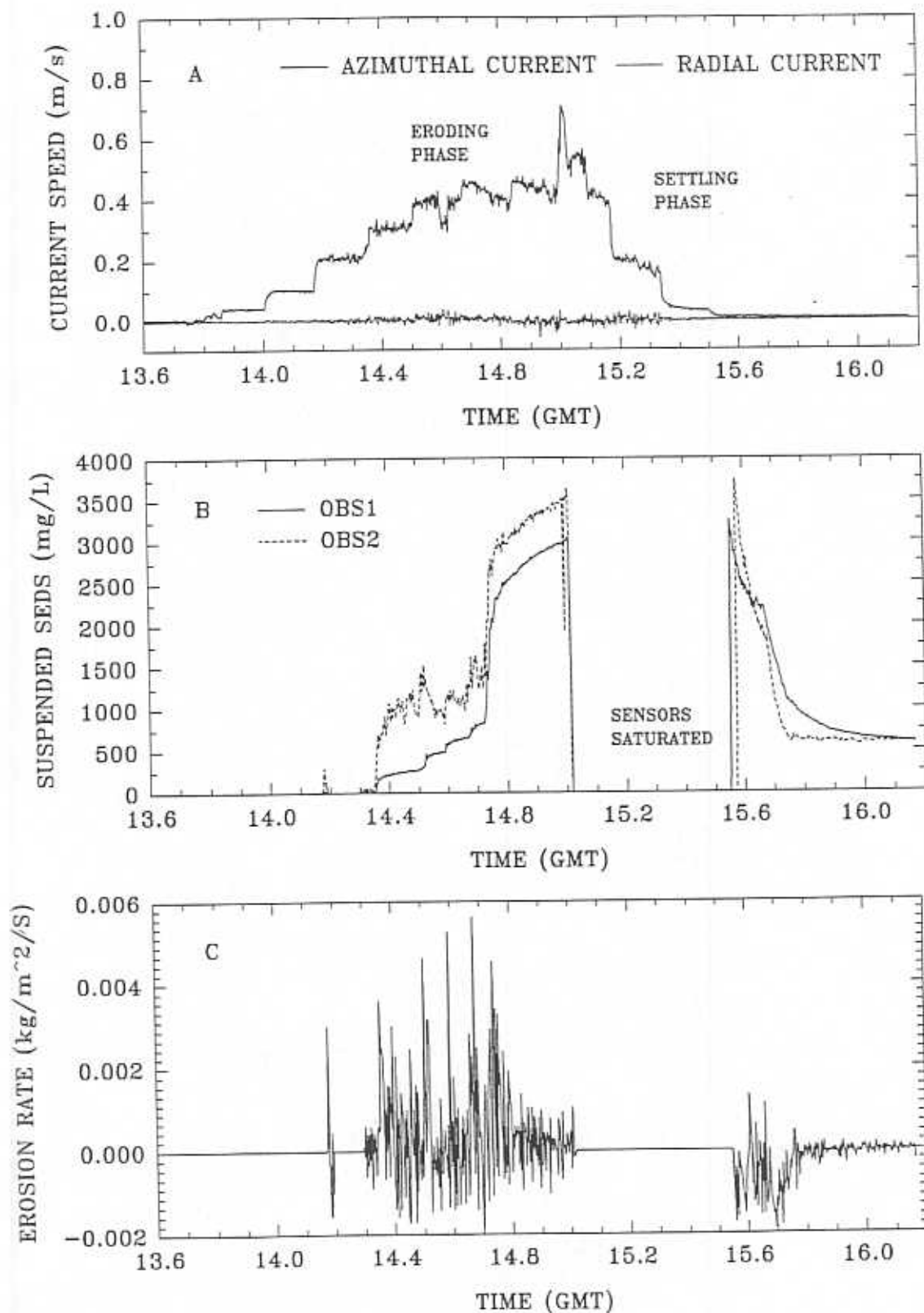


Figure 8.36 Time series of ACER Laboratory Carousel experiment using sediment from anchor station S3, Run 1.

LAB CAROUSEL - EXP2  
FORT ANNE (FA3) - 18 JULY, 1994

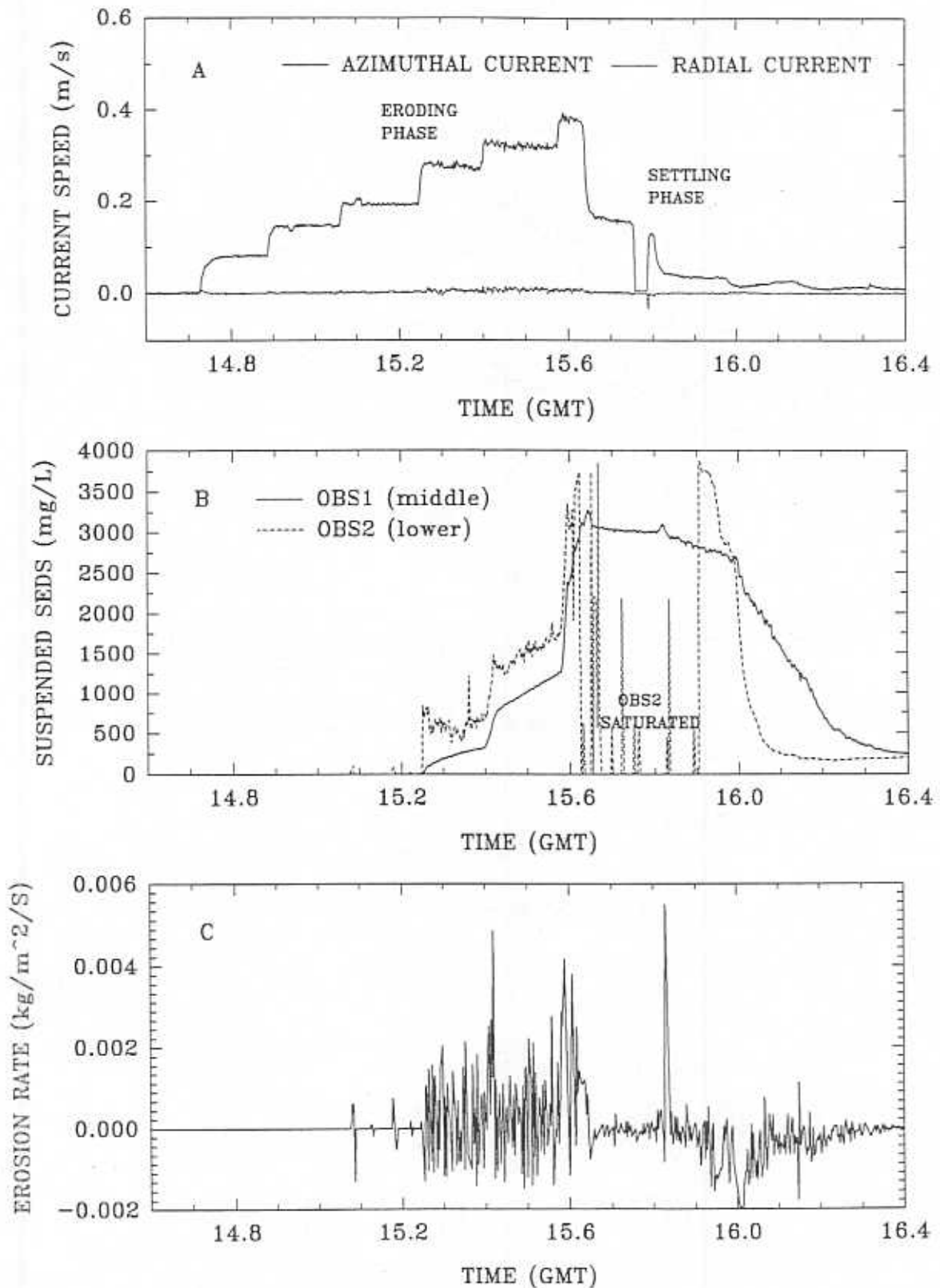


Figure 8.37 Time series of ACER Laboratory Carousel experiment using sediment from anchor station S3, Run 2.

LAB CAROUSEL - EXP3  
FORT ANNE (FA3) - 25 JULY, 1994

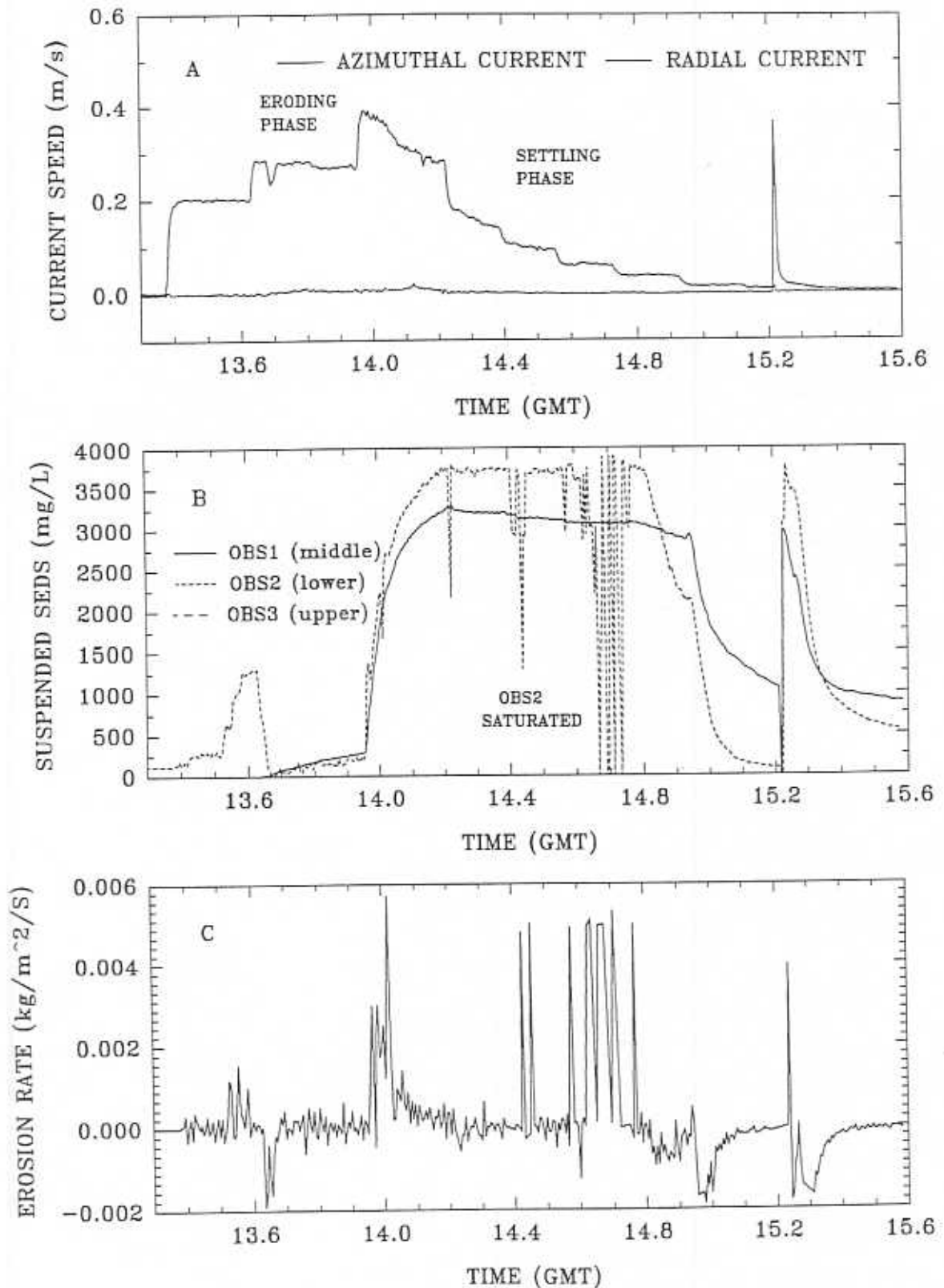


Figure 8.38 Time series of ACER Laboratory Carousel experiment using sediment from anchor station S3, Run 3.

### 8.6.2 Threshold Stresses for Bed Erosion

The threshold for erosion was determined in the same fashion as for Sea Carousel. That is, synthetic cores were produced as described by Amos and Gibson (1994). Plots of the synthetic cores for the three experiments are shown in Figures 8.39 to 8.41. The erosion thresholds are defined as the surface intercept of the failure envelope (solid line) shown in the synthetic core plots. The failure envelope is the line that joins points of minimum bed strength with depth. The sediment strength varied in proportion with the settling time between 0.8 and 1.5 Pa. To reiterate, the initial bed was placed on the flume bed by spatula, and therefore was remoulded in air. The effect on remoulding can be seen in Figure 8.39. Notice the shear zone and the abrupt changes in slope of the failure envelope that are diagnostic of layers of differing strength. Also notice that the greatest strength was in the topmost 2 mm and that strength decreased with depth (resulting in a negative friction angle).

The second and third experiments were undertaken on material that was deposited from suspension during the previous erosion experiment. These beds perhaps simulate nature more accurately than does bed emplacement. The erosion threshold of the second experiment is lower than the emplaced bed threshold, but shows a well ordered distribution of strength against depth that has also been found in the Sea Carousel. Again, the maximum strength is at the surface. This may be related to the development of a biofilm and associated adhesion. The thickness of the film was less than 2 mm in experiment LE2. By the third experiment, the erosion threshold has increased to 1.5 Pa and the "biofilm" had thickened to 4 mm. The strength of these sediments greatly exceeds those reported by Sea Carousel. We propose that water temperature plays a strong role in mediating the Laboratory Carousel results which were undertaken in water between 22 and 24°C (salinity 30 ppt). Microbial (i.e., bacterial and/or fungal) activity may be presumed to be high. The inner stations in Annapolis Basin were at a field water temperature of between 10 and 12°C (salinity 30 ppt) where microbial activity would be expected to be lower.

The obvious outcome of the above findings is that the measured bed strength is a product of the way the bed is laid down, the temperature of the water, and the duration of settling, consolidation, and biostabilization.

### 8.6.3 Erosion Rates

Bed erosion ( $E$ ) in experiment LE1 did not show the well ordered Type I trends, but were highly time-variable (Figure 8.36). Experiment LE2, by contrast, showed continuous erosion beyond an initial erosion peak (Type I/II; Figure 8.37). Experiment LE3 (Figure 8.38) showed a single case of Type I erosion, whereupon the entire bed was eroded at one speed increment. The net bed erosion appeared to be about the same in the laboratory experiments as in Sea Carousel because of the similar final concentrations in suspension (3000 - 4000 mg/L). Also, the erosion rates were of the same order as found *in situ* at station FA2. These erosion rates are plotted with the Sea Carousel results in Figure 8.42. Notice that the laboratory erosion rates appear to be in continuity with the field results, varying in linear proportion with the applied bed shear stress ( $\tau$ ). The best-fit regression line suggests that this function is:

$$E = 0.00026\tau \text{ kg/m}^2/\text{s}; r^2 = 0.63$$

## LAB CAROUSEL EXP1 - ANNAPOLIS BASIN

SAMPLE FA3 - 14 JULY, 1994

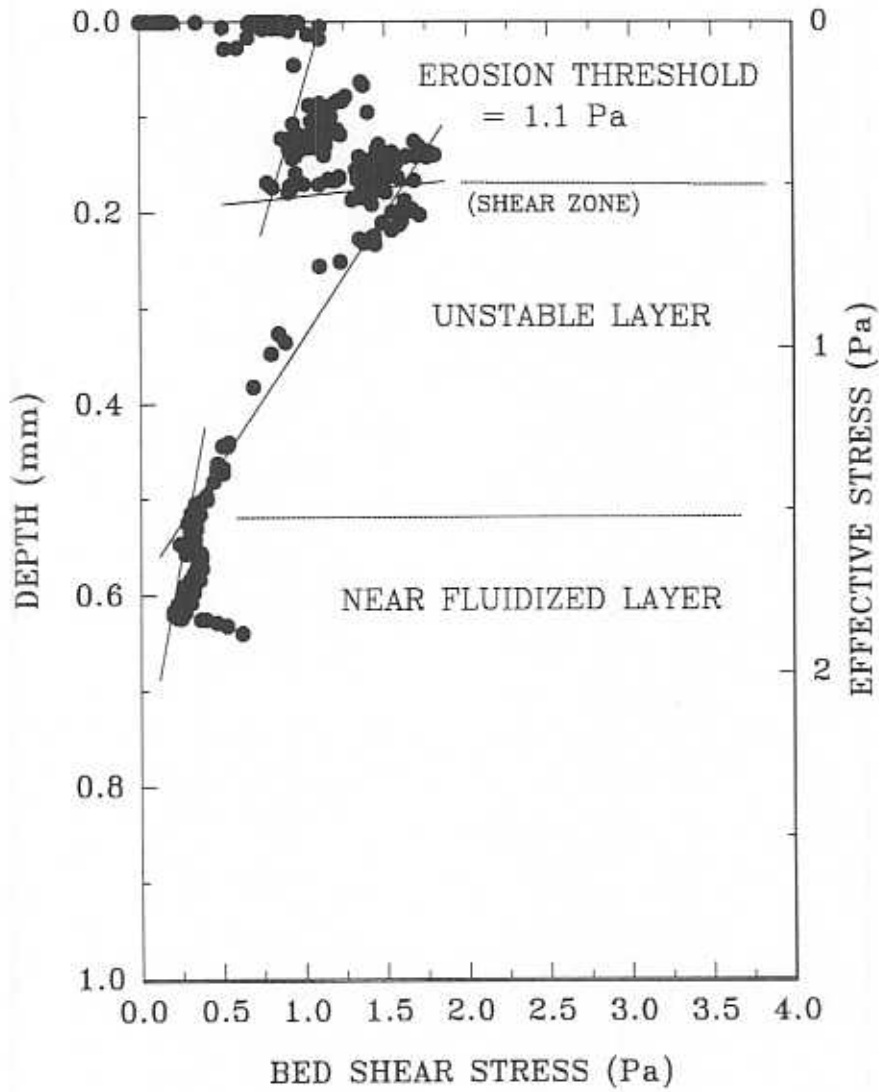


Figure 8.39 Relationship between shear stress and depth in sediment, ACER Laboratory Carousel, Run 1.

## LAB CAROUSEL EXP2 - ANNAPOLIS BASIN

SAMPLE FA3 - 18 JULY, 1994

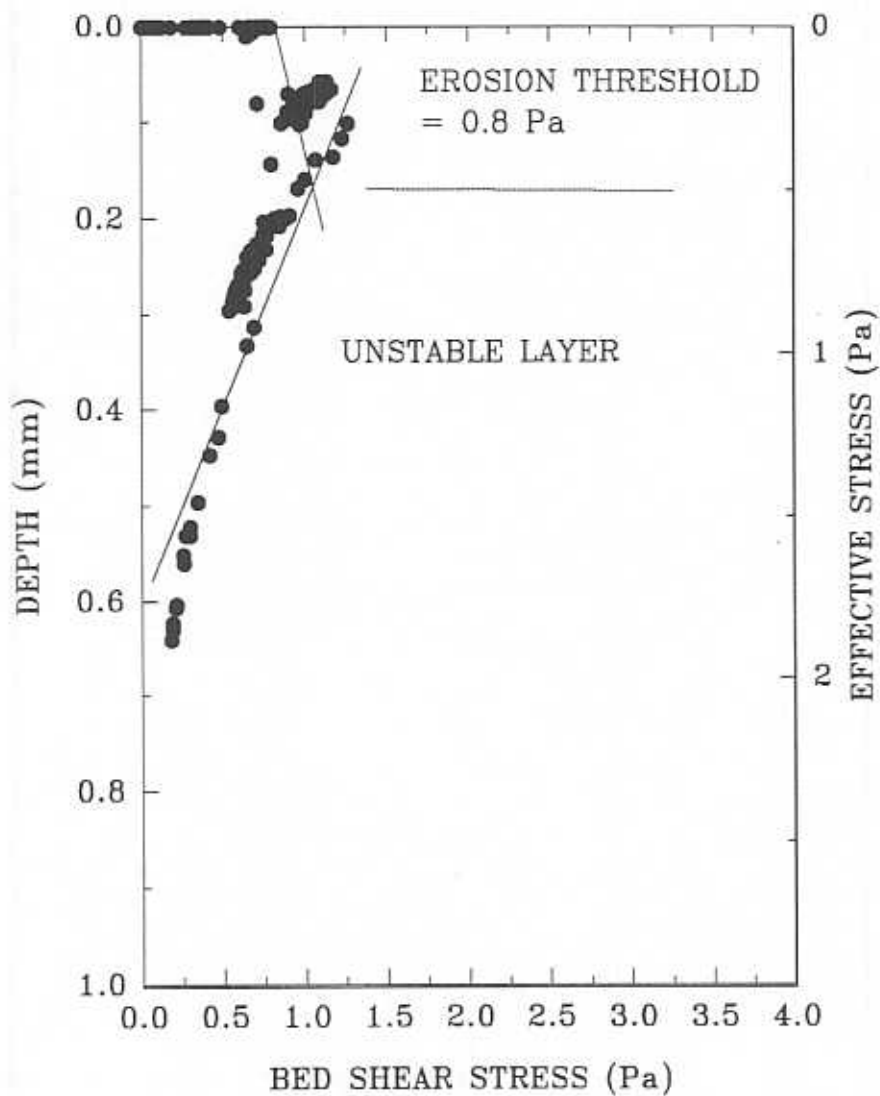


Figure 8.40 Relationship between shear stress and depth in sediment, ACER Laboratory Carousel, Run 2.



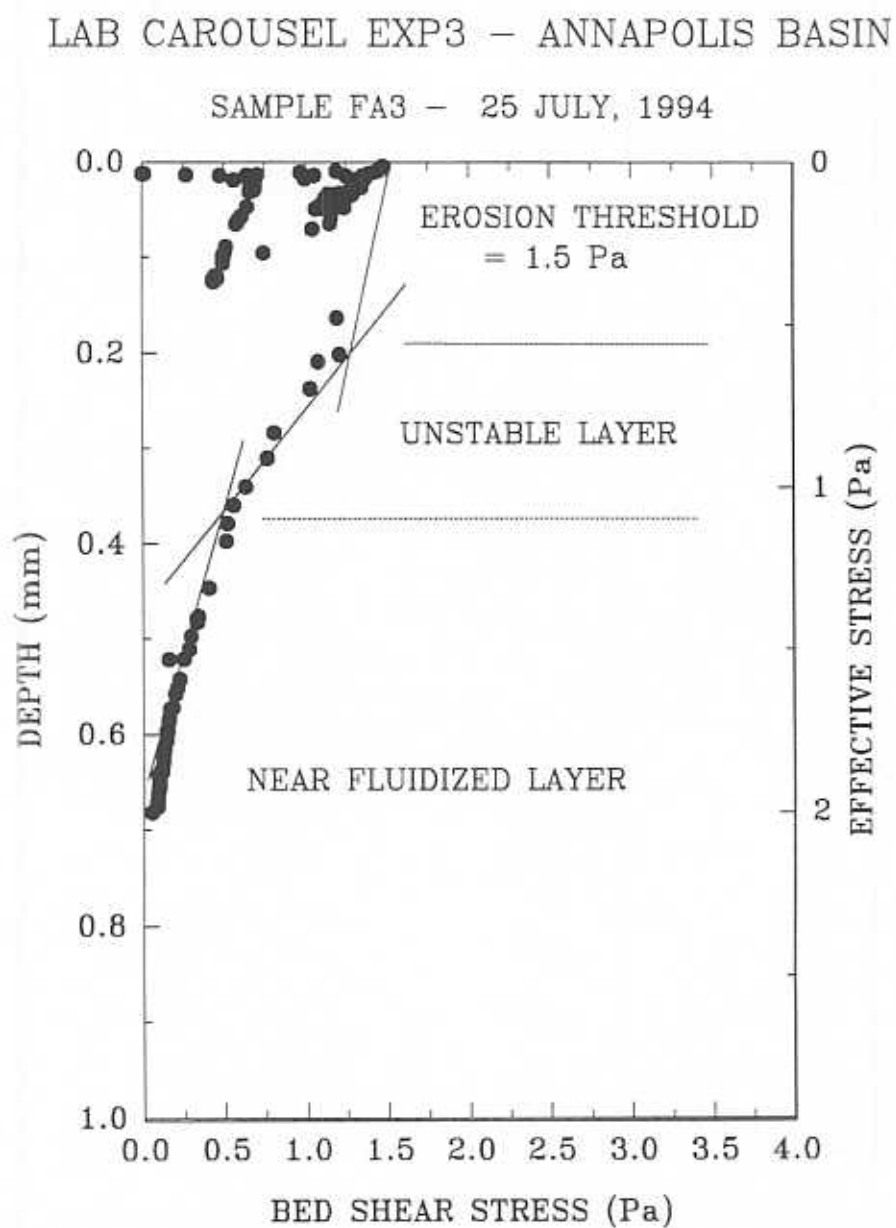


Figure 8.41 Relationship between shear stress and depth in sediment, ACER Laboratory Carousel, Run 3.

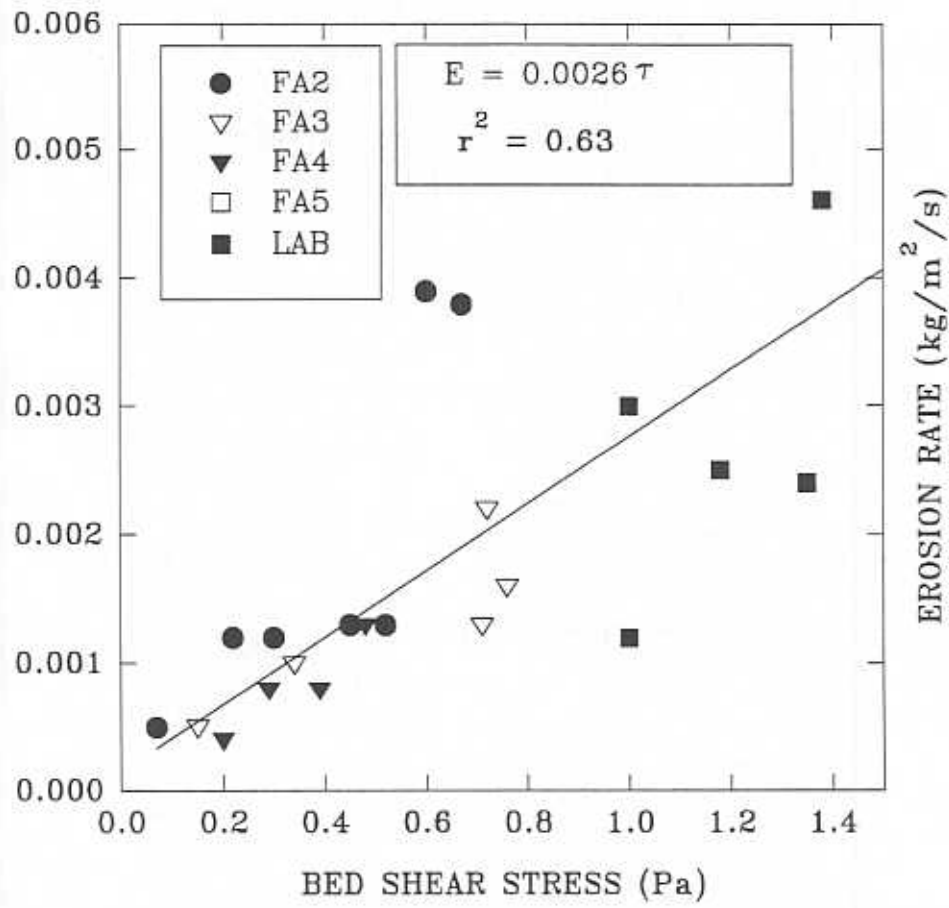


Figure 8.42 Comparison of Laboratory and Sea Carousel determinations of relationship between shear stress and erosion rate.

The regression line appears to pass through the origin, suggesting that the erosion rate is a function of the applied bed shear stress and not the excess stress ( $\tau - \tau_c$ ). The erosion rate versus bed stress for the lab experiments must form a step function:  $\tau_c$  was high (0.8 to 1.5 Pa) and below  $\tau_c$  there was no erosion. Thus we may express the erosion process in a more accurate form as follows:

$$E = 0.00026\tau \text{ kg/m}^2/\text{s}; \tau > \tau_c.$$

STATION	EROSION RATE (kg/m <sup>2</sup> /s)	BED STRESS (Pa)
EXP1	2.4 x 10 <sup>-3</sup>	1.35
EXP1	4.6 x 10 <sup>-3</sup>	1.38
EXP1	5.3 x 10 <sup>-3</sup>	1.68
EXP2	1.1 x 10 <sup>-3</sup>	1.00
EXP2	2.5 x 10 <sup>-3</sup>	1.18
EXP3	3.0 x 10 <sup>-3</sup>	1.00

Table 8.9. The peak erosion rates (EP) and prevailing bed shear stresses during the erosion of station FA3 grey mud in the Laboratory Carousel.

#### 8.6.4 Deposition Rates

The still water mass settling rate for the grey mud has been determined following a method given in Amos and Mosher (1985). The resulting value was  $2.32 \times 10^{-4}$  m/s. This value is approximately 30% of the field values for station FA3, and about 70% of the values reported by Sigouin and MacDonald (1994). We interpret this relatively low settling rate to be the result of remoulding the field sediment during bed emplacement. This would have the effect of breaking down bonds and aggregates to form smaller particles which would thus settle at a slower rate.

The critical threshold for deposition ( $\tau_d$ ) was evaluated following a method given by D. Willis (personal communication, 1994). This method has also been followed by Sigouin and MacDonald (1994). The method involves inverting the following equation:

$$\delta M/\delta t = W_s C_o [(\tau_d - \tau)/\tau_d]$$

where  $\delta M/\delta t$  is the mass deposition rate (kg/m<sup>2</sup>/s), found through the decrease in SSC with time,  $\tau$  is the applied stress of the moving flow in which the sediment is settling, and  $W_s$  is the mass settling rate derived following Amos and Mosher (1985). The only remaining unknown is thus  $\tau_d$ , which can thereafter be derived. Following recent discussions with D. Willis, and applying the above method, the corrected mean values of  $\tau_d$  for the NRC experiments are:

$$\begin{aligned}\tau_d(\text{red mud}) &= 0.23 \text{ Pa} \\ \tau_d(\text{grey mud}) &= 0.20 \text{ Pa}.\end{aligned}$$

We repeated the above method using data from experiment LE2. The variables in this experiment were as follows:

$$C_o = 3057 \text{ kg/m}^3$$

$$\begin{aligned}W_s &= 2.32 \times 10^{-4} \text{ m/s} \\ \tau &= 0.13 \text{ Pa} \\ \delta M/\delta t &= 0.208 \text{ kg/m}^2/\text{s}\end{aligned}$$

Thus the following equation results:

$$0.208 = 0.703(1) - 0.703(0.13/\tau_c)$$

and  $\tau_c = (0.703 \times 0.13)/(0.703 - 0.208) = 0.18 \text{ Pa}$ .

The resulting deposition threshold was estimated to be 0.18 Pa, which is about 10% below the values derived by NRC. Given the uncertainties of the Lab Carousel data and the lack of repetition, the results are remarkably close.

### **8.7 Interpretations**

The laboratory methods reported herein appear to be a valuable adjunct to field work in providing information not always available in the field. In particular, the rate of biostabilization can be evaluated, as well as the factors which influence the stabilization. We have found that the erosion thresholds appear to vary according to settling/biostabilization time, and method of bed emplacement. Consequently, it cannot be considered an accurate representation of field conditions. By contrast, the rate of erosion (once the erosion threshold has been exceeded) appears to fall in continuity with field data, suggesting that lab work can extend limited field observation of this parameter.

The greatest value of this laboratory work has been in defining the critical threshold for deposition. This parameter cannot be determined as yet in the field because of the complicating effects of dispersion from the flume. Estimates on this threshold appear to be consistent between the NRC results and those collected at Acadia University. It is noted, however, that the still water settling rates that we derived were up to 70% lower than field measurements and 30% lower than NRC estimates. The reasons for these discrepancies are unknown.

## **9.0 BIOLOGICAL CONSTITUENTS OF THE ANNAPOLIS BASIN AND ESTUARY**

Graham R. Daborn  
Acadia Centre for Estuarine Research  
Acadia University

### **9.1 Introduction**

The central problem addressed by the present study related to the conditions that have given rise to recent erosion of the shoreline at Fort Anne, and the dynamic relationships that determine the options by which the shoreline can be protected against erosion in the future. In order to design appropriate remedial measures, it was agreed that a hydrodynamic and sedimentological model would be useful. The results described in previous sections of this report relate to a suite of field investigations aimed at providing necessary information for the construction, calibration and verification of the models. Principal among these are the measurements of current velocity, grain size, and the erodibility of deposited sediments (Sections 5 and 8). In addition, factors affecting the stability of the embankment of the Fort were examined to provide a basis for remedial action.

Although grain size and composition are regarded as fundamental factors affecting the erodibility or stability of deposited sediments, it is also well recognised that living organisms and biological processes can significantly affect these phenomena. For these reasons, we investigated the dominant fauna occurring in the sediments at the anchor stations, and at a series of sample sites forming a transect across the beach at Fort Anne. Methods are described in Section 4.

### **9.2 Subtidal Benthic Fauna**

Benthic organisms play varied roles in relation to sediment behaviour. Some polychaetes (worms) and crustaceans construct burrows in the surface sediment that they line with mucus or sand grains glued together, which have the effect of stabilising the deposit, creating a fabric that generally exhibits greater strength than the sediment would otherwise possess. The burrowing activities of some tend to disturb the sediment and destroy any micro-scale fabric that may be important in holding individual grains together. Deposit-feeding animals ingest the sediment, stripping off the diatom, bacteria and organic matter coatings that may be responsible for much particle-particle adhesion, and that coincidentally constitute their food. Since much of their ingestion is inert sediment, they produce copious amounts of undigested (fecal) waste that may be extruded as coils or strings onto the sediment surface, increasing its effective roughness. Suspension-feeding animals filter particles from the overlying water, decreasing the suspended load, and also creating a deposit from their waste. Thus, benthic organisms play diverse and poorly understood roles in the processes leading to accretion and erosion of sediments.

The benthic fauna of subtidal areas of the Annapolis Basin and Estuary includes more than 50 species (cf. Appendix D, Section 13.3), the majority of which are polychaetes. The total number of organisms, and abundance of each of the major taxa found in grab samples are shown in Figures 9.1 and 9.2. Data are presented as the average number ( $\pm 1$  standard deviation) of organisms found in the five or six separate Ekman grab samples taken at each station. No samples were taken at station S1 near the Annapolis Causeway, because the rocky bottom in this location prevented sampling with the equipment available.

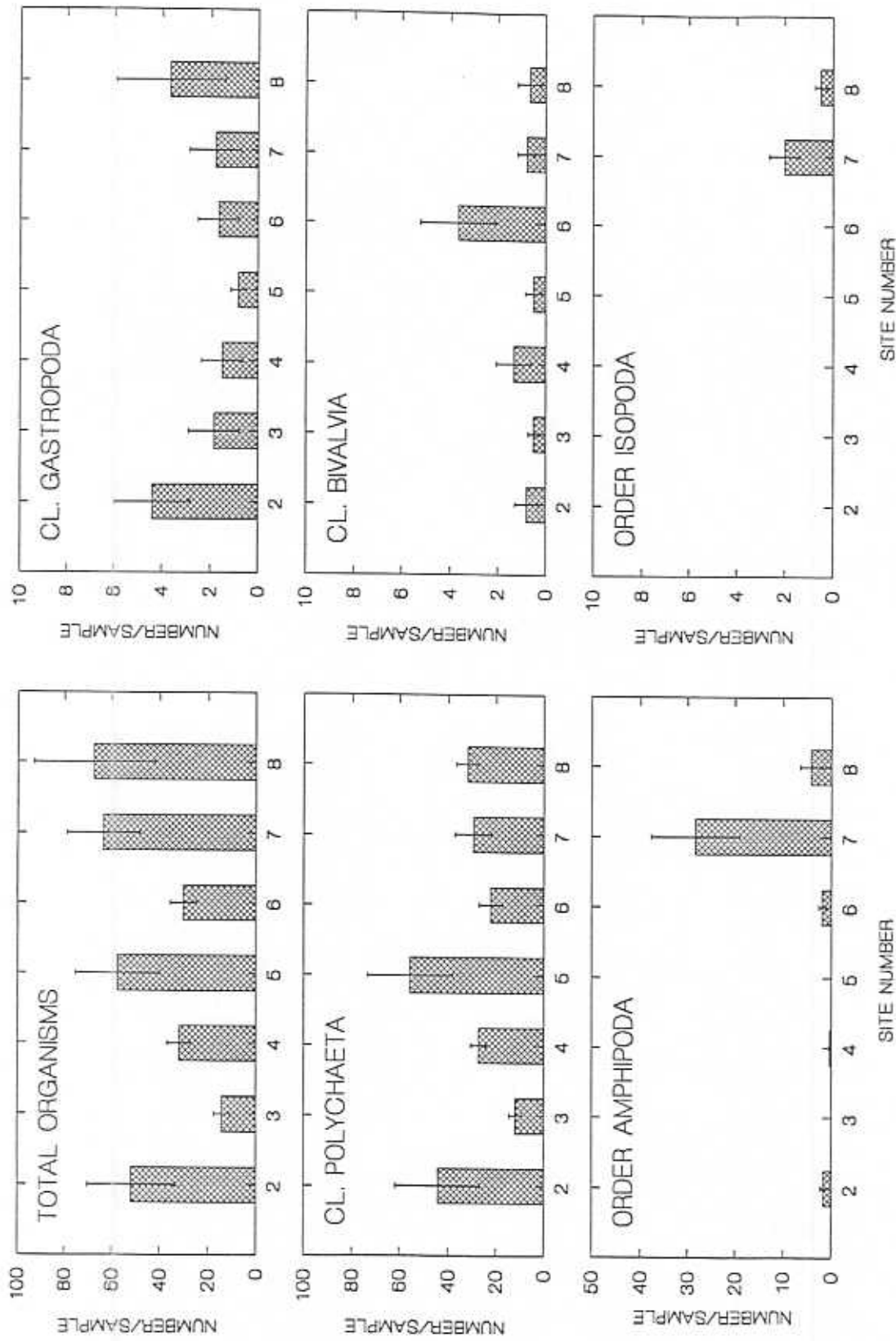


Figure 9.1 Abundance of benthic organisms at stations S2 to S8 in the Annapolis Basin and Estuary, 1994.

Total abundance varied from less than 10 per sample to more than 90 (representing <482 to >4300 organisms.m<sup>-2</sup>, respectively). Relatively high numbers were found at stations S2 and S5 in the Estuary, and stations S7 and S8 in the Basin; lower numbers were encountered at stations S3, S4 and S6.

Station S2, which is nearest to Fort Anne, apparently exhibits a relatively abundant fauna, dominated by polychaetes and gastropods. In fact, the numbers may be inflated by a single sample that contained over 100 worms, constituting almost half of all the animals caught in five samples. Without that sample, the bottom near Fort Anne would be similar to the adjacent estuary stations. Patchy distributions of benthic organisms are commonly found in estuaries, which is why replicated samples need to be taken.

There are clear differences between the faunas of stations in the Estuary (i.e., stations S2 to S5, east of Goat Island) and those in the Basin. These differences are evident in Figures 9.2 and 9.3.

In the Estuary, the fauna is composed of relatively few species (i.e., is less diverse), and generally dominated by a few taxa such as the marine gastropod (snail) *Nassarius trivittatus*, and the polychaete worms *Chaetozone setosa*, and *Nephtys neotenus*. These species are typical of muddy estuarine environments (Brinkhurst *et al.* 1976, Bromley and Bleakney 1984). The dog whelk, *Nassarius*, is a predator of benthic animals, as is the common burrowing polychaete *Nephtys* (Wildish *et al.* 1983). Movements of these species in search of prey tend to disrupt the fabric of the surface sediment, increasing its roughness, and favouring mobilisation. *Chaetozone*, however, is a burrowing deposit-feeder, which may play a complex role in stabilising the sediment by construction of its burrows, or in disturbing the sediment surface through its feeding activities. Control of deposit-feeders by predators may result in growth of microflora, especially benthic diatoms, that often play a role in biostabilisation (Paterson and Daborn 1991, Daborn *et al.* 1993b).

Because of the variation in the numbers found in five adjacent samples (cf. Appendix D), it is not certain whether the subtidal area near Fort Anne (station 2) is really different from the other Estuary stations. Relative abundance of the dominant species is similar at stations S2, S3 and S4, and only slightly different at S5 in the smaller proportion represented by *Chaetozone* (Figure 9.3). Measurements of sediment erodibility using 'Sea Carousel' showed that the surficial sediment at station 2 is much less stable than other stations, and analysis of the gravity core showed that the surface layer consisted of a fine red clay similar to that outcropping on the Fort Anne shoreline (cf. Figure 13.1). It is possible that the greater erodibility and the abundance of *Chaetozone* and *Nassarius* are related, either because the foraging activities of these two species disturb the sediment and break down its structure, or because the red clay at the surface has been redeposited there after being eroded away from the shoreline, and has not undergone consolidation. Observations during 'Sea Carousel' and gravity core sampling indicated that all stations in the Estuary were highly bioturbated, resulting in high water contents (see below and Section 8) and low bulk density.



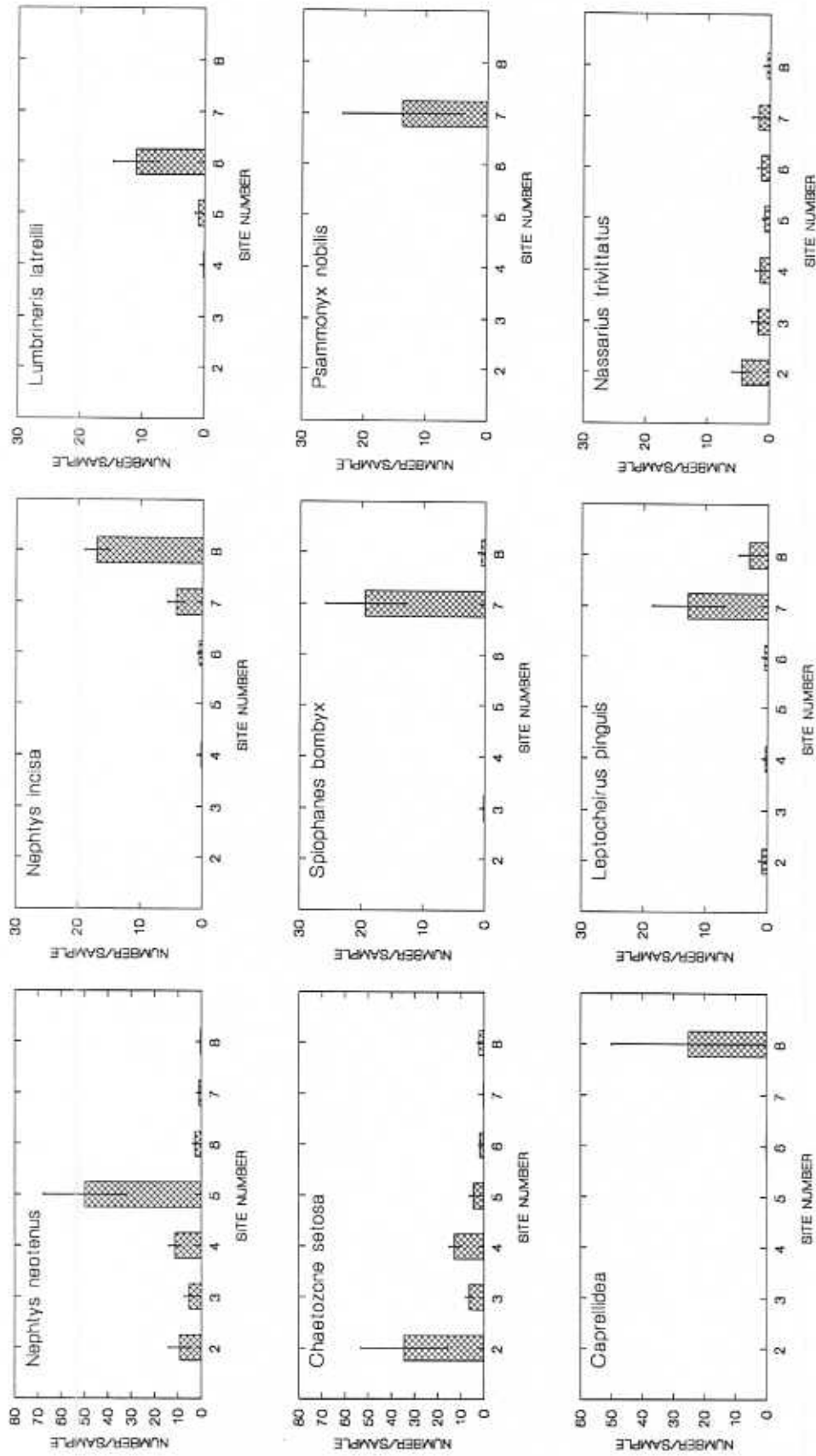


Figure 9.2 Abundance of dominant benthic species in the Annapolis Basin and Estuary, 1994.



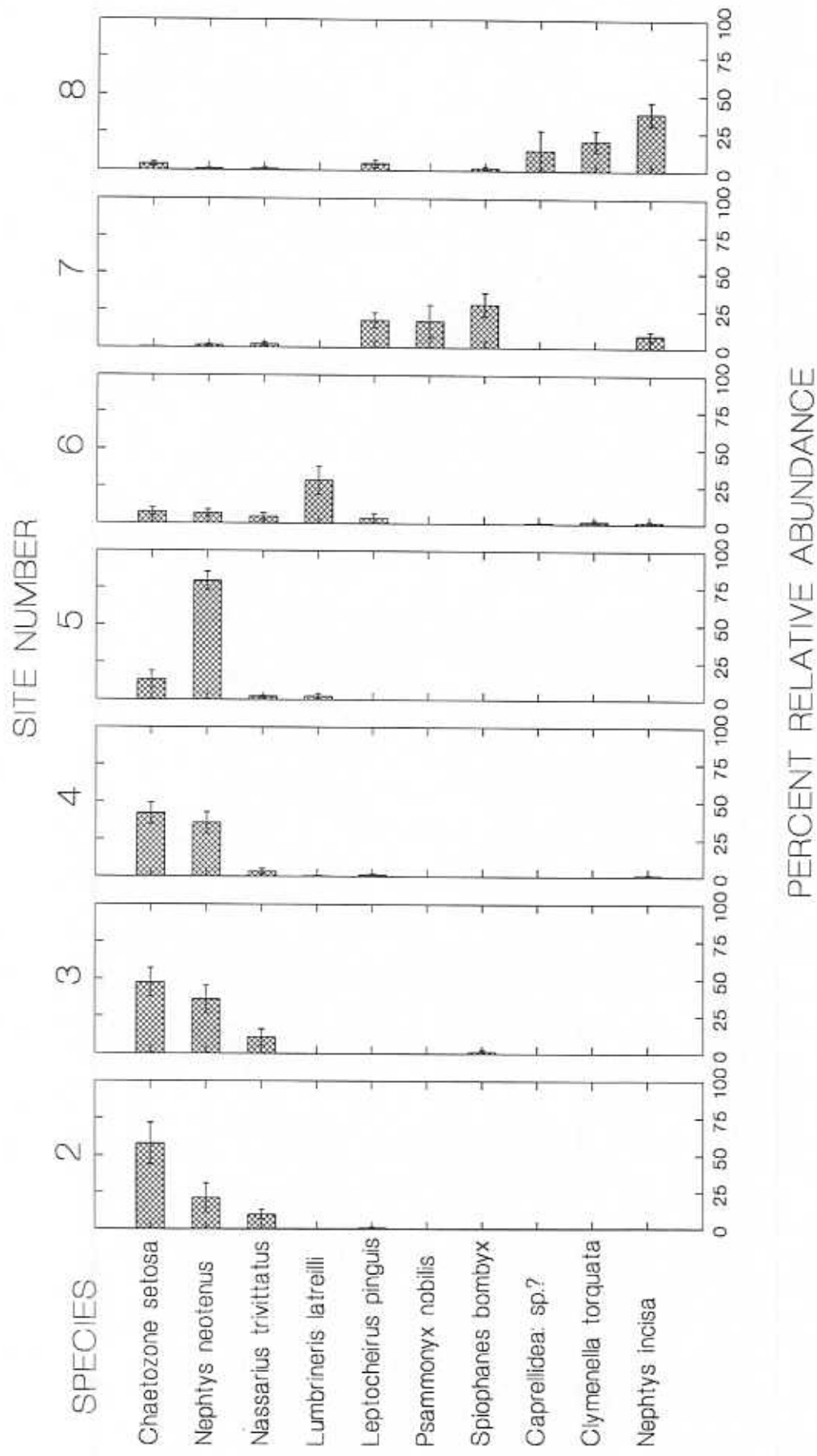


Figure 9.3 Relative abundance of dominant benthic species at stations S2 to S8 in the Annapolis Basin and Estuary, 1994.

These dominant forms of the estuary, however, are largely absent from the Basin stations, where currents are stronger and, consequently, sediments are more sandy. At stations S6 to S8, the variety of species is greater, as well as the abundance. Although polychaetes still dominate, several other taxa are more prevalent, including crustaceans (*Leptocheirus*, *Ampelisca* and *Psammonyx*). Because of the small size and shallow depth of penetration of the Ekman sampler used, some of the deeper-dwelling organisms such as some bivalves, and the more active epibenthic animals (e.g., *Crangon septemspinosa*) are inevitably underrepresented. The fauna, however, is otherwise very typical of a well-sorted silty-sand bottom in a coastal environment. Both current velocities and feeding/burrowing activities of the benthos result in continuous disturbance of the sediment surface.

### 9.3 Biological Properties of Subtidal Sediments

Sediments that are subject to extensive biological activity become modified accordingly. Parameters that provide a measure of some of the important biological processes are water content, organic content, carbohydrate and chlorophyll concentrations.

Water content varies partly with grain size, the finer clay-dominated sediments having higher water contents than coarser ones, but it also varies with the degree of bioturbation. Extensive burrowing by benthic organisms irrigates the sediments to depths of several centimetres, limiting consolidation and favouring resuspension. Organic content reflects the intensity of biological production in the water column or the sediments themselves, or possibly the import of organic production from elsewhere. For the same degree of local production, it is usual to find organic content of the finer sediments to be higher than coarser sediments such as sands. Where sediments are exposed to sufficient light at least periodically (e.g., in estuaries with large tidal range such as the Annapolis), and nutrients are available, the sediment surface may be inhabited by diatoms that photosynthesise actively during daylight exposure, releasing quantities of carbohydrates. These carbohydrate exudates have been shown to increase cohesiveness of deposited sediments (Deccho 1990, Paterson and Daborn 1991, Paterson 1994). Other organisms that may contribute carbohydrates to the sediment are bacteria and fungi. Diatoms in the sediments or the water column also release chlorophyll that may accumulate; chlorophyll content thus reflects to some extent the biological activity of that portion of the estuary.

Results of analyses for biological properties of the sediments are shown in Figures 9.4 to 9.6. Except for station S2, results show a steady decline in water content and % organic carbon<sup>1</sup> as one moves seaward (Figure 9.4), corresponding to the gradual coarsening of the sediment. In contrast, carbohydrate (Figure 9.5) and chlorophyll levels (Figure 9.6) generally increase seawards, despite the increase in abundance and diversity of potential grazing organisms that might control benthic diatom populations. The trends are consistent, and produce statistically significant differences in values between the inner Estuary stations, and those of the Basin. The increases in chlorophyll and carbohydrate levels suggest that light plays an important role, since turbidity (i.e., suspended sediment concentration) decreases seawards.

<sup>1</sup> N.B. In Figure 9.4B, % organic content is expressed relative to the dry weight of the sediment, whereas in Table 8.7, results from gravity core samples are expressed as a % of total or wet weight. Despite the apparent differences, the results are compatible.

It is notable that station S2 near Fort Anne, stands out as distinctly different from these trends. Water content and organic carbon content are somewhat lower, whereas carbohydrate concentration is distinctly higher at S2 than at other Estuary stations. Chlorophyll levels are comparable with those at station S3, but somewhat higher than might be expected from the trend suggested by the rise in levels from station S3 through S6.

#### 9.4 Intertidal Fauna

Previous observations have suggested that the red clay outcropping on the foreshore of Fort Anne (cf. Figure 4.6) may be significantly weakened by the colonisation of burrowing benthic animals that introduce water deeper into the sediment (Daborn *et al.* 1993a). When exposed and inundated by the rising tide, the red clay seems to be extremely susceptible to erosion, resulting in a plume of sediment that forms during the flood. Because of the very low settling rate, much of the resuspended particulate material is probably advected away from the shore rather than redeposited. Water samples taken during the ebb tide from the Fort Anne shoreline on 16 June 1994 showed an average suspended particulate matter concentration of  $20.8 \text{ mg.L}^{-1}$  (cf. Appendix E).

A series of core samples (5.7 cm diam) was taken along a transect across the Fort Anne shoreline starting from a College of Geographic Sciences survey pin above exposed cribwork of the southwest ravelin, and extending normal to the tide line through the position of the S4 current meter station #1 (cf. Figures 4.2 and 4.5). The transect was 140 m in length. At intervals of 20 m, three core samples were taken in close proximity to one another according to a random number series. Each was bagged and labelled separately. In the laboratory, samples were sieved through a 0.4 mm screen. Details of sample locations, and a description of sediment conditions based upon observations are included in Figure 9.7.

Only 14 benthic species were recorded in this study; although numerous other larger species (including the mussel *Mytilus edulis* and the green crab *Carcinus maenas*) were observed, their numbers were too few or their size too great to be included in the samples. The principal species found was the burrowing amphipod, *Corophium volutator* (Figure 9.8). This was present in almost all samples, at an average density of 16 per sample, representing overall densities of about  $6,300 \text{ m}^{-2}$ . This is a very much lower abundance than is found in other intertidal areas of the Bay of Fundy where this species is dominant (Daborn *et al.* 1991). The only other species recorded in significant numbers were two polychaetes, *Nephtys neotenus* and *Scolecopides viridis*.

By comparison with other intertidal areas in the Annapolis Basin and Bay of Fundy, these limited results suggest that the foreshore of Fort Anne has a poorly developed benthic fauna. This may be attributed to the instability of the surface associated with continued resuspension, and the high degree of subsurface compaction which may prevent deep burrowing by invertebrates. The burrowing and foraging activities of *Corophium*, however, probably contribute to resuspension phenomena, and as indicated above, may introduce water deeper into the substrate than would otherwise be the case.

If these preliminary results are borne out by more extensive sampling, the low production of this shoreline suggests that remedial actions that involve covering the red clay will not significantly diminish the biological value of the shore. On the contrary, a stabilised rocky surface would probably exhibit both greater biological diversity and biological production.

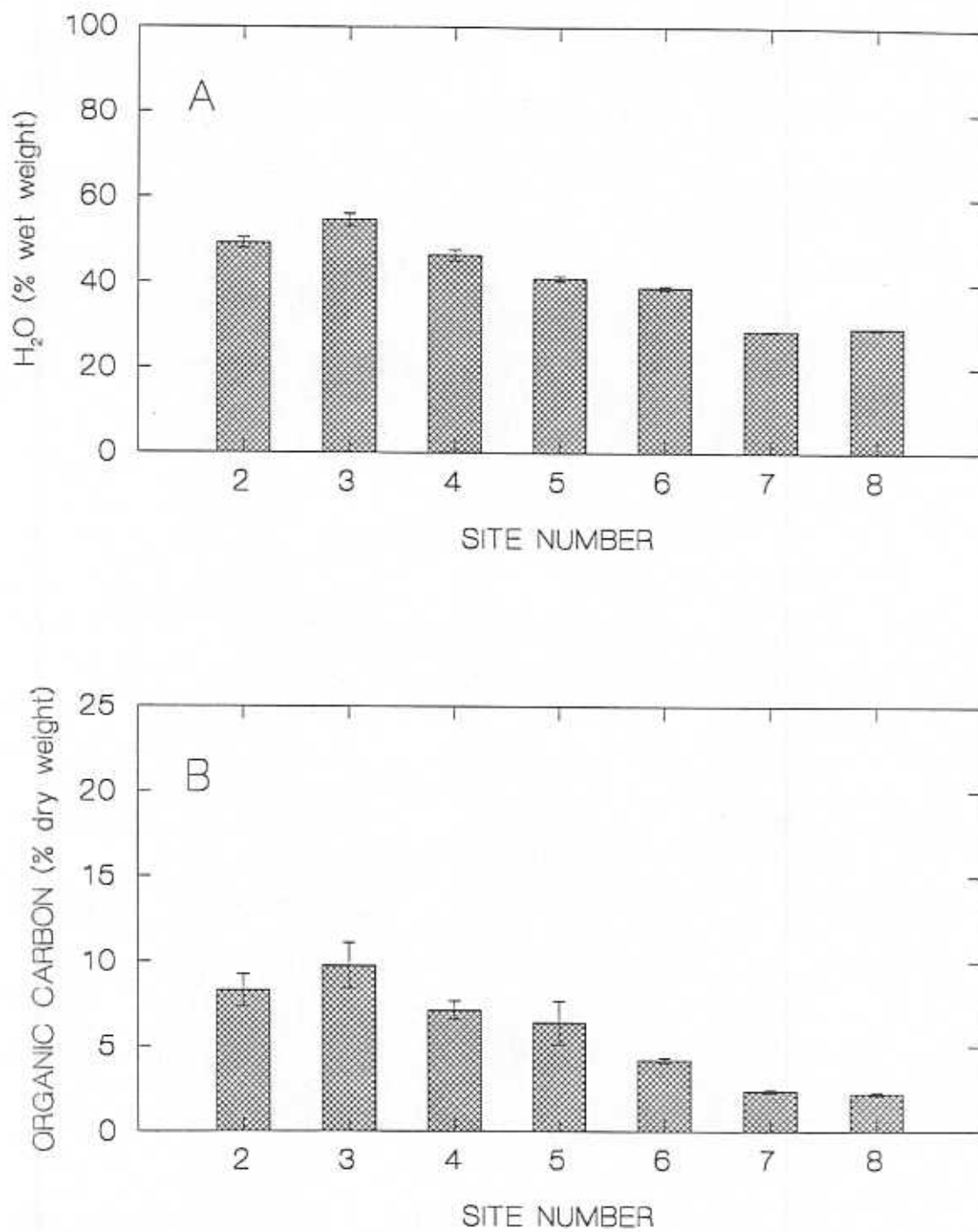


Figure 9.4 Water content and % organic carbon of sediments from stations S2 to S8 in the Annapolis Basin and Estuary, 1994.

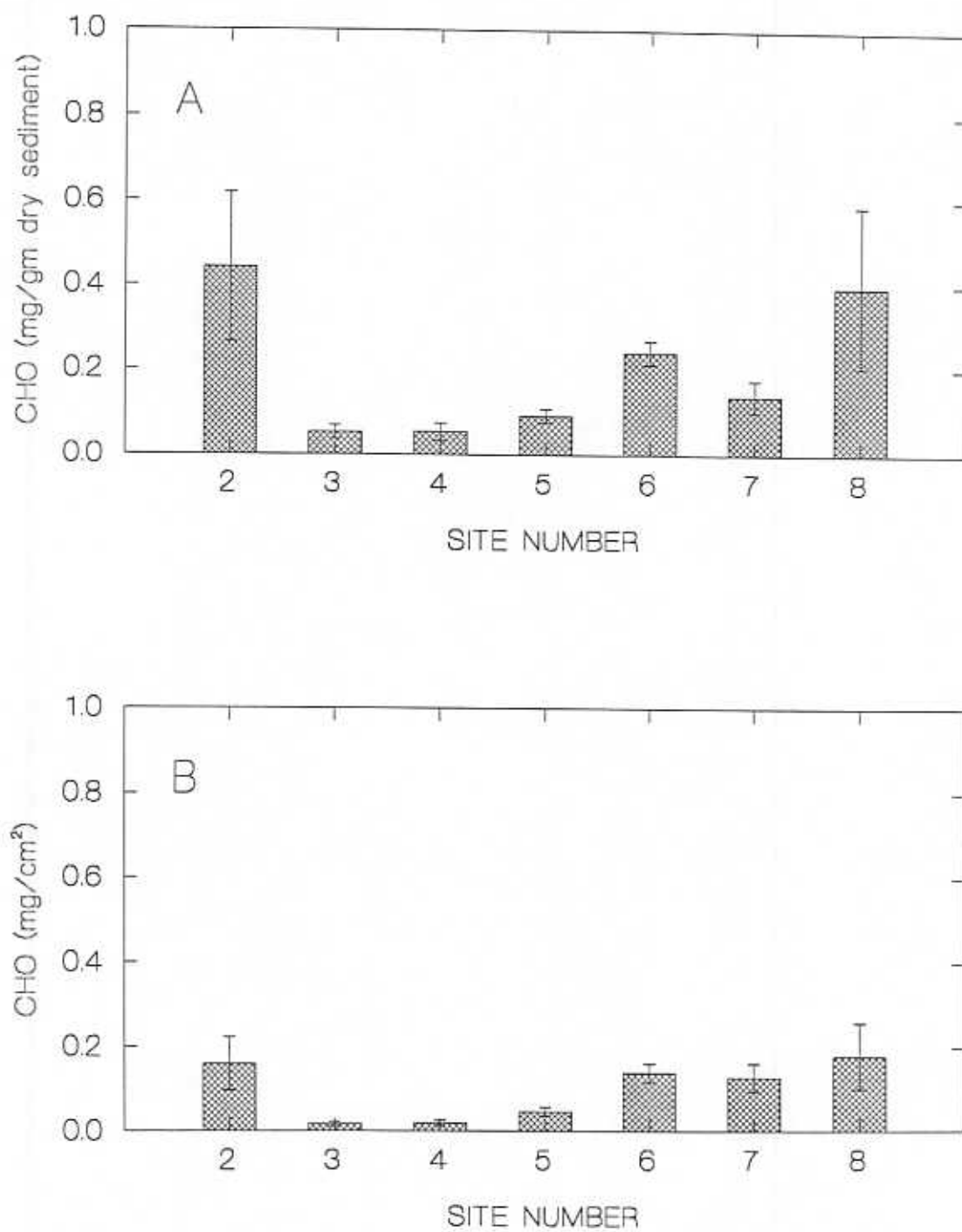


Figure 9.5 Carbohydrate concentrations of sediments at stations S2 to S8 in the Annapolis Basin and Estuary, 1994.

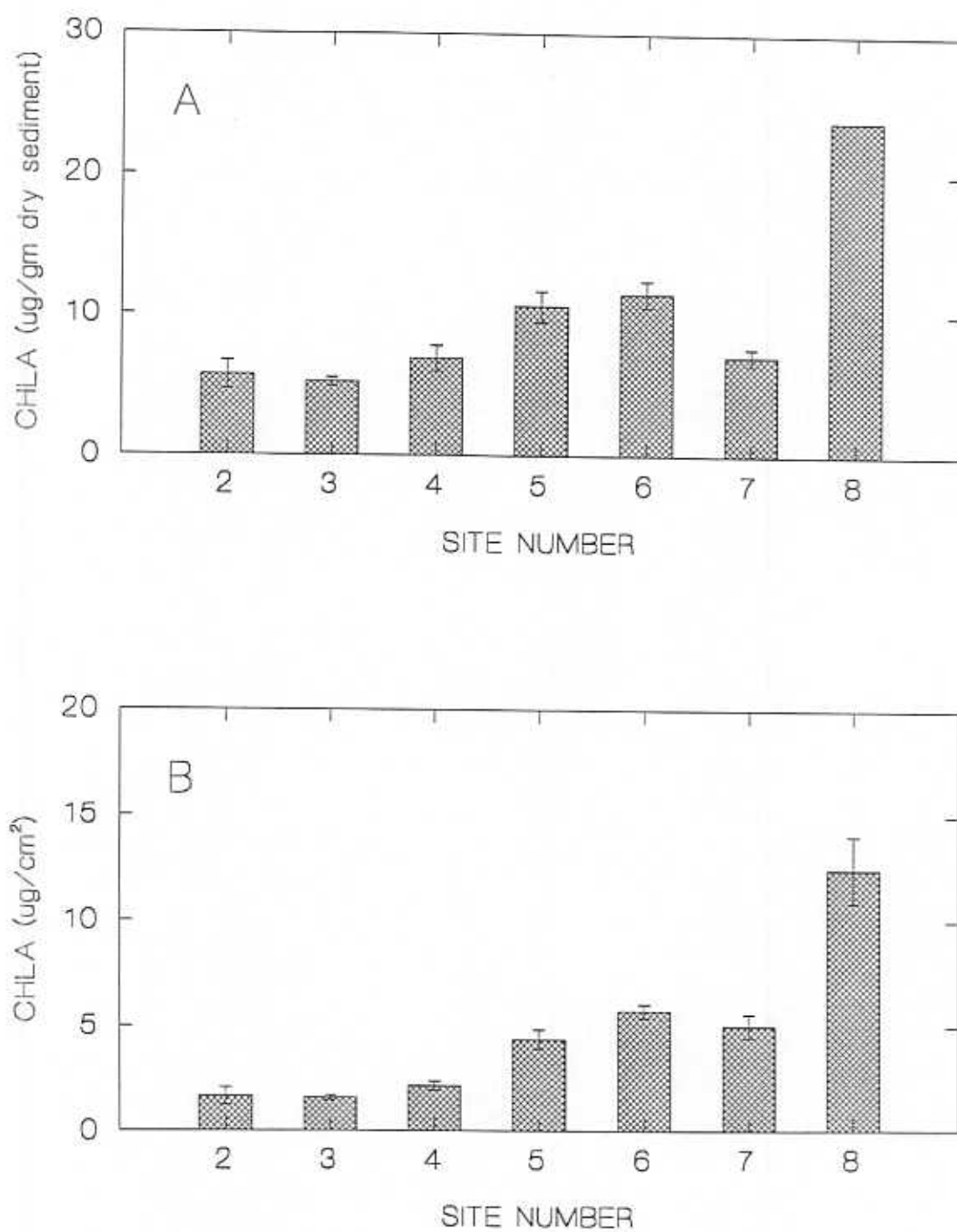


Figure 9.6 Chlorophyll concentrations of sediments at stations S2 to S8 in the Annapolis Basin and Estuary, 1994.

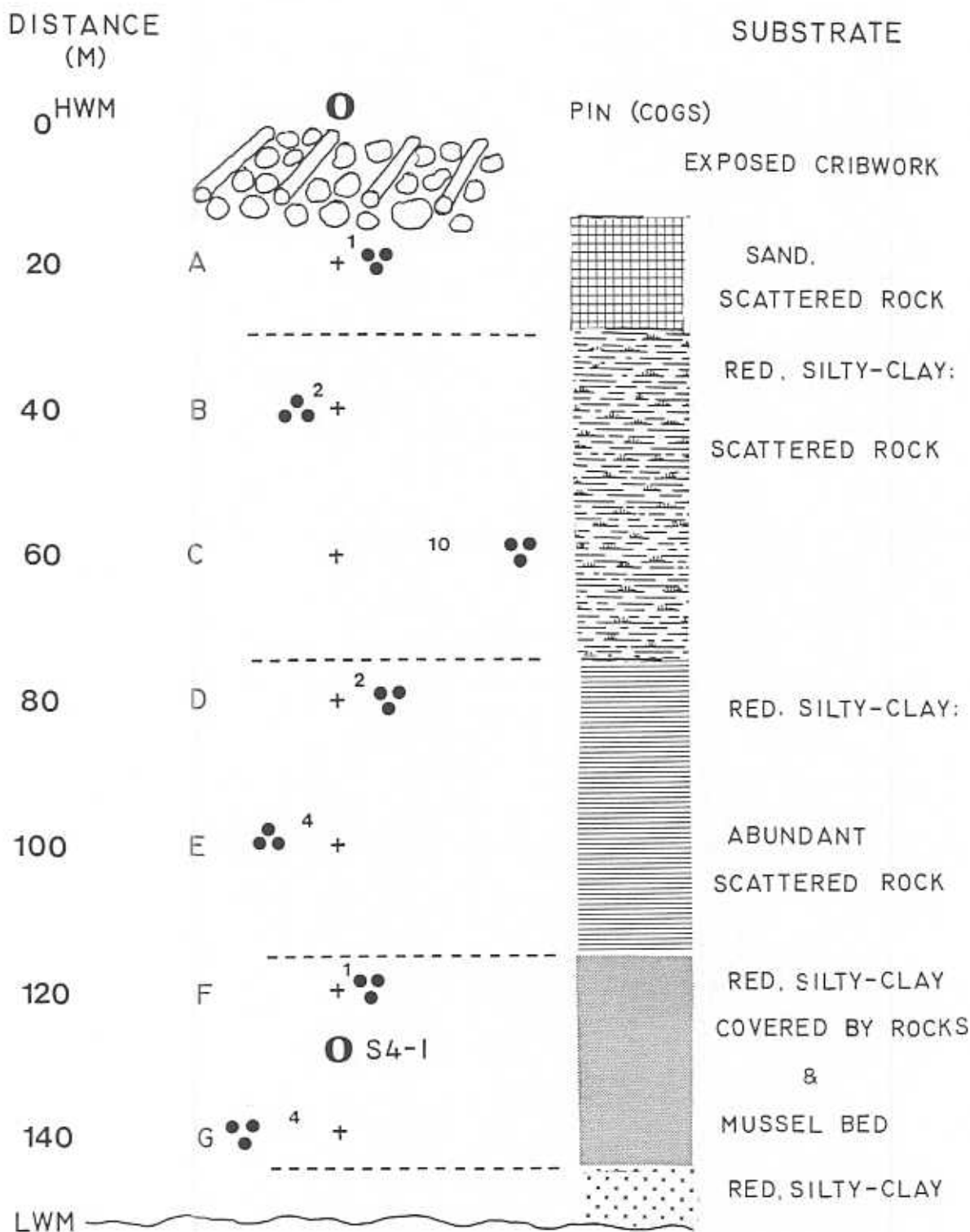


Figure 9.7 Intertidal Transect on Fort Anne Shore.

••<sup>2</sup> - Triplicate core samples at stations A-G along transect. Small numbers indicate randomly selected distance east or west of station.

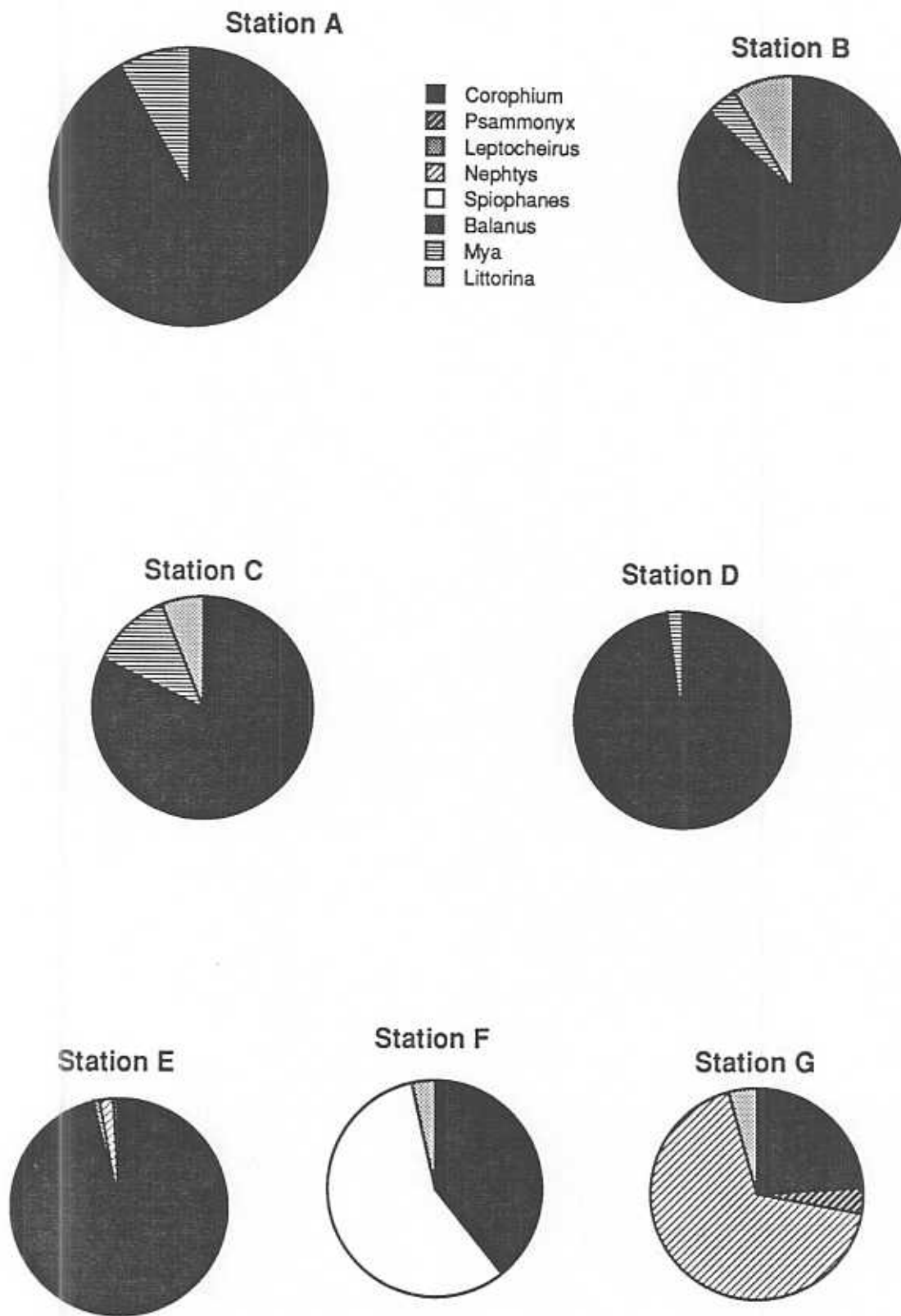


Figure 9.8 Relative abundance of benthic intertidal fauna along Fort Anne transect.



## 10.0 SUMMARY

1. In order to assess the prospects for and appropriate design of remedial works to protect the embankments at Fort Anne National Historic Site from continuing erosion, a research programme to examine hydrodynamic and sedimentological processes in neighbouring portions of the Annapolis Basin and Estuary was conducted from 12 to 18 June 1994.
2. The project was coordinated by the Acadia Centre for Estuarine Research (ACER), and conducted in cooperation with the Atlantic Geoscience Centre (AGC), Bedford Institute of Oceanography, and the Institute for Marine Dynamics, National Research Council of Canada, Ottawa (NRCC).
3. Recording current meters were deployed at three locations in the central axis of the estuary, and at three other locations on the Fort Anne foreshore, to provide data for construction and calibration of a hydrodynamic model. These data were forwarded to the Institute for Marine Dynamics, NRCC, for modelling purposes.
4. Tidal range in the Annapolis Basin and Estuary varied from 5 to 8 m. In the Estuary (landward of Goat Island) water level at high and low water was influenced by generation activities at the Annapolis Tidal Generating Station.
5. Tidal currents in the Basin and Estuary are strongly reversing. Velocities are slightly higher in the Basin ( $< 70 \text{ cm}\cdot\text{sec}^{-1}$ ) than in the Estuary ( $50 - 65 \text{ cm}\cdot\text{sec}^{-1}$ ).
6. Eight anchor station locations along the axis of the Annapolis Basin and Estuary were chosen for studies of physical and sedimentological parameters. The innermost station near the Annapolis Causeway proved to have a rocky substrate and was not suitable for study.
7. Salinity and temperature profiles at each anchor station indicated that in the Estuary, the water column tended to be stratified, with two or occasionally three layers of differing salinity and temperature, or partially mixed. Basin stations tended to be more completely mixed because of tidal and wave turbulence.
8. Boreholes drilled in the embankment of the Fort indicate that the embankment was raised on a natural topographic high made of interbedded sands and silty clays that have been laid down under marine conditions. The boreholes were used to install piezometer pipes for monitoring of groundwater levels.
9. Cores encountered reddish clay at elevations in the embankment corresponding to the deposit that is currently exposed in the intertidal area. This clay is interpreted as a widespread fluvio-glacial deposit from approximately 2000 years ago.
10. Analysis of cores of the red clay taken in 1993 showed it to be a high plasticity clayey-silt, with a plasticity index of 29%. Upon wetting with sea water, exposed red clay loses cohesion and is highly susceptible to erosion by resuspension.
11. Areas of fully liquefied clay were encountered in exposed areas at the foot of the southwest ravelin.

12. Soft, 'squeezing' clay layers were encountered in the boreholes that represent weak strata. These have been associated with previous rotational slippage of the embankment indicated by the step-like topographic profile of the bank, and the rotation of 18<sup>th</sup> century timbers.
13. Monitoring of levelling plates installed on exposed timbers of the southwest ravelin indicate that the slope is currently active. A significant movement occurred in the fall of 1993. Movements of timbers are associated with wave-induced erosion of underlying sediments, and with general slope instability.
14. Analyses of slope stability suggest that the loss of a rockfill berm associated with disappearance of the adjacent saltmarsh was a factor in reactivating a failure along a historically weak internal surface.
15. Tidal movements are an important factor stressing the exposed embankment : on the rising tide, pore pressures increase in the bank, and persist for some time after the tide has fallen. The increased hydrostatic load is added to existing gravitational load, increasing the probability of failure.
16. Replacement of the lost rock mass was recommended and completed during 1994 as a temporary measure to increase slope stability. Stability analyses indicate that this remedial action provides a marginal degree of safety. It needs to be maintained and may require augmentation.
17. Direct measurements of sediment erodibility were made at the seven anchor stations using 'Sea Carousel', a remotely-deployable flume. Some deployments were truncated as a result of wind drift of the vessel used as a platform.
18. Sediments in the Estuary exhibited exceptionally low resistance to erosion and high erosion rates compared with other areas studied in the Bay of Fundy and elsewhere. Erosion thresholds in the Estuary were consistently 0.2 to 0.3 Pa, compared with 0.4 to 0.7 Pa at Basin stations.
19. Station S2, the nearest to Fort Anne, had anomalously high erosion rates compared with other Estuary stations. Furthermore, there was no increase in erosion threshold with depth in the sediment at S2, unlike other stations in the Annapolis system and elsewhere. These observations are consistent with the interpretation that the surface sediment at S2 is unconsolidated.
20. Settling rates of resuspended sediment from Estuary stations measured in 'Sea Carousel' were also unusually low, but (except for S3 below Fort Anne) comparable with results obtained in laboratory flumes at the Acadia Centre for Estuarine Research and the Canada Centre for Inland Waters (CCIW), Burlington, Ont.
21. Gravity cores were taken at anchor stations 2 to 8, resulting in cores 0.6 to 0.8 m in length. Examination of intact cores showed that most Estuary sediments are reduced muds that are highly bioturbated; at S2 near Fort Anne, the surface of the sediment consists of an aerobic layer similar in appearance to the red clay outcropping along the Fort Anne shoreline, and underlying Fort Anne itself. Basin sediments are of mixed lithology and composition, but also bioturbated.

22. Grain size analysis indicates that the sand content increases, and the clay content decreases with distance seaward from the Annapolis Causeway.
23. Studies of remoulded sediments from the Estuary were conducted in the 'Laboratory Carousel' at ACER, and in the carousel at CCIW. A sample from S3 resettled in the ACER Carousel showed that erosion threshold increased with time from 0.8 to 1.5 Pa. Resistance to erosion was greater at the surface than below.
24. Stillwater settling rates of remoulded sediment were <70% lower than field measurements, and 30% lower than estimates obtained and used by NRCC. Reasons for the differences are not known.
25. Grab samples for benthic fauna showed that the abundance of organisms was greater at Basin stations than at those in the Estuary. All Estuary stations were seen to be extensively bioturbated.
26. Although polychaete worms dominated at all sites, diversity of organisms was greater in the Basin than the Estuary. In the Basin various crustaceans were also relatively numerous.
27. In general, water content and organic carbon content of sediments decreased with distance from the Annapolis Causeway, whereas chlorophyll *a* and carbohydrate concentrations increased. The latter suggest higher productivity in the clearer waters of the Annapolis Basin.
28. Station S2, nearest to Fort Anne, departed from the trends shown in other stations : i.e., water and organic carbon contents were lower, and chlorophyll and carbohydrate concentrations higher than expected at this site. These observations correspond with the anomalous behaviour of sediments from this station.
29. Core samples from the Fort Anne shoreline indicate that the intertidal benthic community is sparse and poorly developed. It is dominated by the burrowing amphipod *Corophium volutator*.
30. If further surveys confirm the above, it would appear that there would be no major loss of productivity, and possibly an increase in biological production and diversity if remedial work should convert the intertidal zone into a rocky substrate.

## 11.0 CONCLUSION and RECOMMENDATIONS

Review of the investigations carried out during 1992-94 indicates that sufficient information now exists to permit determination of the remedial measures necessary for protection of Fort Anne National Historic Site against erosion by the sea. We have during these studies obtained a wide array of information on physical oceanography, geology, sedimentology and biology, and have assisted with development of linked hydrodynamic and sedimentological models that allow testing of the efficacy of possible solutions. Although much more specific research could be done to amplify present knowledge, and to increase confidence in the solutions, the degree of vulnerability of the Fort does not permit the luxury of delaying further attempts to define appropriate action.

Recommendation 1. That discussions regarding engineering solutions to the problem of erosion on the Fort Anne site be initiated immediately.

Recommendation 2. That a multidisciplinary team be formed to address the solutions mentioned in Recommendation 1. The team should include : a physical oceanographer, a geotechnical scientist, a sedimentologist, a biologist, and a number of engineers.

Recommendation 3. That the solutions considered should attempt to address the two aspects of the erosion problem : a) continued erosion of the remaining saltmarsh and destabilisation of the bank on the Annapolis Estuary side; and b) erosion of the intertidal sediments caused by resuspension of the exposed fine red silty-clay that is weakening on inundation by water, and through the activities of burrowing organisms. Solutions considered should include :

- 1) rebuilding of Queen's Wharf to its former maximum length;
- 2) reconstruction of the rock groyne at the western end of the Annapolis foreshore (previously referred to as the "Scottish? Wharf");
- 3) protection of the remnant saltmarsh on the Allain River side of the Fort, using fabric and/or rockfill protection;
- 4) protection of the exposed intertidal clay from exposure to seawater.

The remedial work done at the base of the southwest ravelin in 1994 has stabilised the embankment in the short term. However, the margin of safety is only moderate, and it is not certain how long the bank will remain in this state.

Recommendation 4. Water levels in the boreholes established in 1994 should be monitored regularly during wet periods, especially during the spring and early summer.

Recommendation 5. In order to detect any movement of the southwest ravelin, a selected number of rocks placed at the foot of the bank in 1994 should be identified, marked, and carefully surveyed. Positions of these marker rocks should be resurveyed accurately at six-month intervals.

The role(s) of invertebrate infauna in accelerating loss of the exposed intertidal clay suggests that the process will continue more or less indefinitely. Observations in this study suggest that the fauna is not particularly extensive or abundant, however, continued introduction of water into the deposit

will exacerbate the present situation. It seems necessary to consider ways of armouring the sediment to prevent it from being irrigated and resuspended. Undoubtedly, environmental assessment requirements will include an assessment of the abundance and diversity of the biota on the shore, which cannot be derived from the present information.

Recommendation 6. That a comprehensive survey of the benthic fauna be conducted in July/August (when development is at its peak) along a series of transects across the Fort Anne shoreline on both the Annapolis Estuary and Allain River sides.

Recommendation 7. In order to test the feasibility of providing a complete cap to the intertidal sediments, a small experiment should be conducted using an impermeable mattress (e.g., 3 m x 3 m) set out over the sediment as a seal, and then covered with cobbles/boulders. This should be left in place for as long as feasible, to examine the effect on the underlying substrate.

12.0 REFERENCES CITED

- Amos, C.L. and Mosher, D.A. 1985. Erosion and deposition of fine-grained sediments from the Bay of Fundy. *Sedimentology* 32 : 815-832.
- Amos, C.L., Grant, J., Daborn, G.R., and Black, K. 1992. Sea Carousel -- a benthic, annular flume. *Est. Coastal Shelf Sci.* 27 : 1-13.
- Amos, C.L. and Gibson, A.J. 1994. The stability of dredge material at Dumpsite B, Miramichi Bay, New Brunswick, Canada. Geological Survey of Canada, Open Report No. 3020, Dartmouth, Nova Scotia : 51 p + Appendices.
- Amos, C.L., Gibson, A.J., Partridge, V., Atkinson, A., and Jodrey, F. 1994. *MV Navicula* cruise -Miramichi Bay, New Brunswick. Geological Survey of Canada, Open File Report 2939 : 55 p.
- Bjerrum, L. 1971. Subaqueous slope failures in Norwegian fjords. Norwegian Geotechnical Institute, Oslo, Report No. 88, pp. 1-8.
- Brinkhurst, R.O., Linkletter, L.E., Lord, E.I., Connors, S.A., and Dadswell, M.J. 1976. A preliminary guide to the littoral and sublittoral marine invertebrates of Passamaquoddy Bay. Unpublished manual, St. Andrews Biological Station, St. Andrews, New Brunswick : 166 p.
- Bromley, J.E.C. and Bleakney, J.S. 1984. Keys to the Fauna and Flora of Minas Basin. National Research Council of Canada, Atlantic Research Laboratory, Publication No. 24119 : 368 p.
- Brylinsky, M., Gibson, J., Daborn, G.R., Amos, C.L., and Christian, H.A. 1992. Miramichi inner bay sediment stability study. Acadia Centre for Estuarine Research, Publication No. 22 : 57 p.
- Cybulski, J.S. 1994. Analysis of a human skeleton found on the beach at Fort Anne, Nova Scotia, May 16, 1994. Report to the Canadian Parks Service, Atlantic Region, and Canadian Museum of Civilization, April : 18 p.
- Daborn, G.R., Amos, C.L., Brylinsky, M., Christian, H.A., Drapeau, G., Perillo, G., Piccolo, M.C., and Yeo, G. 1991. Littoral Investigation of Sediment Properties. Final Report. Acadia Centre for Estuarine Research, Report No. 17 : 239 p.
- Daborn, G.R., Brylinsky, M., and DeWolfe, D. 1992. Study of current flow patterns in the Annapolis Estuary in the vicinity of Fort Anne National Historic Site. Report to Canadian Parks Service, Environment Canada, Acadia Centre for Estuarine Research, Publication No. 25 : 31 p.
- Daborn, G.R., Christian, H.A., Brylinsky, M. and DeWolfe, D.L. 1993a. An experimental study of factors affecting current flow and sediment stability on the Fort Anne foreshore. Report to Canadian Parks Service, Environment Canada, Acadia Centre for Estuarine Research, Publication No. 29 : 52 p.
- Daborn, G.R., Amos, C.L., Brylinsky, M., Christian, H.A., Drapeau, G., Faas, R.W., Grant, J., Long, B., Paterson, D.M., Perillo, G.M.E., and Piccolo, M.C. 1993b. An ecological



- 'cascade' effect : migratory shorebirds affect stability of intertidal sediments. *Limnol. and Oceanogr.* 38 : 225 - 231.
- Decho, A.W. 1990.** Microbial exopolymer secretions in ocean environments: their role(s) in food webs and marine processes. *Oceanogr. Mar. Biol. Ann. Rev.* 28 : 73-153.
- Dunn, B. 1992.** A preliminary look at the history of erosion at Fort Anne. Report to Parks Canada, November : 32 p.
- Golder Associates. 1982.** Subsurface investigation - proposed Interpretative Centre, Fort Anne National Historic Park. Report to Parks Canada, July.
- Jacques, Whitford & Associates Ltd. 1985.** Geotechnical investigation - Allain Creek bridge abutment stability: Annapolis Royal, Nova Scotia. Report to the Department of Transportation, Province of Nova Scotia, July.
- Jacques, Whitford & Associates Ltd. 1994.** Laboratory tests on shear strength testing of Annapolis Basin Red Clay. Report to the Geological Survey of Canada, December, Contract No. 23420-4-M232/01/HAL.
- Meadows, P.S. and Tufail, A. 1986.** Bioturbation, microbial activity and sediment properties in an estuarine ecosystem. *Proc. R. Soc. Edinb. (Sect. B)* 90 : 1-14.
- Morgenstern, N.R. and Sangrey, D.A. 1978.** Methods of stability analysis. *In* Landslides - Analysis and Control, Transportation Research Board, National Research Council, Special report 176, pp. 155-171.
- Nowell, A.R.M., Jumars, P.A., and Eckman, J.E. 1981.** Effects of biological activity on the entrainment of marine sediments. *Marine Geology* 42 : 133-153.
- Paterson, D. M. and Daborn, G.R. 1991.** Sediment stabilisation by biological action: significance for coastal engineering. *Proceedings of the Conference on Developments in Coastal Engineering*, Bristol, United Kingdom : 111-119.
- Paterson, D.M. 1994.** Microbial mediation of sediment structure and behaviour. *NATO ASI Series G35* : 97-109.
- Sigouin, N. and MacDonald, D. 1994.** Characterization of cohesive sediments. Fort Anne National Historic Site. National Research Council, Laboratory Memorandum IECE-CEP-LM-004 : 17 p.
- Terzaghi, K. 1956.** Varieties of submarine slope failures. *Proceedings of the 8th Texas Conference on Soil Mechanics and Foundation Engineering*, 14-15 September. University of Texas, Austin, Bureau of Building Research, Special Publication No. 29.
- Wallace, B. 1994.** Salvage excavation of skeleton found on the Beach at Fort Anne. Unpublished Report, Parks Canada, Halifax, Nova Scotia, 14 p.

- Wildish, D.J., Peer, D.L., Wilson, A.J., Hines, J., Linkletter, L., and Dadswell, M.J. 1983.**  
Sublittoral macro-infauna of the upper Bay of Fundy. Can. Tech. Rept. Fish. Aquat. Sci. No. 1194 : iii + 64 p.
- Willis, D. 1995.** Fort-Anne National Historic Site, Shoreline Erosion, Progress Report No. 10. Institute for Marine Dynamics, National Research Council of Canada.



**Appendix A**

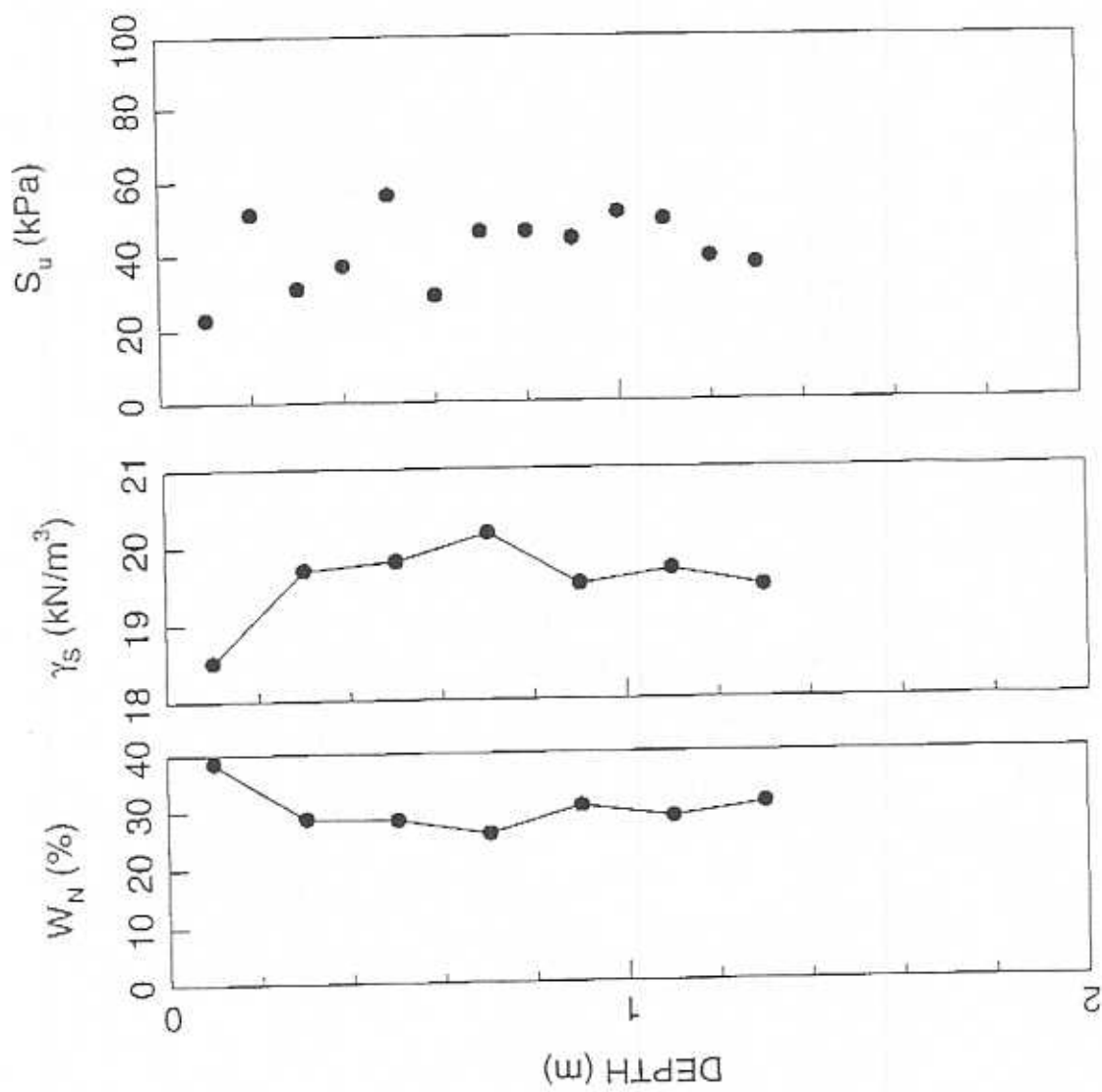
**Graphic Summaries for 1994 Geotechnical Borings on Southwest Ravelin**

#### Appendix A. Graphic summaries for 1994 geotechnical borings on southwest ravelin.

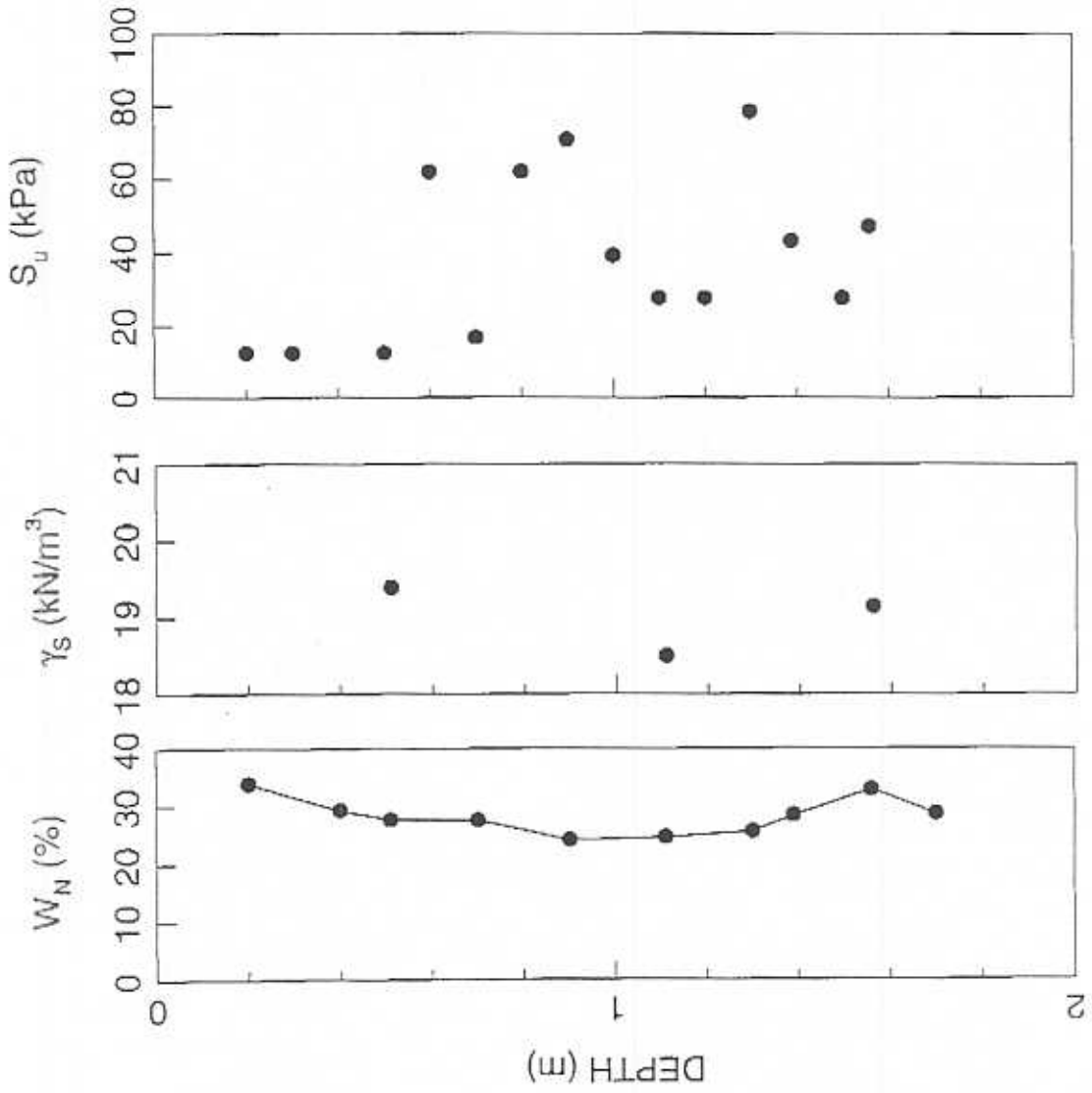
The following three graphs summarize geotechnical index property test results obtained after opening the tube samples collected from the seaward slope of the southwest ravelin. The sample material from the top of the slope (94BH1) showed a uniform water content ( $w_n$ ) over the top 2 m, varying from 35% near the surface to 26% at 1 m below ground surface, below which it increased to 35%. The saturated unit weight (bulk density multiplied by gravitational constant)  $\gamma_s$ , varied between 18.5 and 19  $\text{kn/m}^3$ , as shown. The undrained shear strength was measured with a Swedish fall cone apparatus and showed low levels in loose intervals and higher values in denser fine-grained intervals. The higher values varied between 60 and 80 kPa, which indicated that a significant amount of overlying soil has been eroded away (see previous comments regarding erosion of intertidal zone).

Boreholes from the base embankment (94BH2 and 94BH3) were located at the base of the southwest ravelin, in the area where rockfill was placed during remediation of the worsening landslide, followed similar trends as for 94BH1. The undrained shear strength was lower than in 94BH1, suggesting that the upper portion of the slope was partially dry and therefore somewhat more desiccated. The soils encountered at the base of the slope were identical in appearance and behaviour to those encountered over the intertidal mudflat, in a previous geotechnical investigation.

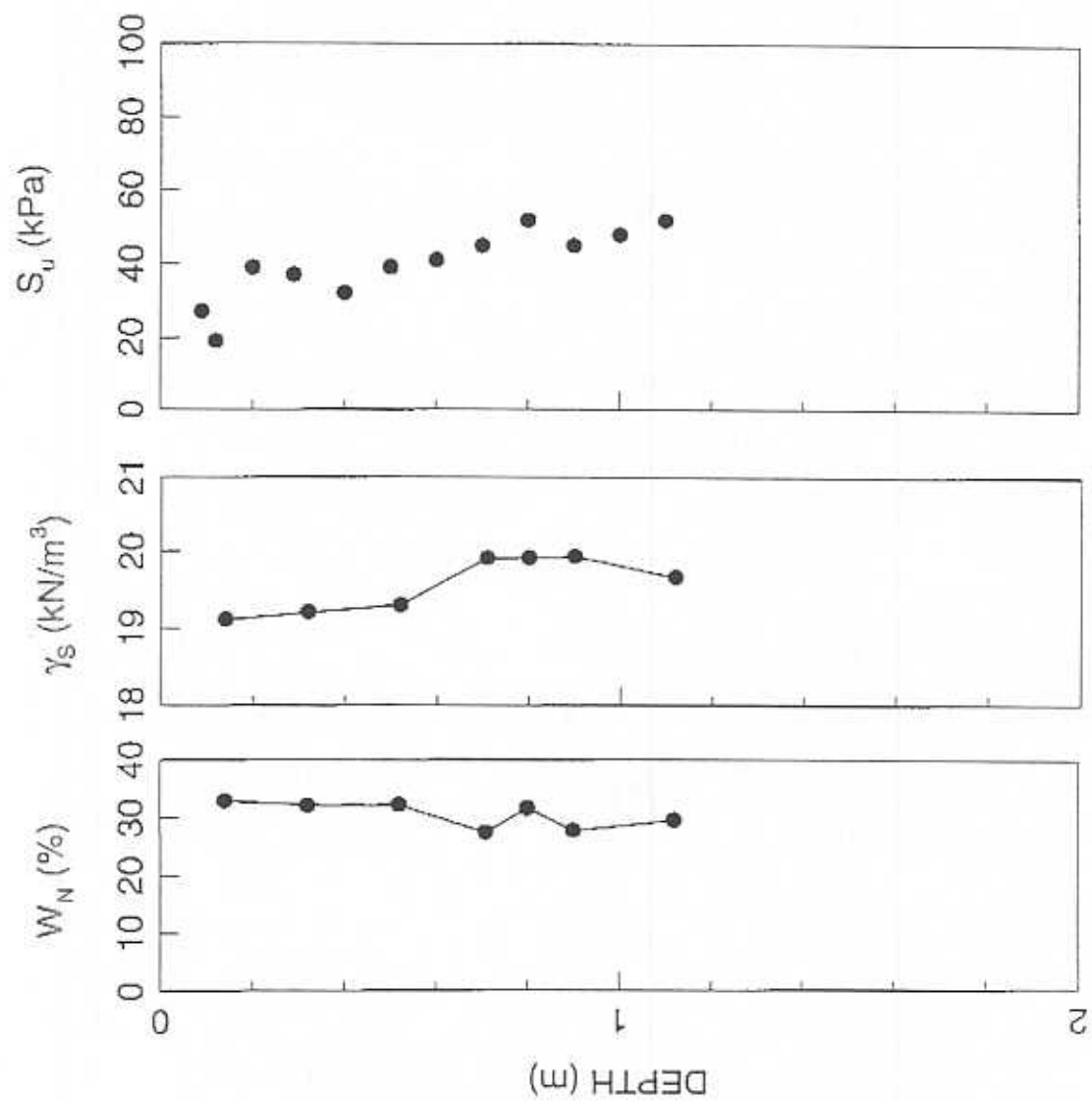
## FORT ANNE 94BH3



**FORT ANNE 94BH1**

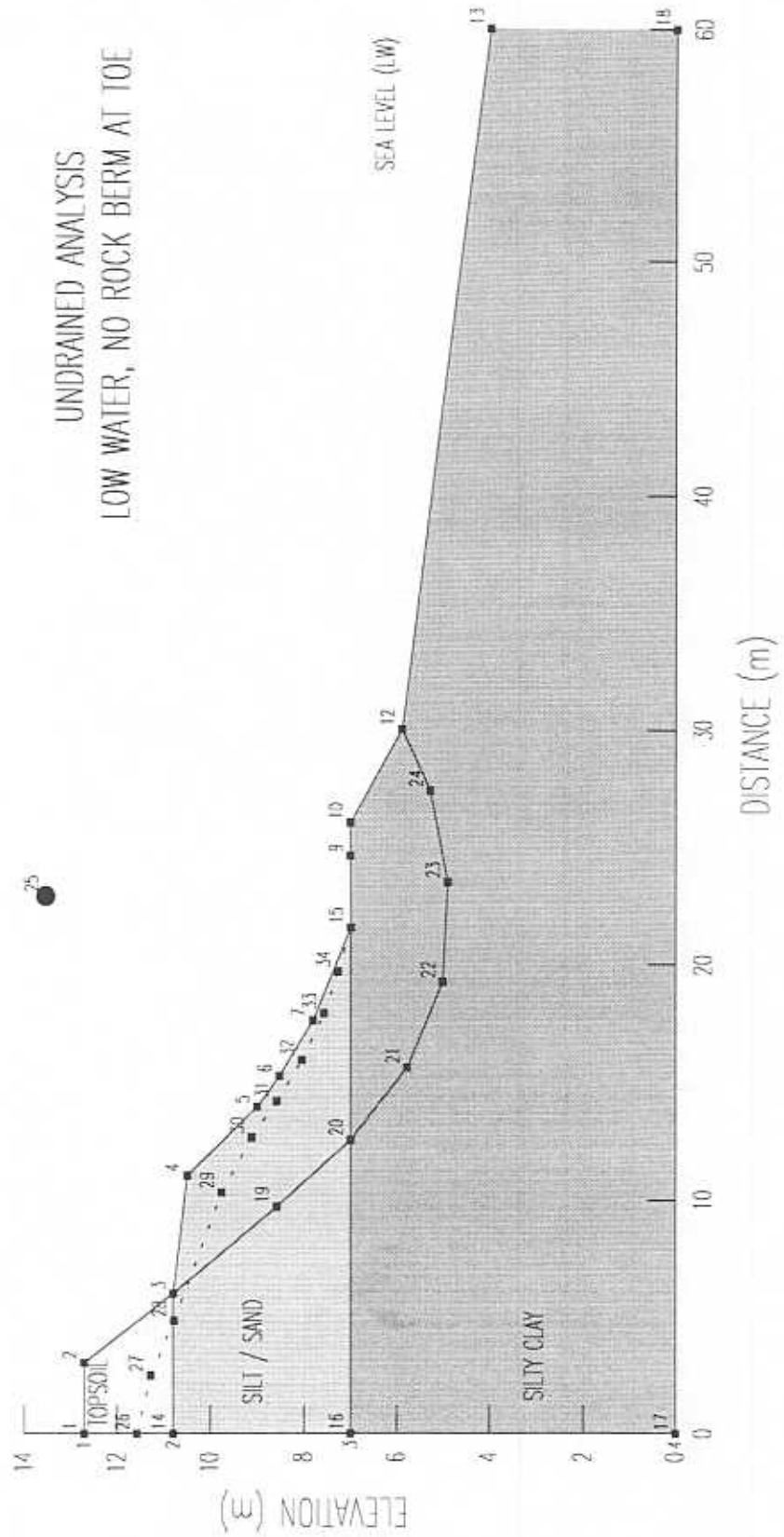


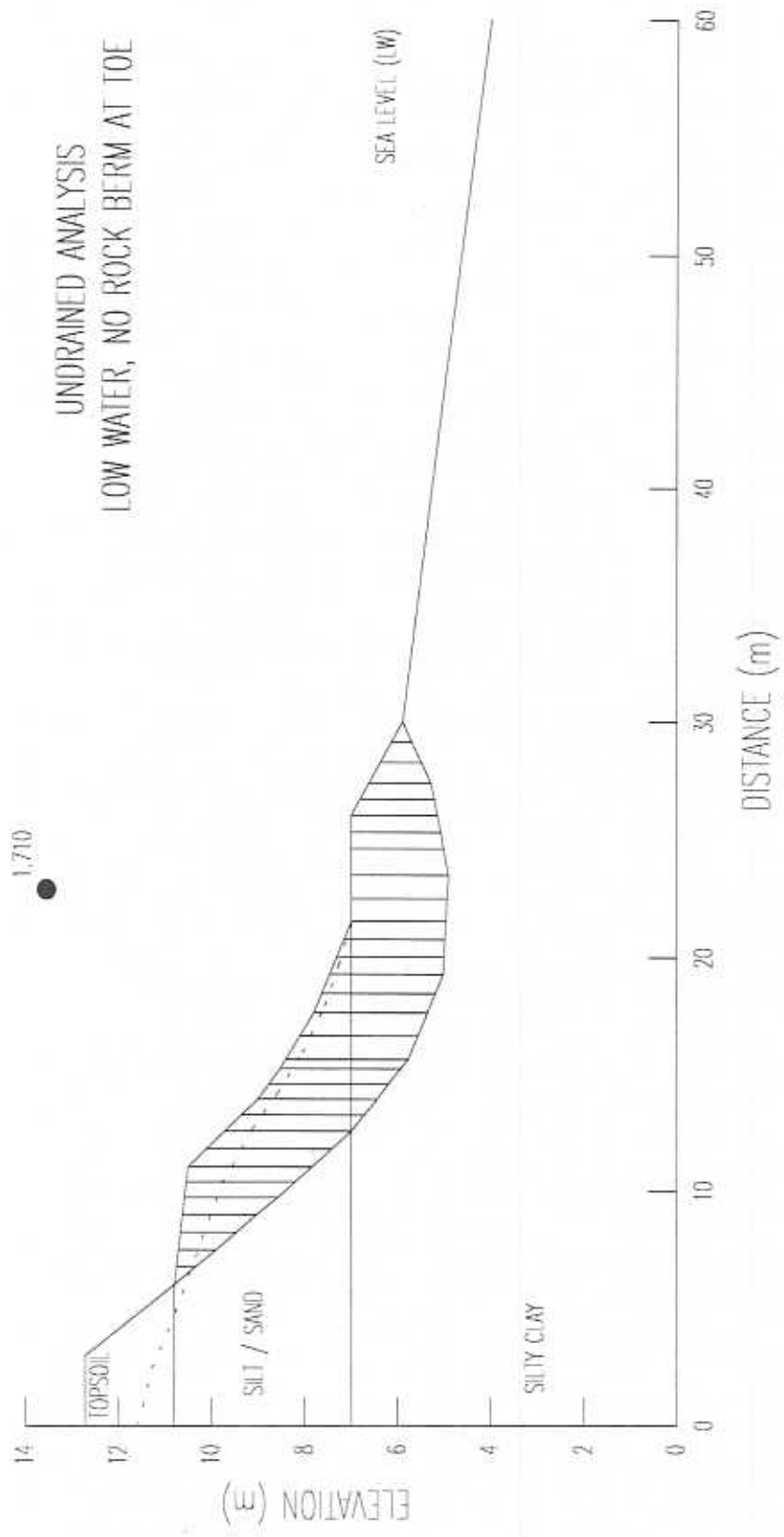
# FORT ANNE 94BH2



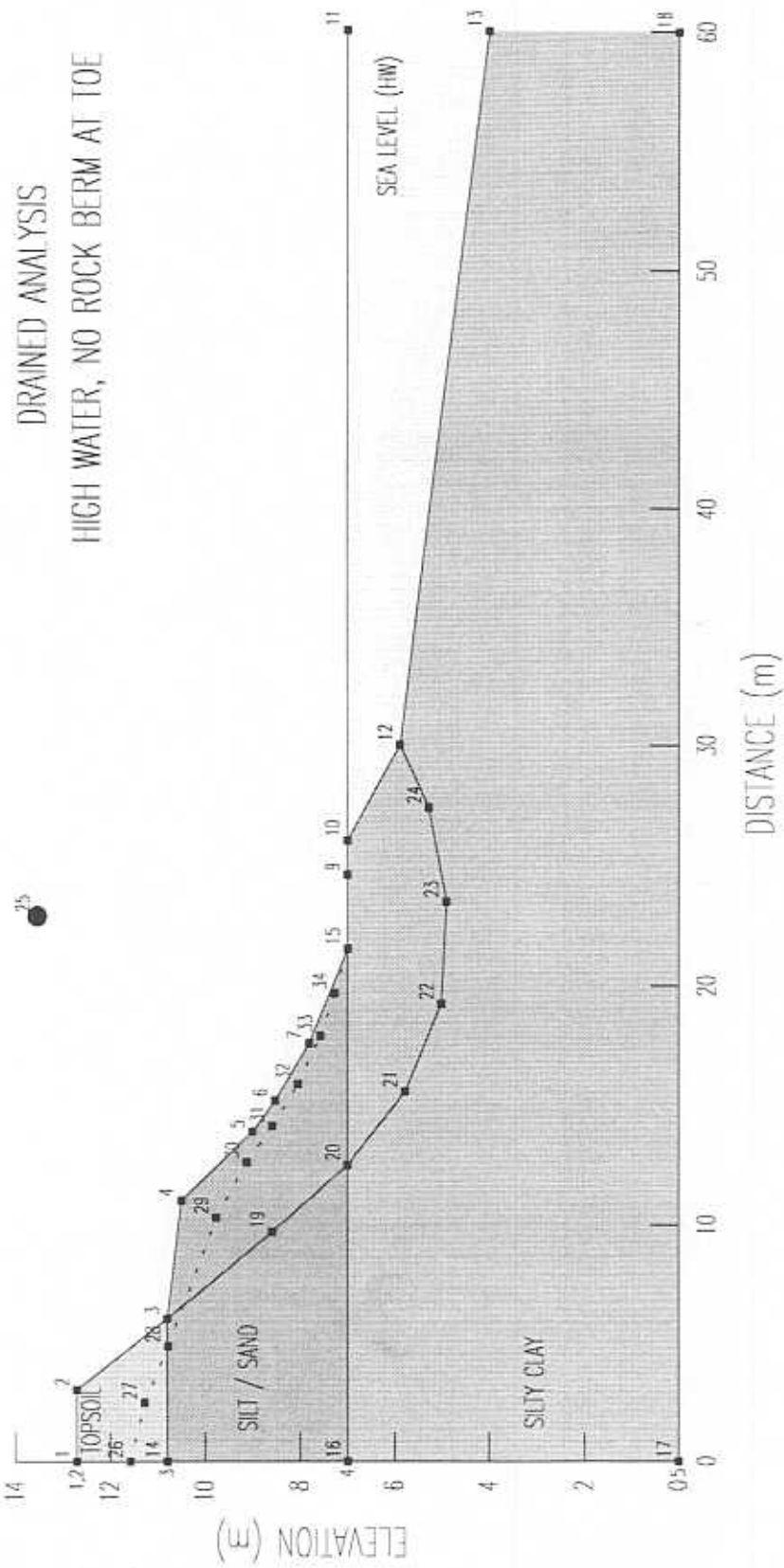
**Appendix B**

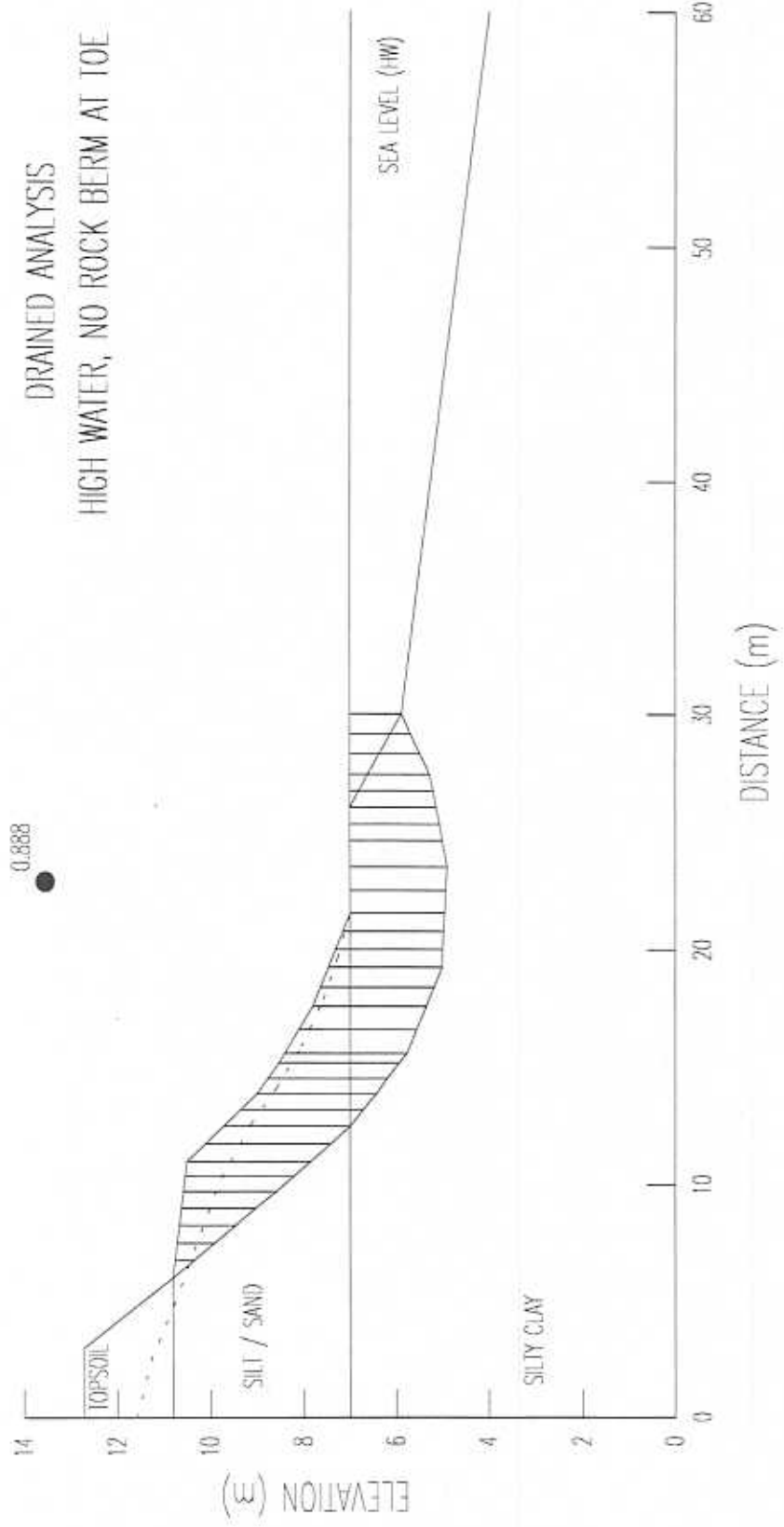
**Boundary Conditions for the Analysis of Slope Stability**



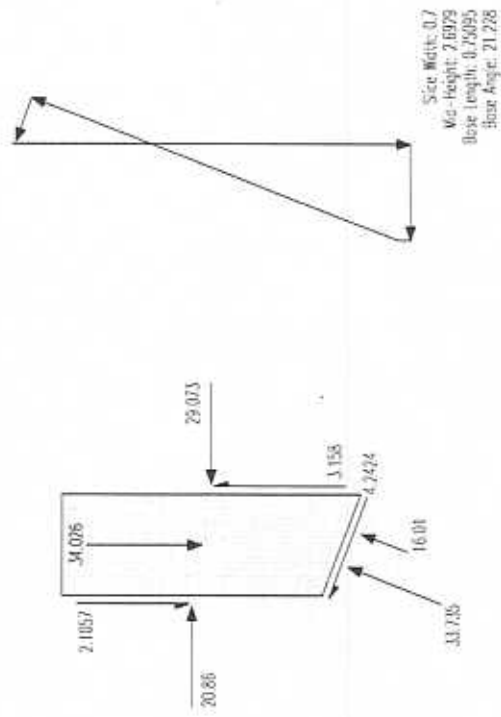


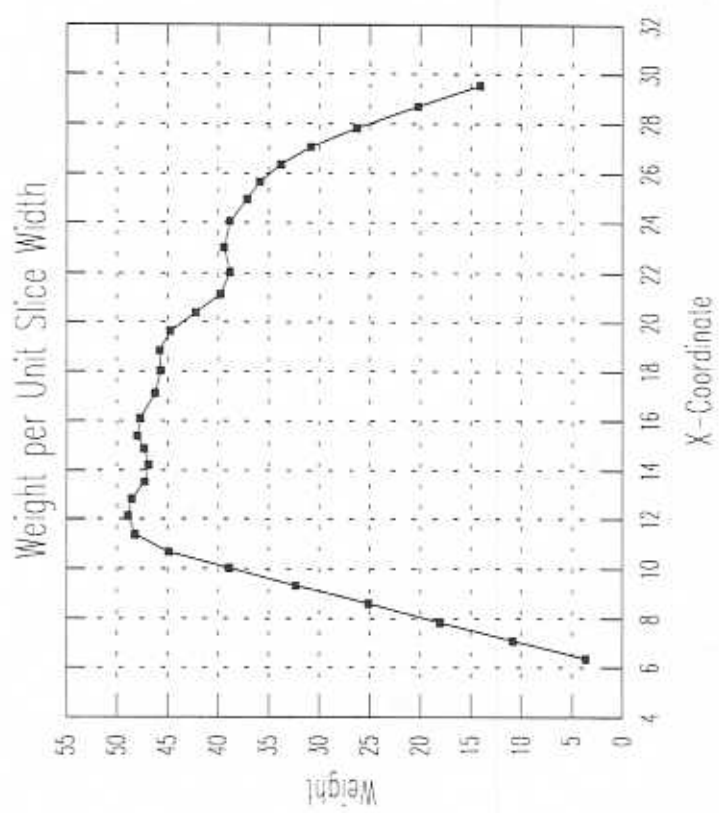


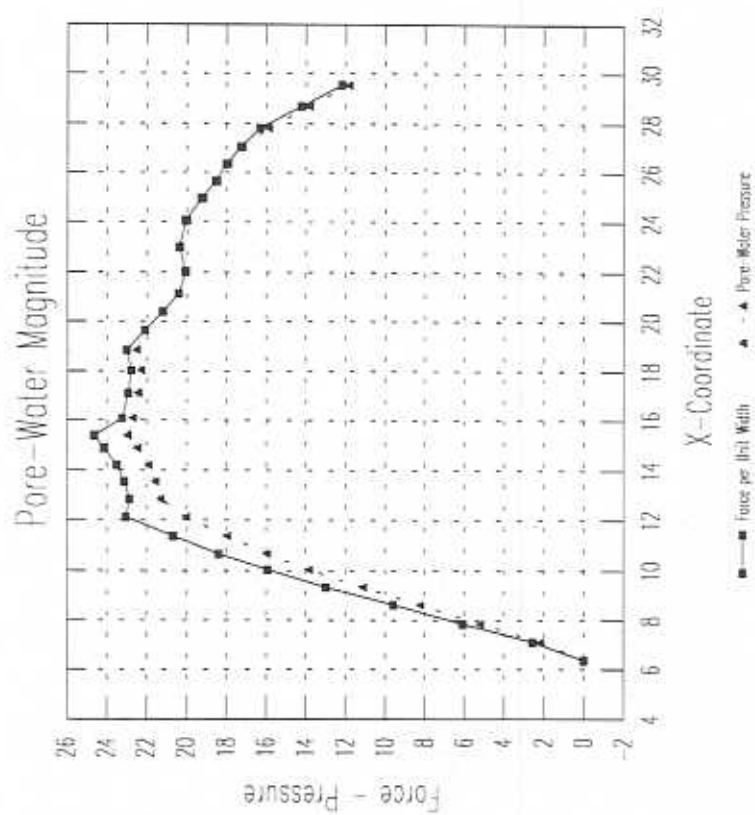


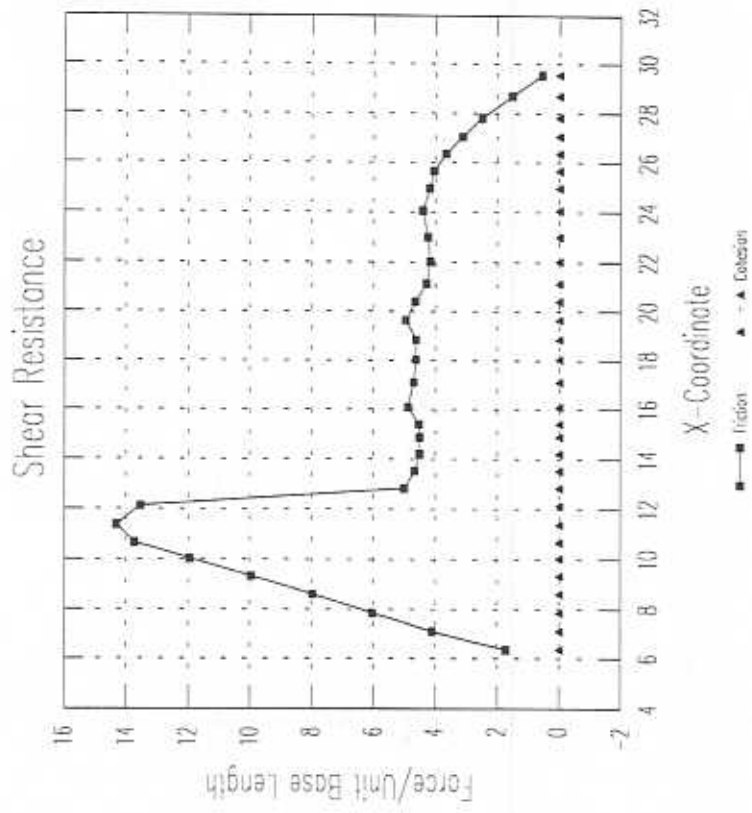


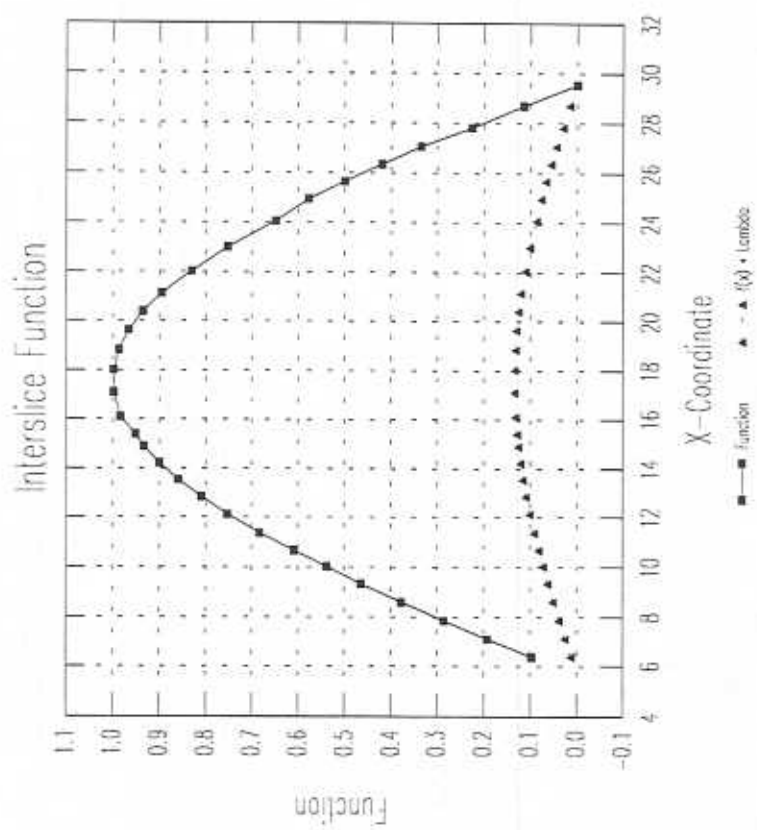
Slice 10 - Morgenstern-Price Method



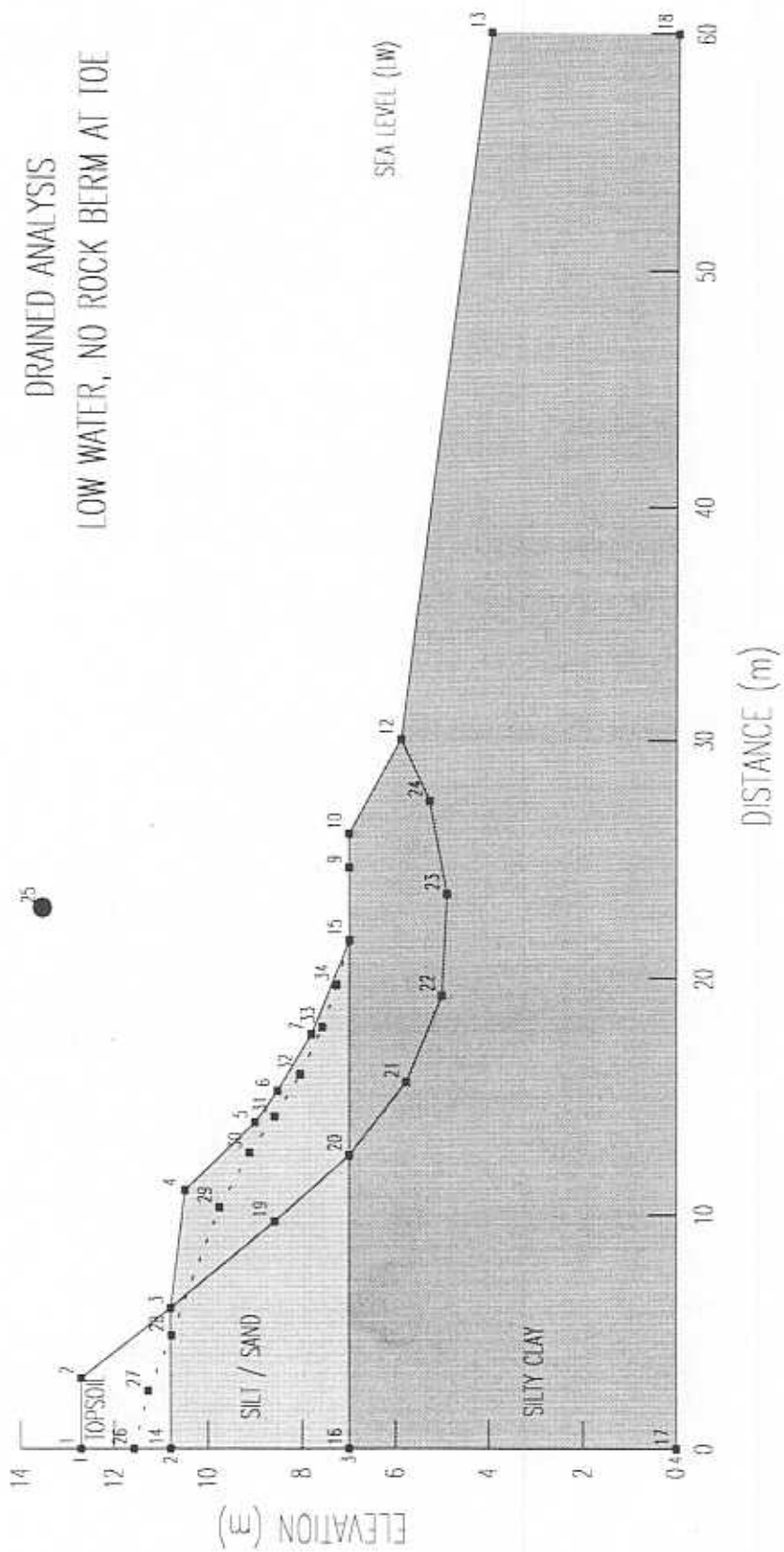




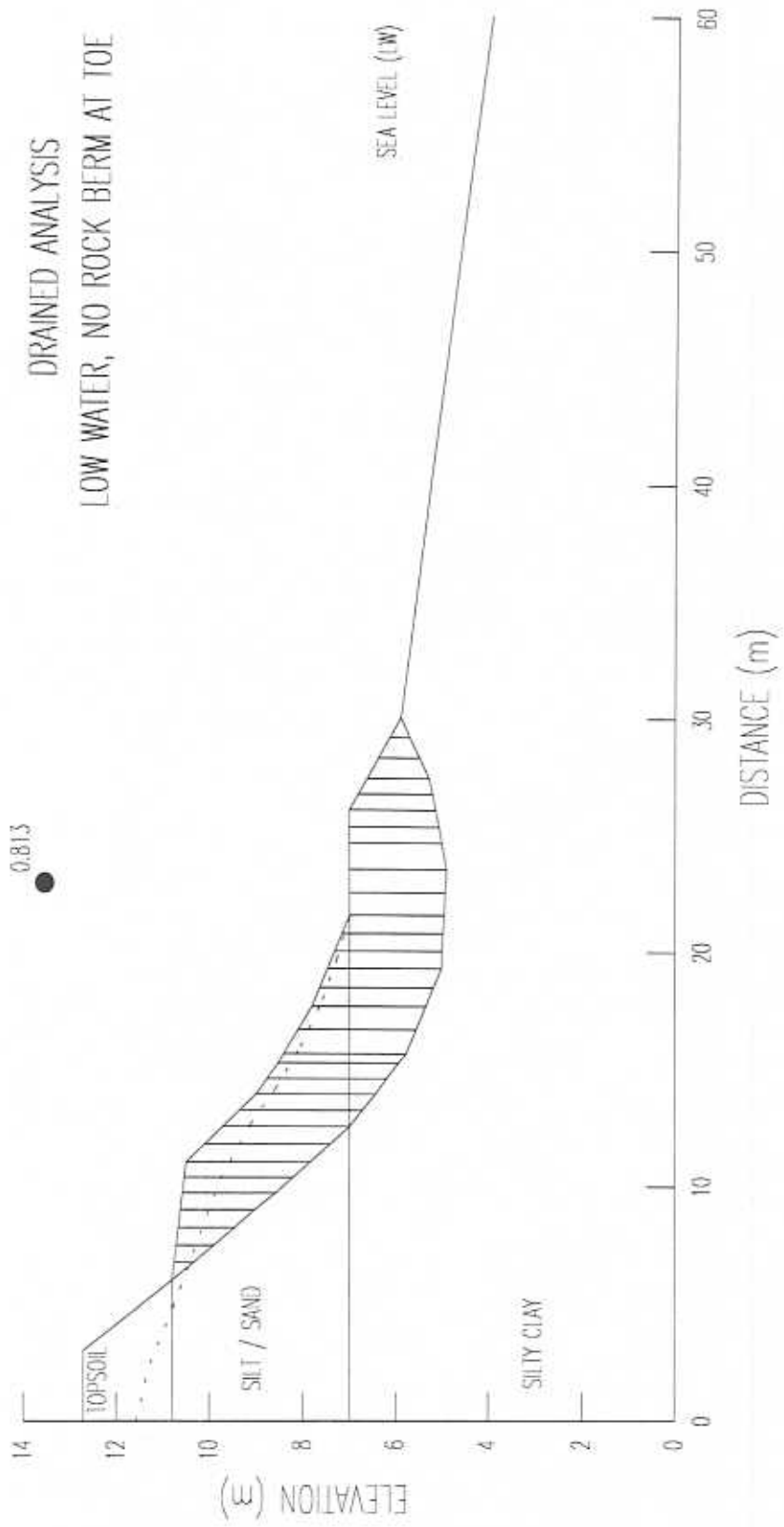




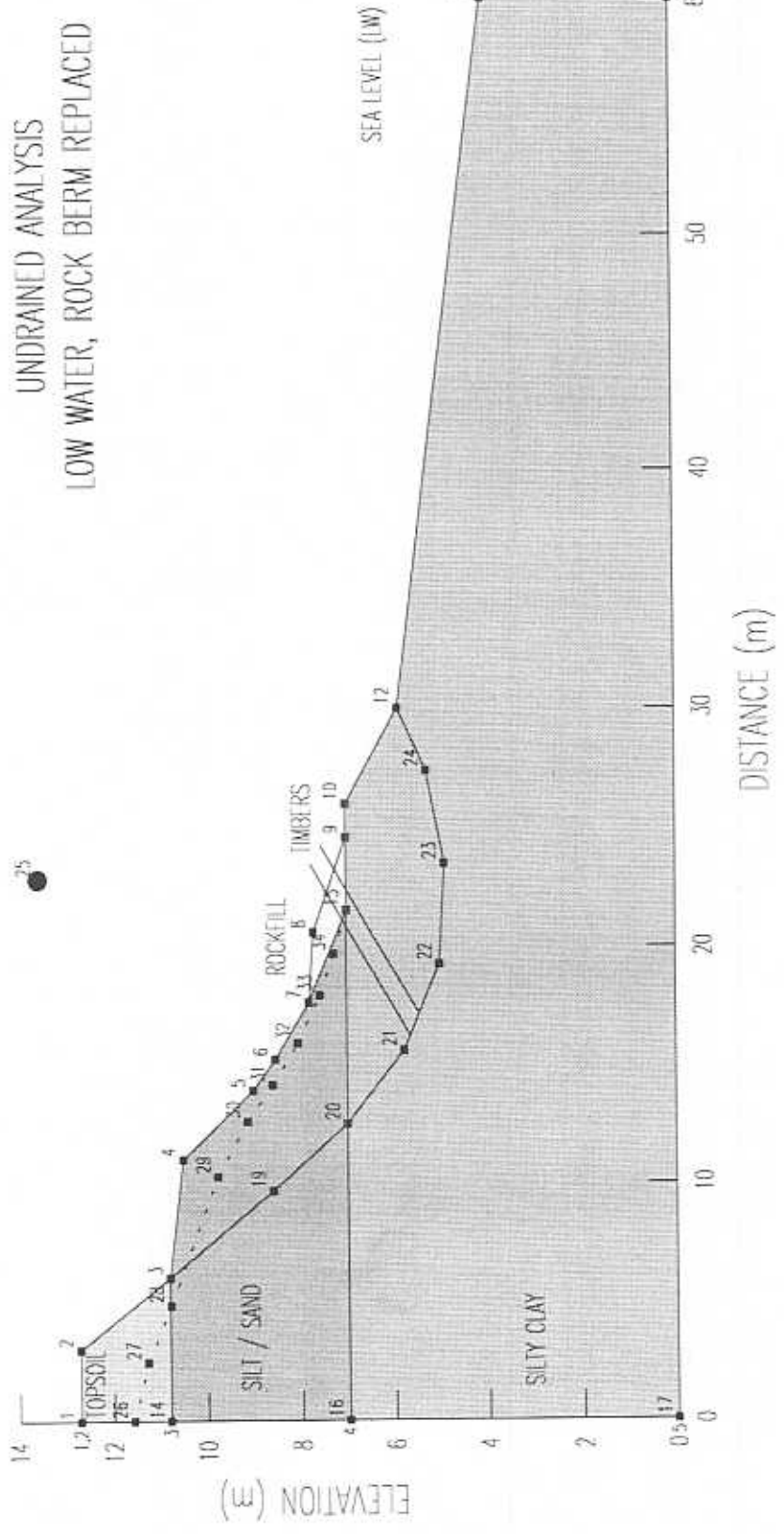
DRAINED ANALYSIS  
 LOW WATER, NO ROCK BERM AT TOE

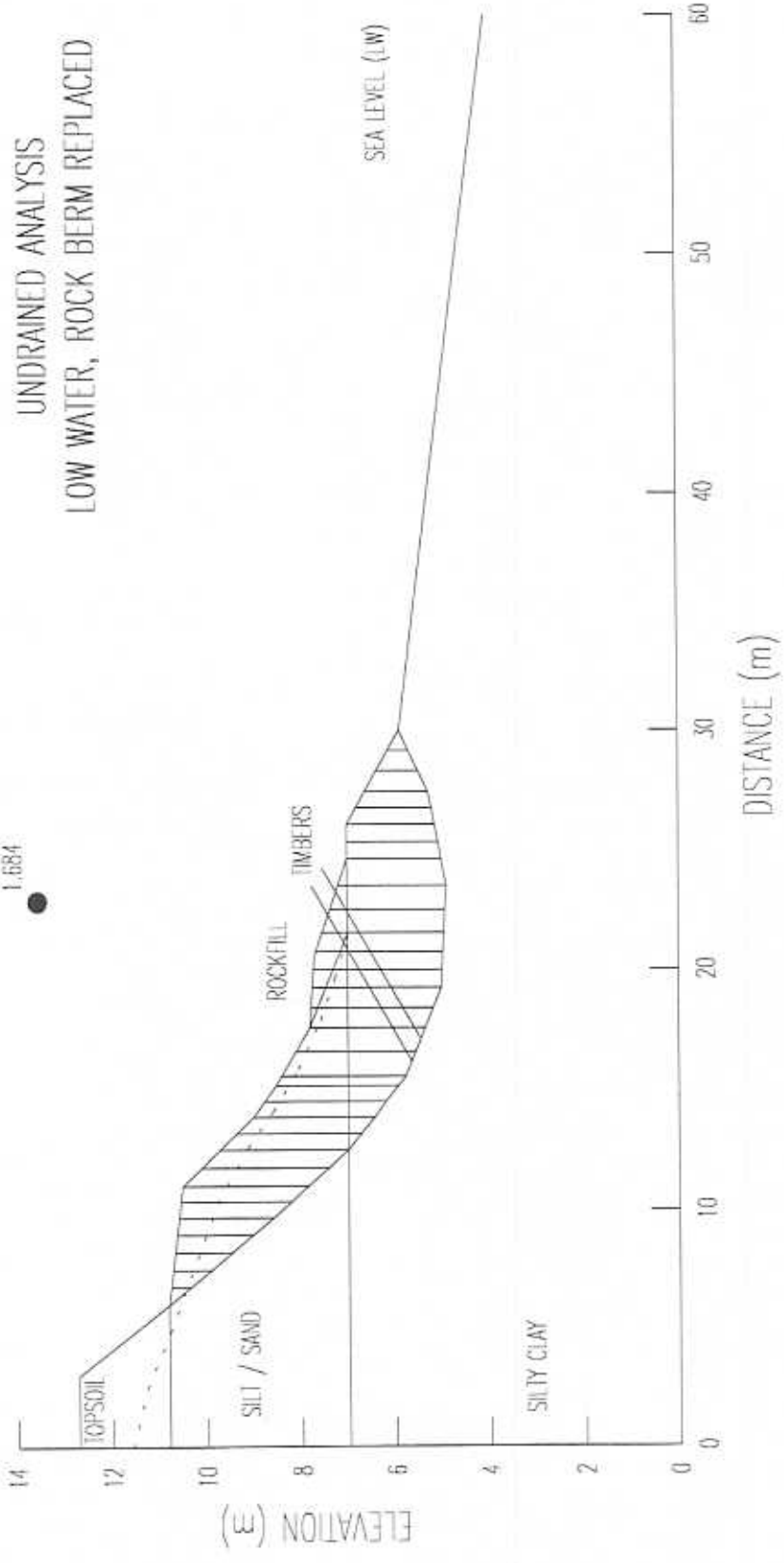


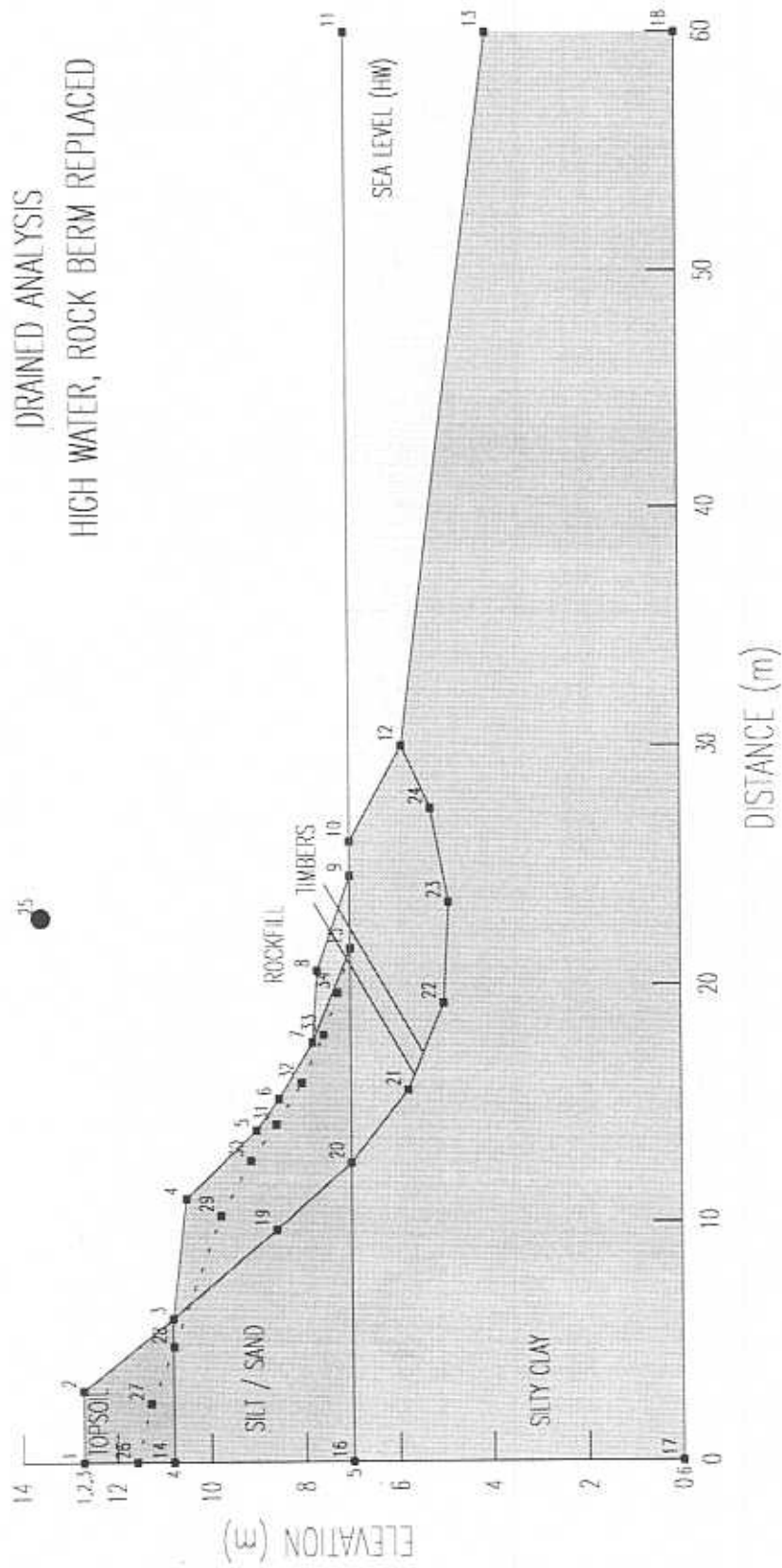


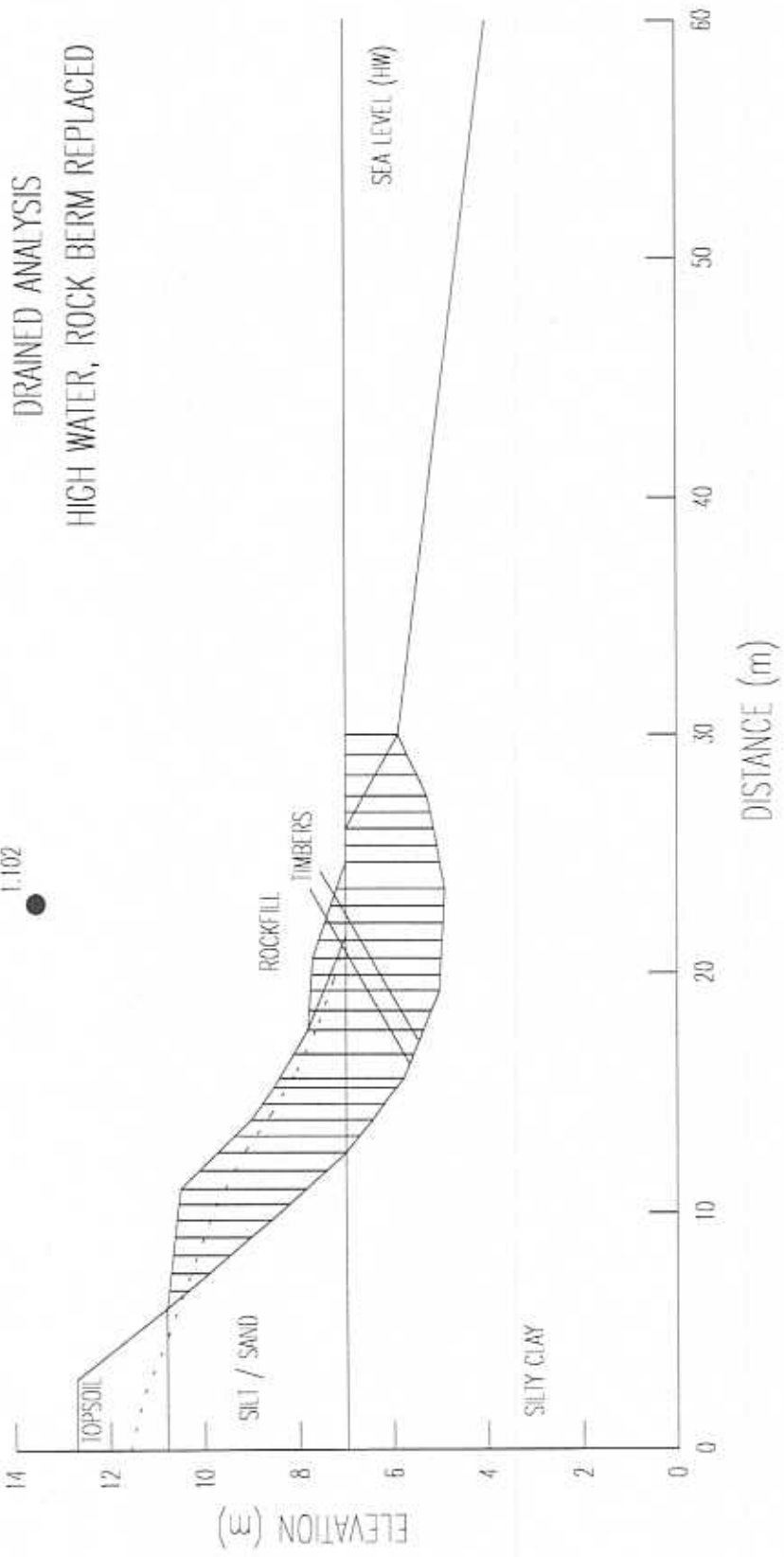




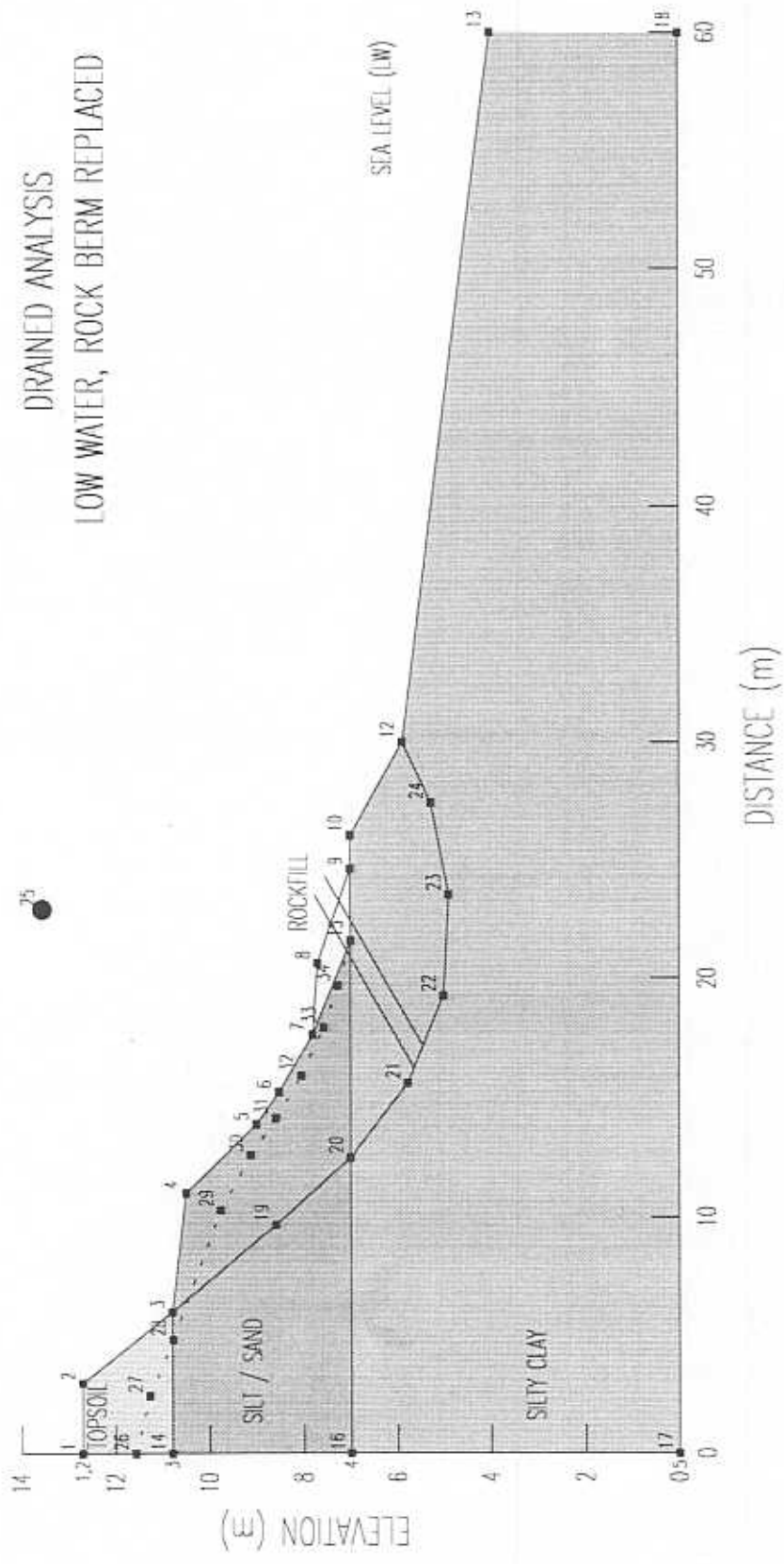


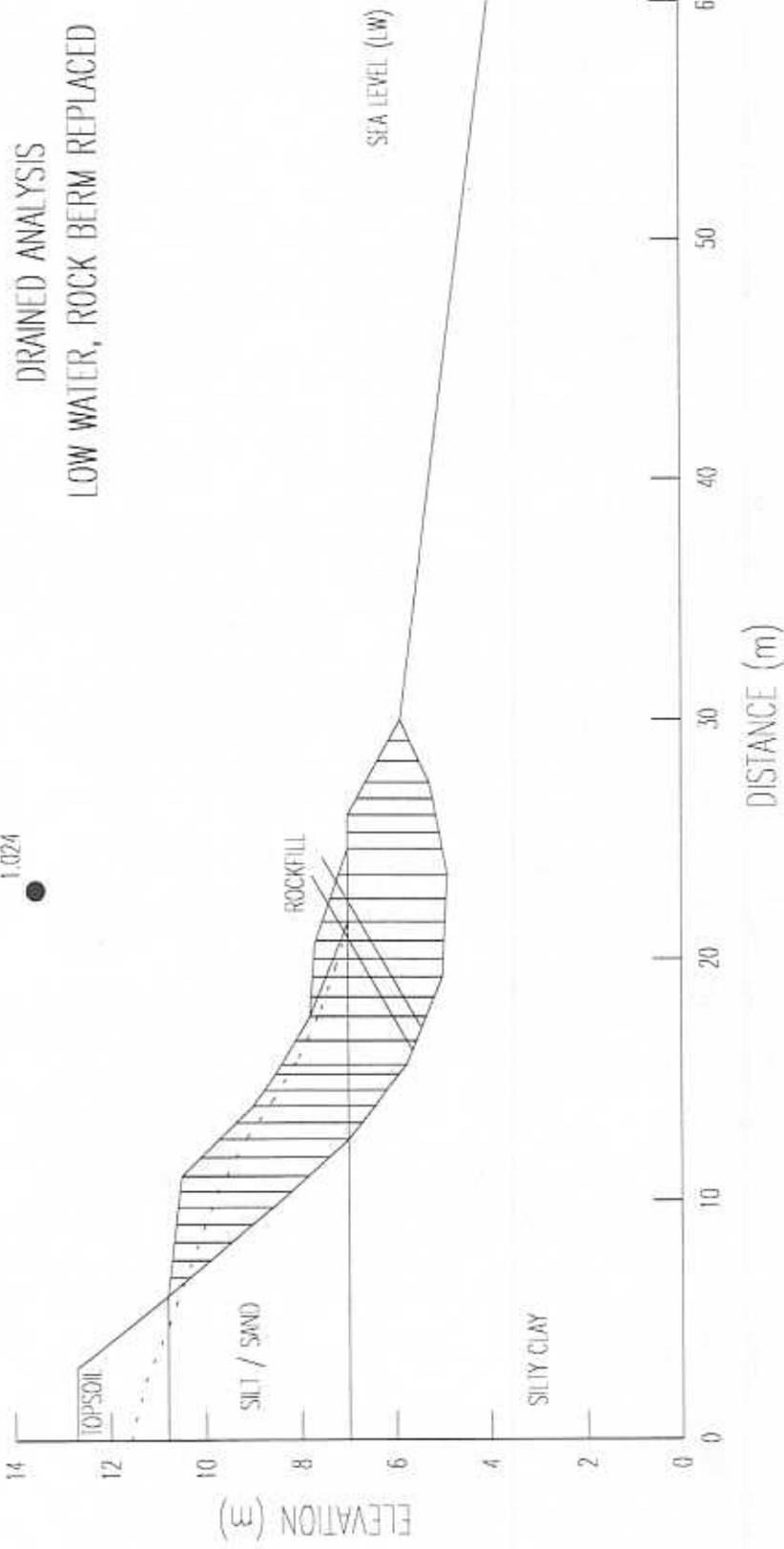






DRAINED ANALYSIS  
LOW WATER, ROCK BERM REPLACED







**Appendix C**

**Photographs of Gravity Cores, Stations S2 to S8, Annapolis Basin and Estuary**

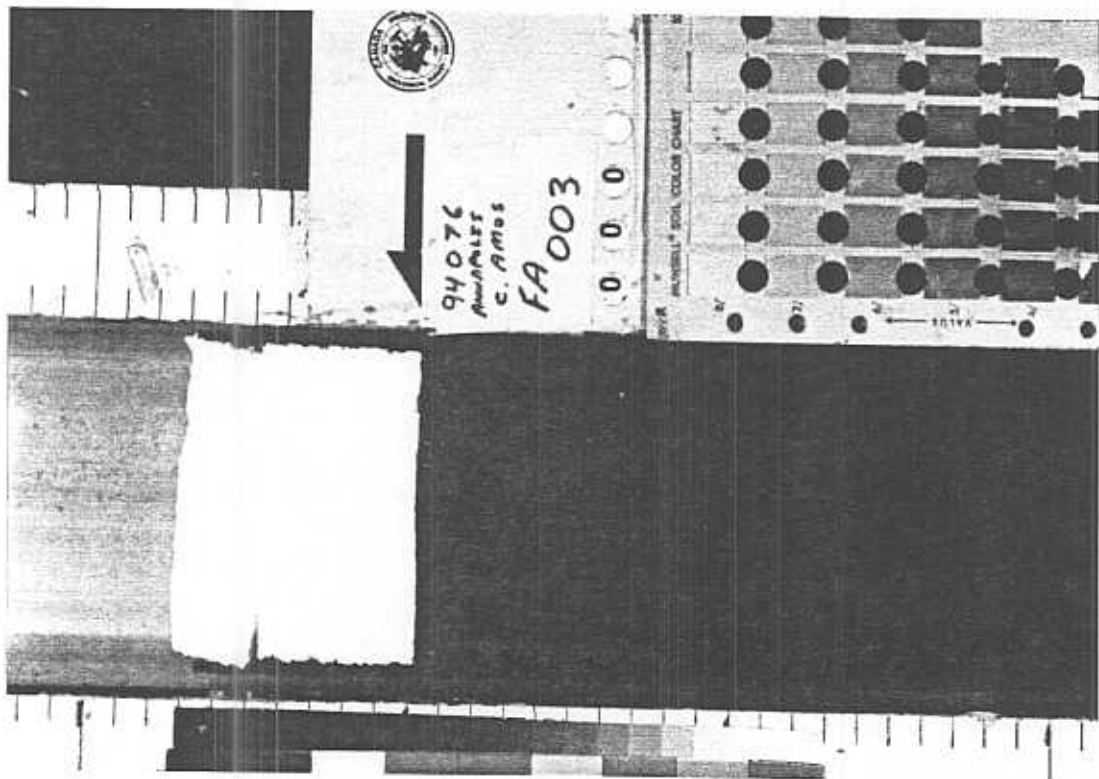


Figure 13.2 Gravity Core FA 003, (Upper Section)  
Anchor Station 3.

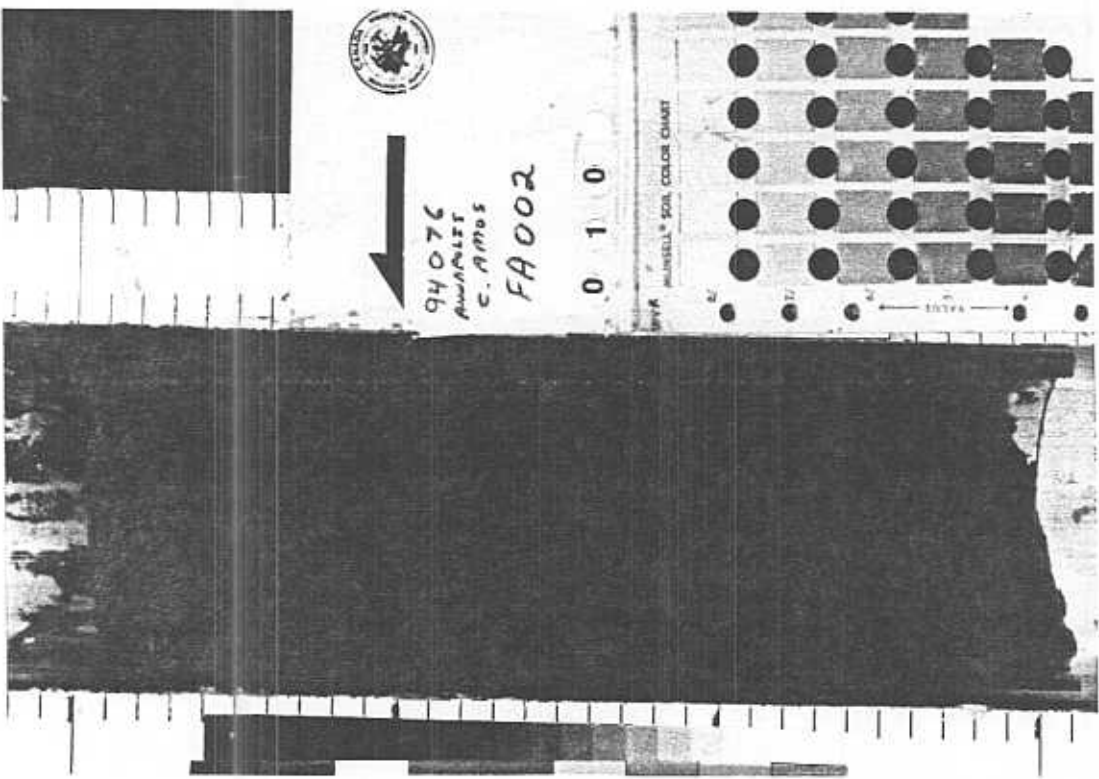


Figure 13.1 Gravity Core FA 002.  
Anchor Station 2.

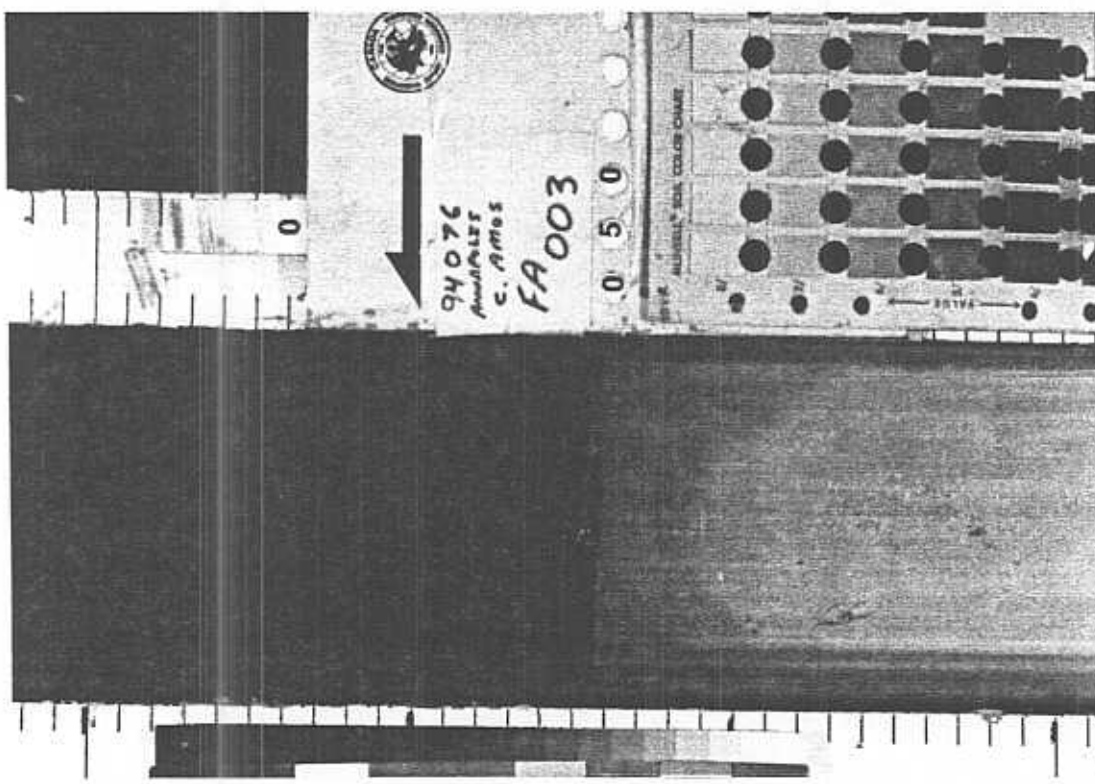


Figure 13.4 Gravity Core FA 003, (Lower Section)  
Anchor Station 3.

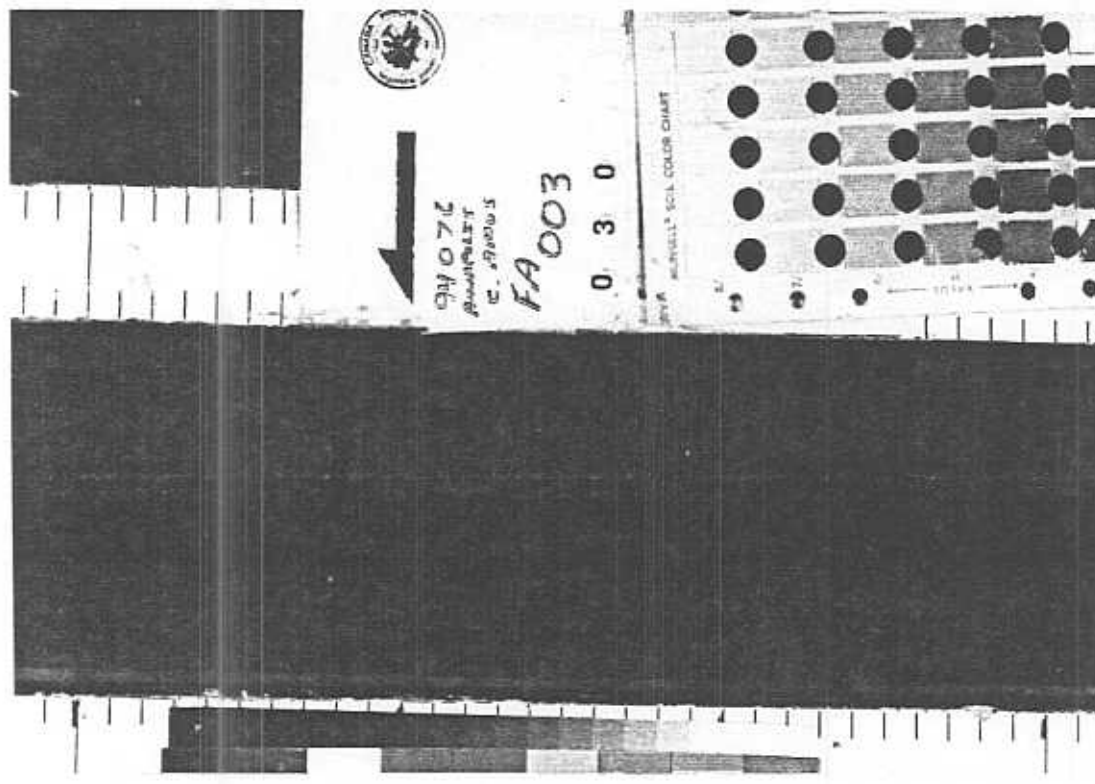


Figure 13.3 Gravity Core FA 003 (Middle Section).  
Anchor Station 3.

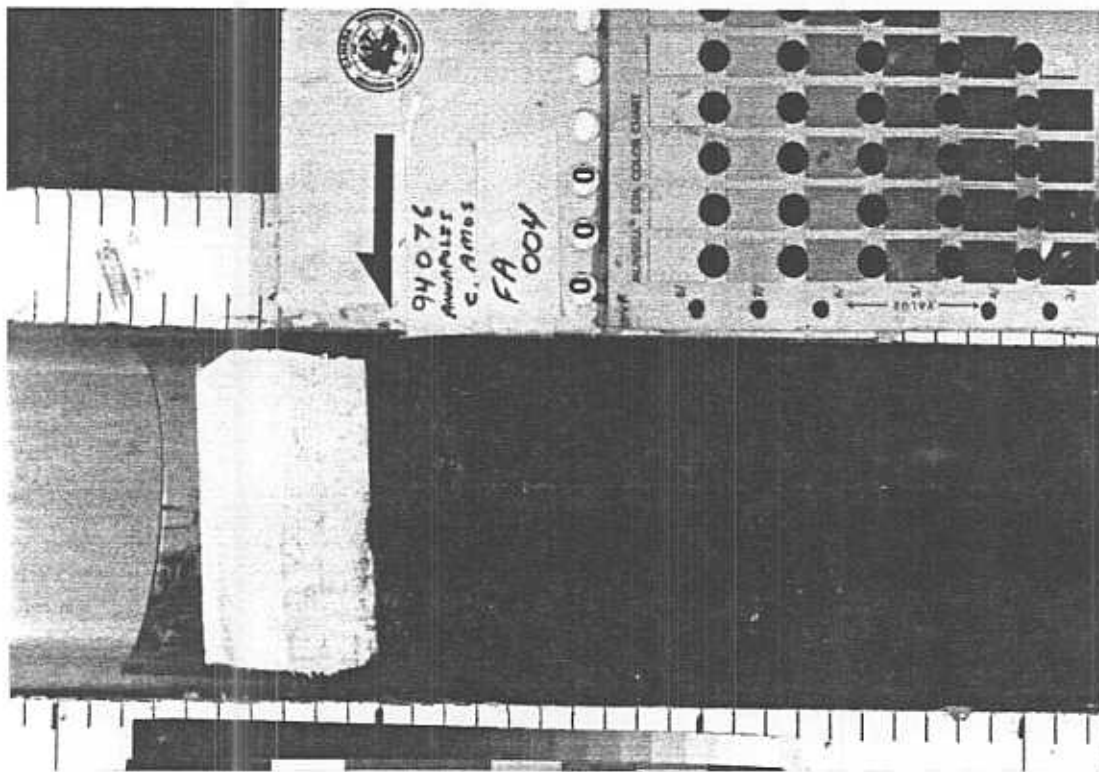


Figure 13.5 Gravity Core FA 004 (Upper Section).  
Anchor Station 4.

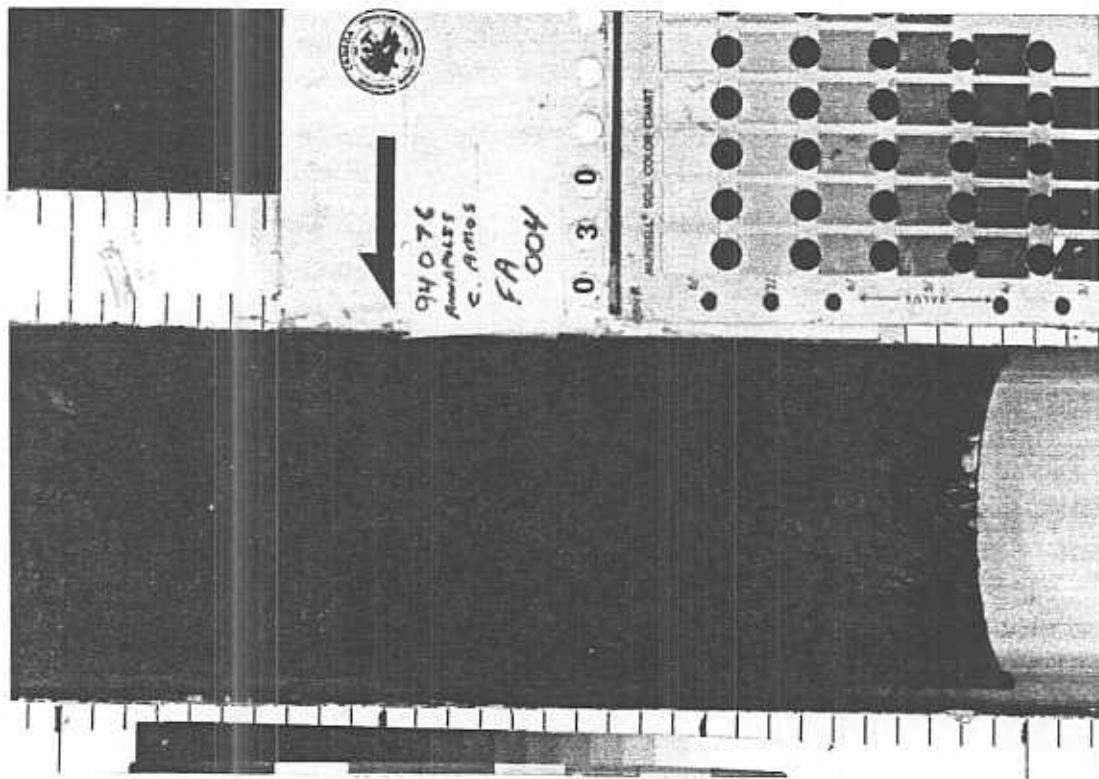


Figure 13.6 Gravity Core FA 004, (Lower Section).  
Anchor Station 4.

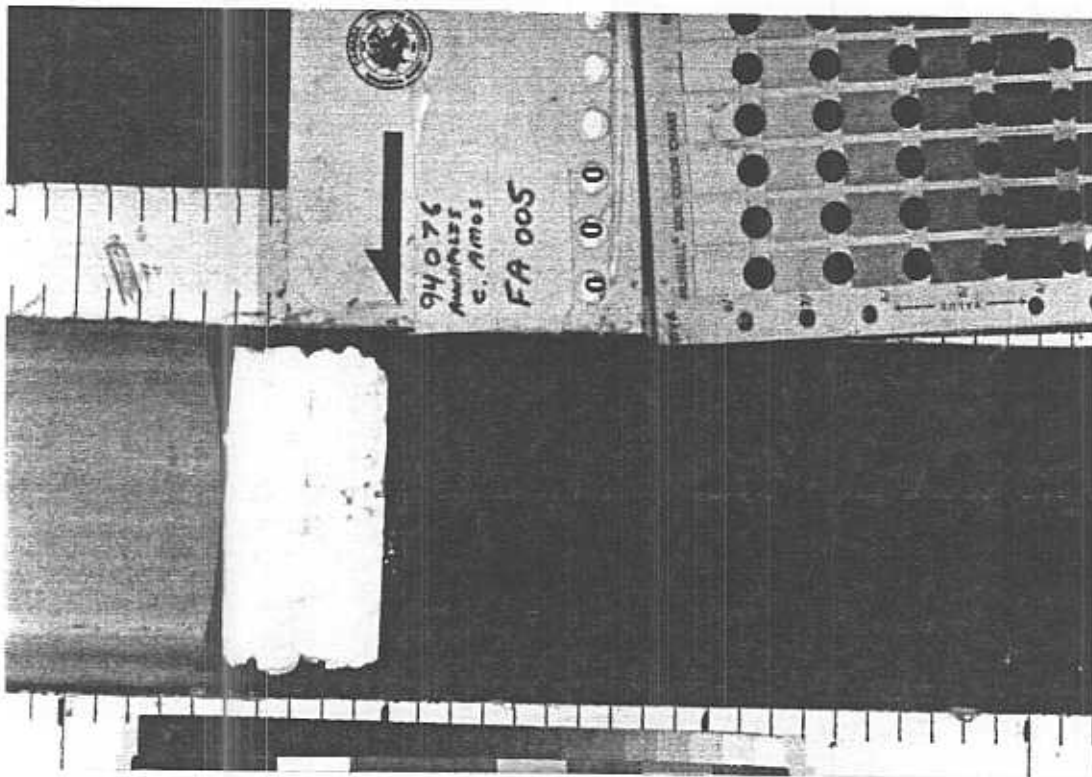


Figure 13.7 Gravity Core FA 005 (Upper Section).  
Anchor Station 5.

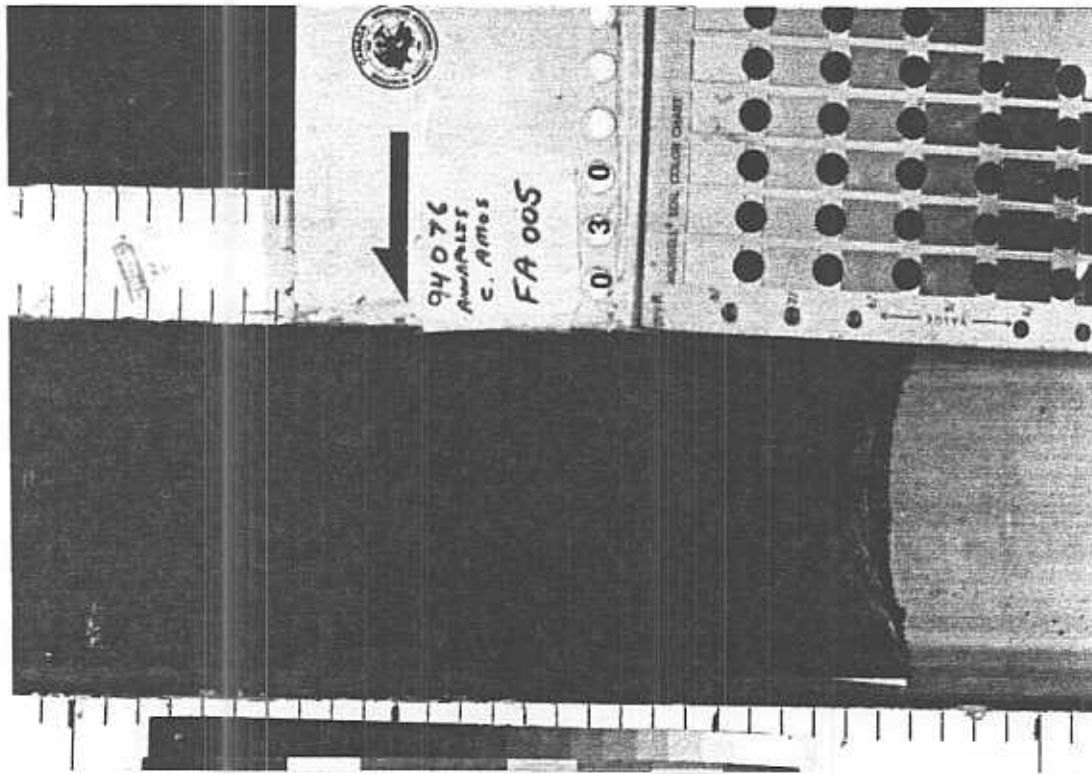


Figure 13.8 Gravity Core FA 005, (Lower Section)  
Anchor Station 5.



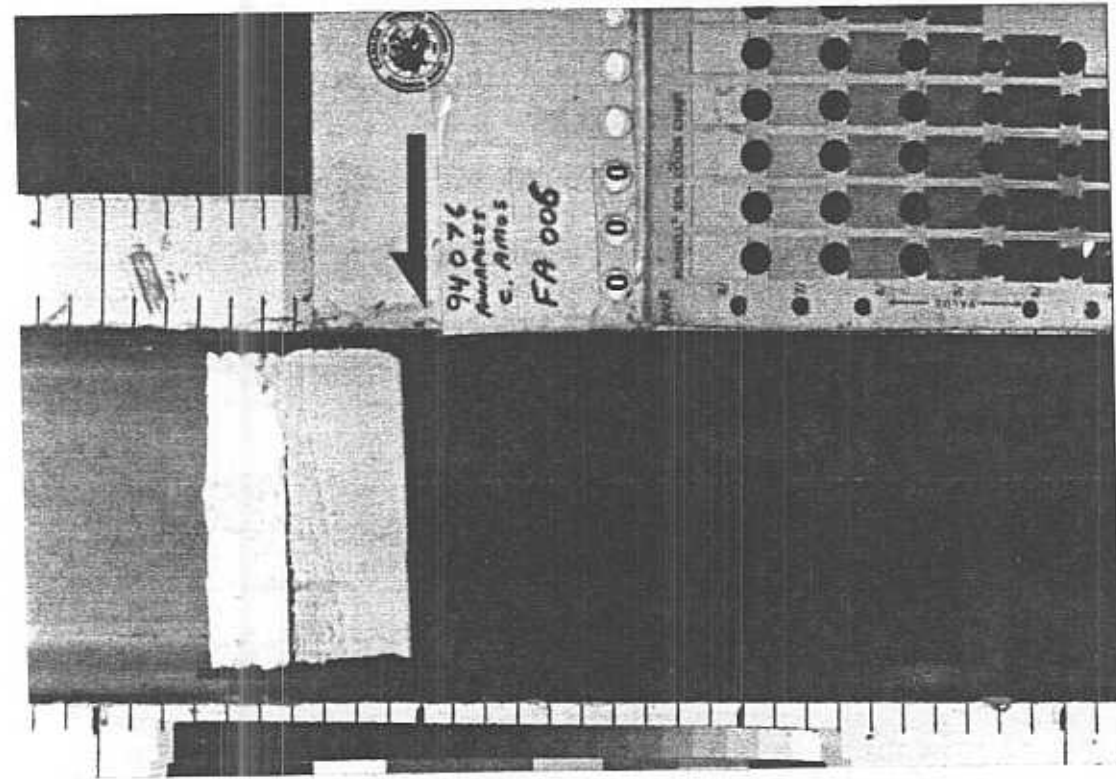


Figure 13.9 Gravity Core FA 006 (Upper Section).  
Anchor Station 6.

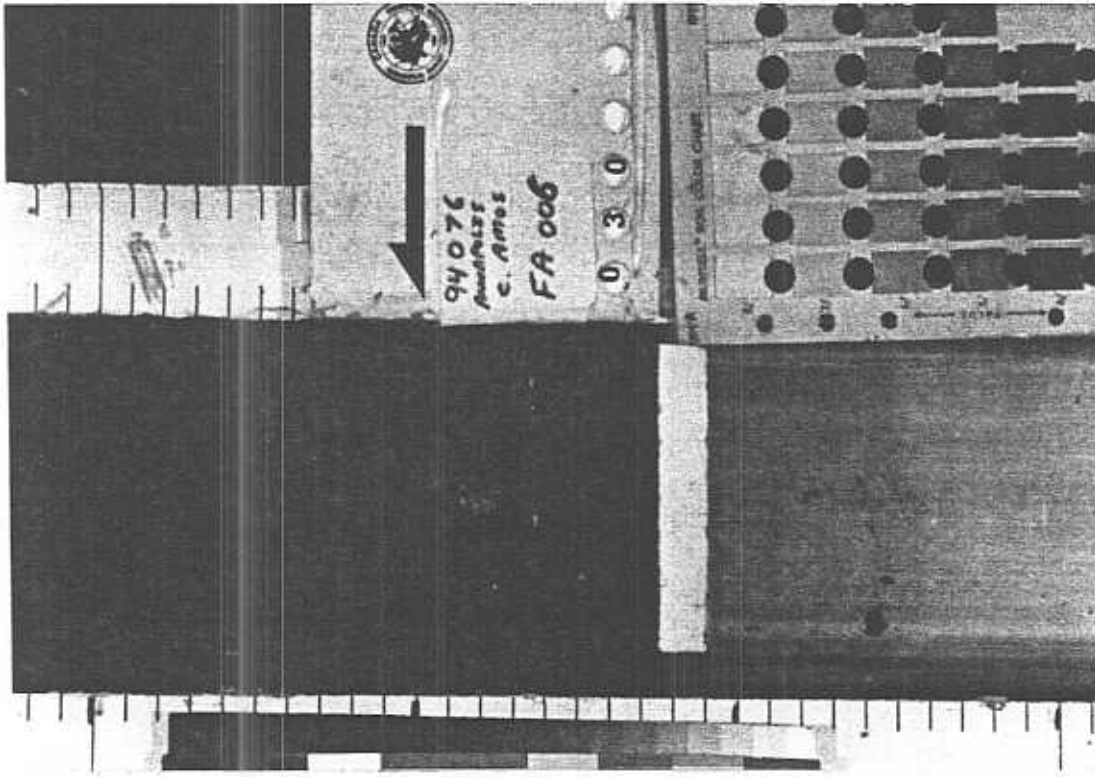


Figure 13.10 Gravity Core FA 006, (Lower Section)  
Anchor Station 6.

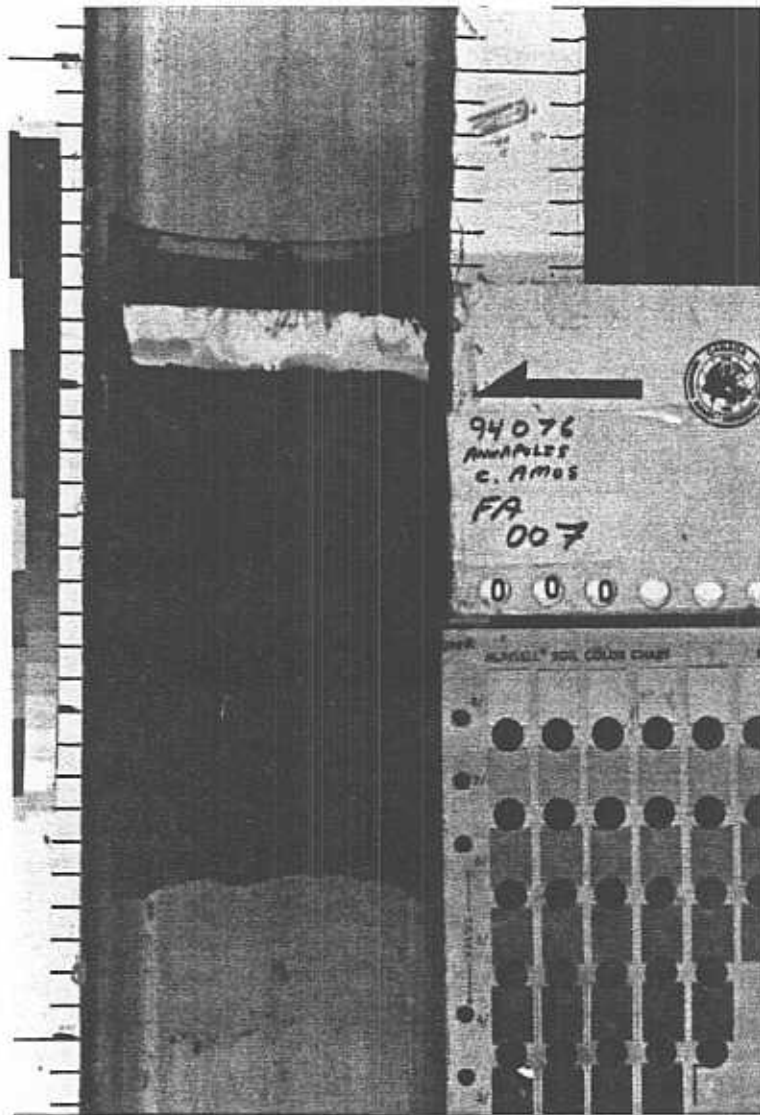


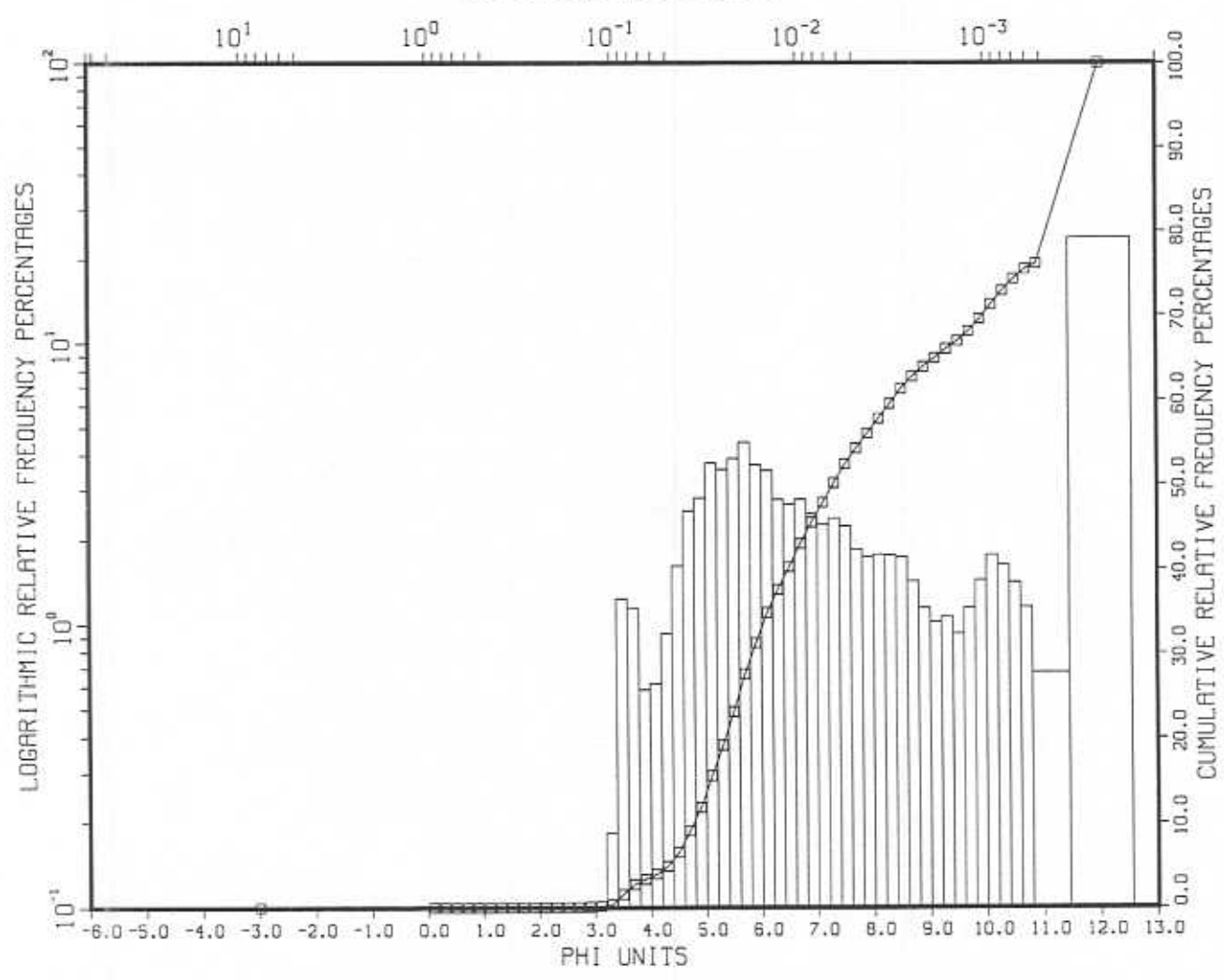
Figure 13.11 Gravity Core FA 007.  
Anchor Station 7.

**Appendix D**

**Grain Size Analyses of Gravity Cores**



94076-FA 02 C 0-2,R0009365, DR. CARL AMOS  
# ,00206, AGC GRAVITY, OFF FORT ANNE, ANNAPOLIS BASIN  
MILLIMETER EQUIVALENTS



CALCULATION RESULTS FOR  
THE SAMPLE WITH THE IDENTIFIER:

94076-FA 02 C 0-2, RD009365, DR. CARL AMOS  
# ,00206, AGC GRAVITY, OFF FORT ANNE, ANNAPOLIS BASIN

## RESULTS

MIDPOINTS		RELATIVE	CUMULATIVE
MM	PHI	FREQUENCY	FREQUENCY
		PERCENTAGES	PERCENTAGES
8.0	-3.00	0.03	0.03
.93	0.10	0.00	0.03
.81	0.30	0.00	0.03
.71	0.50	0.00	0.03
.62	0.70	0.00	0.03
.54	0.90	0.00	0.03
.47	1.10	0.00	0.03
.41	1.30	0.00	0.03
.35	1.50	0.00	0.03
.31	1.70	0.01	0.04
.27	1.90	0.00	0.04
.23	2.10	0.00	0.05
.20	2.30	0.01	0.05
.18	2.50	0.02	0.07
.15	2.70	0.02	0.09
.13	2.90	0.03	0.12
.12	3.10	0.06	0.18
.10	3.30	0.18	0.36
.88E-01	3.50	1.24	1.60
.77E-01	3.70	1.15	2.75
.67E-01	3.90	0.59	3.34
.58E-01	4.10	0.62	3.95
.51E-01	4.30	0.94	4.89
.44E-01	4.50	1.63	6.52
.38E-01	4.70	2.53	9.05
.33E-01	4.90	2.81	11.86
.29E-01	5.10	3.75	15.61
.25E-01	5.30	3.56	19.18
.22E-01	5.50	3.90	23.07
.19E-01	5.70	4.45	27.52
.17E-01	5.90	3.70	31.23
.15E-01	6.10	3.54	34.76
.13E-01	6.30	2.78	37.54
.11E-01	6.50	2.67	40.22
.96E-02	6.70	2.78	43.00
.84E-02	6.90	2.47	45.47
.73E-02	7.10	2.27	47.74
.63E-02	7.30	2.39	50.13
.55E-02	7.50	2.24	52.37
.48E-02	7.70	1.86	54.22

.42E-02	7.90	1.75	55.97
.36E-02	8.10	1.78	57.75
.32E-02	8.30	1.78	59.53
.28E-02	8.50	1.75	61.28
.24E-02	8.70	1.43	62.71
.21E-02	8.90	1.15	63.86
.18E-02	9.10	1.03	64.88
.16E-02	9.30	1.07	65.96
.14E-02	9.50	0.93	66.89
.12E-02	9.70	1.15	68.04
.10E-02	9.90	1.44	69.49
.91E-03	10.10	1.78	71.27
.79E-03	10.30	1.64	72.91
.69E-03	10.50	1.42	74.33
.60E-03	10.70	1.16	75.48
.52E-03	10.90	0.68	76.16
.24E-03	12.00	23.84	100.00

GRAIN SIZE BREAKDOWN				
%	%	%	%	%
GRAVEL	SAND	SILT	CLAY	MUD
0.03	3.30	52.64	44.03	96.66

## STATISTICAL MEASURES

MEAN	STANDARD	KURTOSIS	SKEWNESS
(PHI)	DEVIATION	( NO DIM. )	( NO DIM. )
	(PHI)		
8.05	2.76	1.73	0.25

Calculation Results for  
The Sample with the Identifier:

PSS Version: V2.3  
 Processed (DD-MM-YY): 8-16-94  
 Sed Lab Number: 9365  
 Lines of Raw Data: 57  
 Sed Lab's ID: 94076-FA 02 C 0-2  
 Cruise: 94076  
 Project Number: 303047  
 Scientist Name: DR. CARL AMOS  
 Sed Lab Comments: AGC GRAVITY, OFF FORT ANNE, ANNAPOLIS  
 BASIN  
 Raw Data File: RD009365  
 Sample Work File: SWF00206  
 Top Interval: 0.00 cm.  
 Bottom Interval: 2.00 cm.  
 SID key: 50787  
 Sample Number: FA-2  
 Station Number: FA-2  
 Instrument Type: AGC GRAVITY  
 Sample Type: CORE  
 Latitude: 44:44.55 Degrees North  
 Longitude: 65:31.35 Degrees West  
 Water Depth: 9.20 m.  
 #

Results

Midpoints		Relative Frequency Percentages	Cumulative Frequency Percentages
MM	PHI		
8.00e+00	-3.00	0.03	0.03
9.33e-01	0.10	0.00	0.03
8.12e-01	0.30	0.00	0.03
7.07e-01	0.50	0.00	0.03
6.16e-01	0.70	0.00	0.03
5.36e-01	0.90	0.00	0.03
4.67e-01	1.10	0.00	0.03
4.06e-01	1.30	0.00	0.03
3.54e-01	1.50	0.00	0.03
3.08e-01	1.70	0.01	0.04
2.68e-01	1.90	0.00	0.04
2.33e-01	2.10	0.00	0.05
2.03e-01	2.30	0.01	0.05
1.77e-01	2.50	0.02	0.07
1.54e-01	2.70	0.02	0.09
1.34e-01	2.90	0.03	0.12
1.17e-01	3.10	0.06	0.18
1.02e-01	3.30	0.18	0.36
8.84e-02	3.50	1.24	1.60
7.69e-02	3.70	1.15	2.75
6.70e-02	3.90	0.59	3.34

5.83e-02	4.10	0.62	3.95
5.08e-02	4.30	0.94	4.89
4.42e-02	4.50	1.63	6.52
3.85e-02	4.70	2.53	9.05
3.35e-02	4.90	2.81	11.86
2.92e-02	5.10	3.75	15.61
2.54e-02	5.30	3.56	19.18
2.21e-02	5.50	3.90	23.07
1.92e-02	5.70	4.45	27.52
1.67e-02	5.90	3.70	31.23
1.46e-02	6.10	3.54	34.76
1.27e-02	6.30	2.78	37.54
1.10e-02	6.50	2.67	40.22
9.62e-03	6.70	2.78	43.00
8.37e-03	6.90	2.47	45.47
7.29e-03	7.10	2.27	47.74
6.35e-03	7.30	2.39	50.13
5.52e-03	7.50	2.24	52.37
4.81e-03	7.70	1.86	54.22
4.19e-03	7.90	1.75	55.97
3.64e-03	8.10	1.78	57.75
3.17e-03	8.30	1.78	59.53
2.76e-03	8.50	1.75	61.28
2.40e-03	8.70	1.43	62.71
2.09e-03	8.90	1.15	63.86
1.82e-03	9.10	1.03	64.88
1.59e-03	9.30	1.07	65.96
1.38e-03	9.50	0.93	66.89
1.20e-03	9.70	1.15	68.04
1.05e-03	9.90	1.44	69.49
9.11e-04	10.10	1.78	71.27
7.93e-04	10.30	1.64	72.91
6.91e-04	10.50	1.42	74.33
6.01e-04	10.70	1.16	75.48
5.23e-04	10.90	0.68	76.16
2.44e-04	12.00	23.84	100.00

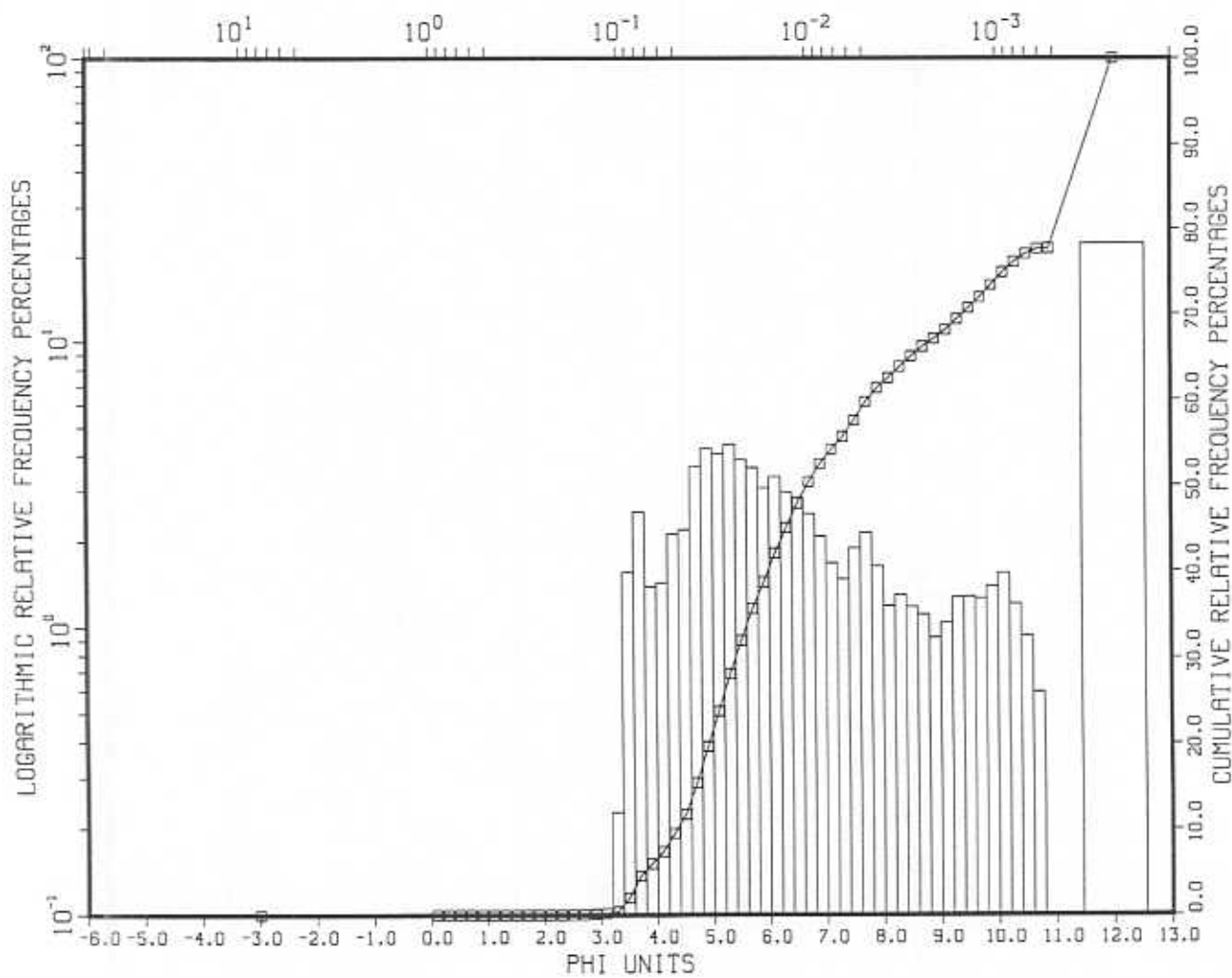
## Grain Size Breakdown

%	%	%	%	%
Gravel	Sand	Silt	Clay	Mud
0.03	3.30	52.64	44.03	96.66

## Statistical Measures

Mean	Standard	Kurtosis	Skewness
(PHI)	Deviation	( No Dim. )	( No Dim. )
(PHI)	(PHI)	( No Dim. )	( No Dim. )
8.05	2.76	1.73	0.25

94076-FA 03 C 0-3,RD009366, DR. CARL AMOS  
 # ,00207, AGC GRAVITY, INNER ANNAPOLIS BASIN  
 MILLIMETER EQUIVALENTS



CALCULATION RESULTS FOR  
THE SAMPLE WITH THE IDENTIFIER:

94076-FA 03 C 0-3, RD009366,  
# ,00207,

DR. CARL AMOS  
AGC GRAVITY, INNER ANNAPOLIS BASIN

## RESULTS

MIDPOINTS		RELATIVE	CUMULATIVE
MM	PHI	FREQUENCY	FREQUENCY
		PERCENTAGES	PERCENTAGES
8.0	-3.00	0.01	0.01
.93	0.10	0.00	0.01
.81	0.30	0.00	0.01
.71	0.50	0.00	0.01
.62	0.70	0.00	0.01
.54	0.90	0.00	0.01
.47	1.10	0.00	0.01
.41	1.30	0.00	0.01
.35	1.50	0.00	0.01
.31	1.70	0.00	0.01
.27	1.90	0.00	0.01
.23	2.10	0.00	0.01
.20	2.30	0.02	0.03
.18	2.50	0.01	0.04
.15	2.70	0.03	0.07
.13	2.90	0.05	0.11
.12	3.10	0.08	0.19
.10	3.30	0.23	0.42
.88E-01	3.50	1.56	1.97
.77E-01	3.70	2.55	4.52
.67E-01	3.90	1.39	5.92
.58E-01	4.10	1.43	7.35
.51E-01	4.30	2.12	9.47
.44E-01	4.50	2.20	11.68
.38E-01	4.70	3.66	15.34
.33E-01	4.90	4.24	19.58
.29E-01	5.10	4.07	23.66
.25E-01	5.30	4.39	28.04
.22E-01	5.50	3.87	31.92
.19E-01	5.70	3.63	35.54
.17E-01	5.90	3.09	38.63
.15E-01	6.10	3.38	42.01
.13E-01	6.30	2.98	45.00
.11E-01	6.50	2.86	47.85
.96E-02	6.70	2.51	50.36
.84E-02	6.90	2.09	52.46
.73E-02	7.10	1.69	54.14
.63E-02	7.30	1.48	55.62
.55E-02	7.50	1.90	57.53
.48E-02	7.70	2.16	59.69

.42E-02	7.90	1.64	61.33
.36E-02	8.10	1.19	62.52
.32E-02	8.30	1.31	63.83
.28E-02	8.50	1.19	65.02
.24E-02	8.70	1.12	66.13
.21E-02	8.90	0.93	67.06
.18E-02	9.10	1.05	68.11
.16E-02	9.30	1.28	69.39
.14E-02	9.50	1.29	70.68
.12E-02	9.70	1.27	71.95
.10E-02	9.90	1.40	73.35
.91E-03	10.10	1.56	74.90
.79E-03	10.30	1.22	76.12
.69E-03	10.50	0.95	77.06
.60E-03	10.70	0.60	77.66
.52E-03	10.90	0.05	77.71
.24E-03	12.00	22.29	100.00

## GRAIN SIZE BREAKDOWN

%	%	%	%	%
GRAVEL	SAND	SILT	CLAY	MUD
0.01	5.90	55.42	38.67	94.08

## STATISTICAL MEASURES

MEAN	STANDARD	KURTOSIS	SKEWNESS
(PHI)	DEVIATION	( NO DIM. )	( NO DIM. )
	(PHI)		
7.66	2.86	1.75	0.40



Calculation Results for  
The Sample with the Identifier:

PSS Version: V2.3  
 Processed (DD-MM-YY): 8-16-94  
 Sed Lab Number: 9366  
 Lines of Raw Data: 57  
 Sed Lab's ID: 94076-FA 03 C 0-3  
 Cruise: 94076  
 Project Number: 303047  
 Scientist Name: DR. CARL AMOS  
 Sed Lab Comments: AGC GRAVITY, INNER ANNAPOLIS BASIN  
 Raw Data File: RD009366  
 Sample Work File: SWF00207  
 Top Interval: 0.00 cm.  
 Bottom Interval: 3.00 cm.  
 SID key: 50789  
 Sample Number: FA-3  
 Station Number: FA-3  
 Instrument Type: AGC GRAVITY  
 Sample Type: CORE  
 Latitude: 44:43.97 Degrees North  
 Longitude: 65:32.12 Degrees West  
 Water Depth: 8.40 m.  
 #

Results

Midpoints		Relative Frequency Percentages	Cumulative Frequency Percentages
MM	PHI		
8.00e+00	-3.00	0.01	0.01
9.33e-01	0.10	0.00	0.01
8.12e-01	0.30	0.00	0.01
7.07e-01	0.50	0.00	0.01
6.16e-01	0.70	0.00	0.01
5.36e-01	0.90	0.00	0.01
4.67e-01	1.10	0.00	0.01
4.06e-01	1.30	0.00	0.01
3.54e-01	1.50	0.00	0.01
3.08e-01	1.70	0.00	0.01
2.68e-01	1.90	0.00	0.01
2.33e-01	2.10	0.00	0.01
2.03e-01	2.30	0.02	0.03
1.77e-01	2.50	0.01	0.04
1.54e-01	2.70	0.03	0.07
1.34e-01	2.90	0.05	0.11
1.17e-01	3.10	0.08	0.19
1.02e-01	3.30	0.23	0.42
8.84e-02	3.50	1.56	1.97
7.69e-02	3.70	2.55	4.52
6.70e-02	3.90	1.39	5.92

5.83e-02	4.10	1.43	7.35
5.08e-02	4.30	2.12	9.47
4.42e-02	4.50	2.20	11.68
3.85e-02	4.70	3.66	15.34
3.35e-02	4.90	4.24	19.58
2.92e-02	5.10	4.07	23.66
2.54e-02	5.30	4.39	28.04
2.21e-02	5.50	3.87	31.92
1.92e-02	5.70	3.63	35.54
1.67e-02	5.90	3.09	38.63
1.46e-02	6.10	3.38	42.01
1.27e-02	6.30	2.98	45.00
1.10e-02	6.50	2.86	47.85
9.62e-03	6.70	2.51	50.36
8.37e-03	6.90	2.09	52.46
7.29e-03	7.10	1.69	54.14
6.35e-03	7.30	1.48	55.62
5.52e-03	7.50	1.90	57.53
4.81e-03	7.70	2.16	59.69
4.19e-03	7.90	1.64	61.33
3.64e-03	8.10	1.19	62.52
3.17e-03	8.30	1.31	63.83
2.76e-03	8.50	1.19	65.02
2.40e-03	8.70	1.12	66.13
2.09e-03	8.90	0.93	67.06
1.82e-03	9.10	1.05	68.11
1.59e-03	9.30	1.28	69.39
1.38e-03	9.50	1.29	70.68
1.20e-03	9.70	1.27	71.95
1.05e-03	9.90	1.40	73.35
9.11e-04	10.10	1.56	74.90
7.93e-04	10.30	1.22	76.12
6.91e-04	10.50	0.95	77.06
6.01e-04	10.70	0.60	77.66
5.23e-04	10.90	0.05	77.71
2.44e-04	12.00	22.29	100.00

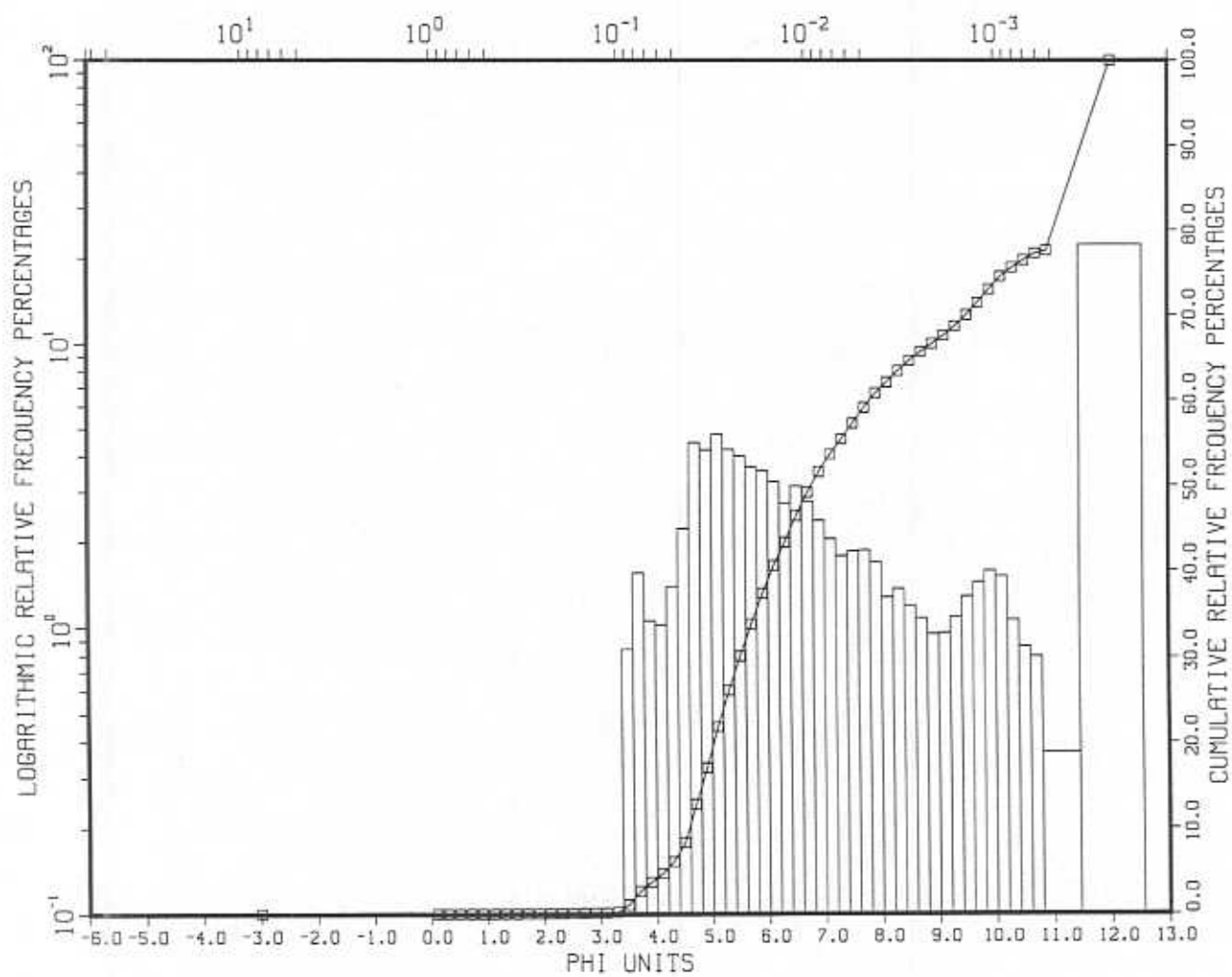
## Grain Size Breakdown

%	%	%	%	%
Gravel	Sand	Silt	Clay	Mud
0.01	5.90	55.42	38.67	94.08

## Statistical Measures

Mean	Standard	Kurtosis	Skewness
(PHI)	Deviation	( No Dim. )	( No Dim. )
	(PHI)		
7.66	2.86	1.75	0.40

94076-FA 04 C 0-3,R0009369, DR. CARL AMOS  
 # ,00207, AGC GRAVITY, INNER ANNAPOLIS BASIN  
 MILLIMETER EQUIVALENTS



CALCULATION RESULTS FOR  
THE SAMPLE WITH THE IDENTIFIER:

94076-FA 04 C 0-3,RD009369, DR. CARL AMOS  
# ,00207, AGC GRAVITY, INNER ANNAPOLIS BASIN

## RESULTS

MIDPOINTS		RELATIVE	CUMULATIVE
MM	PHI	FREQUENCY	FREQUENCY
		PERCENTAGES	PERCENTAGES
8.0	-3.00	0.06	0.06
.93	0.10	0.00	0.06
.81	0.30	0.00	0.06
.71	0.50	0.00	0.06
.62	0.70	0.00	0.06
.54	0.90	0.00	0.06
.47	1.10	0.00	0.06
.41	1.30	0.00	0.06
.35	1.50	0.00	0.07
.31	1.70	0.00	0.07
.27	1.90	0.01	0.07
.23	2.10	0.01	0.08
.20	2.30	0.01	0.09
.18	2.50	0.01	0.10
.15	2.70	0.01	0.12
.13	2.90	0.02	0.14
.12	3.10	0.03	0.17
.10	3.30	0.08	0.25
.88E-01	3.50	0.84	1.09
.77E-01	3.70	1.55	2.64
.67E-01	3.90	1.06	3.70
.58E-01	4.10	1.02	4.72
.51E-01	4.30	1.39	6.11
.44E-01	4.50	2.23	8.34
.38E-01	4.70	4.47	12.81
.33E-01	4.90	4.22	17.03
.29E-01	5.10	4.78	21.81
.25E-01	5.30	4.23	26.04
.22E-01	5.50	4.02	30.07
.19E-01	5.70	3.66	33.72
.17E-01	5.90	3.56	37.29
.15E-01	6.10	3.26	40.55
.13E-01	6.30	2.74	43.28
.11E-01	6.50	3.15	46.43
.96E-02	6.70	2.78	49.21
.84E-02	6.90	2.38	51.59
.73E-02	7.10	2.05	53.64
.63E-02	7.30	1.78	55.42
.55E-02	7.50	1.85	57.27
.48E-02	7.70	1.86	59.13

.42E-02	7.90	1.70	60.82
.36E-02	8.10	1.27	62.10
.32E-02	8.30	1.37	63.46
.28E-02	8.50	1.19	64.66
.24E-02	8.70	1.08	65.73
.21E-02	8.90	0.95	66.69
.18E-02	9.10	0.96	67.65
.16E-02	9.30	1.09	68.74
.14E-02	9.50	1.29	70.03
.12E-02	9.70	1.44	71.47
.10E-02	9.90	1.58	73.05
.91E-03	10.10	1.51	74.57
.79E-03	10.30	1.07	75.63
.69E-03	10.50	0.86	76.49
.60E-03	10.70	0.80	77.29
.52E-03	10.90	0.37	77.66
.24E-03	12.00	22.34	100.00

## GRAIN SIZE BREAKDOWN

%	%	%	%	%
GRAVEL	SAND	SILT	CLAY	MUD
0.06	3.64	57.12	39.18	96.30

## STATISTICAL MEASURES

MEAN	STANDARD	KURTOSIS	SKEWNESS
(PHI)	DEVIATION	( NO DIM. )	( NO DIM. )
	(PHI)		
7.74	2.81	1.83	0.38

Calculation Results for  
The Sample with the Identifier:

PSS Version: V2.3  
 Processed (DD-MM-YY): 8-16-94  
 Sed Lab Number: 9369  
 Lines of Raw Data: 57  
 Sed Lab's ID: 94076-FA 04 C 0-3  
 Cruise: 94076  
 Project Number: 303047  
 Scientist Name: DR. CARL AMOS  
 Sed Lab Comments: AGC GRAVITY, INNER ANNAPOLIS BASIN  
 Raw Data File: RD009369  
 Sample Work File: SWF00207  
 Top Interval: 0.00 cm.  
 Bottom Interval: 3.00 cm.  
 SID key: 50791  
 Sample Number: FA-4  
 Station Number: FA-4  
 Instrument Type: AGC GRAVITY  
 Sample Type: CORE  
 Latitude: 44:43.68 Degrees North  
 Longitude: 65:32.99 Degrees West  
 Water Depth: 7.50 m.  
 #

Results

Midpoints		Relative Frequency Percentages	Cumulative Frequency Percentages
MM	PHI		
8.00e+00	-3.00	0.06	0.06
9.33e-01	0.10	0.00	0.06
8.12e-01	0.30	0.00	0.06
7.07e-01	0.50	0.00	0.06
6.16e-01	0.70	0.00	0.06
5.36e-01	0.90	0.00	0.06
4.67e-01	1.10	0.00	0.06
4.06e-01	1.30	0.00	0.06
3.54e-01	1.50	0.00	0.07
3.08e-01	1.70	0.00	0.07
2.68e-01	1.90	0.01	0.07
2.33e-01	2.10	0.01	0.08
2.03e-01	2.30	0.01	0.09
1.77e-01	2.50	0.01	0.10
1.54e-01	2.70	0.01	0.12
1.34e-01	2.90	0.02	0.14
1.17e-01	3.10	0.03	0.17
1.02e-01	3.30	0.08	0.25
8.84e-02	3.50	0.84	1.09
7.69e-02	3.70	1.55	2.64
6.70e-02	3.90	1.06	3.70

5.83e-02	4.10	1.02	4.72
5.08e-02	4.30	1.39	6.11
4.42e-02	4.50	2.23	8.34
3.85e-02	4.70	4.47	12.81
3.35e-02	4.90	4.22	17.03
2.92e-02	5.10	4.78	21.81
2.54e-02	5.30	4.23	26.04
2.21e-02	5.50	4.02	30.07
1.92e-02	5.70	3.66	33.72
1.67e-02	5.90	3.56	37.29
1.46e-02	6.10	3.26	40.55
1.27e-02	6.30	2.74	43.28
1.10e-02	6.50	3.15	46.43
9.62e-03	6.70	2.78	49.21
8.37e-03	6.90	2.38	51.59
7.29e-03	7.10	2.05	53.64
6.35e-03	7.30	1.78	55.42
5.52e-03	7.50	1.85	57.27
4.81e-03	7.70	1.86	59.13
4.19e-03	7.90	1.70	60.82
3.64e-03	8.10	1.27	62.10
3.17e-03	8.30	1.37	63.46
2.76e-03	8.50	1.19	64.66
2.40e-03	8.70	1.08	65.73
2.09e-03	8.90	0.95	66.69
1.82e-03	9.10	0.96	67.65
1.59e-03	9.30	1.09	68.74
1.38e-03	9.50	1.29	70.03
1.20e-03	9.70	1.44	71.47
1.05e-03	9.90	1.58	73.05
9.11e-04	10.10	1.51	74.57
7.93e-04	10.30	1.07	75.63
6.91e-04	10.50	0.86	76.49
6.01e-04	10.70	0.80	77.29
5.23e-04	10.90	0.37	77.66
2.44e-04	12.00	22.34	100.00

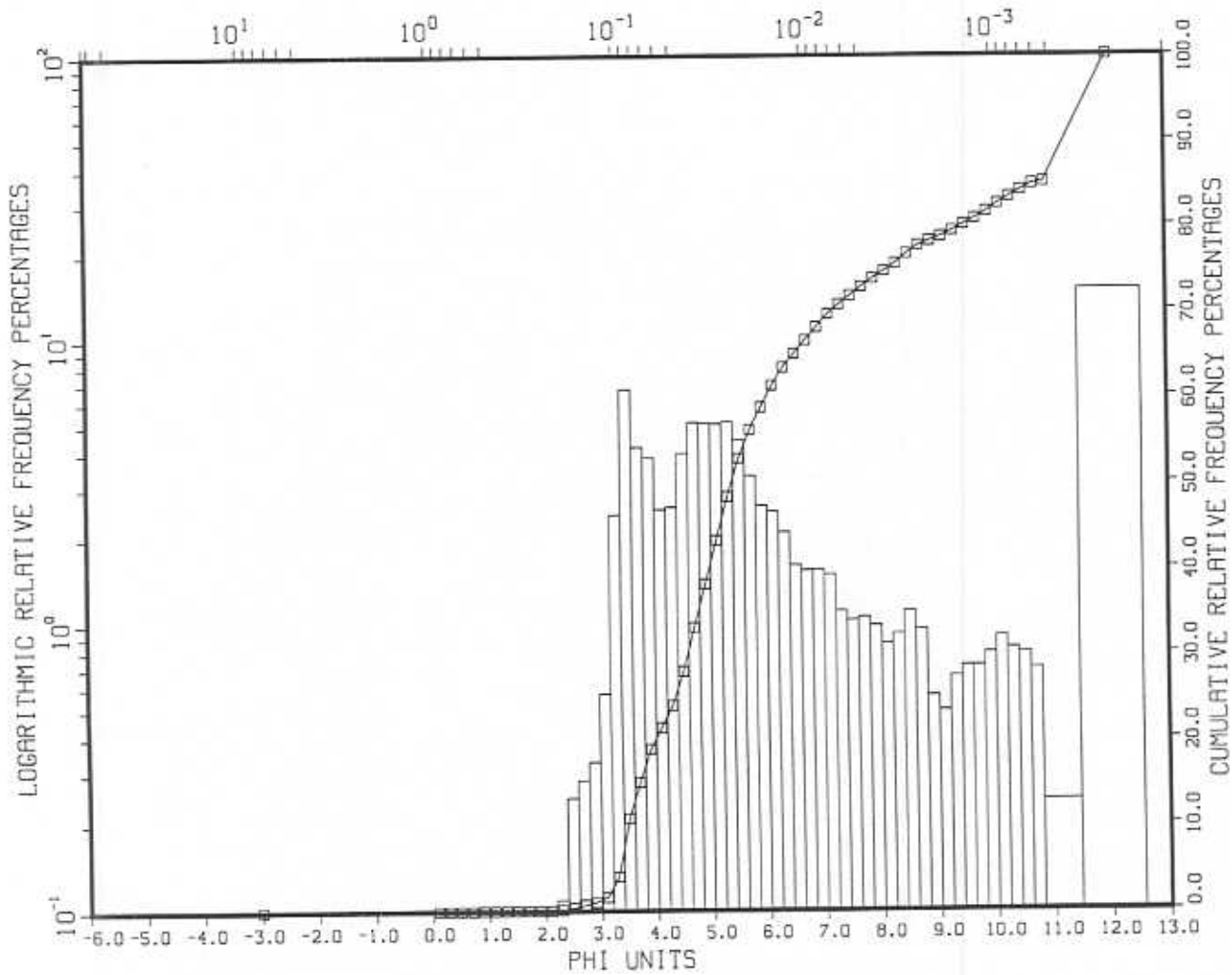
## Grain Size Breakdown

%	%	%	%	%
Gravel	Sand	Silt	Clay	Mud
0.06	3.64	57.12	39.18	96.30

## Statistical Measures

Mean	Standard	Kurtosis	Skewness
(PHI)	Deviation	( No Dim. )	( No Dim. )
	(PHI)		
7.74	2.81	1.83	0.38

94076-FA 05 C 0-3, RD009367, DR. CARL AMOS  
 # ,00208, AGC GRAVITY, BEHIND GOAT ISLAND, ANNAPOLIS BASIN  
 MILLIMETER EQUIVALENTS





CALCULATION RESULTS FOR  
THE SAMPLE WITH THE IDENTIFIER:

94076-FA 05 C 0-3, RD009367, DR. CARL AMOS  
# ,00208, AGC GRAVITY, BEHIND GOAT ISLAND, ANNAPOLIS BASIN

## RESULTS

MIDPOINTS		RELATIVE	CUMULATIVE
MM	PHI	FREQUENCY	FREQUENCY
		PERCENTAGES	PERCENTAGES
8.0	-3.00	0.00	0.00
.93	0.10	0.00	0.00
.81	0.30	0.00	0.00
.71	0.50	0.00	0.00
.62	0.70	0.00	0.00
.54	0.90	0.03	0.03
.47	1.10	0.00	0.03
.41	1.30	0.01	0.04
.35	1.50	0.00	0.04
.31	1.70	0.00	0.04
.27	1.90	0.00	0.04
.23	2.10	0.01	0.06
.20	2.30	0.11	0.16
.18	2.50	0.25	0.41
.15	2.70	0.29	0.70
.13	2.90	0.33	1.03
.12	3.10	0.57	1.60
.10	3.30	2.43	4.04
.88E-01	3.50	6.69	10.73
.77E-01	3.70	4.21	14.94
.67E-01	3.90	3.86	18.80
.58E-01	4.10	2.54	21.34
.51E-01	4.30	2.58	23.92
.44E-01	4.50	4.00	27.92
.38E-01	4.70	5.12	33.04
.33E-01	4.90	5.10	38.14
.29E-01	5.10	5.06	43.19
.25E-01	5.30	5.15	48.34
.22E-01	5.50	4.44	52.78
.19E-01	5.70	3.33	56.11
.17E-01	5.90	2.62	58.73
.15E-01	6.10	2.50	61.22
.13E-01	6.30	2.11	63.34
.11E-01	6.50	1.62	64.96
.96E-02	6.70	1.55	66.51
.84E-02	6.90	1.56	68.07
.73E-02	7.10	1.50	69.58
.63E-02	7.30	1.12	70.70
.55E-02	7.50	1.04	71.73
.48E-02	7.70	1.06	72.80

.42E-02	7.90	0.99	73.79
.36E-02	8.10	0.86	74.65
.32E-02	8.30	0.93	75.58
.28E-02	8.50	1.12	76.70
.24E-02	8.70	0.96	77.66
.21E-02	8.90	0.56	78.23
.18E-02	9.10	0.50	78.73
.16E-02	9.30	0.66	79.39
.14E-02	9.50	0.72	80.11
.12E-02	9.70	0.72	80.82
.10E-02	9.90	0.80	81.62
.91E-03	10.10	0.91	82.53
.79E-03	10.30	0.83	83.36
.69E-03	10.50	0.80	84.16
.60E-03	10.70	0.70	84.87
.52E-03	10.90	0.24	85.11
.24E-03	12.00	14.89	100.00

## GRAIN SIZE BREAKDOWN

% GRAVEL	% SAND	% SILT	% CLAY	% MUD
0.00	18.79	55.00	26.21	81.20

## STATISTICAL MEASURES

MEAN (PHI)	STANDARD DEVIATION (PHI)	KURTOSIS ( NO DIM. )	SKEWNESS ( NO DIM. )
6.55	2.87	2.41	0.86

Calculation Results for  
The Sample with the Identifier:

PSS Version: V2.3  
 Processed (DD-MM-YY): 8-16-94  
 Sed Lab Number: 9367  
 Lines of Raw Data: 57  
 Sed Lab's ID: 94076-FA 05 C 0-3  
 Cruise: 94076  
 Project Number: 303047  
 Scientist Name: DR. CARL AMOS  
 Sed Lab Comments: AGC GRAVITY, BEHIND GOAT ISLAND,  
 ANNAPOLIS BASIN  
 Raw Data File: RD009367  
 Sample Work File: SWF00208  
 Top Interval: 0.00 cm.  
 Bottom Interval: 3.00 cm.  
 SID key: 50793  
 Sample Number: FA-5  
 Station Number: FA-5  
 Instrument Type: AGC GRAVITY  
 Sample Type: CORE  
 Latitude: 44:42.46 Degrees North  
 Longitude: 65:35.51 Degrees West  
 Water Depth: 6.40 m.  
 #

Results

Midpoints		Relative Frequency Percentages	Cumulative Frequency Percentages
MM	PHI		
8.00e+00	-3.00	0.00	0.00
9.33e-01	0.10	0.00	0.00
8.12e-01	0.30	0.00	0.00
7.07e-01	0.50	0.00	0.00
6.16e-01	0.70	0.00	0.00
5.36e-01	0.90	0.03	0.03
4.67e-01	1.10	0.00	0.03
4.06e-01	1.30	0.01	0.04
3.54e-01	1.50	0.00	0.04
3.08e-01	1.70	0.00	0.04
2.68e-01	1.90	0.00	0.04
2.33e-01	2.10	0.01	0.06
2.03e-01	2.30	0.11	0.16
1.77e-01	2.50	0.25	0.41
1.54e-01	2.70	0.29	0.70
1.34e-01	2.90	0.33	1.03
1.17e-01	3.10	0.57	1.60
1.02e-01	3.30	2.43	4.04
8.84e-02	3.50	6.69	10.73
7.69e-02	3.70	4.21	14.94

6.70e-02	3.90	3.86	18.80
5.83e-02	4.10	2.54	21.34
5.08e-02	4.30	2.58	23.92
4.42e-02	4.50	4.00	27.92
3.85e-02	4.70	5.12	33.04
3.35e-02	4.90	5.10	38.14
2.92e-02	5.10	5.06	43.19
2.54e-02	5.30	5.15	48.34
2.21e-02	5.50	4.44	52.78
1.92e-02	5.70	3.33	56.11
1.67e-02	5.90	2.62	58.73
1.46e-02	6.10	2.50	61.22
1.27e-02	6.30	2.11	63.34
1.10e-02	6.50	1.62	64.96
9.62e-03	6.70	1.55	66.51
8.37e-03	6.90	1.56	68.07
7.29e-03	7.10	1.50	69.58
6.35e-03	7.30	1.12	70.70
5.52e-03	7.50	1.04	71.73
4.81e-03	7.70	1.06	72.80
4.19e-03	7.90	0.99	73.79
3.64e-03	8.10	0.86	74.65
3.17e-03	8.30	0.93	75.58
2.76e-03	8.50	1.12	76.70
2.40e-03	8.70	0.96	77.66
2.09e-03	8.90	0.56	78.23
1.82e-03	9.10	0.50	78.73
1.59e-03	9.30	0.66	79.39
1.38e-03	9.50	0.72	80.11
1.20e-03	9.70	0.72	80.82
1.05e-03	9.90	0.80	81.62
9.11e-04	10.10	0.91	82.53
7.93e-04	10.30	0.83	83.36
6.91e-04	10.50	0.80	84.16
6.01e-04	10.70	0.70	84.87
5.23e-04	10.90	0.24	85.11
2.44e-04	12.00	14.89	100.00

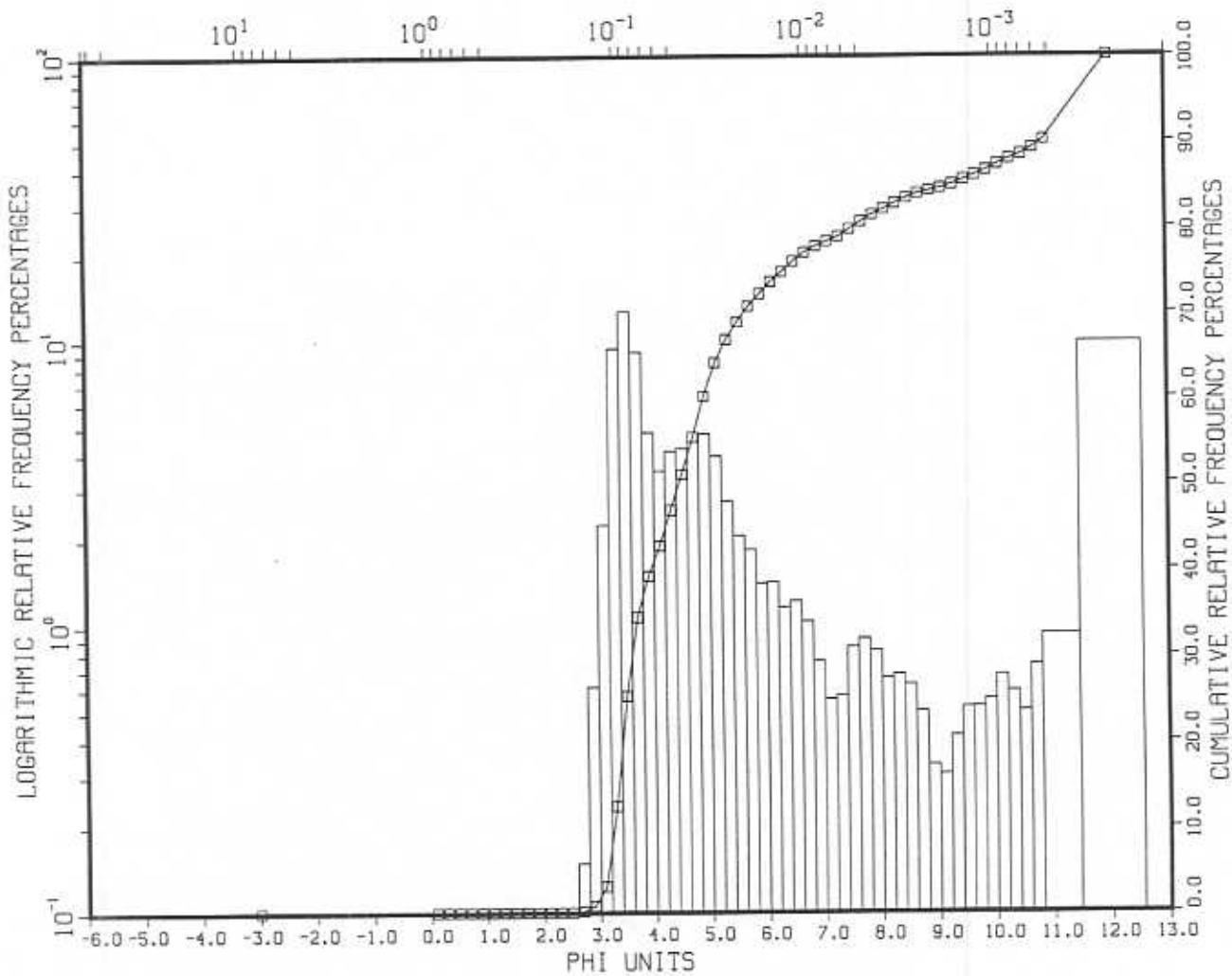
## Grain Size Breakdown

%	%	%	%	%
Gravel	Sand	Silt	Clay	Mud
0.00	18.79	55.00	26.21	81.20

## Statistical Measures

Mean	Standard	Kurtosis	Skewness
(PHI)	Deviation	( No Dim. )	( No Dim. )
	(PHI)		
6.55	2.87	2.41	0.86

94076-FA 06 C 0-3,RD009368, DR. CARL AMOS  
 # ,00209, AGC GRAVITY, ANNAPOLIS BASIN  
 MILLIMETER EQUIVALENTS



CALCULATION RESULTS FOR  
THE SAMPLE WITH THE IDENTIFIER:

94076-FA 06 C 0-3, RD009368,  
# ,00209,

DR. CARL AMOS  
AGC GRAVITY, ANNAPOLIS BASIN

## RESULTS

MIDPOINTS		RELATIVE	CUMULATIVE
MM	PHI	FREQUENCY	FREQUENCY
		PERCENTAGES	PERCENTAGES
8.0	-3.00	0.04	0.04
.93	0.10	0.01	0.05
.81	0.30	0.00	0.05
.71	0.50	0.00	0.05
.62	0.70	0.00	0.05
.54	0.90	0.00	0.05
.47	1.10	0.00	0.05
.41	1.30	0.00	0.05
.35	1.50	0.00	0.05
.31	1.70	0.00	0.05
.27	1.90	0.00	0.05
.23	2.10	0.00	0.05
.20	2.30	0.00	0.05
.18	2.50	0.00	0.05
.15	2.70	0.15	0.20
.13	2.90	0.62	0.81
.12	3.10	2.26	3.07
.10	3.30	9.44	12.51
.88E-01	3.50	12.76	25.27
.77E-01	3.70	9.16	34.43
.67E-01	3.90	4.78	39.21
.58E-01	4.10	3.49	42.71
.51E-01	4.30	4.10	46.81
.44E-01	4.50	4.20	51.01
.38E-01	4.70	4.42	55.43
.33E-01	4.90	4.72	60.15
.29E-01	5.10	3.94	64.09
.25E-01	5.30	2.73	66.83
.22E-01	5.50	2.08	68.90
.19E-01	5.70	1.85	70.76
.17E-01	5.90	1.42	72.17
.15E-01	6.10	1.43	73.61
.13E-01	6.30	1.17	74.77
.11E-01	6.50	1.23	76.00
.96E-02	6.70	1.04	77.05
.84E-02	6.90	0.76	77.80
.73E-02	7.10	0.56	78.36
.63E-02	7.30	0.57	78.94
.55E-02	7.50	0.85	79.79
.48E-02	7.70	0.91	80.70

.42E-02	7.90	0.83	81.52
.36E-02	8.10	0.66	82.19
.32E-02	8.30	0.68	82.87
.28E-02	8.50	0.63	83.50
.24E-02	8.70	0.51	84.00
.21E-02	8.90	0.33	84.33
.18E-02	9.10	0.31	84.64
.16E-02	9.30	0.42	85.05
.14E-02	9.50	0.52	85.58
.12E-02	9.70	0.53	86.11
.10E-02	9.90	0.56	86.66
.91E-03	10.10	0.68	87.34
.79E-03	10.30	0.60	87.94
.69E-03	10.50	0.51	88.45
.60E-03	10.70	0.74	89.19
.52E-03	10.90	0.94	90.13
.24E-03	12.00	9.87	100.00

## GRAIN SIZE BREAKDOWN

% GRAVEL	% SAND	% SILT	% CLAY	% MUD
0.04	39.18	42.31	18.48	60.79

## STATISTICAL MEASURES

MEAN (PHI)	STANDARD DEVIATION (PHI)	KURTOSIS ( NO DIM. )	SKEWNESS ( NO DIM. )
5.62	2.78	3.42	1.30

Calculation Results for  
The Sample with the Identifier:

PSS Version: V2.3  
 Processed (DD-MM-YY): 8-16-94  
 Sed Lab Number: 9368  
 Lines of Raw Data: 57  
 Sed Lab's ID: 94076-FA 06 C 0-3  
 Cruise: 94076  
 Project Number: 303047  
 Scientist Name: DR. CARL AMOS  
 Sed Lab Comments: AGC GRAVITY, ANNAPOLIS BASIN  
 Raw Data File: RD009368  
 Sample Work File: SWF00209  
 Top Interval: 0.00 cm.  
 Bottom Interval: 3.00 cm.  
 SID key: 50795  
 Sample Number: FA-6  
 Station Number: FA-6  
 Instrument Type: AGC GRAVITY  
 Sample Type: CORE  
 Latitude: 44:41.07 Degrees North  
 Longitude: 65:38.78 Degrees West  
 Water Depth: 8.60 m.  
 #

Results

Midpoints		Relative Frequency Percentages	Cumulative Frequency Percentages
MM	PHI		
8.00e+00	-3.00	0.04	0.04
9.33e-01	0.10	0.01	0.05
8.12e-01	0.30	0.00	0.05
7.07e-01	0.50	0.00	0.05
6.16e-01	0.70	0.00	0.05
5.36e-01	0.90	0.00	0.05
4.67e-01	1.10	0.00	0.05
4.06e-01	1.30	0.00	0.05
3.54e-01	1.50	0.00	0.05
3.08e-01	1.70	0.00	0.05
2.68e-01	1.90	0.00	0.05
2.33e-01	2.10	0.00	0.05
2.03e-01	2.30	0.00	0.05
1.77e-01	2.50	0.00	0.05
1.54e-01	2.70	0.15	0.20
1.34e-01	2.90	0.62	0.81
1.17e-01	3.10	2.26	3.07
1.02e-01	3.30	9.44	12.51
8.84e-02	3.50	12.76	25.27
7.69e-02	3.70	9.16	34.43
6.70e-02	3.90	4.78	39.21



5.83e-02	4.10	3.49	42.71
5.08e-02	4.30	4.10	46.81
4.42e-02	4.50	4.20	51.01
3.85e-02	4.70	4.42	55.43
3.35e-02	4.90	4.72	60.15
2.92e-02	5.10	3.94	64.09
2.54e-02	5.30	2.73	66.83
2.21e-02	5.50	2.08	68.90
1.92e-02	5.70	1.85	70.76
1.67e-02	5.90	1.42	72.17
1.46e-02	6.10	1.43	73.61
1.27e-02	6.30	1.17	74.77
1.10e-02	6.50	1.23	76.00
9.62e-03	6.70	1.04	77.05
8.37e-03	6.90	0.76	77.80
7.29e-03	7.10	0.56	78.36
6.35e-03	7.30	0.57	78.94
5.52e-03	7.50	0.85	79.79
4.81e-03	7.70	0.91	80.70
4.19e-03	7.90	0.83	81.52
3.64e-03	8.10	0.66	82.19
3.17e-03	8.30	0.68	82.87
2.76e-03	8.50	0.63	83.50
2.40e-03	8.70	0.51	84.00
2.09e-03	8.90	0.33	84.33
1.82e-03	9.10	0.31	84.64
1.59e-03	9.30	0.42	85.05
1.38e-03	9.50	0.52	85.58
1.20e-03	9.70	0.53	86.11
1.05e-03	9.90	0.56	86.66
9.11e-04	10.10	0.68	87.34
7.93e-04	10.30	0.60	87.94
6.91e-04	10.50	0.51	88.45
6.01e-04	10.70	0.74	89.19
5.23e-04	10.90	0.94	90.13
2.44e-04	12.00	9.87	100.00

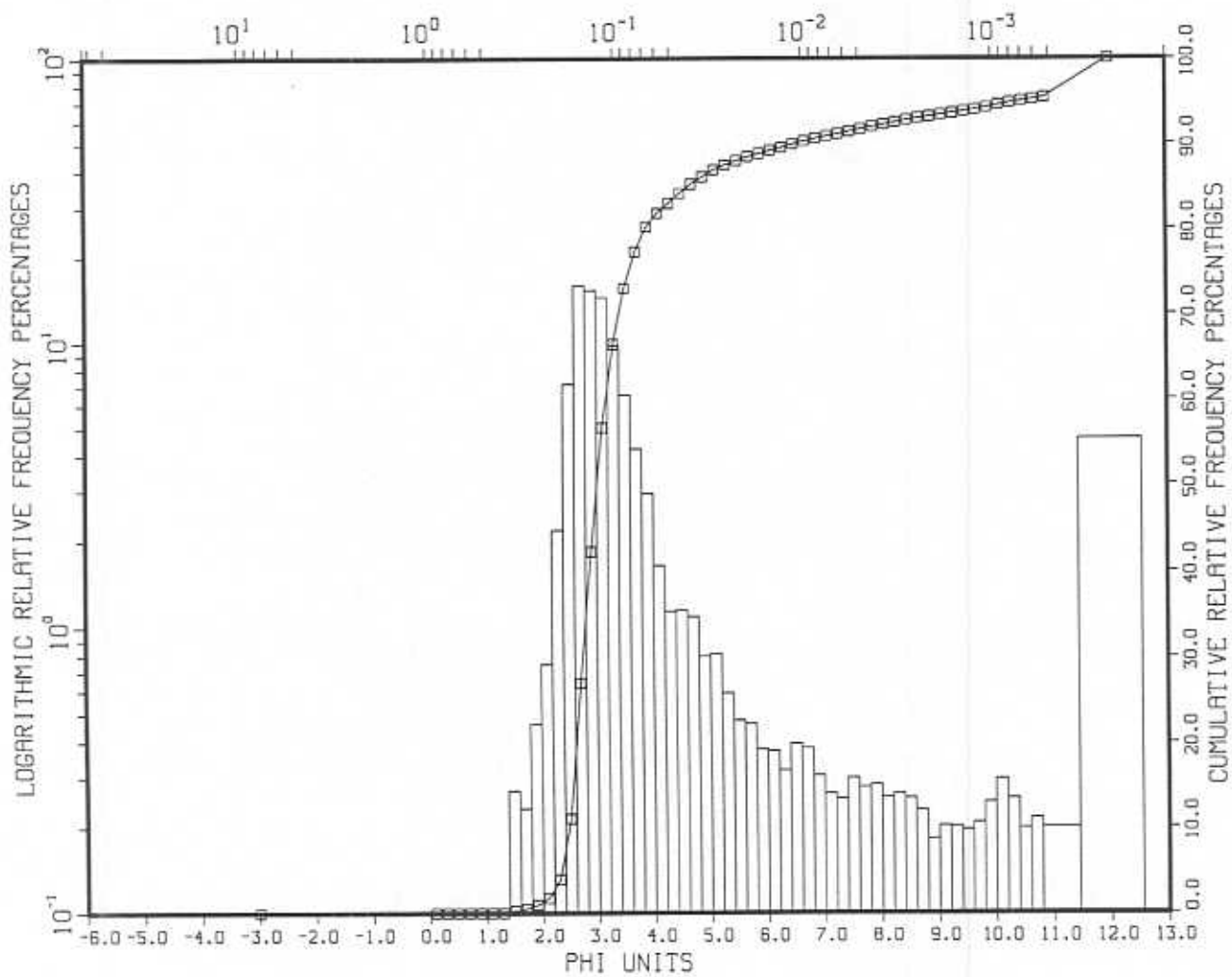
## Grain Size Breakdown

%	%	%	%	%
Gravel	Sand	Silt	Clay	Mud
0.04	39.18	42.31	18.48	60.79

## Statistical Measures

Mean (PHI)	Standard Deviation (PHI)	Kurtosis ( No Dim. )	Skewness ( No Dim. )
5.62	2.78	3.42	1.30

94076-FA 07 C 0-3, R0009370, DR. CARL AMOS  
 # ,00210, AGC GRAVITY, MAIN CHANNEL, OUTER ANNAPOLIS BASIN  
 MILLIMETER EQUIVALENTS



CALCULATION RESULTS FOR  
THE SAMPLE WITH THE IDENTIFIER:

94076-FA 07 C 0-3,RD009370, DR. CARL AMOS  
# ,00210, AGC GRAVITY, MAIN CHANNEL, OUTER ANNAPOLIS BASIN

## RESULTS

MIDPOINTS		RELATIVE	CUMULATIVE
MM	PHI	FREQUENCY	FREQUENCY
		PERCENTAGES	PERCENTAGES
8.0	-3.00	0.02	0.02
.93	0.10	0.00	0.02
.81	0.30	0.00	0.02
.71	0.50	0.00	0.02
.62	0.70	0.00	0.02
.54	0.90	0.00	0.02
.47	1.10	0.00	0.02
.41	1.30	0.01	0.03
.35	1.50	0.27	0.30
.31	1.70	0.23	0.53
.27	1.90	0.46	1.00
.23	2.10	0.75	1.75
.20	2.30	2.20	3.95
.18	2.50	7.14	11.09
.15	2.70	15.89	26.99
.13	2.90	15.29	42.28
.12	3.10	14.44	56.72
.10	3.30	9.78	66.50
.88E-01	3.50	6.56	73.05
.77E-01	3.70	4.24	77.30
.67E-01	3.90	2.95	80.25
.58E-01	4.10	1.66	81.91
.51E-01	4.30	1.15	83.06
.44E-01	4.50	1.16	84.21
.38E-01	4.70	1.10	85.31
.33E-01	4.90	0.80	86.12
.29E-01	5.10	0.82	86.94
.25E-01	5.30	0.60	87.53
.22E-01	5.50	0.48	88.01
.19E-01	5.70	0.47	88.48
.17E-01	5.90	0.38	88.85
.15E-01	6.10	0.37	89.23
.13E-01	6.30	0.32	89.55
.11E-01	6.50	0.40	89.95
.96E-02	6.70	0.38	90.33
.84E-02	6.90	0.31	90.64
.73E-02	7.10	0.26	90.90
.63E-02	7.30	0.25	91.15
.55E-02	7.50	0.30	91.45
.48E-02	7.70	0.28	91.73

.42E-02	7.90	0.28	92.02
.36E-02	8.10	0.26	92.27
.32E-02	8.30	0.26	92.54
.28E-02	8.50	0.25	92.79
.24E-02	8.70	0.23	93.02
.21E-02	8.90	0.18	93.20
.18E-02	9.10	0.20	93.41
.16E-02	9.30	0.20	93.61
.14E-02	9.50	0.20	93.81
.12E-02	9.70	0.21	94.01
.10E-02	9.90	0.25	94.26
.91E-03	10.10	0.30	94.56
.79E-03	10.30	0.25	94.81
.69E-03	10.50	0.20	95.01
.60E-03	10.70	0.22	95.22
.52E-03	10.90	0.20	95.42
.24E-03	12.00	4.58	100.00

GRAIN SIZE BREAKDOWN				
%	%	%	%	%
GRAVEL	SAND	SILT	CLAY	MUD
0.02	80.23	11.77	7.98	19.75

STATISTICAL MEASURES			
MEAN	STANDARD	KURTOSIS	SKEWNESS
(PHI)	DEVIATION	( NO DIM. )	( NO DIM. )
	(PHI)		
3.91	2.30	8.60	2.53

Calculation Results for  
The Sample with the Identifier:

PSS Version: V2.3  
 Processed (DD-MM-YY): 8-16-94  
 Sed Lab Number: 9370  
 Lines of Raw Data: 57  
 Sed Lab's ID: 94076-FA 07 C 0-3  
 Cruise: 94076  
 Project Number: 303047  
 Scientist Name: DR. CARL AMOS  
 Sed Lab Comments: AGC GRAVITY, MAIN CHANNEL, OUTER  
 ANNAPOLIS BASIN  
 Raw Data File: RD009370  
 Sample Work File: SWF00210  
 Top Interval: 0.00 cm.  
 Bottom Interval: 3.00 cm.  
 SID key: 50797  
 Sample Number: FA-7  
 Station Number: FA-7  
 Instrument Type: AGC GRAVITY  
 Sample Type: CORE  
 Latitude: 44:39.62 Degrees North  
 Longitude: 65:40.42 Degrees West  
 Water Depth: 8.50 m.  
 #

Results

Midpoints		Relative Frequency Percentages	Cumulative Frequency Percentages
MM	PHI		
8.00e+00	-3.00	0.02	0.02
9.33e-01	0.10	0.00	0.02
8.12e-01	0.30	0.00	0.02
7.07e-01	0.50	0.00	0.02
6.16e-01	0.70	0.00	0.02
5.36e-01	0.90	0.00	0.02
4.67e-01	1.10	0.00	0.02
4.06e-01	1.30	0.01	0.03
3.54e-01	1.50	0.27	0.30
3.08e-01	1.70	0.23	0.53
2.68e-01	1.90	0.46	1.00
2.33e-01	2.10	0.75	1.75
2.03e-01	2.30	2.20	3.95
1.77e-01	2.50	7.14	11.09
1.54e-01	2.70	15.89	26.99
1.34e-01	2.90	15.29	42.28
1.17e-01	3.10	14.44	56.72
1.02e-01	3.30	9.78	66.50
8.84e-02	3.50	6.56	73.05
7.69e-02	3.70	4.24	77.30

6.70e-02	3.90	2.95	80.25
5.83e-02	4.10	1.66	81.91
5.08e-02	4.30	1.15	83.06
4.42e-02	4.50	1.16	84.21
3.85e-02	4.70	1.10	85.31
3.35e-02	4.90	0.80	86.12
2.92e-02	5.10	0.82	86.94
2.54e-02	5.30	0.60	87.53
2.21e-02	5.50	0.48	88.01
1.92e-02	5.70	0.47	88.48
1.67e-02	5.90	0.38	88.85
1.46e-02	6.10	0.37	89.23
1.27e-02	6.30	0.32	89.55
1.10e-02	6.50	0.40	89.95
9.62e-03	6.70	0.38	90.33
8.37e-03	6.90	0.31	90.64
7.29e-03	7.10	0.26	90.90
6.35e-03	7.30	0.25	91.15
5.52e-03	7.50	0.30	91.45
4.81e-03	7.70	0.28	91.73
4.19e-03	7.90	0.28	92.02
3.64e-03	8.10	0.26	92.27
3.17e-03	8.30	0.26	92.54
2.76e-03	8.50	0.25	92.79
2.40e-03	8.70	0.23	93.02
2.09e-03	8.90	0.18	93.20
1.82e-03	9.10	0.20	93.41
1.59e-03	9.30	0.20	93.61
1.38e-03	9.50	0.20	93.81
1.20e-03	9.70	0.21	94.01
1.05e-03	9.90	0.25	94.26
9.11e-04	10.10	0.30	94.56
7.93e-04	10.30	0.25	94.81
6.91e-04	10.50	0.20	95.01
6.01e-04	10.70	0.22	95.22
5.23e-04	10.90	0.20	95.42
2.44e-04	12.00	4.58	100.00

## Grain Size Breakdown

%	%	%	%	%
Gravel	Sand	Silt	Clay	Mud
0.02	80.23	11.77	7.98	19.75

## Statistical Measures

Mean	Standard	Kurtosis	Skewness
(PHI)	Deviation	( No Dim. )	( No Dim. )
3.91	2.30	8.60	2.53

**Appendix E**

**Benthic Fauna at Subtidal Stations of the Annapolis Basin and Estuary, June 1994**

**Results: Benthic Samples - Fort Anne, 1994**  
**Station: FA-2**

Species	Sample Number					
	1	2	3	4	5	6
Hydrozoa				not preserved properly		
ph. Rhyncocoela		3				
Class Gastropoda						
Nassarius trivittatus	1	8	8		1	4
Littorina littorea						
Aporrhais occidentalis						
Lacuna vineta						
Oenopota bincarinata						
Lunatia triseriata						
unid gastropod						
Class Bivalvia						
Macoma balthica						
Yoldia limatula						
Cyclocardia borealis			1			2
Mya arenaria						
Spisula solidissima						
imid. juv. bivalves			1			
subclass Cirripeda						
Balanus balanoides						
Cucumaria frondosa?						
(echinoderm)						
Order Cumacea						
Oxyurostylis smithi						
Leptocuma minor	1		6			1
Order Isopoda						
Cirolana polita						
Chiridotea tuftsi						
Chiridotea sp.		1				
Ptilanthura tenuis						
suborder Caprellidea						



## FA-2 (cont.)

Species	Sample Number					
	1	2	3	4	5	6
suborder Gammaridea						
<i>Leptocheirus pinguis</i>		3			1	
<i>Ampelisca vadorum</i>	1				1	2
<i>Unciola irrorata</i>						
<i>Edotea montosa</i>						
<i>Psammonyx nobilis</i>						
unid Amphipod						
Order Decapoda						
<i>Crangon septemspinosa</i>						
Class Polychaeta						
Terebellidae	1		1			
<i>Chaetozone setosa</i>	22	107			29	9
<i>Nephtys neotenus</i>	2	5	27		9	3
<i>Nephtys incisa</i>						
<i>Nephtys caeca</i>						
<i>Nephtys ciliata</i>						
<i>Nephtys</i> sp.						
<i>Spiophanes bombyx</i>						
<i>Scolelepis squatus</i>						
<i>Eteone flava</i>						
<i>Eteone longa</i>						1
<i>Lumbrineris latreilli</i>						
<i>Lumbrineris tenuis</i>						
<i>Phyllodoce mucosa</i>						
<i>Scoloplos robustus</i>						
<i>Syllis gracilis</i>						
<i>Sternaspis scutata</i>						
<i>Pherusa affinis</i>						
<i>Potamilla neglecta</i>						
<i>Cossura longocirrata</i>						
<i>Polycirrus eximius</i>						
<i>Asabellides oculata</i>						
<i>Clymenella torquata</i>						
<i>Polydora</i> sp.						
<i>Ophelina acuminata</i>						
<i>Tharyx acutus</i>						
<i>Praxillella gracilis</i>						
<i>Ninoe nigripes</i>						
<i>Prionospio steenstrupi</i>						
unid polychaetes						

**Results: Benthic Samples - Fort Anne, 1994**  
**Station: FA-3**

Species	Sample Number					
	1	2	3	4	5	6
Hydrozoa						
ph. Rhyncocoela						
Class Gastropoda						
<i>Nassarius trivittatus</i>	4	1				6
<i>Littorina littorea</i>						
<i>Aporrhais occidentalis</i>						
<i>Lacuna vincta</i>						
<i>Oenopota bincarinata</i>						
<i>Lunatia triseriata</i>						
unid gastropod						
Class Bivalvia						
<i>Macoma balthica</i>						
<i>Yoldia limatula</i>						
<i>Cyclocardia borealis</i>						1
<i>Mya arenaria</i>						
<i>Spisula solidissima</i>						
inid. juv. bivalves		1	1			
subclass Cirripeda						
<i>Balanus balanoides</i>						
<i>Cucumaria frondosa?</i> (echinoderm)						
Order Cumacea						
<i>Oxyurostylis smithi</i>						
<i>Leptocuma minor</i>			1			
Order Isopoda						
<i>Cirolana polita</i>						
<i>Chiridotea tuftsi</i>						
<i>Chiridotea sp.</i>						
<i>Ptilanthura tenuis</i>						
suborder Caprellidea						

## FA-3 (cont.)

Species	Sample Number					
	1	2	3	4	5	6
suborder Gammaridea						
<i>Leptocheirus pinguis</i>						
<i>Ampelisca vadorum</i>						
<i>Unciola irrorata</i>						
<i>Edotea montosa</i>						
<i>Psammonyx nobilis</i>						
unid Amphipod						
Order Decapoda						
<i>Crangon septemospinosa</i>						
Class Polychaeta						
<i>Chaetozone setosa</i>	9	1	8	7	3	10
<i>Nephtys neotenus</i>		6	11	5	1	9
<i>Nephtys incisa</i>						
<i>Nephtys caeca</i>						
<i>Nephtys ciliata</i>						
<i>Nephtys</i> sp.						
<i>Spiophanes bombyx</i>				1		
<i>Scolelepis squatus</i>						
<i>Eteone flava</i>						
<i>Eteone longa</i>						
<i>Lumbrineris latreilli</i>						
<i>Lumbrineris tenuis</i>						
<i>Phyllodoce mucosa</i>						
<i>Scoloplos robustus</i>						
<i>Syllis gracilis</i>						
<i>Sternaspis scutata</i>						
<i>Pherusa affinis</i>						
<i>Potamilla neglecta</i>						
<i>Cossura longocirrata</i>						
<i>Polycirrus eximius</i>						
<i>Asabellides oculata</i>						
<i>Clymenella torquata</i>						
<i>Polydora</i> sp.						
<i>Ophelina acuminata</i>						
<i>Tharyx acutus</i>						
<i>Praxillella gracilis</i>						
<i>Ninoe nigripes</i>						
<i>Prionospio steenstrupi</i>						
unid polychaetes						

**Results: Benthic Samples - Fort Anne, 1994**  
**Station: FA-4**

Species	Sample Number					
	1	2	3	4	5	6
Hydrozoa						
ph. Rhyncocoela	1					
Class Gastropoda						
Nassarius trivittatus		3		5	1	
Littorina littorea						
Aporrhais occidentalis						
Lacuna vineta						
Oenopota bincarinata						
Lunatia triseriata						
unid gastropod						
Class Bivalvia						
Macoma balthica						
Yoldia limatula						
Cyclocardia borealis		3		1	3	
Mya arenaria						
Spisula solidissima					1	
inid. juv. bivalves						
subclass Cirripeda						
Balanus balanoides						
Cucumaria frondosa?						
(echinoderm)						
Order Cumacea						
Oxyurostylis smithi						
Leptocuma minor	1	2		3	2	
Order Isopoda						
Cirolana polita						
Chiridotea tuftsi						
Chiridotea sp.						
Ptilanthura tenuis						
suborder Caprellidea						

## FA-4 (cont.)

Species	Sample Number					
	1	2	3	4	5	6
suborder Gammaridea						
<i>Leptocheirus pinguis</i>	1				1	
<i>Ampelisca vadorum</i>						
<i>Unciola irrorata</i>						
<i>Edotea montosa</i>						
<i>Psammonyx nobilis</i>						
unid Amphipod						
Order Decapoda						
<i>Crangon septemspinosus</i>				1		
Class Polychaeta						
<i>Chaetozone setosa</i>	17	19	9	17	6	9
<i>Nephtys neotenus</i>	2	9	10	21	14	12
<i>Nephtys incisa</i>			1			
<i>Nephtys caeca</i>						
<i>Nephtys ciliata</i>		1				
<i>Nephtys</i> sp.						
<i>Spiophanes bombyx</i>						
<i>Scolecopsis squatus</i>						
<i>Eteone flava</i>						
<i>Eteone longa</i>						
<i>Lumbrineris latreilli</i>				1		
<i>Lumbrineris tenuis</i>						
<i>Phyllodoce mucosa</i>						
<i>Scoloplos robustus</i>				1		
<i>Syllis gracilis</i>						
<i>Sternaspis scutata</i>						
<i>Pherusa affinis</i>						
<i>Potamilla neglecta</i>		1			9	
<i>Cossura longocirrata</i>						1
Terebellidae	2					
<i>Asabellides oculata</i>	1					
<i>Clymenella torquata</i>						
<i>Polydora</i> sp.						
<i>Ophelina acuminata</i>						
<i>Tharyx acutus</i>						
<i>Praxillella gracilis</i>						
<i>Ninoe nigripes</i>						
<i>Prionospio steenstrupi</i>						
unid polychaetes						

Results: Benthic Samples - Fort Anne, 1994  
Station: FA-5

Species	Sample Number					
	1	2	3	4	5	6
Hydrozoa	"1"	"1"				
ph. Rhyncocoela						1
Class Gastropoda						
Nassarius trivittatus	2	1	1	1		
Littorina littorea						
Aporrhais occidentalis						
Lacuna vincta						
Oenopota bincarinata						
Lunatia triseriata						
unid gastropod						
Class Bivalvia						
Macoma balthica		1				
Yoldia limatula						
Cyclocardia borealis					1	
Mya arenaria						
Spisula solidissima						
imid. juv. bivalves					1	
subclass Cirripeda						
Balanus balanoides						
Cucumaria frondosa?						
(echinoderm)						
Order Cumacea						
Oxyurostylis smithi	1					
Leptocuma minor						
Order Isopoda						
Cirolana polita						
Chiridotea tuftsi						
Chiridotea sp.						
Ptilanthura tenuis						
suborder Caprellidea						

## FA-5 (cont.)

Species	Sample Number					
	1	2	3	4	5	6
suborder Gammaridea						
<i>Leptocheirus pinguis</i>						
<i>Ampelisca vadorum</i>						
<i>Unciola irrorata</i>						
<i>Edotea montosa</i>						
<i>Psammonyx nobilis</i>						
unid Amphipod						
Order Decapoda						
<i>Crangon septemspinosa</i>						
Class Polychaeta						
<i>Chaetozone setosa</i>	11	1	7	6		2
<i>Nephtys neotenus</i>	32	44	11	71	127	14
<i>Nephtys incisa</i>						
<i>Nephtys caeca</i>						
<i>Nephtys ciliata</i>						
<i>Nephtys</i> sp.						
<i>Spiophanes bombyx</i>						
<i>Scolelepis squatus</i>						
<i>Eteone flava</i>						
<i>Eteone longa</i>						
<i>Lumbrineris latreilli</i>				1	3	2
<i>Lumbrineris tenuis</i>						
<i>Phyllodoce mucosa</i>						
<i>Scoloplos robustus</i>						
<i>Syllis gracilis</i>						
<i>Sternaspis scutata</i>						
<i>Pherusa affinis</i>					1	
<i>Potamilla neglecta</i>				1		
<i>Cossura longocirrata</i>						
<i>Polycirrus examinus</i>						
<i>Asabellides oculata</i>						
<i>Clymenella torquata</i>						
<i>Polydora</i> sp.						
<i>Ophelina acuminata</i>						
<i>Tharyx acutus</i>						
<i>Praxillella gracilis</i>						
<i>Ninoe nigripes</i>						
<i>Prionospio steenstrupi</i>						
unid polychaetes						

Results: Benthic Samples - Fort Anne, 1994  
Station: FA-6

Species	Sample Number					
	1	2	3	4	5	6
Hydrozoa						
ph. Rhyncocoela		2				
Class Gastropoda						
<i>Nassarius trivittatus</i>		4		2	2	
<i>Littorina littorea</i>						
<i>Aporrhais occidentalis</i>						
<i>Lacuna vincta</i>				1		
<i>Oenopota bincarinata</i>						
<i>Lunatia triseriata</i>		1				
unid gastropod						
Class Bivalvia						
<i>Macoma balthica</i>						
<i>Yoldia limatula</i>	1				1	
<i>Cyclocardia borealis</i>		1				
<i>Mya arenaria</i>						
<i>Spisula solidissima</i>		8				
inid. juv. bivalves			6		6	
subclass Cirripeda						
<i>Balanus balanoides</i>						
<i>Cucumaria frondosa?</i> (echinoderm)						
Order Cumacea						
<i>Oxyurostylis smithi</i>					1	
<i>Leptocuma minor</i>				1		
Order Isopoda						
<i>Cirolana polita</i>						
<i>Chiridotea tuftsi</i>						
<i>Chiridotea sp.</i>						
<i>Ptilanthura tenuis</i>						
suborder Caprellidea			1			



## FA-6 (cont.)

Species	Sample Number					
	1	2	3	4	5	6
suborder Gammaridea						
<i>Leptocheirus pinguis</i>	2					1
<i>Ampelisca vadorum</i>	1		3	1		3
<i>Unciola irrorata</i>						
<i>Edotea montosa</i>						
<i>Psammonyx nobilis</i>						
unid Amphipod						
Order Decapoda						
<i>Crangon septemspinosa</i>						
Class Polychaeta						
Terebellidae						
<i>Chaetozone setosa</i>	2		2	1	2	3
<i>Nephtys neotenus</i>		4	3	3		6
<i>Nephtys incisa</i>			1	1		1
<i>Nephtys caeca</i>		1			1	
<i>Nephtys ciliata</i>						
<i>Nephtys</i> sp.						
<i>Spiophanes bombyx</i>						
<i>Scolelepis squatus</i>						
<i>Eteone flava</i>			1	1		1
<i>Eteone longa</i>						
<i>Lumbrineris latreilli</i>		16	13	16		21
<i>Lumbrineris tenuis</i>						
<i>Phyllodoce mucosa</i>			1			
<i>Scoloplos robustus</i>			2		1	
<i>Syllis gracilis</i>			2	1		
<i>Sternaspis scutata</i>		2	2	2	1	3
<i>Pherusa affinis</i>				1		
<i>Potamilla neglecta</i>						
<i>Cossura longocirrata</i>						
<i>Polycirrus examinus</i>						
<i>Asabellides oculata</i>						
<i>Clymenella torquata</i>		1				3
<i>Polydora</i> sp.						
<i>Ophelina acuminata</i>						
<i>Tharyx acutus</i>						
<i>Praxillella gracilis</i>		2				
<i>Ninoe nigripes</i>	4				4	
<i>Prionospio steenstrupi</i>						
unid polychaetes	1					

## Results: Benthic Samples - Fort Anne, 1994

Station: FA-7

Species	Sample Number					
	1	2	3	4	5	6
Hydrozoa					sample not preserved properly	
ph. Rhyncocoela						
Class Gastropoda						
Nassarius trivittatus	1	1	6	1		
Littorina littorea						
Aporrhais occidentalis						
Lacuna vineta						
Oenopota bincarinata						
Lunatia triseriata						
unid gastropod						
Class Bivalvia						
Macoma balthica						
Yoldia limatula						
Cyclocardia borealis						
Mya arenaria	1	1				
Spisula solidissima						
imid. juv. bivalves			2			
subclass Cirripeda						
Balanus balanoides						
Cucumaria frondosa?						
(echinoderm)						
Order Cumacea						
Oxyurostylis smithi		2	1			1
Leptocuma minor	1					1
Order Isopoda						
Cirolana polita	3	2		2		
Chiridotea tuftsi						
Chiridotea sp.						
Ptilanthura tenuis		1		1		1
suborder Caprellidea						

## FA-7 (cont.)

Species	Sample Number					
	1	2	3	4	5	6
suborder Gammaridea						
<i>Leptocheirus pinguis</i>	20	3	32	4		5
<i>Ampelisca vadorum</i>		1				
<i>Unciola irrorata</i>	5	2				1
<i>Edotea montosa</i>						
<i>Psammonyx nobilis</i>	9	1	5	52		2
unid Amphipod						
Order Decapoda						
<i>Crangon septemspinosa</i>						
Class Polychaeta						
<i>S. viridus</i>						
<i>Chaetozone setosa</i>				1		
<i>Nephtys neotenus</i>	1	1	1	2		
<i>Nephtys incisa</i>	3	5	9	1		3
<i>Nephtys caeca</i>	1					
<i>Nephtys ciliata</i>						
<i>Nephtys</i> sp.						
<i>Spiophanes bombyx</i>	22	1	41	19		14
<i>Scolelepis squatus</i>			2			
<i>Eteone flava</i>						
<i>Eteone longa</i>			1			
<i>Lumbrineris latreilli</i>						
<i>Lumbrineris tenuis</i>						
<i>Phyllodoce mucosa</i>	1		3			2
<i>Scoloplos robustus</i>				1		
<i>Syllis gracilis</i>						
<i>Sternaspis scutata</i>						
<i>Pherusa affinis</i>						
<i>Potamilla neglecta</i>						
<i>Cossura longocirrata</i>						
<i>Polycirrus examinus</i>						
<i>Asabellides oculata</i>						
<i>Clymenella torquata</i>						
<i>Polydora</i> sp.	1					
<i>Ophelina acuminata</i>	1					
<i>Tharyx acutus</i>	1	4				
<i>Praxillella gracilis</i>			3	2		
<i>Ninoe nigripes</i>						
<i>Prionospio steenstrupi</i>						1
unid polychaetes		1				

Results: Benthic Samples - Fort Anne, 1994  
Station: FA-8

Species	Sample Number					
	1	2	3	4	5	6
Hydrozoa						
ph. Rhyncocoela	1					
Class Gastropoda						
Nassarius trivittatus				3		
Littorina littorea						
Aporrhais occidentalis		1				
Lacuna vineta			13	4		
Oenopota bicarinata				1		
Lunatia triseriata						
unid gastropod				1		
Class Bivalvia						
Macoma balthica						
Yoldia limatula						
Cyclocardia borealis		3				
Mya arenaria						
Spisula solidissima					1	
inid. juv. bivalves						
subclass Cirripeda						
Balanus balanoides						
Cucumaria frondosa? (echinoderm)	3		1	2		
Order Cumacea						
Oxyurostylis smithi						
Leptocuma minor						1
Order Isopoda						
Cirolana polita		1				
Chiridotea tuftsi				1		
Chiridotea sp.						
Ptilanthura tenuis			1			
Edotea montosa			2			
suborder Caprellidea			149	2		

## FA-8 (cont.)

Species	Sample Number					
	1	2	3	4	5	6
suborder Gammaridea						
Leptocheirus pinguis			7	9		2
Ampelisca vadorum						
Unciola irrorata			1			
Edotea montosa						
Psammonyx nobilis						
unid Amphipod	1			3		
Order Decapoda						
Crangon septemspinosa						
Class Polychaeta						
Terebellidae	2		1		2	
Chaetozone setosa		1	2	4	4	1
Nephtys neotenus		1		1		
Nephtys incisa	17	15	14	26	13	17
Nephtys caeca						
Nephtys ciliata						
Nephtys sp.						
Spiophanes bombyx		1			3	
Scolecopsis squatus	2					
Eteone flava			1			
Eteone longa				1	1	
Lumbrineris latreilli						
Lumbrineris tenuis						
Phyllodoce mucosa						
Scoloplos robustus	2	1		2		1
Syllis gracilis		1			3	
Sternaspis scutata						
Pherusa affinis						
Potamilla neglecta						
Cossura longocirrata						
Polycirrus eximius						
Asabellides oculata						
Clymenella torquata	18	5		4	19	4
Polydora sp.					1	1
Ophelina acuminata						
Tharyx acutus						
Praxillella gracilis						
Ninoe nigripes						
Prionospio steenstrupi						
unid polychaetes						